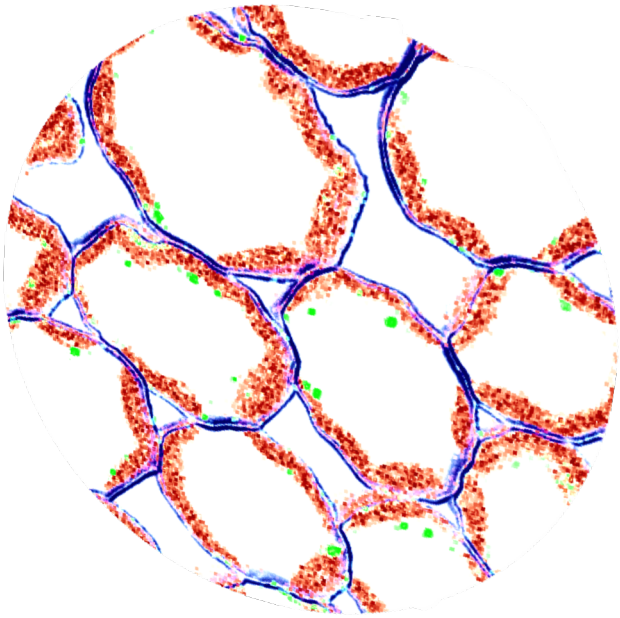

Interaction between class III peroxidases and arabinogalactan proteins in plant cell physiology

Sara Bettencourt Saraiva Alves Ramos
Doutoramento em Biologia
Departamento de Biologia
2014

Orientadora
Mariana Sottomayor, Professora Auxiliar, Faculdade de Ciências

Aos meus pais

ACKNOWLEDGMENTS

Em primeiro lugar gostaria de agradecer à minha orientadora, Mariana Sottomayor, uma mente brilhante, inspiradora, com quem muito aprendi e a quem devo este projeto e todo o conhecimento adquirido durante estes anos. Obrigada por me ensinares a pensar, a planear e a desenvolver o meu espírito crítico. Por todo o entusiasmo e dedicação empregues neste projeto, e, principalmente, pelo teu otimismo e energia, que me faziam ver as coisas de outra forma e me davam ânimo para continuar. Obrigada por "apostares" em mim!

I want to thank to professor Fry for welcoming me in your lab and for the opportunity to work and study in such great research group.

A todos os membros do grupo BNP do IBMC, tanto aos atuais como aos que já partiram, por todo o apoio, companheirismo e boa disposição! O bom ambiente de trabalho do nosso grupo foi fundamental para eu conseguir levantar-me de manhã e ter ânimo quando o trabalho não estava a correr bem… muito obrigada por isso! Em particular, gostaria de agradecer à Raquel por toda a calma e paciência, e por me responder prontamente a todos os e-mails com pedidos de ajuda. À nossa colombiana, Mafe, pelo riso contagiante. À Aninhas por estar sempre pronta para ajudar no que for preciso. Às nossas espanholas, Lore e Tere, por animarem os nossos dias. Lore, obrigada pelas boas gargalhadas… fazes falta! Tere, por toda a paciência para me aturares durante a reta final e por todas as tentativas para me animar… muito obrigada! Um agradecimento muito especial à Inês e à Pat, as minhas "muletas", por toda a ajuda e *brainstorming* durante este percurso e sobretudo por me ajudarem a chegar até ao fim. Inês, tu foste o meu exemplo durante estes anos. Contigo aprendi a ser mais expedita e sociável… já não sou tão "ranhosa", certo?! Pat, tu foste o meu ombro amigo, no qual eu chorei, por tudo e por nada… Obrigada por ouvires e por teres sempre uma palavra de apoio.

Aos membros do grupo MBNA do IBMC, por todo o apoio, convívio e troca de conhecimentos. Um especial agradecimento à Lili.

Ao Frederico Silva, Paula Sampaio e Rui Fernandes do IBMC, pela vossa paciência e por todos os resultados que obtive com a vossa ajuda. Muito obrigada!

Às minhas amigas desde sempre, Carla, Cláudia, Isa, Ju e Sara, por (ainda) serem minhas amigas! Obrigada pelos bons momentos, pelas jantaradas e por estarem sempre do meu lado, sempre disponíveis.

Às minhas amigas Joana, Marisa e Marta, que apesar de não passar muito tempo com vocês, eu sei que vocês estão aí… para o que der e vier!

À minha família por todos os momentos de descontração e boa disposição… vocês foram essenciais para a minha saúde mental! Em especial ao meu irmão e à minha cunhada pela minha pequena grande alegria, o meu sobrinho. Graças a ti, pestinha, estes dois últimos anos foram simplesmente especiais.

Aos meus pais, a quem dedico esta tese, por me deixarem seguir o meu caminho, mesmo acreditando que não seria o melhor para mim. Obrigada por toda a compreensão, por acreditarem em mim, por aturarem a minha cara emburrada e o meu mau feitio durante estes anos… vocês são o meu porto de abrigo!

E finalmente, ao Nuno… simplesmente por existires! Por me fazeres sentir a pessoa mais especial do teu mundo, por não me deixares esmorecer, por me dizeres constantemente que eu sou o teu orgulho e, sobretudo, por me fazeres acreditar em mim mesma… muito obrigada!

This work was financially co-supported by Fundação para a Ciência e a Tecnologia - FCT (SFRH/BD/48283/2008) and POPH-QREN (European Social Fund), and by a Scientific Mecenate Grant from Grupo Jerónimo Martins SA to the host laboratory of Bioactive Natural Products at IBMC – Instituto de Biologia Molecular e Celular.

ABSTRACT

The primary cell wall of plant cells is a highly plastic structure with a major role during development, mainly due to the function of several classes of proteins whose precise functions and mechanisms of action are still poorly understood. These include, among others, arabinogalactan proteins (AGPs) and class III peroxidases (Prxs). Discovering the way these proteins influence cell wall remodelling and signalling integration during morphogenesis and interaction with the environment is essential to understand plant cell physiology and development.

The main objective of this thesis was to investigate the occurrence of an interaction between AGPs and Prxs in the model plants *Catharanthus roseus* and *Arabidopsis thaliana*, using a set of *in vitro* and *in vivo* experiments, and to investigate the possible role of the Prx-AGP interaction.

In order to pursuit this aim, it was necessary to first investigate the localization of AGPs in both model plants. This study delivered a picture of AGPs cell/tissue localization patterns, as well as of their subcellular distribution in both plants. Some of the AGP epitopes presented highly specific labelling profiles, marking specific cell types in *C. roseus* and Arabidopsis, such as LM2 and JIM16, while others labelled most cell types, such as JIM14. On the other hand, the labelling by MAC207, JIM8 and JIM13 was clearly distinct between the two species analysed, showing that the localization of AGP epitopes does not always bear the same morphogenetic identity in different species. Interestingly, MAC207 labelled specifically the *C. roseus* alkaloid accumulating laticifers and idioblast cells. This immunolabelling study and complementary cell fractionation studies revealed that AGPs are conspicuously localized in the vacuoles, suggesting a functional relevance and challenging the paradigm of AGPs as just cell wall proteoglycans. Finally, it was shown that both AGPs and Prx are co-localized in membrane microdomains both at the level of the plasma membrane and the tonoplast, suggesting a possible *in vivo* interaction important for signalling.

It was shown that *C. roseus* and Arabidopsis Prxs, as well as horseradish peroxidase, all accept AGPs as substrates, and that Prx mediated oxidative cross-linking of AGPs, *in vitro* and *in vivo*, putatively relevant to the dynamics and remodelling of cell wall properties, and leading to *de novo* formation of AGP glycosidic epitopes that have been implicated in important aspects of plant development and plant cell physiology. Considered as a whole, the data points to a model where the interaction Prx-AGP may function as a signalling platform responsive to the important

regulatory molecule H_2O_2, where Prx uses this signalling molecule to cross-link co-localized AGPs that then interact with down-stream signalling molecules also present in the membrane microdomain.

The studies performed with root hairs, where H_2O_2 signalling has been implicated in tip growth indeed supported a role for Prx and AGPs compatible with the proposed model. The AGP blocker Yariv, the Prx inhibitor SHAM and the ROS scavengers KI and ascorbate all inhibited root hair differentiation. Moreover, AGP and Prx antibodies, as well as gum arabic, negatively affected the rate of root hair tip growth, while Prx and ectopic expression of *AtAGP9* and *AtAGP58* all stimulated that rate.

In order to investigate the occurrence of *in planta* interaction of AGPs and Prx, fluorescent protein (FP) fusions with specific AGP and Prx genes were generated and used for a range of transient and stable transformation strategies with inconclusive results. However, two FP-fusions, one with AtAGP58 and the other with AtPrx34, were shown to be excellent molecular markers for the plasma membrane and the vacuole, respectively, presenting consistent results in different transient expression assays for both homologous and heterologous systems that validate their use as useful tools for protein subcellular localization experiments.

Finally, the use of the endogenous promoters with the FP fusions enabled to determine the expression profile of the *AtAGP9* and *AtAGP58* genes, selected due to their high level of expression in Arabidopsis leaves. Both AGPs presented different expression profiles throughout the aerial organs of the plant and in the seedlings, with *AtAGP58* being mainly expressed in green organs and *AtAGP9* being mostly expressed in roots, styles and stamens. These studies point out several functions for these two AGPs.

Overall, the results obtained in the course of this thesis have provided novel knowledge about a noteworthy link between two important groups of plant cell wall proteins and the mechanisms by which they may be involved in signalling and morphogenesis, with important implications for the understanding of the physiology of plant cells and plant development.

RESUMO

A parede celular primária das células vegetais é uma estrutura altamente plástica com um papel importante durante o desenvolvimento, principalmente devido ao papel de várias classes de proteínas cujas funções e mecanismos de ação continuam por esclarecer. Estas classes de proteínas incluem, entre outras, as proteínas arabinogalactânicas (AGPs) e as peroxidases de classe III (Prxs). Descobrir a forma como estas duas famílias de proteínas influenciam a remodelação da parede celular e a integração de sinais durante a morfogénese e interação com o meio ambiente é essencial para compreender a fisiologia da célula vegetal e o seu desenvolvimento.

O principal objetivo desta tese foi investigar a existência duma interação entre AGPs e Prxs nas plantas modelo *Catharanthus roseus* e *Arabidopsis thaliana*, usando para tal um conjunto de experiências *in vitro* e *in vivo*, e para estudar a possível função da interação Prx-AGP.

Em busca deste objetivo, primeiro foi necessário investigar a localização das AGPs em ambas as plantas modelo. Este estudo desvendou um quadro de padrões de localização das AGPs nas células/tecidos, bem como a sua distribuição subcelular em ambas as plantas. Alguns dos epítopos das AGPs apresentaram perfis de marcação altamente específicos, marcando tipos de célula específicos em *C. roseus* e Arabidopsis, como o LM2 e o JIM16, enquanto outros marcaram a maioria das células, como o JIM14. Por outro lado, a marcação com o MAC207, JIM8 e JIM13 era claramente distinta entre as duas espécies analisadas, mostrando que a localização de epítopos de AGPs não exibe sempre a mesma identidade morfogenética em espécies diferentes. Curiosamente, o MAC207 marcou especificamente as células em *C. roseus* que acumulam os alcalóides, os lactíferos e os idioblastos. Este estudo de imunolocalização e estudos complementares de fracionamento celular revelaram que as AGPs estão conspicuamente localizadas nos vacúolos, sugerindo uma relevância funcional e desafiando o paradigma das AGPs como proteoglicanos apenas da parede celular. Finalmente, foi demonstrado que ambas, AGPs e Prxs, estão co-localizadas em microdomínios da membrana, tanto ao nível da membrana citoplasmática como do tonoplasto, sugerindo uma possível interação *in vivo* importante para a sinalização.

Foi mostrado que as Prxs de *C. roseus* e Arabidopsis, bem como a peroxidase de rábano, aceitam as AGPs como substratos, e que as Prxs medeiam o *cross-linking* oxidativo das AGPs, *in vitro* e *in vivo*, sendo este putativamente relevante para a dinâmica e remodelação da parede celular, e levando à formação de novos epítopos glicosídicos das AGPs que têm sido implicados em aspetos importantes do

desenvolvimento da planta e da fisiologia da célula vegetal. Considerado como um todo, os dados apontam para um modelo onde a interação Prx-AGP pode funcionar como uma plataforma de sinalização que responde a uma molécula sinalizadora importante, o H_2O_2, onde as Prxs usam esta molécula de sinalização para o *cross-linking* das AGPs co-localizadas, que por sua vez interagem com moléculas de sinalização a jusante e que também estão presentes no microdomínio membranar.

Os estudos realizados com os pelos radiculares, onde a sinalização pelo meio de H_2O_2 tem sido implicada no *tip growth*, de facto apoiaram um papel para as Prxs e as AGPs compatível com o modelo proposto. O bloqueador de AGPs, Yariv, o inibidor de Prxs, SHAM, e os *scavengers* de ROS, KI e ascorbato, todos inibiram a diferenciação do pelo radicular. Além disso, anticorpos contra AGPs e contra Prxs, bem como a goma arábica, afetaram negativamente a taxa de crescimento do pelo radicular, enquanto que Prx e a expressão ectópica de *AtAGP9* e *AtAGP58* estimularam essa taxa.

A fim de investigar a presença de interação entre AGPs e Prx *in planta*, foram geradas fusões de genes específicos de AGPs e Prx com uma proteína fluorescente (PF), que foram utilizadas numa série de estratégias de transformações transientes e estáveis com resultados inconclusivos. No entanto, duas fusões com PF, uma com a AtAGP58 e outra com a AtPrx34, mostraram ser uns excelentes marcadores moleculares para a membrana citoplasmática e para o vacúolo, respectivamente, apresentando resultados consistentes em diferentes ensaios de expressão transiente, tanto em sistemas homólogos como heterólogos, que validam o seu uso como ferramentas úteis em ensaios de localização subcelular de proteínas.

Finalmente, o uso de promotores endógenos com as fusões com a PF serviu para determinar o perfil de expressão dos genes *AtAGP9* e *AtAGP58*, os quais foram seleccionados devido ao seu elevado nível de expressão em folhas de Arabidopsis. Ambos os genes de AGPs apresentaram diferentes perfis de expressão ao longo dos órgãos aéreos da planta e nas plântulas, com o *AtAGP58* sendo expresso principalmente nos órgãos verdes e o *AtAGP9* sendo principalmente expresso nas raízes, estiletes e estames. Estes estudos apontam para várias possíveis funções para estas duas AGPs.

No geral, os resultados obtidos no decurso deste trabalho foram proporcionando novos conhecimentos sobre uma ligação entre dois grupos importantes de proteínas da parede celular e os mecanismos pelos quais elas podem estar envolvidas na

sinalização e na morfogénese, com implicações importantes para a compreensão da fisiologia das células vegetais e do desenvolvimento da planta.

TABLE OF CONTENTS

ABBREVIATIONS

35S	Cauliflower mosaic virus promoter
AG	Arabinogalactan
AGP	Arabinogalactan protein
Ala	Alanine
Ara	Arabinose
Asn	Asparagine
At	*Arabidopsis thaliana*
AVLB	α-3',4'-anhydrovinblastine
Ca^{2+}	Calcium
cDNA	Complementary DNA
CFP	Cyan fluorescent protein
Col0	Arabidopsis ecotype Columbia 0
Cro	*Catharanthus roseus*
CTE	C-terminal extension
Cys	Cysteine
DNA	Deoxyribonucleic acid
DTT	Dithiothreitol
EDTA	Ethylenediaminetetraacetic acid
ER	Endoplasmic reticulum
Fuc	Fucose
Gal	Galactose
GalA	Galacturonic acid
GFP	Green fluorescent protein
GlcA	Glucoronic acid
Gly	Glycine
GPI	Glycosylphosphatidylinositol
h	Hour
HrPrxII	Horseradish class III peroxidase type II
H_2O_2	Hydrogen peroxide
$HO^{\bullet}$	Hydroxyl radical
$HOO^{\bullet}$	Hydroperoxide radical
Hyp	Hydroxyproline
IBCWSF	Soluble proteins ionically bound to the cell wall fraction
IEF	Isoelectric focusing electrophoresis

IPTG	Isopropyl-β-D-thiogalactopyranoside
KI	Potassium iodide
K_m	Michaelis-Menten constant
Lys	Lysine
mAb	Monoclonal antibody
min	Minute
4-MN	4-methoxy-α-naphtol
MP	Mature protein
mRNA	Messenger RNA
NADPH	Nicotinamide adenine dinucleotide phosphate
nos ter	NOS terminator from the nopaline synthase gene from *A. tumefaciens*
$O_2^{\bullet-}$	Superoxide anion
OH^-	Hydroxide anion
$^{\bullet}OH$	Hydroxyl radicals
ON	Overnight
PCD	Programmed cell death
PCR	Polymerase chain reaction
PEG	Polyethylene glycol
Pro	Proline
Prx	Class III peroxidase
Rha	Rhamnose
ROS	Reactive oxygen species
RT	Room temperature
s	Second
SDS-PAGE	SDS-Polyacrylamide gel electrophoresis
Ser	Serine
SHAM	Salicylhydroxamic acid
SP	Signal peptide
Thr	Threonine
TIA	Terpenoid indole alkaloid
v/v	volume/volume
Val	Valine
w/v	weight/volume
YFP	Yellow fluorescent protein
Xyl	Xylose

LIST OF FIGURES

I. INTRODUCTION

III. RESULTS AND DISCUSSION

III.1 Cell wall and vacuolar arabinogalactan proteins are markers of cell differentiation in the leaves of the medicinal plant *Catharanthus roseus*

III.2 Class III peroxidases and arabinogalactan proteins in *Catharanthus roseus*

III.3 Class III peroxidases and arabinogalactan proteins in *Arabidopsis thaliana*

III.4 Do AGPs and Prx cooperate to regulate tip growth in Arabidopsis root hairs?

III.5 Genetic approaches to investigate the *in vivo* interaction between Prx and AGPs

III.6 Expression profiles of *AtAGP9* and *AtAGP58* in *Arabidopsis thaliana* using FP reporter genes under the control of the endogenous promoters

III.7 Fluorescent protein fusions with an AGP and a Prx as plasma membrane and vacuole markers for live plant cell imaging

IV. FINAL DISCUSSION AND FUTURE PERSPECTIVES

LIST OF TABLES

I. INTRODUCTION

III. RESULTS AND DISCUSSION

III.2 Class III peroxidases and arabinogalactan proteins in *Catharanthus roseus*

III.3 Class III peroxidases and arabinogalactan proteins in *Arabidopsis thaliana*

I.

INTRODUCTION

I.1 The Plant Cell Wall

Plant cells encase themselves within a complex structure, called the cell wall, which provides enough rigidity to support the heavy weight of high trees as large as 100 m height, but are also flexible and elastic allowing growth during expansion and differentiation. Plant cell walls are of utmost importance in our daily lives, because they constitute the raw material in the manufacture of textiles, paper and wood. They are also the source of lignocellulosic biomass, used as a feedstock for biofuel production, as an alternative to fossil fuels.

The plant cell wall is a dynamic network highly organized which changes throughout the life of the cell. In growing cells, the “primary wall” is typically a thin, flexible layer (0.1–1 µm) that consists of complex polysaccharides and a small amount of proteins. Despite its thinness, the primary wall combines extreme tensile strength with extensibility, conferring shape to the protoplast within and allowing growth. Moreover, because the cell wall constitutes an interface between adjacent cells, it plays an important role in communication/signalling. In some cells, like water-conducting vessels, once the final cell size is reached, a “secondary cell wall” is deposited on the “primary cell wall” providing great mechanical strength and structural reinforcement (Figure I.1). These characteristics of cell walls allow plants to grow to remarkable heights, to avoid predation, to minimize water loss, and to function and reproduce successfully in diverse habitats (Cosgrove, 2005).

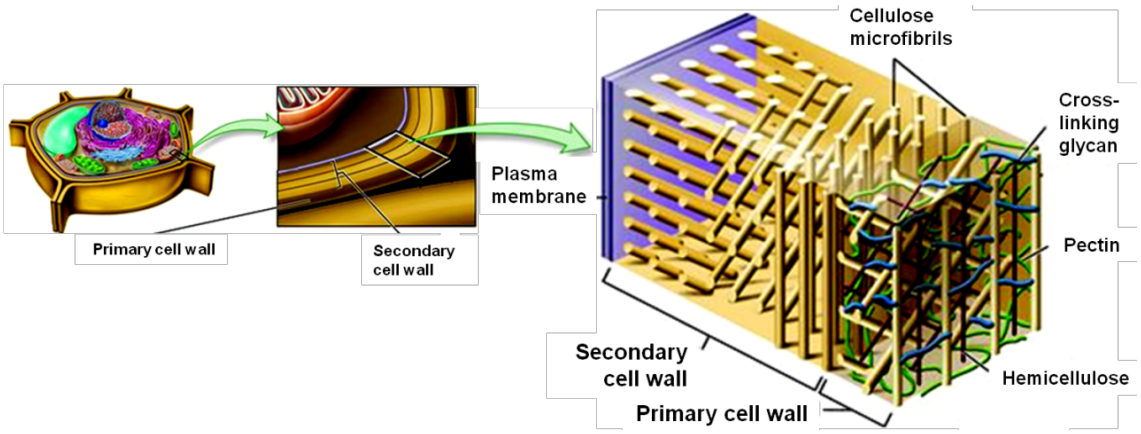

Figure I.1 – The plant cell wall. The primary cell wall is relatively thin and flexible. The secondary cell wall, which is produced only by certain plant cells, is synthesized after the primary cell wall in successive layers. Adapted from Brooker et al. (2010).

Cell wall properties vary not only among different taxa of the plant kingdom, but also within the same plant and throughout the individual plant’s life. Variations in cell wall composition have been detected among different organs, different cell types within

one tissue, and even within a single cell (Knox, 2008). Despite this diversity, all primary cell walls consist of a highly organized composite of cellulose fibers embedded in a matrix of hemicellulosic and pectic polysaccharides (~90%) (Figure I.2), along with small amounts of structural and enzymatic proteins (~10%) (Caffall and Mohnen, 2009). Cellulose is the most abundant wall polysaccharide, existing in the form of highly resistant microfibrils constituted by paracrystalline assemblies of several dozen linear chains of β(1→4) linked D-glucose units, maintained together by hydrogen bonds along their length. In the matrix, hemicelluloses are polysaccharides that cross-bind cellulose microfibrils to form a network that is strong yet plastic, while pectin polysaccharides provide fluidity to the gelatinous matrix (Cosgrove, 2005). Cellulose microfibrils are synthesized by large hexameric complexes of cellulose synthase located in the plasma membrane (Figure I.2), that move along cortical microtubules to determine the directional deposition of the microfibrils, which will ultimately determine the shape and anisotropic growth of plant cells (Bringmann et al., 2012). On the other hand, hemicelluloses and pectins are synthesized in the Golgi apparatus and are deposited to the wall surface by vesicles (Figure I.2). Cell wall structural proteins include glycine-rich proteins (GRPs), hydroxyproline-rich glycoproteins (HRGPs) that comprise extensins, arabinogalactan-proteins (AGPs) and proline-rich proteins (PRPs). Cell walls may be modified by specific enzymes, such as expansins, hydrolases, proteases, esterases, class III peroxidases (Prxs) and transglycosylases that cut, trim and cross-link the wall polymers, contributing decisively to wall assembly and remodelling during growth and development, and in stress responses.

The new primary cell wall is formed during cell division from a developing cell plate built from noncellulosic polysaccharides delivered by Golgi vesicles. It has been proposed that, within the cell plate, the rod shaped glycoproteins extensins suffer self-assembly and Prx-mediated cross-linking to originate a positively charged scaffold that templates the *in muro* deposition of pectin to originate the new wall at cytokinesis - the middle lamella (Cannon et al., 2008). Each new cell then starts the synthesis of a new primary wall through the directional deposition do cellulose microfibrils and the exocytosis of matrix polysaccharides. After achieving its final size and shape, cells needing special structural reinforcement will elaborate a secondary cell wall that may have distinct compositions. Secondary cell walls all have a cellulose network, as the primary cell wall, but they have distinct sets of hemicelluloses, or lower levels of pectins compared with primary cell walls, and they may show the deposition of specific polymers such as lignin, suberin or cutin (Buchanan et al., 2002; Knox, 2008). Noteworthy, lignins are the major component of the secondary cell walls of fibers,

xylem vessels, tracheids, and sclereids, and they are heteropolymers resulting from oxidative coupling of three *p*-hydroxycinnamyl alcohols (monolignols) in a reaction mediated by Prxs.

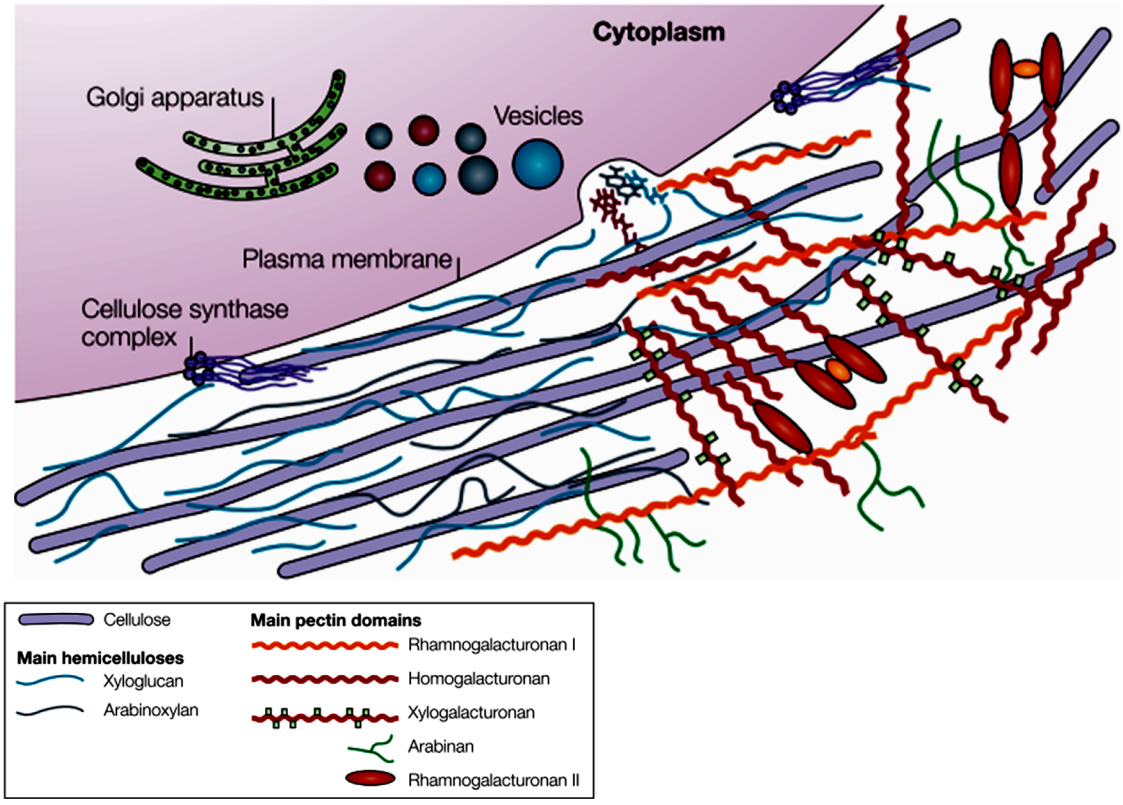

Figure I.2 – The primary cell wall polysaccharides. For clarity, the hemicelluloses-cellulose network is shown on the left part of the cell wall without pectins, which are emphasized on the right part of the figure. In most plant species the main hemicellulose is xyloglucan, while arabinoxylans and mannans (not shown) are found in lesser amounts. The main pectin polysaccharides include rhamnogalacturonan I and homogalacturonan, with smaller amounts of xylogalacturonan, arabinan, arabinogalactan I (not shown) and rhamnogalacturonan II. Pectin domains are believed to be covalently linked together and to bind to xyloglucan by covalent and non-covalent bonds. Arabinans are also able to bind to cellulose surfaces. From Cosgrove (2005).

To assemble the plant cell wall polysaccharides and glycoproteins, the plant needs an extensive biosynthetic machinery, and it has been estimated that over 2,000 gene products are involved in the dynamic construction and deconstruction of the cell wall (Keegstra, 2010). Unveiling the dynamics of the cell wall is the key to establish the molecular mechanisms by which plant cells adapt their walls to control growth and development, cell mechanics, water relations, and other properties. Although the composition and structure of plant cell walls are well known, the conformations of their interveners and their interactions to build a dynamic functional network with high tensile strength but resilient, with ability to expand and suffer extensive remodelling, are still poorly understood. Moreover, the cell wall/plasma membrane interface is capable of

perceiving morphogenesis clues and environmental challenges through signalling mechanisms that are also largely unknown. Underpinning the remodelling and communication/signalling properties of the plant cell surface are a number of different classes of proteins whose precise functions and mechanisms of action are still scarcely characterized. Among these, arabinogalactan proteins (AGPs) are particularly interesting due to their implications in many aspects of plant development and plant cell physiology and due to their potential involvement in cell signalling.

I.2 Arabinogalactan proteins

Arabinogalactan proteins (AGPs) are a diverse class of highly glycosylated proteoglycans ubiquitous at the surface of every cell from every plant, from bryophytes to angiosperms. They consist of a hydroxyproline (Hyp)-rich core-protein *O*-glycosylated with complex arabinogalactan (AG) polysaccharides and arabinose (Ara) oligosaccharides, and they usually contain no more than 1-10% of protein (Nothnagel, 1997). Most of the AGPs, but not all, possess an hydrophobic C-terminal domain for the addition of a glycosylphosphatidylinositol (GPI) anchor, binding AGPs to the plasma membrane (see section I.2.3) (Youl et al., 1998). This GPI anchor can be cleaved by the action of phospholipases leading to the release of AGPs from the plasma membrane (Svetek et al., 1999). Historically, proteoglycans were defined as AGPs if they met three criteria: the presence of arabinogalactan chains, a Hyp-rich protein backbone, and the ability to bind to β-Yariv reagent (see section I.2.4.1) (Du et al., 1996). AGPs are found in the plasma membrane, in the wall, in the apoplastic space, and in secretions. They have also been found in detergent-resistant membranes in *Arabidopsis thaliana*, suggesting their presence in membrane microdomains (Borner et al., 2005). The abundance of AGP genes and the high degree of posttranslational modifications of AGPs suggest a high investment in the synthesis of AGPs, indicating that these proteins have conserved important roles in plants. The functions of AGPs have been investigated namely using a set of monoclonal antibodies that recognize their carbohydrate epitopes (Knox, 1997), and a group of artificial phenylglycosides dyes, Yariv reagents, that specifically bind, stain and neutralize the biological function of many AGP (Yariv et al., 1967). These studies, together with recent functional and reverse genetics studies indicated that AGPs are implicated in cell proliferation and differentiation, cell expansion and adhesion, tip growth, somatic embryogenesis, plant microbe interactions, male and female gametogenesis, and programmed cell death (Majewska-Sawka and Nothnagel, 2000; Showalter, 2001; Seifert and Roberts, 2007).

However, the precise mechanisms of action of AGPs remain largely unknown, including their direct interacting co-actors.

AGPs have also important commercial applications. They are used for several industrial purposes due to their emulsifying, adhesive, and water-holding properties, with the most important AGPs in this field being the ones that constitute gum arabic. Gum arabic, an exudate collected from *Acacia senegal* trees, is one of the most commercially important gums (Renard et al., 2006). The ability of gum arabic to suspend flavourings and colourings, and to do so with low viscosity, makes it an extremely valuable additive in the food industry. Moreover, gum arabic is used in the candy industry to slow the hardening process in the manufacture of hard candy and as an adhesive in postage stamp, envelopes and cigarette papers (Showalter, 2001). AGPs have further potential applications in medicine, since they have been shown to stimulate the animal immune systems, in some cases by activation of the complement system and in other cases by enhancing the cytotoxic activity of natural killer cells (Yamada and Kiyohara, 1999; Classen et al., 2006; Nosáľová et al., 2011). AGPs have other potential pharmaceutical applications, such as fat absorbers, in the treatment of diabetes, and for the coating of medical tablets (Ozaki and Kitamura, 2005; Fang and Li, 2007; Malainine, 2007).

I.2.1 Protein structure and gene family

Molecular cloning of several confirmed and putative AGP protein backbones has greatly contributed to the understanding of their structure and diversity (Chen et al., 1994; Mau et al., 1995; Gao et al., 1999; Shpak et al., 1999; Tan et al., 2004; Shimizu et al., 2005; Estévez et al., 2006). The variety of protein backbones has led to a classification of AGPs into different subclasses based on the presence/absence of particular domains (Figure I.3). **Classical** AGPs consist of a single central hydrophilic domain rich in proline/hydroxyproline (Pro/Hyp), alanine (Ala), serine (Ser), threonine (Thr) and glycine (Gly), flanked by an N-terminal signal peptide, which is removed from the mature protein, and a C-terminal hydrophobic domain, which is replaced by a GPI anchor (Schultz et al., 2000). **AG peptides** are classical AGPs with short protein backbones of about 10–15 amino acids residues and they were first identified in wheat (Borner et al., 2003). Some AGPs contain a lysine (Lys) rich domain and are termed **Lys-rich AGPs** (Gilson et al., 2001). The fasciclin-like AGPs (**FLAs**) are chimeras and constitute a fourth distinct subclass of AGPs that contain one or two fasciclin domains, thought to be involved in protein-protein interactions (Johnson et al., 2003). Finally, there are other **chimeric AGPs** with other domains in their backbones, for instance

domains rich in asparagine (Asn) or cysteine (Cys) residues in addition to domains containing Pro/Hyp (Du et al., 1996).

The initial analysis of the Arabidopsis genome enabled the identification of 47 AGP genes (Schultz et al., 2002), but a new bioinformatics software program, based on biased amino acid composition and specific amino acid motifs, BIO OHIO, has recently identified 85 AGP genes in Arabidopsis (Showalter et al., 2010). These included 22 classical AGPs, 16 AG peptides, 3 Lys-rich AGPs, 21 FLAs, and 23 chimeric AGPs (Showalter et al., 2010). Investigation of the rice genome enabled, so far, identification of 69 AGPs, including 11 classical AGPs, 15 AG peptides, 2 Lys-rich AGPs, 27 FLAs and 14 chimeric AGPs (Ma and Zhao, 2010).

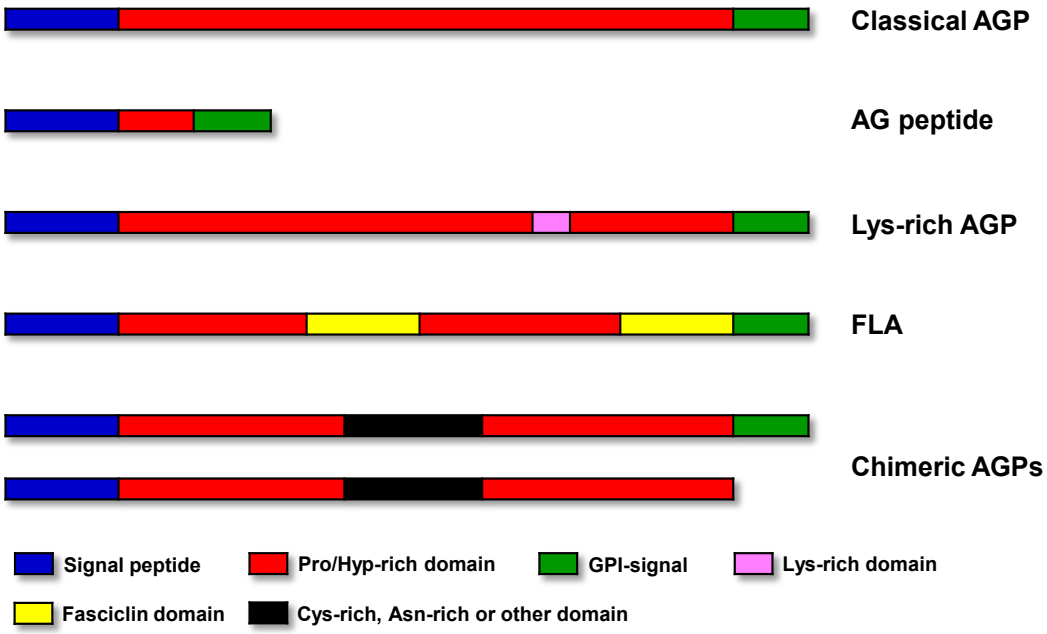

Figure I.3 – Schematic representation of the different classes of AGPs. Classical AGPs are characterized by a signal peptide domain, a Pro/Hyp-rich domain and a C-terminal GPI-signal sequence. AG peptides are classical AGPs with a short Pro/Hyp-rich domain. Lys-rich AGPs and FLAs consist of classical AGPs which may contain Lys-rich or fasciclin domains, respectively, within their sequences. Chimeric AGPs often lack the C-terminal domain for GPI anchorage.

I.2.2 Carbohydrate moiety and global molecular shape

Generally, for most glycoproteins, function is primarily associated with the polypeptide backbone rather than the carbohydrate portion. However, for AGPs the situation may be reversed because typical AGPs contain less than 10% protein, suggesting that the carbohydrate domain is the functional part of the molecule (Clarke et al., 1979; Kieliszewski and Lamport, 1994; Borner et al., 2003; Xu et al., 2008). Thus, the characterization of the structural details of the carbohydrate chains of AGPs is likely the key to understand AGP functions.

The glycosidic chains of AGPs are attached to Hyp residues in the polypeptide chain. In fact, one of the earliest post-translationally modifications suffered by AGPs is the hydroxylation of Pro residues to Hyp. The enzyme responsible for this process is the prolyl 4-hydroxylase (P4H; EC 1.14.11.2) (Gorres and Raines, 2010). *A. thaliana* encodes 13 P4Hs, but only P4H1 and P4H2 have been cloned and characterized (Hieta and Myllyharju, 2002; Tiainen et al., 2005). P4H does not hydroxylate all Pro residues: for instance, Lys-Pro is never hydroxylated, whereas Pro-Val is always hydroxylated, and Thr-Pro is hydroxylated only sometimes (Kieliszewski and Lamport, 1994; Schultz et al., 2000). Pro residues in extensins and AGPs, such as those occurring as Ser-Pro_4, Ala-Pro and Ser-Pro repeats, are almost always hydroxylated (Shpak et al., 2001). The *in vivo* location of P4H in plants remains unclear. Immunolocalization of P4H in *Phaseolus vulgaris* and *Tropaeolum majus* showed close association with the endoplasmic reticulum (ER) and Golgi apparatus in root tip cells (Wojtaszek et al., 1999), and Yuasa et al. (2005) identified a tobacco P4H as an ER- and Golgi-localizing type II membrane protein (N-terminal region at the cytosol and C-terminal region in the lumen) with a cytosolic ER export signal. The Pro hydroxylation of *O*-glycosylated cell wall proteins is of broad importance to polarized growth of root hairs, as shown by Velasquez et al. (2011). In this study, they demonstrated that inhibition of P4H activity blocked root hair growth and reduced the *O*-glycosylation of cell wall proteins. It is possible that the downstream mediator of this effect may be an AGP.

The conversion of Pro to Hyp affects protein conformation and protein-protein interactions but, above all, provides reactive hydroxyl groups for further modification including glycosylation by glycosyltransferases (GTs) (Kieliszewski and Shpak, 2001). The type of glycosylation is dependent on the contiguous or non-contiguous nature of the Hyp residues. Actually, the identification of different types of Hyp repeats in various plant glycoproteins and subsequent analysis of artificial peptides, led to the Hyp-contiguity hypothesis, which predicts that blocks of contiguous Hyp residues, such as those occurring in extensins (Ser-Pro_{3-5}), are arabinosylated with oligoarabinosides, whereas noncontiguous Hyp residues, separated by Ala or Ser residues, such as those occurring in AGPs, are exclusively substituted with AG polysaccharide chains (Kieliszewski and Lamport, 1994; Kieliszewski and Shpak, 2001). When AGP protein backbones contain both contiguous and noncontiguous Hyp residues, such as gum arabic AGP, then both AG polysaccharide chains and short Ara oligosaccharides are found (Goodrum et al., 2000). In mammals, the *O*-linked glycosylation has been extensively studied, and many GTs have been cloned and characterized (Coutinho et

al., 2003). However, in plants only a few GTs have been purified and cloned (Doblin et al., 2010). In Arabidopsis, the AGs on AGPs are synthesized by type II ER/Golgi-located GTs, including members of the CAZy family that possess (1,3)-β-GalT activity (Strasser et al., 2007; Qu et al., 2008; Egelund et al., 2010). A particular GT, peptidyl Hyp *O*-galactosyltransferase (HGT), is required to add the first Gal residue to a Hyp residue in the protein backbone and, in Arabidopsis cells, this enzyme is predominantly located in ER fractions (Oka et al., 2010). So, a model has been proposed in which the addition of the first Gal onto Hyp occurs in the ER (Oka et al., 2010). It is uncertain whether the addition of the remaining sugars that make up the AG chains occurs one residue at a time or blockwise, as is the case of *N*-linked glycans (Kelly et al., 2006), although recent results support the former mechanism (Qu et al., 2008; Oka et al., 2010). Therefore, there are likely multiple GTs involved in the assembly of AG chains, such as *O*-galactosyltransferases and arabinosyltransferases, as well as GTs for the terminal sugars. On the other hand, these enzymes have to work hierarchically to regulate the final density, length, and sequence of AG chains (Breton et al., 1998). Two members of CAZy family, AtFUT4 and AtFUT6, were recently characterized as α-(1,2)-fucosyltransferases (FUTs) that are specific for AGPs (Wu et al., 2010). These are the first enzymes to be characterized that are specific for AGP glycosylation. An AtFUT6-GFP was localized in the Golgi apparatus, supporting the evidence that much of the biosynthesis of the AG side chains occurs within this organelle (Wu et al., 2010). However, nothing is known about the determination of the supposedly specific arrangements of sugars within the *O*-glycan chains, which are thought to be the key to both the physicochemical properties and the function of AGPs.

AGPs, as their name implies, are rich in Ara and galactose (Gal). The carbohydrate domain is usually in the form of type II arabinogalactan polysaccharides (type II AGs), that are *O*-glycosidically linked to Hyp residues on the protein backbone (Figure I.4). These type II AGs vary in size from 30–150 sugar residues and consist of a (1,3)-β-D-galactan backbone having (1,6)-β-D-galactan side chains, usually terminating in Ara and other less-abundant sugars, including rhamnose (Rha), xylose (Xyl), fucose (Fuc), galacturonic acid (GalA) and glucuronic acid (GlcA) (Clarke et al., 1979; Nothnagel, 1997). Chemical analyses of some AG chains suggests that the (1,3)-β-D-galactan backbone contains repeat blocks of approximately seven Gal residues interrupted by a periodate-sensitive linkage that is postulated to be either (1,6)-β-D-Gal or (1,5)-α-L-Ara (Gaspar et al., 2001). Like in extensins, short oligoarabinosides linked *O*-glycosidically to Hyp residues are also found on some AGPs (Figure I.4) (Qi et al., 1991; Kieliszewski et al., 1992; Goodrum et al., 2000).

Classical AGPs are not *N*-glycosylated, but some chimeric AGPs, including FLAs, are thought to be *N*-glycosylated, since they contain the predicted conserved sequence Asn-X-Ser/Thr, where X can be any amino acid except Pro, and *N*-glycosylation was demonstrated for two of this AGPs (Sommer-Knudsen et al., 1996; Johnson et al., 2003). Although most AGPs share the above mentioned characteristics in their polysaccharides, considerable diversity arises through variations in the galactan structure, in the size of the glycan chains, and in the type and proportions of sugars attached to the galactan structure.

Another important aspect of AGP structure is the global molecular shape of AGPs (Figure I.4). Two models have been proposed: the "wattle blossom" model (Fincher et al., 1983) and the "twisted hairy rope" model (Qi et al., 1991). In the "wattle blossom" model, most Hyp residues are noncontiguous and are predicted to bear type II AG chains, which are folded into globular units generating an overall spheroidal shape (Figure I.4A). In the “twisted hairy rope” model, the polysaccharide chains as well as oligoarabinosides have an extended conformation and are attached in repetitive blocks along the protein backbone (Figure I.4B). The overall shape of the AGP is elongated with short projections ("hairs") along its length. One or both of these models may prove to be correct, as different AGPs may have different molecular shapes. Visualization of different AGPs using transmission electron microscopy has provided support for both models. Images of AGPs from the culture medium of carrot cells, and images of AGPs from the tobacco style seem consistent with the predictions of the "wattle blossom" model (Baldwin et al., 1993; Cheung et al., 1995). In contrast, a fraction from gum arabic appeared as a rodlike structure, consistent with the "twisted hairy rope" model (Qi et al., 1991). Mahendran et al. (2008) demonstrated that the other fraction from gum arabic was consistent with the “wattle blossom” model, whereas Sanchez et al. (2008) showed that the last fraction from gum arabic was a thin oblate ellipsoid that led to the formulation of a third model, the “disc-like” model, which was difficult to reconcile with the “wattle blossom” model. Therefore, it appears that the three fractions from gum arabic have different tertiary structures that unquestionably reflect the vast primary structural diversity of both the type II AG chains and the protein backbones of these AGPs.

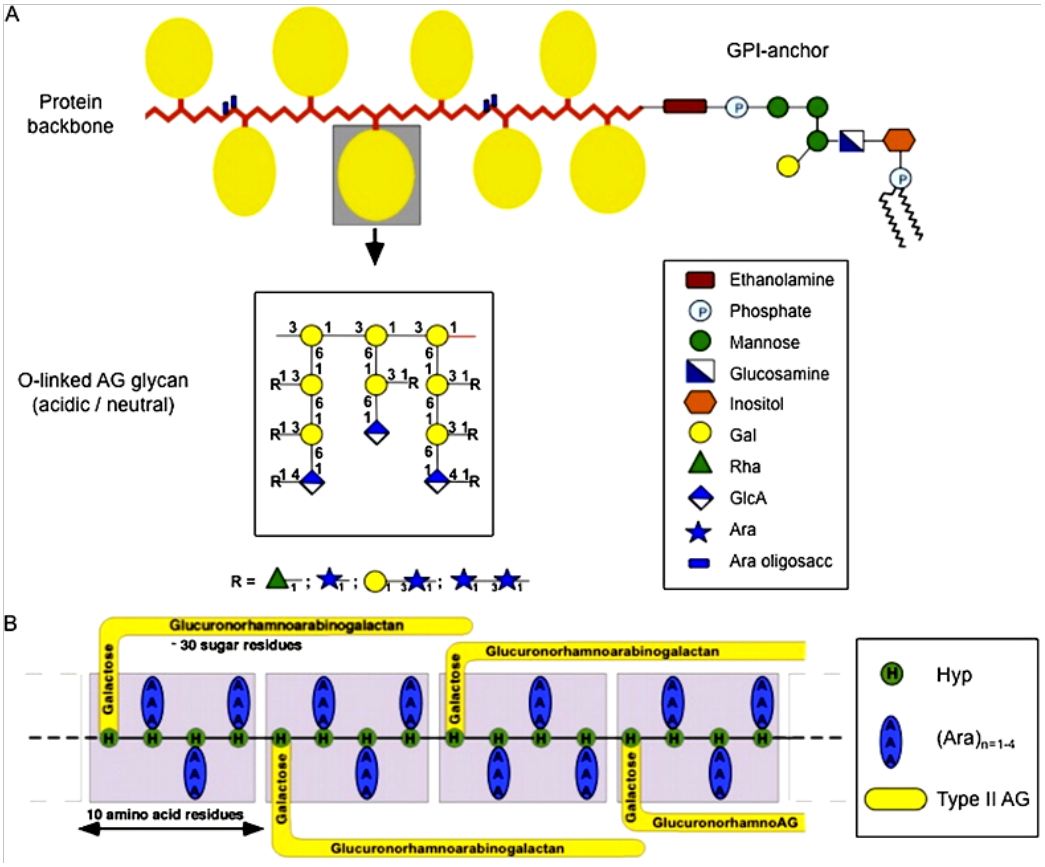

Figure I.4 – Tertiary structure of AGPs. (A) The wattle blossom model of the structure of AGPs with a GPI membrane anchor attached. The molecule as a whole is spheroidal. (B) The twisted hairy rope model of the structure of the gum arabic AGP. The glucuronorhamnoarabinogalactan has a galactan backbone with GlcA, Rha, and Ara side chains similar to that shown in the AG schematic in A. Adapted from Ellis et al. (2010).

I.2.3 Glycosylphosphatidylinositol (GPI) anchor

The glycosylphosphatidylinositol (GPI) anchor is a post-translational modification, added at the C-terminus of many eukaryotic proteins, that anchors the proteins in the outer leaflet of the cell membrane (Paulick and Bertozzi, 2008). An important advance in AGPs research came with the finding that some AGPs are synthesized with a GPI anchor (Youl et al., 1998; Oxley and Bacic, 1999; Svetek et al., 1999). A bioinformatics search of the Arabidopsis genome reveals that approximately 248 proteins contain the C-terminal hydrophobic signal sequence for the addition of a GPI anchor, and approximately 40% of these contain AG glycomodules (Borner et al., 2002; Borner et al., 2003).

The C-terminal GPI signal sequence contains small aliphatic amino acids at the ω (cleavage) and ω+2 sites, followed by a short spacer, and terminates in a stretch of small hydrophobic amino acids. An AGP GPI anchor from pear has been fully sequenced and contains the conserved minimal core oligosaccharide structure found in

all eukaryotic GPI anchors, α-D-Man-(1,2)-α-D-Man-(1,6)-α-D-Man-(1,4)-α-D-GlcN-inositol, but with a plant-specific substitution of a β-galactosyl on *O*-4 of the 6-linked mannosyl residue. This oligosaccharide is linked to the AGP protein backbone via a phosphoethanolamine, in the ER. The lipid moiety of this GPI anchor is a phosphoceramide, rather than the glycerolipid present in other kingdoms (Oxley and Bacic, 1999).

The pathway of GPI anchor synthesis established for mammals and yeast (Figure I.5) occurs in several phases, beginning with the early steps of the synthesis of the GPI moiety on the cytoplasmic surface of the ER (Orlean and Menon, 2007; Kinoshita et al., 2008). The protein backbone is inserted into the ER lumen co-translationally, and eventually the two processes converge, after the flipping of the anchor from one face of the ER to the other. A similar pathway likely exists in plants, since orthologs of the mammalian and yeast genes have been found in plants (Ellis et al., 2010). The synthesis of the GPI anchor is initiated by the enzymatic complex GPI-GlcNac transferase, with at least 6 subunits, that transfers the *N*-acetylglucosamine (GlcNAc) to phosphatidylinositol (PI). Following this, the enzyme GlcNAc-PI de-*N*-acetylase acetylates GlcNAc-PI to yield glucosamine-PI (Gn-PI). Then, the synthesis switches from the cytoplasmic to the lumenal face of the ER, where three mannose residues are added by an α-mannosyltransferase, and a phosphorylethanolamine (PE) is added by an EtNP transferase. Finally, a transamidase complex (Eisenhaber et al., 2003) removes the hydrophobic C-terminal signal sequence of the candidate protein and attaches the GPI-anchor to its *ω* site. AGPs then undergo prolyl hydroxylation and galactosylation, which begins within the ER and is completed within the Golgi network. At last, AGPs are transported in vesicles to the plasma membrane, where they are either temporarily anchored to the plasma membrane, before being released by phospholipases (Griffith and Ryan, 1999; Svetek et al., 1999), or endocytosed (Schultz et al., 1998).

Deficiencies in GPI biosynthesis lead to drastic effects in animals and yeasts by blocking cell growth, cell division, or morphogenesis (Leidich et al., 1995; Rosti, 2000). In Arabidopsis, mutations in *SETH1* and *SETH2*, which encode homologs of two conserved proteins involved in the first step of the GPI biosynthetic pathway, resulted in reduced pollen germination and tube growth, suggesting that GPI anchoring is required during both phases of post-pollination development (Lalanne et al., 2004). Likewise, the GPI anchor of AGPs has been implicated in their functions and mechanisms of action (see section I.2.6).

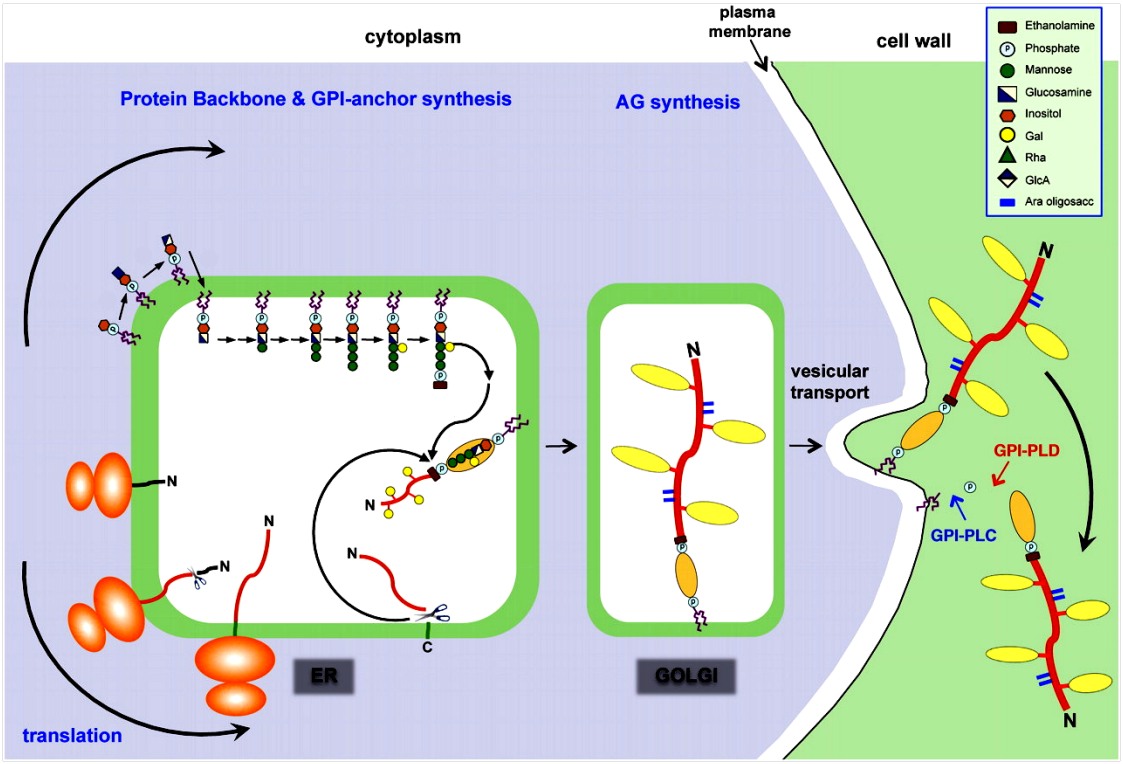

Figure I.5 – Proposed mechanism for the synthesis and addition of a GPI anchor to an AGP. The addition of a GPI anchor to an AGP likely occurs in several phases, beginning with the synthesis of the GPI moiety on the cytoplasmic surface of the ER. The protein backbone is inserted into the ER co-translationally, and eventually the two processes converge. The GPI anchor synthesis pathway shown is a composite of that established for mammals and yeast. From Ellis et al. (2010).

I.2.4 Probes for AGPs

Over the years, the functions and interactions of AGPs have been studied using biochemical and immunohistochemical techniques, with the most commonly approaches including the use of the probes called Yariv phenylglycosides and of monoclonal antibodies raised against several AGP carbohydrate epitopes.

I.2.4.1 Yariv reagents

Yariv phenylglycosides are a group of chemical compounds that were initially developed as carbohydrate antigens for the production of an anti-glycoside antibody (Yariv et al., 1962). It then turned out that these Yariv reagents specifically interact with AGPs, forming a brown-red precipitate (Yariv et al., 1967; Jermyn et al., 1975). This interaction has been used as a criterion in the definition of AGPs, although some AGPs do not react with Yariv reagents. Nevertheless, the structure involved in the interaction with Yariv reagents is presumed to be conserved in many AGPs. The interaction of Yariv reagents with AGPs depends on the glycosyl residues of the Yariv reagent. In

particular, β-glucosyl Yariv (β-Glc-Yariv) and β-galactosyl Yariv (β-Gal-Yariv) bind to AGPs, whereas α-forms and β-mannosyl do not bind to AGPs, and, for that reason, are often used as experimental controls (Jermyn et al., 1975; Larkin, 1977, 1978; Nothnagel and Lyon, 1986). Therefore, the β-Yarivs are useful tools for staining, detection, quantification and purification of AGPs. As the treatment with β-Yarivs causes the perturbation of AGPs in plants and cell cultures, disrupting their normal distribution and *in vivo* function, β-Yarivs are reliable reagents to be used to investigate AGPs functional roles. Until now, the target structures on AGPs required for the interaction with β-Yarivs have not been identified. However, Kitazawa et al. (2013) demonstrated, by sequentially trimming the AG moieties of AGPs, that β-Gal-Yariv binds to the β-(1,3)-galactan main chains of radish root AGP.

I.2.4.2 Monoclonal Antibodies

Monoclonal antibodies (mAbs) developed against cell wall polymers have emerged as an important tool for the study of plant cell wall structure and function (Table I.1) (Knox, 2008). AGPs are antigenic and are capable of generating several mAbs, which are used to track and/or perturb the AGPs in order to identify their roles. For many mAbs, the knowledge of their epitope specificity is still limited, because the immunogen used was a mixture of AGPs (like gums), membrane vesicles or even whole protoplasts (Knox et al., 1989; Pennell et al., 1991; Smallwood et al., 1996). Epitope identification has been successful when oligosaccharides with known structures have been available for use as competitive inhibitors in binding assays (Knox et al., 1991; Yates et al., 1996). For instance, β-GlcA-(1,3)-α-GalA-(1,2)-α-Rha from a partial acid hydrolysate of gum karaya was found to be a very effective inhibitor of the binding of MAC207, JIM4 and JIM13 (Yates et al., 1996). Furthermore, while this oligosaccharide inhibited the binding of all these three antibodies, each of these antibodies exhibited different labelling patterns in plant tissues (Knox et al., 1991). These results seemed to indicate that a portion of the binding site of each antibody recognized a portion of the oligosaccharide, while another portion of the binding site recognized some distinctive adjacent residues in AGPs. More recently, Pattathil et al. (2010) generated 130 new mAbs that bind to diverse epitopes present on a broad spectrum of plant cell wall glycans, including AGPs glycans (not included in Table I.1).

The world-wide collection of cell wall glycan-directed mAbs is now satisfactorily large and diverse to constitute a comprehensive resource that will prove invaluable for detailed studies of the structure, dynamics, function, and biosynthesis of plant cell walls.

Table I.1 – List of antibodies directed against AGP carbohydrate epitopes.

mAb	Antigen	Epitope	References
JIM4	AGP from carrot	β-GlcA-(1,3)-α-GalA-(1,2)-α-Rha	Yates et al. (1996)
JIM8	AG from sugar beet	Unknown	Pennell et al. (1991)
JIM13	AGP from carrot	β-GlcA-(1,3)-α-GalA-(1,2)-α-Rha	Knox et al. (1991); Yates et al. (1996)
JIM14	AGP from carrot	Unknown	Knox et al. (1991); Yates et al. (1996)
JIM15	AGP from carrot	Unknown	Knox et al. (1991); Yates et al. (1996)
JIM16	AGP from carrot	Unknown	Knox et al. (1991); Yates et al. (1996)
LM2	AGP from rice	β-linked GlcA	Smallwood et al. (1996); Yates et al. (1996)
LM6	Sugar beet arabinan	α-(1,5)-arabinans	Willats et al. (1998); Verhertbruggen et al. (2009)
LM14	AGP from carrot	Arabinose- and galactose-enriched chains	Moller et al. (2008)
MAC204	AGP from pea	Unknown	Bradley et al. (1988); VandenBosch et al. (1989)
MAC207	AGP from pea	β-GlcA-(1,3)-α-GalA-(1,2)-α-Rha	Bradley et al. (1988); Yates et al. (1996)
MAC265	AGP from pea	Unknown	VandenBosch et al. (1989)
PCBC3	AGP from *N. alata*	Unknown	Ferguson et al. (1999)
CCRC-M7	Rhamnogalacturonan I	Arabinosylated β-(1,6)-galactan	Steffan et al. (1995)
PN 16-4B4	AG from *N. glutinosa*	Unknown	Norman et al. (1986)
MH4-3E5	AG from *N. tabacum*	Unknown	Hahn et al. (1987)

AG, Arabinogalactan; AGP, arabinogalactan protein; GalA, galacturonic acid; GlcA, glucuronic acid; Rha, rhamnose; mAb, monoclonal antibody

I.2.5 Roles of AGPs in biological processes

AGPs have been implicated in many developmental and growth processes at the whole plant, cellular and molecular level, that are discussed in the following sections.

I.2.5.1 Cell division and expansion

The functions of AGPs in growth mechanisms have been investigated mainly using mAbs and Yariv reagents to bind, aggregate and inactivate AGPs. The effect on growth is related to inhibition of cell division or inhibition of cell expansion.

The treatment of 'Paul's Scarlet rose (Rosa sp.) cell suspensions with β-Yariv caused a reversible inhibition of cell growth in a concentration-dependent manner, without affecting cell viability. Moreover, cell sizes in β-Yariv-treated cultures were similar to the control, indicating that β-Yariv was involved in suppression of cell division (Serpe and Nothnagel, 1994). Langan and Nothnagel (1997) also demonstrated that the proliferation of two rose cell suspensions, Rosa 57 and Rosa 93, was strongly inhibited by β-Yariv, but while the effect was readily reversible with Rosa 57, the viability of Rosa 93 was severely compromised. They further demonstrated that Rosa 57 and Rosa 93 differ in both the numbers and abundances of AGPs isolated from the cell walls and the culture medium, which could explain the different behaviour of these two cell suspensions. The addition of the monoclonal antibodies JIM13 and JIM8 to the medium of sugar beet protoplasts inhibited proliferation but did not affect short-term

viability (Butowt et al., 1999). More recently, Shibaya and Sugawara (2009) observed that β-Yariv inhibited cell division of protoplast-regenerated cells of the liverwort *Marchantia polymorpha* L., due to interference with cell plate formation and not with mitosis. Also indicating a role for AGPs in cell division, the Arabidopsis *agp19* mutant has fewer abaxial epidermal cells in rosette leaves, indicative of a decrease in cell division. However, this mutant also shows shorter hypocotyl cells, smaller rosette epidermal cells and more regularly shaped spongy mesophyll cells leading Yang et al. (2007) to conclude that the Lys-rich AGP19 is involved both in cell division and cell expansion in Arabidopsis plants.

In fact, many studies have implicated AGPs in cell elongation. Arabidopsis seedlings treated with β-Yariv showed reduced root growth, due to the accumulation of β-Yariv in root tissues, which caused a reduction in cell elongation during the post-proliferation phase of elongation at the root apex. In addition, β-Yariv treatment of carrot suspension-cultured cells, that had been induced to elongate rather than proliferate, inhibited cell elongation (Willats and Knox, 1996). Similarly, Ding and Zhu (1997) demonstrated that β-Yariv-treated Arabidopsis seedlings exhibit reduced root growth and inappropriate cell expansion at the root epidermis, indicating a role of cell surface AGPs in root growth and control of root epidermal cell expansion. Likewise, treatment with β-Yariv inhibited cell elongation of cultured tobacco cells, interfering with cellulose deposition in the cell wall, inhibited the GA- or IAA-promoted elongation of cucumber seedling hypocotyls, and also inhibited apical cell extension in *Physcomitrella patens* (Vissenberg et al., 2001; Park et al., 2003; Lee et al., 2005). Finally, genetic approaches have already implicated specific AGPs with cell elongation. Under salt stress, the root tips of an Arabidopsis salt-hypersensitive mutant, *sos5* (*salt overly sensitive5*), swell and root growth is arrested (Shi et al., 2003). The *SOS5* gene was shown to encode a FLA, belonging to a group of AGPs considered as cell surface adhesion proteins. This was the first described AGP mutant with a clearly defined phenotype. The root-swelling phenotype in *sos5* mutant is caused by abnormal cell expansion at the root tip. This mutant also demonstrated a defective cell-to-cell adhesion. In *P. patens* the knock-out of AGP1 resulted in a ~25% reduction in both colony growth and cell length (Lee et al., 2005).

I.2.5.2 Tip growth

In higher plants, most cells expand by diffuse expansion, whereas root hairs and pollen tubes expand by tip growth, which is a rapid elongation that occurs exclusively at the tip and requires synthesis of new cell wall material, a tip-focused calcium gradient,

control of actin cytoskeleton dynamics, and formation and targeting of secretory vesicles (Cole and Fowler, 2006). AGPs have been consistently implicated in tip growth of both root hairs and pollen tubes.

In the case of pollen tubes, immunolocalization shows that tip cell wall in tobacco, lily, and Arabidopsis all contain specific AGPs (Li et al., 1995; Jauh and Lord, 1996; Mollet et al., 2002; Pereira et al., 2006; Dardelle et al., 2010). Moreover, it is known that pollen tube tip growth is inhibited by β-Yariv treatment and also by genetic interference with GPI-anchor biosynthesis, leading to ectopic callose deposition and pectin alteration (Jauh and Lord, 1996; Roy et al., 1999; Mollet et al., 2002; Lalanne et al., 2004; Qin et al., 2007). The Yariv effect was specially characterized for lily pollen tubes, whose growth was inhibited by Yariv with the production of a bulbous morphology at the pollen tube tip (Jauh and Lord, 1996; Roy et al., 1999). Contrary to the observed for other inhibitors, where cessation of pollen tube growth was correlated with cessation of exocytosis and dissipation of the intracellular calcium gradient, Yariv did no inhibit exocytosis in the lily pollen tube tips, and calcium influx was also not affected (Roy et al., 1999).

On the other hand, investigation of the root epidermal cell bulging mutant, *reb1-1*, defective in root AGPs, showed that trichoblasts were unable to form root hairs and became bulged instead, implicating AGPs in root hair tip growth (Ding and Zhu, 1997; Andème-Onzighi et al., 2002). Additional investigation showed that the AGP mAbs JIM14 and LM2 labelled trichoblasts in the wild type but not in the mutant, further implicating AGPs in tip growth (Andème-Onzighi et al., 2002). Moreover, the bulging phenotype of root epidermal cells was also mimicked by treating wild type roots with the Yariv reagent (Ding and Zhu, 1997). In other studies, Šamaj et al. (1999) showed that an AGP epitope containing glucuronic acid is localized specifically at the surface of maize root hairs. The strongest expression of the epitope was observed during root hair initiation, at the bulge initiation sites within the cell wall and within the tip of elongating root hairs, while it was reduced after cessation of root hair growth. Moreover, differential transcriptomic screenings between a hairless mutant and wild type plants, one in Arabidopsis and the other in barley, both revealed that several AGP genes are highly over-represented in the root hair transcriptome (Jones et al., 2006; Kwasniewski et al., 2010).

I.2.5.3 Programmed cell death

Programmed cell death (PCD) can be triggered in *in vitro* cultures by several biotic and abiotic stimuli. Gao and Showalter (1999) showed that the treatment of Arabidopsis cell

suspension cultures with the β-Yariv reagent induced killing of cell through PCD as evidenced by the presence of internucleosomal DNA fragmentation and structural changes characteristic of PCD, including cytoplasmic shrinkage and condensation, chromatin condensation and nuclear membrane blebbing. These authors suggested that β-Yariv disrupts plasma membrane-cell wall connections and thereby activates a signalling cascade resulting in PCD. Similarly, Chaves et al. (2002) demonstrated that β-Yariv completely inhibited cell growth and induced PCD in tobacco BY-2 suspension cultured cells. These findings implicate AGPs in PCD in plants, suggesting that they may be part of the PCD signalling transduction pathway triggered by external biotic and abiotic stimuli. However, the mechanisms by which AGP perturbation could be induced by those signals and then trigger PCD are not known.

AGPs have also been implicated in developmental PCD, since it was observed by immunocytochemical detection that AGP expression is highly regulated during xylem development in Arabidopsis and maize, with certain AGPs seeming to mark cells destined for PCD (Dolan et al., 1995; Schindler et al., 1995).

I.2.5.4 Cell differentiation

The patterns of AGP epitopes change dramatically during differentiation and morphogenesis suggesting they are implicated in these processes, although the functional meaning of these changes remains unclear. Many researchers hypothesized that AGPs are involved in these processes as markers of cell identity or even as regulatory molecules. Such specific patterns have been specially characterized during embryogenesis and reproductive development and are described in the following two subsections. In what concerns vegetative cells, specific AGP patterns have also been observed, namely in the root. Depending on the species, different AGP epitopes recognized by mAbs were specifically localized at the root epidermal cells, at the root cap and border-like cells, at the pericycle or the apical meristem of roots (Nguema-Ona et al., 2013). In *A. thaliana,* JIM13 is expressed in the single initial of the central metaxylem vessel that lies immediately above the four central cells of the quiescent centre of the root apical meristem. Later, it spreads to the entire ring of eight endodermal cell files and to those pericycle cell files next to the xylem pole (Dolan et al., 1995). The role of AGPs during tracheary elements differentiation in *Zinnia elegans* has been particularly investigated, with an AGP called xylogen seemingly operating as a diffusible signal, since it was able to transdifferentiate *Z. elegans* mesophyll cells into tracheary elements in a strictly time limited way (Stacey et al., 1995; Motose et al., 2001; Motose et al., 2001). Xylogen expression preceded differentiation of tracheary

elements *in vitro* and was expressed in cambium and immature xylem. In the xylem, xylogen had a polar localization in the cell walls of differentiating tracheary elements. In Arabidopsis, double knockouts lacking the two genes that encode xylogen proteins showed defects in vascular development, indicating that xylogen might act as a mediator of inductive cell-cell communication in vascular development (Motose et al., 2004). In radiate pine cultures, β-Yariv reduced the overall tracheid differentiation rate in a concentration dependent manner, ultimately resulting in cell death, providing further evidence that AGPs play an important role in tracheid differentiation, and thus may be an important biological target for improving wood quality (Putoczki et al., 2007).

I.2.5.5 Somatic and zygotic embryogenesis

AGPs have been implicated in the development of both zygotic and somatic embryos. Certain AGP epitopes are differentially expressed during zygotic embryogenesis. The AGP JIM8 epitope is expressed in the two-cell embryo in oilseed rape, but subsequently JIM8 expression is lost from the embryo proper and continues to be expressed in the suspensor (Pennell et al., 1991). In *A. thaliana*, the AGP JIM13 epitope presented a highly specific labelling pattern that changed during embryo development, and β-Yariv treatment decreased harshly the frequency of embryo germination and differentiation (Hu et al., 2006; Zhong et al., 2011). β-Yariv reagent also suppressed the first asymmetric division in tobacco zygotes, demonstrating a requirement for AGPs in establishing the polarity of the zygote (Qin and Zhao, 2006). More recently, Yu and Zhao (2012) demonstrated that β-Yariv increased remarkably the frequency of aberrant division in cultured tobacco zygotes and proembryos, and reduced greatly the cell plate specific localization of AGPs, concluding that AGPs not only contribute to the formation of the new cell plate but also play a role in zygotic division and proembryo pattern establishment.

The AGP epitope JIM4 was shown to be an early structural marker of somatic embryogenesis in carrot and maize cultures, since it was abundant in the extracellular surface matrix network (ECMSN) typical of embryogenic cells, and was totally absent in non-embryogenic cells (Kreuger and Holst, 1996; Šamaj et al., 1999). Moreover, JIM8 labelled a subpopulation of embryogenic cells in carrot cell cultures that produces signal molecules considered essential for progression to embryo formation (McCabe et al., 1997). More recently and for the first time in gymnosperms, it was shown that a specific AGP epitope was secreted and deposited into the ECMSN of cells showing high embryogenesis and regeneration capacity in cell cultures of hybrid fir (Šamaj et al., 2008). In *Trifolium nigrescens,* strong detection of the LM2 epitope was observed in

the meristematic cells from which somatic embryos were produced, with no signal being detected in mature embryos (Pilarska et al., 2013).

Convincing evidence for a role of AGPs in somatic embryogenesis was based on studies showing that the addition of exogenous AGPs to the culture media either induces or inhibits somatic embryogenesis depending of the type of AGP added. For instance, the addition of carrot-seed AGPs to a non-embryogenic carrot cell culture (Kreuger and Holst, 1993) can stimulate the formation of embryos, showing that specific AGPs are essential in somatic embryogenesis and are able to direct development of cells. AGPs isolated with the monoclonal antibody ZUM18 were also shown to increase the percentage of embryogenic cells in carrot suspension cultures, while the AGPs isolated with ZUM15 antibody decreased the percentage of embryogenic cells. The effect of ZUM15 was similar to AGPs isolated from non-embryogenic suspension cultures. These results demonstrated that the ratio of different AGPs in carrot suspension cultures will determine the embryogenic potential of those cells (Kreuger and Holst, 1995).

More recently, Poon et al. (2012) found that a chimeric AGP purified from embryogenic cotton calli was capable to promote somatic embryogenesis when incorporated into tissue culture medium. However, they demonstrated that it was the non-AGP domain that was directly responsible for the somatic embryogenesis-promoting activity, and suggested that a possible role for the AGP domain might involve the passage of this chimera through the cell wall to the cell surface.

I.2.5.6 Reproductive development

Studies using AGP monoclonal antibodies demonstrate that the patterns of AGP localization are highly dynamic during the sporophyte-to-gametophyte transition and gametogenesis, suggesting that AGPs might represent molecular markers of reproductive development (Pennell et al., 1989; Pennell and Roberts, 1990; Pennell et al., 1991; Coimbra et al., 2007; Nguema-Ona et al., 2012). For instance, JIM13 labelled the pollen tube of lily at the tip and the pollen tube of tobacco uniformly or in a ring-like deposition while, in Arabidopsis, MAC207 labelled the tip of the pollen tube and LM2 labelled a ring-like region near the tip (Mollet et al., 2002; Pereira et al., 2006; Qin et al., 2007). These results suggest a role of AGPs in pollen germination and suggest that the carbohydrate epitopes of AGPs are species and/or cell type specific or that the cell wall organization is different between species possibly altering the accessibility of the epitopes. In fact, the Yariv reagent clearly inhibited pollen tube growth in lily and *Annona cherimola,* and its removal from the medium allowed regeneration of new tip

growth in both species (Jauh and Lord, 1996; Roy et al., 1999). Moreover, the secretion of AGPs at the site of emergence of the new tube was observed for both species, implying an important role for AGPs in polarized growth (Mollet et al., 2002). On the other hand, Mollet et al. (2002) reported that the Yariv reagent had no effect on pollen tube growth of *Lycopersicon pimpinellifolium*, *Aquilegia eximia*, and *N. tabacum.*

At the AGP gene level, it was shown that Arabidopsis *AGP6* and *AGP11* are expressed specifically in pollen tubes and pollen grains (Pereira et al., 2006). Additionally, double knockout and knockdown lines showed aberrant pollen development, including pollen grain collapse and retraction of the plasma membrane from pollen walls (Coimbra et al., 2009). In another study, double knockdowns of the same genes presented reduced fertility, at least partly as a result of inhibition of pollen tube growth and hampered pollen release (Levitin et al., 2008). More recently, Coimbra et al. (2010) observed that the *agp6 agp11* double null mutant also shows a precocious germination of pollen inside the anthers. Furthermore, microarray and yeast two-hybrid studies suggested the involvement of AGP6 and AGP11 in multiple signalling pathways, in particular those involved in developmental processes such as endocytosis-mediated plasma membrane remodelling during Arabidopsis pollen development (Costa et al., 2013). In rice, many AGP-encoding genes were highly expressed during sexual reproduction, especially during pollen development and two classical AGP-encoding genes, *OsAGP7* and *OsAGP10*, were highly expressed in pollen, similarly to *AtAGP6* and *AtAGP11* (Ma and Zhao, 2010). Furthermore, Anand and Tyagi (2010) isolated an AGP cDNA from rice preferentially expressed in the inflorescence and analysis of its promoter showed it was a late pollen-expressing gene that was also active during germination and pollen-tube growth (Anand and Tyagi, 2010).

Several studies have indicated that stylar AGPs play also important roles in pollen-tube growth, guidance, nutrition and pollen-tube rejection. In *Nicotiana alata*, an AGP was exclusively expressed in the stigma and a 120-kDa protein with both extensin and AGP properties was abundant in stylar transmitting tissue, with its mRNA accumulating specifically in the style (Lind et al., 1994; Du et al., 1996; Schultz et al., 1997). Furthermore, this 120-kDa protein was taken up into the cytosol of *in vivo* elongating pollen tubes, clearly indicating a role in pollen-tube growth (Lind et al., 1996). Another protein from stylar transmitting tissue recognized by the Yariv reagent, pistil extensin-like protein III (PELP III) from *N. tabacum,* is directly and completely translocated from the transmitting tissue into the elongating pollen tubes callose walls (Graaf et al., 2000; Bosch et al., 2001). But the more clear evidence implicating AGPs

in pollen-tube growth and guidance comes from the studies with the AGP called transmitting tissue-specific protein (TTS) from tobacco. TTS is present in the stylar transmitting tissue and was shown to stimulate pollen tube growth *in vivo* and *in vitro* and to attract pollen tubes grown in a semi-*in vivo* system (Cheung et al., 1995). Moreover, within the transmitting tissue, TTS displayed a gradient of increasing glycosylation from the stigmatic end to the ovarian end of the style, coincident with the direction of pollen tube growth (Wu et al., 1995). These results strongly suggest that the TTS protein-bound sugar gradient may contribute to guiding pollen tubes from the stigma to the ovary. TTS-proteins were also found to incorporate in the pollen tube wall in a de-glycosylated form, suggesting that TTS proteins may contribute to pollen tube nutrition via sugar donation, unlike PELPIII described above, which retained its high molecular weight and high solubility after translocation to the pollen tube wall (Wu et al., 1995; de Graaf et al., 2003). Interestingly, TTS, the 120-kDa protein and PELPIII are all able to bind *in vitro* to S-RNase, suggesting that AGPs may be involved indirectly in pollen rejection during self-incompatibility, by forming a complex with the S-RNase (Cruz-Garcia et al., 2005). Related with the results described above for Solanaceae, it was observed that, in Arabidopsis, specific AGP epitopes labelled specifically the integument micropylar cells, outlining the pollen tube pathway into its final target and suggesting a guidance role for AGPs (Coimbra et al., 2007).

AGPs have also been implicated in female gametogenesis. The JIM8 AGP epitope in oilseed rape specifically labelled the nucellar epidermis, synergid cells, and the egg cell (Pennell et al., 1991). In Arabidopsis, specific labelling of the first gametophytic cells in the pistil, of the secretory cells of the embryo sac and of the synergid cells was also observed for several AGP mAbs (Coimbra et al., 2007). At the gene level, Acosta-Garcia and Vielle-Calzada (2004) demonstrated that AtAGP18 is essential for the initiation of female gametogenesis, since the silenced lines are sterile and exhibit normally differentiated ovules with functional megaspores arrested before the first haploid mitotic division. In a follow-up study, Demesa-Arévalo and Vielle-Calzada (2013) showed that, before meiosis, AtAGP18 was uniformly localized in the ovule primordium but was absent from the megaspore mother cell, and that, following meiosis, it localized to the functional megaspore and the neighbouring sporophytic nucellar cells. Moreover, AtAGP18 overexpression lines exhibited reduced fertility, with developing ovules containing one to three supernumerary cells resulting from meiosis. With these findings, the authors conclude that AtAGP18 is actively involved in selecting the surviving megaspore.

I.2.5.7 Plant microbe interactions

A number of studies concerning plant microbe interactions implicate AGPs in the colonization process, which involves adhesion and cell division. In *Medicago truncatula,* a putative AGP gene was shown to be significantly induced following colonization by a mycorrhizal fungus (van Buuren et al., 1999). This putative AGP was expressed specifically in cortical cells containing arbuscules, suggesting that it might be involved in mediating the interaction between the plant cortical cell and fungal hypha during arbuscule development. More recently, Schultz and Harrison (2008) proposed that *M. truncatula* AGPs could physically interact with the mycorrhizal fungus *Glomus intraradices* AGP-like proteins in the apoplastic compartment hosting the arbuscules.

The phenotype of the Arabidopsis *rat1* mutant, previously characterized as resistant to *Agrobacterium tumefaciens* root transformation, correlates with a mutation in a Lys-rich AGP, AtAGP17 (Gaspar et al., 2004). Furthermore, transformation of *rat1* plants with *AGP17* can restore the wild-type phenotype. The authors suggest that AtAGP17 deficiency may either affect a physical association between the root cell surface and bacteria at the initial stage of infection, or interfere with a signalling cascade in which AtAGP17 acts as an elicitor-like signalling molecule.

Border cells and border-like cells are released from the root tip, either individually or as a group of attached cells, and are thought to play a major role in plant microbe interactions within the rhizosphere and provide protection to the root (Hawes et al., 2000; Driouich et al., 2013). Vicré et al. (2005) observed that root border-like cells of Arabidopsis were highly enriched in AGPs and that, when seedlings were grown in the presence of β-Yariv, the colonization of the root tip cells by *Rhizobium* was altered, implying an involvement of these AGPs in the process. Analysis of the effects of pea root exudates on biofilm formation by *Rhizobium leguminosarum* showed that a putative AGP is able to induce polar attachment of the bacteria *in vitro* (Xie et al., 2012). Treatments of the glycoprotein with proteases or glycosidases suppress the polar attachment, suggesting that both the carbohydrate moiety and the protein backbone are required for function. Xie et al. (2012) proposed that AGPs could be important for attachment of rhizobia to roots of both legumes and non-legumes by acting in a complementary manner to the previously described legume-specific polar attachment mediated via specific lectins and glucomannan (Laus et al., 2006). Curiously, both rhizobia and agrobacteria attach in a polar manner to the plant root surface (Matthysse and Kijne, 1998), meaning that maybe there is a common AGP mediated mechanism acting during rhizobia colonization and agrobacteria transformation (also involving AGPs - previous paragraph).

Little data is available on the role of AGPs at the root surface in a pathogenesis context. Xie et al. (2011) showed that the AGP CCRC-M7 epitope was enhanced in a wax gourd cultivar resistant to infection by *Fusarium oxysporum*, indicating that this epitope is likely to contribute to resistance. In contrast, other AGP epitopes (recognized by LM2 and JIM16) were equivalently expressed in both cultivars, resistant and susceptible, before and after infection. In pea roots, AGPs secreted by border cells are shown to be capable of attracting zoospores of the pathogenic oomycete *Aphanomyces euteiches* and then preventing their germination (Cannesan et al., 2012). In theory, specific root-secreted enzymes involved in degradation and remodelling of cell wall glycoproteins and polysaccharides could release specific oligosaccharides from AGPs in the rhizosphere, which could act as signals of infection (Wen et al., 2007). In fact, this was already demonstrated by Cervone et al. (1989) for pectin-derived oligosaccharides and by Fry et al. (1993) for xyloglucan-derived oligosaccharides.

Interactions between roots and microbes are crucial for plant health and AGPs clearly play a significant role in such interactions.

I.2.5.8 Interaction with plant hormones

AGPs might interact with plant-growth regulator signalling and thereby influence development and growth. The involvement of AGPs in the phytohormone function was firstly demonstrated by Suzuki et al. (2002). In this study, β-Yariv was shown to suppress gibberelic acid-promoted induction of α-amylase in barley aleurone protoplasts, without affecting the ABA-regulated dehydrin promoter or cell viability. This was interpreted as AGPs possibly acting as signalling molecules in the gibberellin signal-transduction pathway, anywhere between signal perception and α-amylase transcription. In cucumber hypocotyls, the transcription level of *CsAGP1*, increased in response not only to GA but also to IAA (Park et al., 2003). Moreover, β-Yariv inhibited the hormone-promoted elongation of cucumber seedling hypocotyls. The authors hypothesized that since GA and auxin are the major stimuli controlling microtubule alignment, AGPs may also play a role in stabilizing the microtubules or in cellulose synthesis after the microtubule alignment (Park et al., 2003).

Loss of function of AtAGP30 results in a suppression of the ABA-induced delay in germination and altered expression of some ABA-regulated genes, indicating that AtAGP30 regulates the timing of germination by modulating ABA perception (Van Hengel and Roberts, 2003). Also in Arabidopsis, the transcript levels of the AGPs *FLA1/2/8* were all downregulated in the presence of ABA (Johnson et al., 2003).

Furthermore, expression of *AtFLA2* was decreased about two-fold after ABA treatment, suggesting that AtFLAs are involved in ABA signal transduction pathways (Xin et al., 2005). In rice, *OsAGP1* and *OsAGP15* were significantly up-regulated by drought and salt stresses, and by ABA, indicating that they may be stress-inducible genes and also participate in the ABA signalling pathway (Ma and Zhao, 2010).

Overexpression of tomato *LeAGP-1* leads to a reduction of apical dominance, suppression of flower maturation and fruit production, and delayed senescence, suggesting an altered balance of the auxin versus cytokinin signal transduction pathway (Sun et al., 2004). In fact, the observed regulation of *LeAGP-1* transcript levels by auxins and cytokinins corroborates this hypothesis. Moreover, the smaller seeds produced by LeAGP-1-overexpressing plants may result from limited production and deposition of storage proteins and nutrient reserves, indicating that LeAGP-1 might act as a negative mediator of ABA signalling. Arabidopsis AtAGP18 overexpressors have a bushy phenotype similar to the tomato LeAGP-1 overexpressors, indicating that AtAGP18 is also likely associated with the cytokinin signal transduction pathway (Zhang et al., 2011).

All these studies point out possible modes of action of AGPs in the interaction with phytohormones. On the one hand, AGPs might have a signalling function acting downstream of growth regulators, namely to stimulate cell division. On the other hand, it was suggested that AGPs might modulate the sensitivity of receptors by either interacting with and modifying receptor properties, or by serving as a co-receptor to present the growth regulator to a low-affinity receptor in a more concentrated form.

I.2.5.9 Cell Wall-Plasma Membrane-Cytoskeleton Continuum

Accumulating evidence has shown that there is a cell wall–plasma membrane–cytoskeleton continuum in plant cells involving interactors such as wall associated kinases (WAKs), AGPs, cellulose synthases, formins, plant specific class VIII myosin, phospholipase D, callose synthase and the recently discovered cellulose synthases interacting (CSI1) protein (Kohorn, 2000; Baluška et al., 2003; Bringmann et al., 2012). Several lines of evidence point to a role of AGPs in mediating this cell wall-plasma membrane-cytoskeleton continuum. Many AGPs are GPI anchored to the plasma membrane and, at the same time, their glycosidic moiety may interact with cell wall components, therefore providing cell wall / plasma membrane attachment. Importantly, AGPs were shown to bind to cell wall pectins, and they might interact also with WAKs, because they seem to localize to the same domains at the plasma membrane of BY-2 protoplasts (Baldwin et al., 1993; Nothnagel, 1997; Scott Gens et al., 2000). Moreover,

adhesion functions may be provided specifically by the AGP multigenic sub-family FLA, similarly to animals, insects, algae, and bacteria, in which fasciclin-like domains are confirmedly involved in cell adhesion (Kawamoto et al., 1998). Shi et al. (2003) observed that the root cells of the Arabidopsis FLA *sos5* mutant (*salt overly sensitive5,* described in section I.2.5.1) have thinner cell walls, aberrant cell shapes, and inhibited expansion, resembling not only WAK mutants, but also mutants of the actin cytoskeleton or mutants having aberrant F-actin distribution (Baluška et al., 2001; Dong et al., 2001; Lally et al., 2001). The involvement of AGPs in the interaction between the cell wall and plasma membrane is demonstrated by data obtained with GFP-tagged LeAGP-1 in tobacco BY2 cells (Sardar et al., 2006). In plasmolysed cells, this AGP was located in Hechtian strands connecting the cell wall and plasma membrane. Treatment with microtubule and F-actin inhibitors resulted in re-localization of LeAGP-1 on Hechtian strands and indicate roles for cytoskeleton in AGP organization at the cell surface and in Hechtian strands. Moreover, β-Yariv treatment resulted in depolymerization/disorganization of microtubules and thicker actin filaments, indicating a reciprocal role for AGPs in microtubule organization and actin polymerization. Similar results were obtained with Arabidopsis roots, where β-Yariv and AGP antibodies, but not pectin or xyloglucan antibodies, disorganized cortical microtubules independently of calcium influx (Nguema-Ona et al., 2007). These results clearly indicate a role of the GPI-anchored AGPs in mediating a plasma membrane-cytoskeleton connection important for its organization.

I.2.6 Mechanisms of action

Despite all the studies described above that implicate AGPs in a plethora of functions in the plant, the precise mechanisms of action of AGPs remain elusive. This diversity of functions and the heterogeneous nature of AGPs suggest the existence of more than one mode of action. It is seemingly expected that the protein backbone, the GPI anchor and the AG component all play roles in AGPs functions.

Concerning cell expansion, Vissenberg et al. (2001) and Park et al. (2003) suggested that the observed effect of β-Yariv in elongation could be due to the involvement of AGPs in the oriented deposition of cellulose microfibrils by possibly acting on the linkage between cortical microtubules and the cellulose microfibrils. In fact, as refered above, plasma membrane AGPs have been shown to indeed interact with microtubules and actin, with blocking of AGPs leading to cytoskeleton disorganization and consequent loss of directional cell expansion (Sardar et al., 2006;

Nguema-Ona et al., 2007). Ding and Zhu (1997) proposed other possible models of action for the role of AGPs in growth. For instance, cell wall AGPs could be involved in wall biosynthesis or assembly, with the loss or interference with the function of these AGPs by Yariv reagents leading to disruption/weakening of the cell wall structure, which is necessary for controlled cell expansion. Alternatively, the Yariv reagent could activate a signal-transduction cascade through cell surface AGPs and their interacting cellular components, and indirectly lead to growth inhibition and other responses.

The signalling capacity of AGPs could be associated with the cleavage of the GPI lipid anchor by phospholipases (Schultz et al., 1998). This process has the potential to generate both intra- and extracellular messengers, by the way of the lipid anchor or the proteoglycan components, respectively. On one hand, the remaining part of the GPI anchor can be recycled with production of secondary messengers, such as phosphatidylinositol, phosphoglycan, and ceramide (Munnik et al., 1998). On the other hand, cleaved AGPs, with their highly complex and variable glycan chains, are ideal candidates for diffusible signalling molecules. In fact, AGPs released from the surface of cells with embryogenic potential have the ability to stimulate non-embryogenic cells to undergo embryogenesis (McCabe et al., 1997) and the soluble form of xylogen contains sufficient information for transdifferentiation of *Z. elegans* mesophyll cells into tracheary elements (Motose et al., 2001). Furthermore, AGPs are a potential source of small signalling molecules, in the form of active oligosaccharides putatively released from AGPs by the action of endoglycanases. Likewise, the treatment of AGPs from immature carrot seed with endochitinases resulted in the activation of the somatic embryogenesis capacity of those AGPs (van Hengel et al., 2001). Another possible mode of signalling involves GPI-anchored proteins in signal transduction pathways as has been shown in animals (Peles et al., 1997; Kleeff et al., 1998; Resta et al., 1998). These interactions can be with proteins in the same cell or in neighbouring cells. Because the signal is transduced via interaction with other transmembrane proteins, the plant AGPs would interact with molecules having both intra- and extracellular domains, such as wall-associated kinases (WAKs), somatic embryogenesis receptor kinase (SERK), and Clavata1 (Lease et al., 1998). Nevertheless, at present the interaction of AGPs with WAKs was shown only indirectly, based on their co-localization in immunofluorescence studies (Scott Gens et al., 2000). It is also plausible that the AGPs core protein could serve as a signalling molecule. The core proteins of the classical AGPs are covered by carbohydrate, and would require at least some degree of deglycosylation before the core protein would be exposed enough for further processing or signalling. However, the non-classical AGPs possess proteolytic non-

AGP protein domains that could act in signalling or other functions. Therefore, under certain environmental conditions and in the presence of enzymes, such as endochitinases, endoglycanases, phospholipases, etc, AGPs could putatively produce a variety of molecules that could be involved in many processes.

In plant cells, numerous plasma membrane proteins, including AGPs and other GPI-anchored proteins, are associated with detergent-resistant membrane microdomains (Borner et al., 2005; Jones et al., 2006), that in animal cells are called lipid rafts and act as centres of signalling cascades (Simons and Toomre, 2000). In animal lipid rafts there are some proteins that interact with the microtubules dynamics or with the actin cytosqueleton (Wickström et al., 2003; Lallemand-Breitenbach et al., 2004). In plants, it was demonstrated an interaction between cell surface AGPs and the cytosqueleton (Sardar et al., 2006; Nguema-Ona et al., 2007). Thus, these studies indicate that, in plants, detergent-resistant membrane microdomains/lipid rafts may potentially perceive signals via GPI-anchored AGPs and transduce them downstream to the cytosqueleton, thereby controlling its organization and, indirectly, the directionally restricted mobility of cellulose synthase complexes, which depends on the orientation of cortical microtubules (Paredez et al., 2006; Bringmann et al., 2012). Therefore, AGPs may in fact influence cell wall assembly and cell expansion, determined to great extent by the orientation of the deposition of cellulose microfibrils.

Sardar and Showalter (2007) suggest a model that predicts a few possible modes of interaction between cell surface AGPs and the cytoskeleton, including direct interaction via a transmembrane protein, such as WAKs, cellulose synthases, endo-1-4-β-D-glucanases, Pro-rich extensin-like receptor kinases, formins, phospholipase D, and lectin receptor kinases, or indirect interaction via detergent-resistant membrane microdomains. In fact, a recent study in Arabidopsis showed that detergent-resistant membranes microdomains are enriched in GPI-anchored proteins, including GPI-anchored AGPs (Borner et al., 2005). Likewise, Sardar et al. (2006) also suggest that detergent-resistant membrane microdomains may potentially perceive signals via a GPI-anchored AGP acting as a cell-surface receptor and transduce them downstream to the cytosol or cytoskeleton via various signalling molecules. On the other hand, it was suggested that AGPs might modulate the sensitivity of receptors by either interacting with and modifying receptor properties, or by serving as a co-receptor to present the growth regulator to a low-affinity receptor in a more concentrated form. This is exactly what has been proposed by Zhang et al. (2011) for the functioning of AtAGP18 in Arabidopsis, that it acts as a co-receptor either by binding to signalling molecules and directly interacting with transmembrane proteins in the membrane

microdomain (Figure I.6A) or by binding to signalling molecules and bringing them to transmembrane receptor proteins (Figure I.6B).

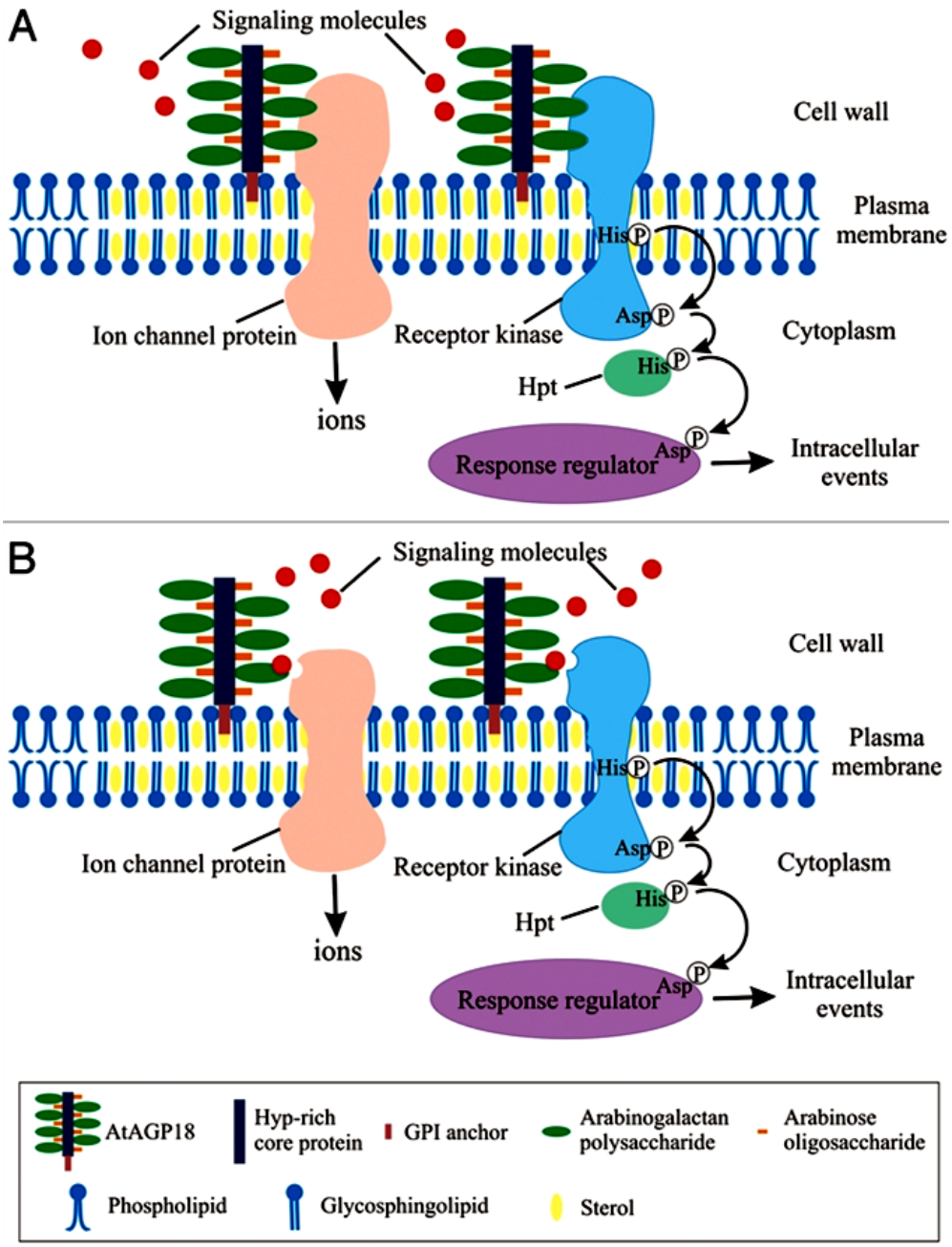

Figure I.6 – Possible models for AGP functioning in cellular signalling to control plant growth and development. In this model, lipid rafts are enriched in glycosphingolipids, sterols, transmembrane proteins (such as receptors, receptor kinases and ion channel proteins) and GPI-anchored proteins including AGPs. (A) AGPs act as a co-receptor by binding to signalling molecules and directly interacting with transmembrane proteins in the lipid rafts. (B) AGPs act as a co-receptor by binding to signalling molecules and bringing the signalling molecules to transmembrane proteins in the lipid rafts. Upon activation by the extracellular signals, the transmembrane proteins initiate signalling and lead to various intracellular events (e.g. phosphorylation similar to the two-component signalling system, influx of calcium ions). Hpt, histidine phosphotransfer protein. From Zhang et al. (2011).

The binding of AGPs to β-Yariv reagent suggests that analogous phenyl-β-glycosides structures might be present in the cell wall polysaccharides and AGPs might be able to bind to these wall components to exert their function. Flavonol glycosides are one possible class of plant phenyl-β-glycosides analogs, because they are capable of inhibiting the interaction between Yariv reagent and AGPs (Jermyn, 1978). Moreover, association of AGPs with cell wall components, such as pectins, has sometimes been observed (Baldwin et al., 1993; Nothnagel, 1997; Tan et al., 2013). A function of AGPs as "plasticizers" has indeed been postulated based on the relative distribution of different AGP fractions in salt-adapted suspension cells (Lamport and Kieliszewski, 2005). It was proposed that the porosity of the pectic network *in muro* increases when AGPs are upregulated because they decrease pectin cross-linking. Thus, AGPs should enhance cell expansion through direct interaction with pectins. The Yariv reagent can abolish this plasticizing capacity of AGPs by converting them into a multimeric AGP–Yariv network (Lamport and Kieliszewski, 2005). Other possible mechanical role of AGPs in the cell wall might be rigidification by oxidative cross-linking (Kjellbom et al., 1997), similarly to what was reported before for PRPs (Bradley et al., 1992) and HRGPs (Brisson et al., 1994) as a mechanism of cell defence. The AGP oxidative cross-linking mediated by cell wall class III peroxidases (Prxs) (Kjellbom et al., 1997) may indeed have a relevant signalling role, since Sottomayor et al. (2008) have observed that Prx and AGPs both localize in membrane microdomains in *Catharanthus roseus* leaf cells. This suggests the hypothesis investigated in this thesis, that the H_2O_2 produced by the plasma membrane NADPH oxidase under stress conditions could be used by Prxs to cross-link co-located AGPs, changing their interaction with other co-located transmembrane signalling proteins to launch a cytosolic response.

I.3 Class III Peroxidases

Class III peroxidases (Prxs) (EC 1.11.1.7), also known as classical or guaiacol peroxidases, were first described in 1810, by Louis Antoine Planche, who reported that a tincture of guaiacum developed a strong blue colour after a piece of fresh horseradish root was soaked in it (historical review by Paul (1986)). Since then, the extraordinary stability of these enzymes, allied to their striking reactivity towards a variety of natural and artificial substrates, resulting very often in the formation of coloured products, made of Prx one of the best characterized redox enzymatic systems, and enabled their commercial application as labels in all sorts of detection assays.

Peroxidases in general are heme-containing enzymes that catalyze the single one-electron oxidation of small molecules at the expense of H_2O_2, and they are classified in two unrelated superfamilies, i) animal peroxidases and ii) peroxidases present in bacteria, fungi and plants, the latter being subdivided in three classes, I, II and III, based on structural divergence (Welinder, 1992). Prx are typical of plants and are targeted to the secretory pathway by an N-terminal signal peptide. Although they are defined as enzymes that catalyze the oxidation of small molecules at the expense of H_2O_2, they have a complex catalytic cycle that may also lead to the production of reactive oxygen species (section I.3.3). As detailed in the following sections, Prxs are secretory proteins localized in the cell wall or in the vacuole, they show a remarkable polymorphism, they are capable of recognizing a broad range of substrates and are implicated in many physiological processes vital for plant life from "seed to senescence" (Sottomayor and Ros Barceló, 2004; Passardi et al., 2005; De Gara et al., 2010).

I.3.1 Chemical structure

Prxs have a molecular weight between 32 kDa and 45 kDa and are composed of a single polypeptide chain of approximately 300 amino acid residues, presenting variable degrees of glycosylation. Sites of *N*-glycosylation occur within surface turns or loop regions, with the glycans being presented to the exterior of the molecule (Veitch, 2004). Most Prxs have several *N*-linked glycans, and the total carbohydrate content can be as high as 25%. In horseradish Prx isoenzyme C a branched heptasaccharide accounts for 75 to 80% of the glycans, but several other minor glycans have also been characterised. These glycans invariably contain two terminal GlcNAc and several mannose residues (Veitch, 2004). Since glycans are large, those close to substrate-binding residues are likely to affect substrate access and reaction dynamics (Nielsen et al., 2001; Cosio and Dunand, 2009). Nine potential *N*-glycosylation sites can be recognized in the primary sequence of horseradish peroxidase isoenzyme C and six in the primary sequence of the *Catharanthus roseus* Prx1 (CroPrx1) (Veitch, 2004; Costa et al., 2008). The external glycosylation of Prxs is one of the main factors determining their kinetic stability (Tams and Welinder, 1998).

All Prxs show four conserved disulphide bridges between cysteine residues and a buried salt bridge. The salt bridge may play an important role in the proper attachment of the N- and C-terminal domains during protein folding (Welinder et al., 2002). Prxs also contain as prosthetic group an iron (III) protoporphyrin IX (usually referred to as the heme group) and two calcium atoms. Both are essential for the structural and

functional integrity of the enzyme. The heme group is situated between the so-called 'distal' (above the heme) and 'proximal' (below the heme) domains. During catalysis, H_2O_2 binds to the distal side of the heme plane (Veitch, 2004). The two calcium binding sites are located at positions distal and proximal to the heme plane and are linked to the heme-binding region by a network of hydrogen bonds. Loss of calcium results in a decrease of both enzyme activity and thermal stability and in subtle changes in the heme environment that can be detected spectroscopically (Veitch, 2004). The three dimensional structure of the Prx enzyme is predominantly α-helical, with ten helices, and a small region of β-sheet.

The Prx core protein initially comprises a N-terminal signal peptide responsible for targeting to the ER and, in some isoenzymes, there is also a heterogeneous C-terminal extension that may target the protein to the vacuole (see section I.3.5) (Welinder et al., 2002; Costa et al., 2008).

I.3.2 Multigenic family and isoenzyme diversity

Prxs show a remarkable polymorphism, with the presence of a high number of isoenzymes in a single plant (Ros Barceló and Muñoz, 2000). This diversity is determined, to a great extent, at the gene level, since it has been shown that Prxs constitute large and varied multigene families in land plants, with 73 genes identified in the *Arabidopsis* genome and 138 in the rice genome (Tognolli et al., 2002; Passardi et al., 2004). This diversification may be related with land colonization by plants, either by allowing formation of a rigid vasculature resulting from the peroxidase mediated synthesis of lignin, or by contributing to the adaptation to a more oxygenated environment (Duroux and Welinder, 2003; Passardi et al., 2004). Similar examples of large gene families in plants have been reported where evolution has multiplied by extensive duplications of genes, such as plant cytochrome P450 proteins and ABC transporters (Paquette et al., 2000; Sánchez-Fernández et al., 2001). In Prxs, this large gene diversity is reflected in the high degree of polymorphism at the protein level, which has been observed by isoelectric focusing, with the detection of many anionic and cationic forms. In Arabidopsis, the Prx pI ranges from 4.5 to 9 with a higher proportion of isoforms around 8.5 (Valério et al., 2004). Furthermore, differences in the glycosylation patterns can further add on the diversity of Prx isoenzymes observed (Mathé et al., 2010).

The coding sequence of the majority of the Prx genes is interrupted by three introns at perfectly conserved positions, suggesting a common ancestral gene with a

classical pattern of four exons and three introns (Østergaard et al., 2000; Welinder et al., 2002). On the other hand, Prx protein sequences also contain significantly variable domains, but the highly conserved protein structure, key amino acid residues and molecular size of Prxs are never compromised (Cosio and Dunand, 2009). The conservation of protein structure is accompanied by a redundancy in substrate acceptance by Prxs *in vitro*. However, it has been proposed that differences in the glycosylation patterns and surface charges among Prxs could potentially be involved in the determination of some level of substrate specificity *in planta* (Douroupi et al., 2005). The shared structural features of Prxs may indicate similar mechanisms but perhaps not similar specific functions. Indeed, Kumari et al. (2008) demonstrated that despite high protein sequence similarity, *Prx62* and *Prx69* from Arabidopsis exhibited a different transcript profile in response to aluminium stress. In contrast, *AtPrx62* and *AtPrx49* had comparable temporal expression profiles (Kumari et al., 2008), even though their protein sequences are evolutionarily distant (Tognolli et al., 2002; Welinder et al., 2002). Even genes resulting from recent tandem duplication such as *AtPrx33* and *AtPrx34* are differentially expressed (Passardi et al., 2006; Figueiredo, 2011). These data support the idea that given the substrate overlapping profile of different Prxs (at least based on *in vitro* studies), it might be the targeting of a given Prx to a certain spatial/temporal window and not substrate specificity that determine the role of individual peroxidase isoforms *in planta* (Cosio and Dunand, 2009). Therefore, the classification based only on sequence similarity is probably not a good indicator for functional assignment among Prxs.

I.3.3 The catalytic cycle

Prxs have a complex catalytic cycle, with the heme prosthetic group assuming different oxidation states and interacting with substrates and H_2O_2 in several possible ways. In general, the reaction catalyzed by Prxs involves the single electron oxidation of several substrates at the expense of H_2O_2 and can be represented as follows, where RH represents the reducing substrate and $R^{\bullet}$ represents the oxidized radical product:

$$H_2O_2 + 2RH \longrightarrow 2H_2O + 2R^{\bullet}$$

The $R^{\bullet}$ products may experience structural rearrangements, oxidize other molecules or react among themselves or with other molecules to produce coupled products (Ros Barceló, 2000). Prxs have a strong activity and accept a wide range of

low molecular weight compounds as reducing substrates, including aromatic phenols, phenolic acids, indoles, amines and sulfonates.

The regular catalytic cycle of Prxs, also called peroxidative cycle, can be expressed by the following set of equations 1-3, where E represents Prx, and the oxidation state of the heme iron atom and the status of the porphyrin (P) are indicated in parenthesis (Veitch, 2004). First, H_2O_2 oxidizes the native ferric form (Fe^{III} resting state) of Prx in a two electron oxidation, and originates the high oxidation state intermediate Compound I, comprising an Fe^{IV} oxyferryl centre and a porphyrin-based cation radical:

$$\underset{\text{Native state Ferric form}}{E\ (Fe^{III}, P)} + H_2O_2 \xrightarrow{k_1} \underset{\text{Compound I}}{E\ (Fe^{IV} = O, P^{\bullet +})} + H_2O \qquad (1)$$

Then, two subsequent one-electron reduction steps of the enzyme occur. Compound I accepts one electron and one proton from a reducing substrate (RH) yielding the intermediate Compound II (Fe^{IV} oxyferryl heme), while RH is oxidized to the radical product $R^{\bullet}$. Both compound I and compound II are powerful oxidants:

$$\underset{\text{Compound I}}{E\ (Fe^{IV} = O, P^{\bullet +})} + RH \xrightarrow{k_2} \underset{\text{Compound II}}{E\ (Fe^{IV} = O, P)} + R^{\bullet} \qquad (2)$$

The reaction cycle is completed by the second one-electron reduction step, in which another molecule of the reducing substrate is oxidized to the corresponding radical enabling the reduction of compound II to restore the ferric native form of Prx:

$$\underset{\text{Compound II}}{E\ (Fe^{IV} = O, P)} + RH \xrightarrow{k_3} \underset{\text{Native state Ferric form}}{E\ (Fe^{III}, P)} + R^{\bullet} + H_2O \qquad (3)$$

The rate constants k_1, k_2 and k_3 refer to the rate of compound I formation, rate of compound I reduction and rate of compound II reduction, respectively. Usually k_3 is the lowest constant, meaning that reduction of compound II is the rate-limiting step in peroxidase catalyzed reactions (Barceló et al., 2003).

Prx may still assume alternative redox states in particular conditions (Ros Barceló, 2000; Veitch, 2004). Thus, the reaction of the native ferric Prx with $O_2^{\bullet -}$ or excess H_2O_2 will produce compound III (equation 4), where the heme assumes the interchangeable states Fe^{II}-dioxygen / Fe^{III}-superoxide (Ros Barceló, 2000; Liszkay et al., 2003). Compound III can also be produced by reaction of Prx directly with a

reductant leading to production of Fe^{II} Prx, which will react with O_2 to yield Compound III as seen in equations 5 and 6 (Ros Barceló, 2000):

$$\underset{\text{Native state Ferric form}}{E(Fe^{III}, P)} + O_2^{\bullet -} \longrightarrow \underbrace{E(Fe^{III} - O_2^{\bullet -}, P) \longleftrightarrow E(Fe^{II} - O_2, P)}_{\text{Compound III}} \quad (4)$$

$$\underset{\text{Native state Ferric form}}{E(Fe^{III}, P)} + R^{\bullet} \longrightarrow \underset{\text{Ferrous form}}{E(Fe^{II}, P)} + R^{+} \quad (5)$$

$$\underset{\text{Ferrous form}}{E(Fe^{II}, P)} + O_2 \longrightarrow \underbrace{E(Fe^{III} - O_2^{\bullet -}, P) \longleftrightarrow E(Fe^{II} - O_2, P)}_{\text{Compound III}} \quad (6)$$

Compound III is a slow electron acceptor and is considered a reversible inactive form of Prx which can either undergo irreversible inactivation to verdohemoprotein (P-670) in the presence of specific compounds (Kawano, 2003), or a slow spontaneous decay back to the native form implicating a transient generation of $O_2^{\bullet -}$ and H_2O_2 (Ros Barceló, 2000). However, Bolwell and Wojtaszek (1997) have proposed that compound III, at neutral to basic pH and in the presence of a suitable reductant will efficiently generate H_2O_2:

$$\underset{\text{Compound III}}{E(Fe^{II} - O_2, P)} + RH_2 \longrightarrow \underset{\text{Native state Ferric form}}{E(Fe^{III}, P)} + H_2O_2 \quad (7)$$

Thiols such as cysteine and glutathione were reported to give high activities as reductants for the generation of H_2O_2 from compound III through equation 7, with NAD(P)H and ascorbate sustaining lower activities (Bolwell and Wojtaszek, 1997).

Finally, it has been proposed that Prx can also undergo a hydroxylic cycle responsible for the generation of hydroxyl radicals ($^{\bullet}OH$) capable of mediating cell wall loosening during extension growth (Chen and Schopfer, 1999; Liszkay et al., 2003; Passardi et al., 2004). The hydroxylic cycle starts by the reduction of the Prx native enzyme to compound III (equations 4-6), which will react with H_2O_2 and reduce it to $^{\bullet}OH$ and the hydroxide anion (OH^-), reverting back to the native form:

$$E(Fe^{II} - O_2, P) + H_2O_2 \longrightarrow E(Fe^{III}, P) + {}^{\bullet}OH + OH^- + O_2 \quad (8)$$

Compound III — Native state Ferric form

Thus, in the presence of a source of $O_2^{\bullet -}$ and availability of H_2O_2, Prxs may produce hydroxyl radicals.

As a consequence of the complex catalytic cycles that Prx can undergo, the enzyme has been implicated in opposite actions concerning ROS: in the scavenging of H_2O_2 through the peroxidative cycle, and in the generation of ROS ($O_2^{\bullet -}/H_2O_2$) through compound III and the hydroxylic cycle. There is some debate whether generation of ROS by peroxidase may actually happen under physiological conditions (Bolwell and Wojtaszek, 1997; Ros Barceló, 2000; Mika et al., 2004), and much of the evidence pointing to that functions is circumstantial. For a better understanding of the balance of ROS during the complex catalytic cycles of Prx, the equations described above are assembled together in Figure I.7.

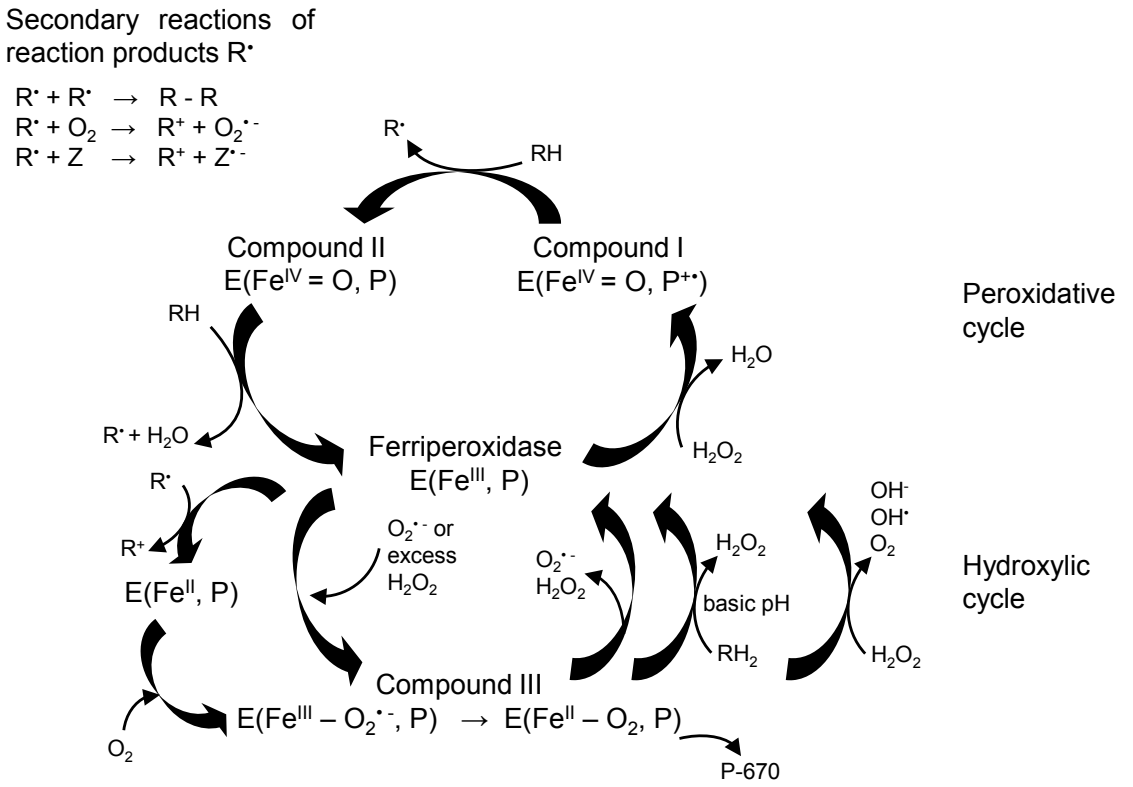

Figure I.7 – Catalytic cycles of Prx. E, Prx. P, porphyrin. RH, reducing substrate. R•, radical product. Z, secondary substrates. Compound I, F^{IV} oxyferryl porphyrin cation. Compound II, F^{IV} oxyferryl heme. E ($Fe^{III} - O_2^{\bullet -}$, P), Fe^{III} – superoxide. E ($Fe^{II} - O_2$, P), Fe^{II} – dioxygen. E (Fe^{II}, P), ferrous form. P-670, verdohemoprotein.

Looking at the general picture shown in Figure I.7, it is clear that most of the possible cycles, although involving steps generating $O_2^{\bullet -}$, H_2O_2, or $^{\bullet}OH$, also include

initiating steps involving ROS consumption, with the overall balance of ROS being null. The only possibility leading to a new generation of ROS is when compound III is formed through reduction of the native Prx to the ferrous form of Prx by an appropriate reductant (equation 5) followed by reaction with O_2 (equation 6), and compound III is then involved in reactions which restore the native Prx with production of ROS (equations 7 and 8). Whether this cycle may indeed happen *in vivo* is still a matter of debate (Ros Barceló, 2000; Almagro et al., 2009), and its experimental *in vitro* occurrence has been reported only for a few Prx isoenzymes (Bolwell and Wojtaszek, 1997; Passardi et al., 2004).

Another interesting characteristic of Prx reactions is that the radical products ($R^{\bullet}$) formed during the peroxidative cycle (equations 2 and 3) may undergo redox mediation reactions resulting on the reduction of secondary substrates (Ros Barceló, 2000):

$$R^{\bullet} + Z \longrightarrow R^{+} + Z^{\bullet -} \quad (9)$$

For particular substrates such as NADH or related reduced compounds, the Prx produced NADH radical initiates a non-enzymatic oxidative cycle by reacting with O_2 (Z in equation 9) to produce $O_2^{\bullet -}$. This radical may then dismutate to H_2O_2 which can be used by Prx to continue to oxidize the initial substrate (Chen and Schopfer, 1999).

I.3.4 Substrate profile

Prxs are versatile enzymes that are capable of accepting a broad range of natural compounds as substrates, such as phenolic compounds, aromatic amines, indoles, alkaloids and sulfonates. The numerous different substrates accepted by Prx *in vitro* has led to their implication in a large number of physiological processes. Prxs react equally towards a variety of artificial substrates leading to the formation of coloured/luminescent/dense products that are the bases for the use of Prx in many labelling procedures commercially valuable.

Prxs generally react to compounds with hydroxyls group(s) attached to an aromatic ring, especially phenolic rings (Hiraga et al., 2001). When the oxidized substrate is a phenolic compound, the reaction leads to the generation of phenoxy radicals that couple spontaneously to form complex phenolic polymers, for instance hydroxycinnamyl alcohol species are polymerized to lignin and hydroxycinnamic acids are incorporated into suberin (Hiraga et al., 2001). Prxs also promote the oxidative phenolic coupling of the feruloyl residues of cell wall polysaccharides, such as

hemicelluloses, and of the tyrosine residues of cell wall hydroxyproline-rich glycoproteins, such as extensins, resulting in the formation of more complex and large molecules in the cell wall (Fry, 2004). These macromolecules strengthen the cell wall, thereby restricting cell expansion and pathogen invasion, and confer structural strength to the plant body.

The oxidative decarboxylation of auxin mediated by Prx is thought to be one of the auxin inactivation processes, although auxin is equally inactivated via conjugation with amino acids or sugars and via conversion to oxindole-3-acetic acid by oxidation without Prx (Hiraga et al., 2001).

Prxs are further involved in the oxidation of flavonoids, particularly ortho-diphenols, to their corresponding semiquinones and quinones. These are highly reactive species that react spontaneously and non-enzymatically with phenols, amino acids or proteins, yielding a complex mixture of brown components. Browning reactions are observed during programmed developmental events such as seed desiccation and plant senescence. Flavonoid oxidation also plays a role in defending the plant against various biotic and abiotic stresses (Pourcel et al., 2007).

Alkaloids have also been described as Prxs substrates. For instance, a leaf basic Prx isoenzyme from *C. roseus* has been suggested to be responsible for the oxidative coupling of the plant terpenoid indole alkaloids catharanthine and vindoline into an unstable dimeric iminium cation that is easily reduced to α-3',4'-anhydrovinblastine (AVLB), a direct biosynthetic intermediate of the anticancer drugs vinblastine and vincristine (Costa et al., 2008). Furthermore, Prxs have also been implicated in the conversion of the alkaloid ajmalicine into serpentine in *C. roseus* (Sottomayor et al., 2004). Other proposed substrates of Prx are vacuolar capsaicinoids (acid amides) in *Capsicum annuum* and catechins in *Camellia sinensis* (Díaz et al., 2004; Sang et al., 2004).

Interestingly, ascorbate has also been proposed to be an indirect substrate of Prx, since it was shown that phenol radicals resulting from Prx mediated oxidation may oxidise ascorbate, regenerating the Prx phenolic reductant substrate, and establishing a cycle that will be quite efficient in the scavenging of H_2O_2 (Figure I.8) (Yamasaki et al., 1997; Takahama, 2004; Ferreres et al., 2011).

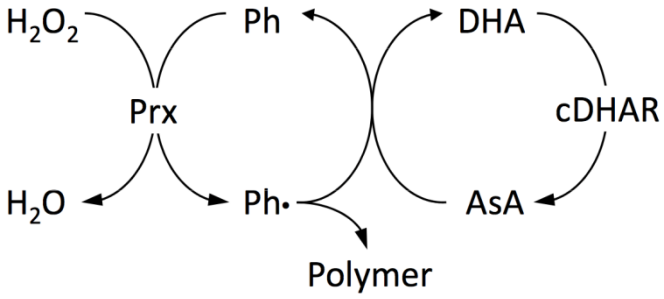

Figure I.8 – Oxidation of ascorbic acid by phenolic radicals originated from Prx mediated oxidation, generating a self-sustained Prx substrate regeneration cycle. A phenolic compound (Ph) is oxidized into a phenolic radical (Ph•) by Prx, which in turn oxidizes ascorbic acid (AsA) to monodehydroascorbate (MDHA) returning to the original form. MDHA will interact spontaneously to produce AsA+dehydroascorbic acid (DHA), which may be reduced back to AsA by dehydroascorbic acid reductase (cDHAR). Adapted from Yamasaki et al. (1997).

Undoubtedly, the broad range of substrates accepted by Prx is mainly determined by the strong oxidizing potential of their activated intermediates, Col I and Col II, which make them suitable oxidizing agents for many reactions (Ros Barceló, 2000). If such a putative substrate is actually a real substrate of the enzyme *in vivo* will depend most probably on specific subcellular compartmentalization and channeling mechanisms.

I.3.5 Subcellular localization and sorting

In the plant cell, Prxs are targeted to the secretory pathway by an N-terminal signal peptide and are thereafter sorted to the cell wall or the vacuole. According to the current dogma, cell wall sorting constitutes the default pathway, and the vacuolar localization implies that the protein sequence possesses a further signalling sequence or patch (Bassham et al., 2008). Prxs have been shown to have a vacuolar localization by direct detection of peroxidase activity / isoenzymes in the vacuoles (Birecka and Catalfamo, 1976; Thom et al., 1982; Bernal et al., 1993; Ferreres et al., 2011),or based on vacuolar localization of GFP fusions (Costa et al., 2008; Matsui et al., 2011). In fact, when compared to any characterized mature plant Prx, all vacuolar Prxs show the presence of a C-terminal extension (CTE) in their deduced amino acid sequence that has, therefore, been putatively considered the vacuolar-sorting signal (Welinder et al., 2002). Moreover, processing of this CTE was demonstrated for the vacuolar barley peroxidase 1 and horseradish peroxidase C indicating that the CTE is a propeptide in the case of these enzymes (Morita et al., 1991; Johansson et al., 1992; Tognolli et al., 2002; Welinder et al., 2002). In *Arabidopsis*, only 10 out of the 73 Prxs possess the CTE and are therefore predicted to be vacuolar (Welinder et al., 2002). A proteomic study of vacuoles isolated from the rosette leaf tissue of Arabidopsis indeed identified

the presence of six Prxs (Carter et al., 2004). Recently, it was shown that the presence of a Prx CTE was indeed sufficient and necessary for vacuolar sorting of Prx-GFP fusions and, therefore, the presence of a CTE in a Prx sequence most certainly indicates a vacuolar localization (Costa et al., 2008; Schnell et al., 2010; Matsui et al., 2011). In conclusion, Prx proteins are initially synthesized as a polypeptide chain composed of a maximum of three domains: an N-terminal propeptide sequence which constitutes an ER signal peptide (SP), a C-terminal propeptide sequence which constitutes a vacuolar sorting signal peptide and is present only in vacuolar isoenzymes (CTE), and the mature protein sequence, which terminates six to eight residues after the last conserved Cys residue in all characterized mature Prxs (Welinder et al., 2002).

Several studies based on cell-component fractionation suggest a clear distribution among the different peroxidase isoenzymes: whereas the complete set of Prxs, from acid to basic, can be found in the cell wall and free apoplastic space, only the most basic Prxs seem to be present in vacuoles (Schloß et al., 1987; Garcia-Florenciano et al., 1991; Sottomayor et al., 2004; Zipor and Oren-Shamir, 2013).

I.3.6 Physiological functions

As a consequence of the large number of genes, the two possible catalytic cycles, and the multitude of putative substrates, Prxs are implicated in a broad range of physiological processes throughout the plant life cycle. The observed redundancy of peroxidase genes and proteins with similar reactivity properties may reflect the importance of this group of enzymes to plant fitness and survival, but also makes it very difficult to determine conclusively the functions of individual isoenzymes. Studies of expression and localization of Prxs on different organs, developmental stages, and under stress conditions, have also accumulated a body of evidence that strongly supports the involvement of Prxs in key processes for the plant life. Two difficulties are inherent in the study of Prxs: the modification of the expression of a single gene often results in no visible mutant phenotype, because it is compensated by redundant peroxidase genes, and peroxidases have the ability to react with numerous plant compounds *in vitro*, being extremely difficult to determine which of these compounds are indeed *in planta* substrates.

Studies on the catalytic properties *in vitro* and of subcellular localization and gene expression consistently support the involvement of cell wall Prxs in cross-linking reactions determining the architecture and defense properties of the plant cell wall, including lignin and suberin biosynthesis, cross-linking of cell wall glycoproteins like

extensin, and cross-linking of cell wall polysaccharides like pectin (Bernards et al., 2004; Fry, 2004; Ralph et al., 2004; Sottomayor and Ros Barceló, 2004; Gabaldón et al., 2005; Cannon et al., 2008). Lignins are plant polymers responsible for the high rigidity of the xylem walls and were therefore essential for the capacity of plants to build a vascular system and colonize dry land. Using H_2O_2 as oxidant, Prxs can generate monolignol phenoxy radicals that spontaneously form lignin polymers (Ralph et al., 2004; Ros Barceló et al., 2004). In fact, several studies showed that some Prxs such as HRP A2 from horseradish, AtPrx21 (ATP2) from *A. thaliana*, various anionic peroxidases from poplar, and cationic peroxidases from tomato (TPX1) and *Zinnia* seem to be involved in the lignification process, namely due to their specific localization in lignifying plant tissues (Østergaard et al., 2000; Quiroga et al., 2000; Holst Christensen et al., 2001; Nielsen et al., 2001; López-Serrano et al., 2004). Suberin is another plant cell wall polymer that is found in specialized cells, for instance in the 'cork' cells found in bark. Prxs have also been implicated in the cross-linking reactions leading to the biosynthesis of the polyphenolic domain of suberin (Bernards et al., 2004; Keren-Keiserman et al., 2004). Cell wall Prxs are extensively described as participating in the control of cell wall rigidification through the cross-linking between cell wall components, including the formation of diphenyl bridges between cell wall proteins such as extensin, and the cross-linking of feruloyl residues of wall polysaccharides (Fry, 2004). Prxs involved in extensin cross-linking have been isolated from a large variety of plant species (Schnabelrauch et al., 1996; Magliano and Casal, 1998; Jackson et al., 2001). Recently, it has been suggested that extensin undergoes self-assembly into a scaffold stabilized by Prx cross-linking during the formation of the cell plate, forming a template for the orderly deposition of the new cross wall at cytokinesis (Cannon et al., 2008). Additionally, Prxs may also regulate growth by their ability for oxidative coupling of phenolic groups present in the polysaccharide network, namely ferulates (Fry, 2004). Growth and cell wall extensibility are indeed inversely correlated with the increase in the content of diferulates in the cell wall, resulting from Prx activity (Sanchez et al., 1996; Kawamura et al., 2000; MacAdam and Grabber, 2002). For instance, an increase in the expression of *AtPrx37* resulted in an increase in the amount of esterified phenolic material associated with their walls and in the cessation of growth in rosette leaves, as well as along the flower stem (Pedreira et al., 2011). On the other hand, Prxs have also been suggested to have an opposite role during root growth, by generating ROS radicals through their alternative catalytic cycle, with these ROS leading to cleavage of cell wall polysaccharides resulting in cell wall loosening and elongation (Passardi et al., 2004). For instance, transcripts of *APRX*, an

anionic peroxidase from zucchini, accumulated strongly in the elongation zone of the hypocotyl and its accumulation was inversely correlated with lignin level (Dunand et al., 2003). Tsukagoshi et al. (2010) also implicated Prx in root growth, but due to a decrease in Prx expression in the transition from proliferative to differentiation growth, which allowed a higher accumulation of H_2O_2, needed for the onset of differentiation.

Prxs have been further suggested to influence cell elongation through degradation of the hormone auxin (Normanly, 1997). The role of peroxidases in IAA catabolism *in planta*, was demonstrated by the decrease of IAA levels in transgenic *Nicotiana sylvestris* overexpressing the tobacco anionic peroxidase, and the rise in IAA in the corresponding antisense line (Lagrimini et al., 1997; Lagrimini* et al., 1997). This degradation of auxin by Prxs seems to be dependent on the phenolic compounds present, with chlorogenic acid, caffeic acid, sinapic acid and quercetin inhibiting this reaction whereas coumaric acid, ferulic acid and kaempferol stimulate it (Potters et al., 2009).

Plant Prxs have been proposed to have different biochemical functions during plant pathogen defence (Almagro et al., 2009). The hydrophobic heteropolymers, lignin and suberin, produced by Prx-mediated H_2O_2-consuming oxidative cross-coupling of monolignol radicals constitute structural barriers that stop pathogen progression and survival. Moreover, most plant cells respond to pathogens through Prx-mediated H_2O_2-consuming cross-linking of extensin and of ferulic acid groups in cell wall components, in a rapid and transitory event. The resulting dense and solid network in the host plant cell wall prevents pathogen penetration and colonization both by cell wall hardening and by diminishing cell wall susceptibility to digestion (Almagro et al., 2009). Some Prx isoenzymes have actually been classified as pathogenesis-related proteins since they are consistently induced in host plant tissues by pathogen infection (van Loon et al., 2006). Plant defence against pathogen infection often involves the build up of an oxidative burst which origin has also sometimes been ascribed to Prxs. In Arabidopsis, Prxs were implicated in ROS generation upon elicitation of both Arabidopsis cells and plants (Bindschedler et al., 2006; Davies et al., 2006). Prxs were also related with other types of stress, including metal, high light and UV stresses (Jansen et al., 2004; Yannarelli et al., 2006; Führs et al., 2010; Ferreres et al., 2011).

Cell wall Prxs have been extensively investigated and have been undoubtedly implicated in a series of physiological processes *in planta*, as discussed above. On the other hand, much less is known about the functions of vacuolar Prxs, with few studies investigating and/or proposing physiological roles for those Prx isoenzymes. Vacuolar Prxs have been mainly implicated in the metabolism of vacuolar compounds, such as

phenolics, alkaloids and anthocyanins (Takahama, 2004; Zipor and Oren-Shamir, 2013). The implication of the main leaf Prx from *C. roseus*, CroPrx1, in the biosynthesis of the terpenoid indole alkaloid α-3',4'-anhydrovinblastine is one of the few examples of extensive characterization of a vacuolar Prx (Sottomayor et al., 1998; Costa et al., 2008). Furthermore, CroPrx1 was shown to efficiently oxidise vacuolar phenolic compounds, including caffeoylquinic acids and flavonoids, and the authors proposed that the vacuolar Prx/phenol/ascorbate system could have an important regulatory role of H_2O_2 levels in leaf cells, not only by scavenging potentially damaging H_2O_2, but also in the fine homeostasis of H_2O_2 levels needed to fulfil its signalling functions (Ferreres et al., 2011). Vacuolar Prxs have also been implicated in anthocyanin degradation, particularly in *Brunfelsia calycina* flowers. In this plant, the flower colour changes rapidly from purple to white during normal development, and this process is accompanied by a significant increase in peroxidase activity, due in part to newly synthesized enzymes, suggesting their involvement in the *in planta* anthocyanin degradation (Vaknin et al., 2005).

Prx activity is one of the quantitatively measured symptoms of plant senescence (Lim et al., 2007). In *C. roseus*, *CroPrx1* gene showed increased expression in senescent leaves, and Prx activity also increased in senescent leaves (Costa et al., 2008). In Arabidopsis, a transcriptome characterization of senescence showed a dramatic increase in the transcript levels of three particular Prx genes, *AtPrx21*, *34* and *42* (Buchanan-Wollaston et al., 2005). The role of Prxs during senescence has been proposed to be related to chlorophyll degradation in the vacuole. *In vitro*, chlorophyll is readily bleached by Prxs in the presence of H_2O_2 and a phenolic compound (Matile et al., 1999).

I.4 AGPs *versus* Prxs

AGPs and Prxs are important families of proteins of the plant cell wall that have been implicated in important aspects of plant cell physiology through mechanisms still poorly characterized. Namely in what concerns AGPs, in spite of all the studies implicating them in fundamental roles for plants, their precise mechanisms of action and direct interacting co-actors remain largely unknown. Some reports have shown the interaction of AGPs with pectins and it has been proposed that they act as *in muro* plasticizers (Immerzeel et al., 2006; Lamport et al., 2006). Highly interesting is the recent proposal that AGPs interact with the cytoskeleton, functioning as an important link for the cytoskeleton-plasma membrane-cell wall continuum (Sardar et al., 2006; Nguema-Ona et al., 2007). On the other hand, Prxs are implicated in the cross-linking of cell wall

components, such as extensins or hemicelluloses (Fry, 2004), leading to cell wall toughening. Kjellbom et al. (1997) demonstrated that sugar beet leaf excision causes plasma membrane AGPs to cross-link and form high-molecular-weight complexes, suggesting that AGPs cross-linking is involved in responses to wounding. Moreover, they showed that H_2O_2 together with horseradish peroxidase mediated a similar *in vitro* cross-linking of those plasma membrane AGPs, so they proposed that wounding was inducing AGP cross-linking due to the induction of an endogenous source of H_2O_2, which was then used by an endogenous cell wall Prx to perform the AGP cross-linking (Kjellbom et al., 1997).

The possibility that AGPs may be cross-linked by Prxs may have structural consequences but will also most certainly affect their signalling properties. In fact, an interaction between Prxs and AGPs could function as a cell surface signalling switch in which H_2O_2 production triggered by stress could be used by Prx to perform cross-linking of AGPs, leading to changes on their interaction with other proteins, and to activation of intracellular signalling. Significantly, Sottomayor et al. (2008) have observed that Prx and AGPs both localize in membrane microdomains in *Catharanthus roseus* leaf cells, further supporting a possible interaction. In fact, a recent set of data indicates the existence in plant plasma membranes of sterol-rich detergent-resistant microdomains (Bhat and Panstruga, 2005). These microdomains are proposed to host GPI-anchored proteins, such as AGPs, and a subset of integral and peripheral cell surface proteins, which could interact to perform specific functions. Actually, recent proteomic studies have detected the presence of AGPs and Prxs in these microdomains of certain tissues (Borner et al., 2005; Lefebvre et al., 2007), and Sardar et al. (2006) specifically suggested a model in which GPI-anchored AGPs localized in membrane microdomains may mediate signalling in plants through interaction with other proteins co-localized in these microdomains. Furthermore, AGPs, Prxs and H_2O_2 have all been implicated in cell expansion so, the fact that they interact may indicate that they cooperate in the regulation of this process (Ding and Zhu, 1997; Foreman et al., 2003; Passardi et al., 2006).

I.5 Model plants

I.5.1 *Catharanthus roseus*

Catharanthus roseus (L.) G. Don. (Figure I.9) is a perennial semi-shrub known as the Madagascar periwinkle, highly appreciated as an ornamental plant. *C. roseus* belongs to the family Apocynaceae and it was first published by Linnaeus as *Vinca rosea*, in his

"Systema Naturae" in 1759. This species was later published as *Catharanthus* by George Don in his "General System of Gardening and Botany" (1835). The genus *Catharanthus* has originated in Madagascar, except for the species *Catharanthus pusillus*, which originated in India. Nonetheless, *C. roseus* has today a pantropical distribution, being naturalized in Africa, America's, Asia, Australia, Southern Europe, and in some islands in the Pacific Ocean. *C. roseus* accumulates in the leaves the dimeric terpenoid indole alkaloids (TIAs) vinblastine and vincristine, which were the first natural anticancer products to be clinically used, and are still among the most valuable agents used in cancer chemotherapy.

Figure I.9 – Flowering plant of *Catharanthus roseus* cv. Little Bright Eye.

The highly prolific TIA metabolism of *C. roseus* involves two specifically differentiated cell types: idioblasts and laticifers. These two cell types appear in all organs of the plant and are easily detected by their conspicuous blue fluorescence, credited to the accumulation of TIAs (Brown et al., 1984). Laticifers are specialized cells that appear in over 20 plant families and contain a milky, chemically complex fluid called latex, composed of specialized metabolites, such as cardenolides, alkaloids or natural rubber (Hagel et al., 2008). During development, laticifers initiate as single cells that grow to a large size, elongating intrusively by tip extension, with penetration probably depending on an equilibrium between cell wall synthesis and cell wall disassembly (Serpe et al., 2002). On the other hand, idioblasts are isolated cells which differ in their form, size, contents, and wall structure from neighboring tissue cells, and they may appear in any of the tissues or tissue-systems of a plant (Foster, 1956). The so-called excretory idioblasts distinctively accumulate specific compounds, such as oil, alkaloids, resin, tannin, pigments or mineral crystals as calcium oxalate. In *C. roseus*,

the term idioblast has been applied to isolated cells appearing in parenchyma tissues that are identified by their distinctive autofluorescence, TIA accumulation, and larger size than surrounding cells (Yoder and Mahlberg, 1976; Mersey and Cutler, 1986; St-Pierre et al., 1999; Mahroug et al., 2007). *C. roseus* leaf laticifers and idioblasts have been shown to be actively involved in TIA biosynthesis and accumulation, and are likely to be the single site in the plant where the biosynthesis of the medicinal anticancer TIAs is completed (Mahroug et al., 2007).

The great pharmacological importance of the TIAs, associated with the low abundance of the anticancer alkaloids in the plant, stimulated an intensive research of *C. roseus,* which has become one of the most studied medicinal plants (van der Heijden et al., 2004; Verpoorte et al., 2007; Costa et al., 2008).

I.5.2 *Arabidopsis thaliana*

Arabidopsis thaliana (L.) Heyn (Figure I.10) is a small flowering plant native to Europe, Asia and North Africa, and is the model organism most widely used in plant research.

Figure I.10 – *Arabidopsis thaliana* (L.) Heyn.

It plays the role in plant biology that mice and *Drosophila* play in animal biology. *A. thaliana* belongs to the family Brassicaceae and it was first described in 1577 in the Harz Mountains by Johannes Thal, who called it *Pilosella siliquosa*. In 1753, Carl Linnaeus renamed the plant *Arabis thaliana* and then in 1842 Gustav Heynhold came up with the new genus *Arabidopsis* and placed the plant in that genus. It was the first plant genome to be sequenced, completed in 2000 by the Arabidopsis Genome Initiative. *A. thaliana* has several traits that make it a useful model for understanding the genetic, cellular, and molecular biology of plants: small size, rapid life cycle, easily

transformed by *Agrobacterium*, produces thousands of seeds, and can self-pollinate and be cross-pollinated. The Arabidopsis gene knockout collections are a unique resource for plant biology made possible by the availability of high-throughput transformation and funding for genomics resources. The site of T-DNA insertions has been determined for over 300,000 independent transgenic lines, with the information and seeds accessible through online T-DNA databases. Through these collections, mutants are available for most genes in Arabidopsis.

I.6 Main objectives of the thesis

Prxs and AGPs have been implicated in vital functions for the plant, influencing the development and physiology of the plant. However, their involvement in many of these functions is still hypothetical, with the mechanisms of action remaining often unsolved. Previous reports have suggested the possibility of an interaction between AGPs and Prxs (Kjellbom et al., 1997; Sottomayor et al., 2008). Therefore, the main objective of this thesis was to investigate the occurrence of an interaction between AGPs and Prxs in the model plants *Catharanthus roseus* and *Arabidopsis thaliana*, using a set of *in vitro* and *in vivo* experiments, and to investigate the possible role of the Prx-AGP interaction. In order to do that, it was necessary to first investigate the localization of AGPs in both model plants, a study that delivered a picture of AGPs cell/tissue localization patterns, as well as of their subcellular distribution in both plants. As a means to try to understand the physiological significance of the Prx-AGP cooperation, the influence of the putative Prx-AGP interaction in the regulation of plant cell expansion was also investigated. Finally, in order to investigate the occurrence of *in planta* (co)-localization of AGPs and Prxs, fluorescent protein (FP) fusions with specific AGP and Prx genes were generated, which revealed to be good subcellular markers useful for future *in vivo* localization experiments. Additionally, the use of the endogenous promoters with the FP fusions enabled to determine the expression profile of previously uncharacterized AGP genes.

This work produced important knowledge about a noteworthy link between two important groups of plant cell wall proteins, AGPs and Prxs, with important implications for plant development and signalling.

II.

METHODOLOGY

II.1 Cell wall and vacuolar arabinogalactan proteins are markers of cell differentiation in the leaves of the medicinal plant *Catharanthus roseus*

II.1.1 Plant material

Catharanthus roseus (L.) G. Don (cv. Little Bright Eye) plants were maintained at 25ºC, in a growth chamber, under a 16 h white fluorescent light photoperiod, at 70 µmol m^{-2} s^{-1}. Leaves from the third pair counting from the shoot apex of mature flowering plants were used for immunolabelling. Plants used were 6 to 8 months old.

II.1.2 Immunolabelling

Monoclonal antibodies (mAbs) used were JIM8, JIM13, JIM14, JIM16, LM2 and MAC207, which were kindly provided by Prof. Paul Knox from the Cell Wall Lab at the University of Leeds (www.plantprobes.net). Leaves were cut in 1 mm wide strips and fixed in 0.4% (v/v) glutaraldehyde and 3.2% (v/v) paraformaldehyde in 1% NaPIPES (pH 7.2) ON at 4ºC. The pieces were dehydrated in an ethanol series, infiltrated in ethanol-resin mixtures and embedded in LR White (TAAB). Semi-thin sections of leaf were collected on silane treated glass slides in an area delimited with hydrophobic pen. After a 10 min wash in PBS, the sections were incubated with blocking solution (10% goat serum in PBS), for 1 h, at RT. Exposure ON at 4ºC to the primary antibody at dilution 1:10 in blocking solution, followed. Sections were thoroughly washed with blocking solution (5 times for 5 min) and labelled in the dark for 3 h at RT with a dilution 1:2,000 goat anti-rat IgG (H+L) secondary antibody conjugated with AlexaFluor488 (Molecular Probes) in blocking solution. Sections were then rinsed in abundant blocking solution (5 times for 5 min), then with PBS for 10 min. In order to stain the cell walls, sections were incubated 5 min with 0.01% calcofluor in PBS and washed with water. Finally, sections were mounted in anti-fading mounting medium (Vectashield mounting medium, Vector Laboratories) and observed using a confocal microscope (Leica SP2 AOBS SE). Visualization of the fluorescence was performed using an excitation wavelength of 488 nm.

II.1.3 Isolation of protoplasts and vacuoles

C. roseus mesophyll protoplasts were obtained using a protocol adapted from Zheng et al. (1997) and Sottomayor et al. (1996). Leaves of adult plants (usually second and

third pairs from the tip) were cut into approximately 1 mm strips and transferred to a Petri dish with digestion medium composed of 2% (w/v) cellulase (Onozuka R-10), 0.3%(w/v) macerozyme (Onozuka R-10) and 0.1% (v/v) pectinase (Sigma) dissolved in MM buffer (0.4 M mannitol in 20 mM MES pH 5.8). The medium was vacuum infiltrated for 15 min, and then leaf strips were incubated for 3 h at 25ºC in the dark. The suspension was then filtered through a 100 µm nylon mesh, and the filtrate was transferred into 15 mL Falcon tubes. The protoplast suspension was centrifuged at 65 *g* for 5 min at RT, the supernatant was removed, and the protoplasts were washed four times in MM buffer. After the final wash, protoplasts were counted using a haemocytometer. The integrity of the isolated protoplasts was checked by observation under an optical microscope (Olympus).

Isolation of *C. roseus* leaf vacuoles was performed according to Robert et al. (2007) with minor modifications. The isolated leaf protoplasts were centrifuged at 65 *g* for 5 min at RT, and the protoplast pellets were chilled for at least 30 min on ice. Vacuoles were released by ressuspending the protoplasts in lysis buffer (0.2 M mannitol, 10% (w/v) Ficoll 400, 10 mM EDTA and 5 mM sodium phosphate pH 8.0) at 37ºC, pipetting up and down 5-8 times with a 5 mL serological pipette, and incubating at room temperature (RT) for 4 min. 6 mL of lysed suspension was transferred into a chilled ultra-clear centrifuge tube using a 5 mL micropipette and overlaid with 3.6 mL of 4% Ficoll in a 4.5:3 mixture of lysis and vacuole buffers at RT, and with 1 mL of ice-cold vacuole buffer (0.45 M mannitol, 2 mM EDTA, 2 mM DTT and 5 mM sodium phosphate pH 7.5). Isolated vacuoles were recovered in the interface between 0 and 4% Ficoll after centrifugation at 71,000 *g*, for 1 h, at 10ºC, in an ultracentrifuge (Beckman Optima™ L80-XP) with acceleration and deceleration in level 6. Vacuoles were stained with neutral red for visualization under the optical microscope and counted using a haemocytometer.

II.1.4 Protein extraction from protoplasts and vacuoles

The protoplasts and vacuoles fractions were diluted in 1 M KCl and 50 mM Tris-HCL pH 7.0 and were broken by freeze/thawing. Soluble and membrane proteins were separated by centrifuging the samples at 100,000 *g* for 45 min at 4ºC. The pellets (membrane proteins) were ressuspended in 1% NaCl and the supernatants (soluble proteins) were concentrated and changed to 1% NaCl using Amicon Ultra 15 mL Centrifugal Filter (Millipore).

II.1.5 Protein extraction from leaves

C. roseus leaves were homogenized in 1 M KCl and 50 mM Tris-HCl pH 7.0 at 4ºC. The homogenate was filtered through a 200 µm nylon mesh and centrifuged at 1,000 rpm for 5 min at 4ºC. The supernatant was centrifuged at 5,000 rpm for 30 min at 4ºC. Soluble and membrane proteins were separated by centrifuging the supernatant at 100,000 *g* for 45 min at 4ºC. The pellets (membrane proteins) were ressuspended in 1% NaCl and the supernatants (soluble proteins) were concentrated and changed to 1% NaCl using Amicon Ultra 15 mL Centrifugal Filter (Millipore).

II.1.6 Rocket gel electrophoresis

AGPs were quantified by rocket electrophoresis, using known concentrations of gum arabic as standards, according to the method described by Gane et al. (1995) and Ding and Zhu (1997). The 1% agarose gel contained 20 µM β-Yariv reagent for AGP precipitation, and electrophoresis was performed at 150 V and 20 mA, at 4ºC, until the rockets were well developed (3 h). Gels were then washed ON with 1% (w/v) NaCl, at 4ºC, and dried onto filter paper. The concentration of AGPs in the samples was estimated in relation to the peak area times staining intensity of gum arabic.

II.1.7 Dot-blot immuno analysis

Protein samples were transferred to a nitrocellulose membrane, through vacuum, using the Dot Blotter Minifold I (Schleicher & Schuell) or the Bio-Dot Apparatus (Bio-Rad). After transfer, the membrane was incubated in blocking solution, 5% milk powder in PBS with 0.05% Tween-20 (PBS-T), for 1 h RT. The membrane was then incubated for 30 min in 30% H_2O_2 in the dark to inactivate endogenous peroxidases, which was confirmed with a chemiluminescence kit (Roche Diagnostics GmbH), according to the manufacturer's instructions. The mAb was diluted 1:100 in blocking solution and used to probe the membrane ON at 4ºC. The membrane was then briefly rinsed three times in water and washed once in PBS-T for 5 min. Horseradish peroxidase-conjugated anti-rat antibody (GE Healthcare) was used at a 1:25,000 dilution in blocking solution for 1 h at RT. The membrane was then briefly rinsed three times in water and washed once in PBS-T for 5 min, followed by a final rinse in water. Development of the activity reaction was performed with the chemiluminescence kit, according to the manufacturer's instructions. Membrane was exposed and films were revealed automatically in a X-OMAT M43 Processor (Kodak). Quantification of labelling was performed using the densitometer Molecular Imager GS800 (Bio-Rad) and the Quantity One® (Bio-Rad) software.

II.2 Class III peroxidases and arabinogalactan proteins in *Catharanthus roseus*

II.2.1 Plant material and treatments

Catharanthus roseus (L.) G. Don cv. 'Little Bright Eye' plants were grown at 25ºC in a growth chamber, under a 16 h photoperiod, using white fluorescent light with a maximum intensity of 70 µmol m^{-2} s^{-1}. Leaves from the third pair counting from the tip were used for immunolabelling. In some instances, 30 min prior to fixation, leaves were syringe infiltrated through the abaxial face with bi-distilled water and 10 mM H_2O_2 or with 2 mM KCN and NaN_3 (Davies et al., 2006) in 10 mM H_2O_2.

II.2.2 Protein extraction from leaves

Leaves were homogenized in 50 mM Tris-HCL pH 7.5, 1 M KCL and 6 mM ascorbic acid at 4ºC. The homogenate was filtered through cheese cloth and centrifuged at 13,000 rpm for 30 min at 4ºC. The obtained supernatant was collected and dialysed against 1 mM NaCl, 1 mM $CaCl_2$, 1 mM $MgCl_2$ and 1 mM $MnCl_2.4H_2O$.

II.2.3 Extraction of the apoplastic fluid from leaves

Leaves were cut into 3 mm wide strips and immediately put in 50 mM Tris-HCL pH 7.5 at 4ºC. The leaf strips were briefly rinsed with the same buffer, put in 50 mM Tris-HCL pH 7.5 and 1 M KCl and submitted to several pulses of mild vacuum for 10 min at 4ºC. The buffer was removed and the cell wall fluid was recovered by centrifugation of the infiltrated leaf strips at 1,000 *g* for 5 min at 4ºC. The fluid was collected and the contamination of the fluid by cytosolic sap was assayed using glucose-6-phosphate dehydrogenase as an enzyme marker (Ros Barceló et al., 1991). The sample was dialysed against 1 mM NaCl, 1 mM $CaCl_2$, 1 mM $MgCl_2$ and 1 mM $MnCl_2.4H_2O$.

II.2.4 Isolation of protoplasts and vacuoles from leaves

See section II.1.3.

II.2.5 Protein extraction from vacuoles

Vacuoles were broken by freeze/thawing, freeze-dried for 2 days, reconstituted in 1 mM NaCl, 1 mM $CaCl_2$, 1 mM $MgCl_2$ and 1 mM $MnCl_2.4H_2O$ and dialysed against the same saline solution.

II.2.6 Determination of peroxidase activity

Peroxidase activity was estimated at 25ºC with 4-methoxy-α-naphthol (4-MN) as substrate according to Ferrer et al. (1990). The assay was performed on a 1 mL assay volume, containing enzyme, 1 mM 4-MN and 0.33 mM H_2O_2 in 0.1 M Tris-acetate buffer at pH 5.0. The reaction was initiated by adding the H_2O_2, and the increase in absorbance at 593 nm was recorded (ε_{593} = 21.0 mM^{-1} cm^{-1}). Enzymatic activity was expressed in katal (kat), and defined as the amount of enzyme that converts 1 mol of substrate into products s^{-1}.

II.2.7 Isoelectric focusing and *in gel* Prx activity

IEF was performed at 4ºC. The gel was composed of 20% (w/v) sucrose, 5% (w/v) acrylamide (Bio-Rad), 0.7% (w/v) ammonium persulfate (APS), 1% (v/v) TEMED and 6% ampholytes pH 3-10 (GE Healthcare). The electrolytes used were 0.5 M sodium hydroxide for the cathode and 0.125 M phosphoric acid for the anode. The run was performed in an horizontal refrigerated box (IsoBox Hoefer Scientific Instruments) under limiting conditions of 15 W. The samples were loaded once the voltage reached 700 V (end of the pre-focusing) and the run ended 5 min after reaching 2,000 V. In gel peroxidase activity was performed by incubation in the same reaction buffer used in section II.2.6. Image was acquired using the densitometer Molecular Imager GS800 (Bio-Rad) and processed with the Quantity One® (Bio-Rad) software.

II.2.8 Purification of CroPrx1 from *C. roseus* leaves

Purification of CroPrx1 was performed according to Sottomayor (1998) with some modifications. 300 g leaves were homogenized in 50 mM Tris-HCl pH 7.5, 1 M KCl, 6 mM ascorbic acid, 1 mM NaCl, 1 mM $CaCl_2$, 1 mM $MgCl_2$ and 1 mM $MnCl_2.4H_2O$ at 4ºC. The homogenate was filtered through cheese cloth and centrifuged at 10,000 rpm for 60 min at 4ºC. The supernatant was collected and solid ammonium sulphate was slowly added with gentle stir at 4ºC, until reaching a 30% (w/v) final concentration. The mixture was then centrifuged at 10,000 rpm for 30 min at 4ºC. The supernatant was collected and submitted to a series of 4 chromatographic steps with selection of the fractions with higher Prx activity in each step. All chromatographies were performed in an ÄKTAprime TM plus (GE Healthcare) low pressure liquid chromatography system at 4ºC. The ammonium sulphate supernatant was applied to a phenyl-Sepharose 6 Fast Flow (high sub) (GE Healthcare), 20 x 1.6 cm column, equilibrated with 1.5 M ammonium sulphate in 50 mM Tris-HCl pH 7.5, 1 mM NaCl, 1 mM $CaCl_2$, 1 mM $MgCl_2$ and 1 mM $MnCl_2.4H_2O$, and proteins were eluted with a linear gradient from 1.5 to 0 M

ammonium sulphate in 50 mM Tris-HCl pH 7.5, 1 mM NaCl, 1 mM $CaCl_2$, 1 mM $MgCl_2$ and 1 mM $MnCl_2.4H_2O$, with a flow rate of 1.5 mL min^{-1}. The 2 mL fractions collected were screened for Prx activity and the fractions with the highest Prx activity were pooled and dialysed ON against 50 mM Tris-HCl pH 7.5, 1 mM NaCl, 1 mM $CaCl_2$, 1 mM $MgCl_2$ and 1 mM $MnCl_2.4H_2O$. The dialysed sample was then applied to a concanavalinA Sepharose 4B (GE Healthcare), 20 x 1.6 cm column, equilibrated with 50 mM Tris-HCl pH 7.5, 1 mM NaCl, 1 mM $CaCl_2$, 1 mM $MgCl_2$ and 1 mM $MnCl_2.4H_2O$. The elution was performed with a gradient from 0 to 2.5 M NaCl, 0.5 M α-D-mannopyranoside (Sigma) in 50 mM Tris-HCl pH 7.5, 1 mM NaCl, 1 mM $CaCl_2$, 1 mM $MgCl_2$ and 1 mM $MnCl_2.4H_2O$, with a 1.5 mL min^{-1} flow rate, and 2 mL fractions were collected. The fractions with the highest Prx activity were pooled and concentrated and directly injected on a Sephacryl S-200 HR (GE Healthcare), 60 x 1.6 cm column, equilibrated with 20 mM MES pH 6.0. The bounded proteins were eluted with the same buffer at a 0.5 mL min^{-1} flow rate and 2 mL fractions were collected. The fractions with higher Prx activity were pooled and applied to a cation exchange HiTrap CaptoS 1 mL column (GE Healthcare) equilibrated with 20 mM MES pH 6.0. Basic proteins were eluted with a linear gradient of 0 to 30% of 20 mM MES, 1 mM NaCl, 1 mM $CaCl_2$, 1 mM $MgCl_2$, 1 mM $MnCl_2.4H_2O$ and 1M KCl, with a flow rate of 1 mL min^{-1}. Fractions of 2 mL were collected and the fractions with higher Prx activity were dialysed against 1 mM NaCl, 1 mM $CaCl_2$, 1 mM $MgCl_2$ and 1 mM $MnCl_2.4H_2O$ and analysed for purity by IEF and SDS-PAGE.

II.2.9 Isolation of AGPs from leaves

The extraction of AGPs from leaves was performed as previous described by Schultz et al. (2000), with some modifications. Leaves were homogenized in liquid nitrogen with a mortar and pestle and were ressuspended in 10 mM EDTA, 0.1% β-mercaptoethanol, 1% (w/v) Triton X-100 and 50 mM Tris-HCl pH 8.0 at 4ºC. The homogenate was filtered through 200 μm nylon mesh and centrifuged at 5,000 rpm for 20 min. The supernatant was precipitated with 5 volumes of cold ethanol for ON at 4ºC. The mixture was centrifuged at 5,000 rpm for 30 min and the supernatant was discarded. The pellet was ressuspended in 50 mM Tris-HCl pH 8.0. The insoluble material was removed by centrifugation, and the supernatant was retained. The pellet was again ressuspended in additional 50 mM Tris-HCl, pH 8.0, and the soluble material (after centrifugation) was pooled with the first supernatant. The buffer-soluble material was dialyzed against water at 4ºC and then it was freeze-dried ON to concentrate the sample. The dried samples were ressuspended in 250 to 500 μL of 1% (w/v) NaCl and transferred to 2-

mL microcentrifuge. AGPs were precipitated with the β-Yariv reagent by mixing the ressuspended samples in an equal volume of β-Yariv [2 mg mL^{-1} in 1% (w/v) NaCl] and leaving ON at 4ºC. The insoluble Yariv–AGP complex was collected by centrifugation at 13,000 rpm in a microcentrifuge for 1 h and washed 3 times with 1% NaCl. To wash the excess of β-Yariv, the complex was dissolved in DMSO, then cold acetone and 1% NaCl were added, forming a flocculate. After centrifugation at 3,000 rpm for 10 min at 4ºC, the process was repeated 3 times. The β-Yariv was removed by dissolving the complex in 10% (w/v) sodium dithionite (Sigma) and incubating at 50ºC until the mixture became a clear yellow colour. The resulting yellow solution was immediately dialyzed against water and finally the sample was freeze-dried.

II.2.10 Spectrophotometric assays of the HrPrxII and CroPrx1 catalytic cycle

The spectrophotometric assays contained 0.25 μM HrPrxII or CroPrx1 and 0.5 μM H_2O_2 in 0.1 M Tris-acetate buffer pH 5.0. The enzymes concentration was calculated using a ε_{403} = 102.0 mM^{-1} cm^{-1} (Dunford, 1982). For kinetics measurements, the concentration of the ferric form of the enzyme (Fe^{3+}) and compound II (CoII) were determined using ε_{403}(CoII) = 61.85 mM^{-1} cm^{-1}, ε_{418}(CoII) = 96.51 mM^{-1} cm^{-1} and $\varepsilon_{418}(Fe^{3+})$ = 53.26 mM^{-1} cm^{-1}, according to the following formulae: $A_{403} = [Fe^{3+}] \times \varepsilon_{403}(Fe^{3+}) + [CoII] \times \varepsilon_{403}(CoII)$, and $A_{418} = [CoII] \times \varepsilon_{418}(CoII) + [Fe^{3+}] \times \varepsilon_{418}(Fe^{3+})$. It was assumed that compound I (CoI) concentration was not significant compared with concentrations of Fe^{3+} and CoII. CoII reduction rates were estimated from the progress curves of CoII.

II.2.11 Protein extraction for cross-linking reactions

Leaves without the midrib were homogenized in liquid nitrogen with a mortar and pestle and were ressuspended in 6 mM ascorbic acid and 50 mM Tris-HCl, pH 7.5. The homogenate was filtered through 200 μm nylon mesh, centrifuged at 10,000 rpm for 5 min to discard the cell wall and organelles pellet, and the supernatant was centrifuged at 100,000 *g* for 30 min to yield the soluble fraction as the supernatant, which was dialysed against 50 mM Tris-HCl, pH 7.5. The membrane fraction was recovered through ressuspension of the pellet on 50 mM Tris-HCl, pH 7.5. All procedures were carried out at 4ºC.

II.2.12 *In vitro* cross-linking in the presence of CroPrx1

The soluble and membrane fractions of proteins were incubated in the presence of 100 nM CroPrx1 and 1 mM H_2O_2 in 50 mM Tris-HCl, pH 7.0, on a final volume of 1 mL, for

1 h at 25ºC. Controls either without CroPrx1 or without H_2O_2 were performed. The reaction was stopped by freezing in liquid nitrogen and stored at -80^{0}C until gel filtration analysis.

II.2.13 Gel filtration

The reaction mixtures were loaded on a Sephacryl S-300 HR (GE Healthcare), 70 x 1.6 cm column, equilibrated with 50 mM Tris-HCl, pH 7.0, which was also used for elution at a flow rate of 0.5 mL min^{-1}.

II.2.14 Dot-blot immuno analysis

Equal volumes of protein samples were transferred to a nitrocellulose membrane through vacuum, using the Bio-Dot Apparatus (Bio-Rad). See section II.1.7.

II.2.15 Immunolabelling and quantification of signal intensity

For immunolabelling see section II.1.2. Sections were observed using a fluorescent microscope (Axioskop, Carl Zeiss). The quantification of the signal intensity obtained was performed using ImageJ (http://rsb.info.nih.gov/ij/) with correction of the background signal.

II.2.16 Preparation of anti-Prx

The anti-Prx was done against Arabidopsis Prx12 mature protein (MP). The 906 bp sequence encoding the Prx12 MP was PCR amplified from λFLC-1-B cDNA, clone pda09996, purchased from Riken BioResource Center. The PCR product was cloned in frame in pET28a (Novagen) with *Nco*I/*Eco*RI. The sequences of the individual primers are as follows (engineered restriction sites are underlined): PL12, 5'-AAGAAGCGGAGTACCATGGCTCCTATAGTGAAA-3' and PR12, 5'-AACGGACATGAAGAATTCTTAGTTTCTGGCTGA-3'. The recombinant vector was transformed in *Escherichia coli* BL21 (DE3) (Novagen). The induction of the recombinant protein was done through the addition of 0.4 mM IPTG (isopropyl-β-D-thiogalactopyranoside) for 4 h. The recombinant protein was purified through acrylamide extraction from SDS-PAGE gel. For the production of polyclonal antibody the purified Prx12 MP was injected subcutaneously into Wistar rabbits and the antiserum was collected (Animal Facility, IBMC). The specificity of the anti-Prx antibody to Prxs was tested, at dilution 1:100, by Western-blot.

II.2.17 Western-blot

SDS-PAGE gel proteins were transferred into a nitrocellulose membrane for 1 h, at 100 V, in transfer buffer, according to the method described by Burnette (1981). The membrane was blocked for 45 min at RT in 5% skimmed milk powder in TBS containing 0.1% Tween-20 (TBS-T). The membranes were probed ON, at 4ºC, with 1:100 anti-Prx in blocking solution. Alkaline-phosphatase conjugated secondary antibody (Sigma) was used at 1:5,000 dilution in TBS-T for 45 min at RT. Activity was revealed using the Western blue stabilized substrate for alkaline phosphatase (Promega), according to the manufacturer's instructions. Image was obtained using the GS-800 densitometer (Bio-Rad) and processed with the Quantity One® (Bio-Rad) software.

II.2.18 Co-immunolabelling

Semi-thin sections of leaves were collected on silane treated glass slides in an area delimited with hydrophobic pen. After a 10 min wash in PBS, the sections were incubated with blocking solution (10% goat serum in PBS), for 1 h, at RT. Exposure ON at 4ºC to the primary antibody mAb at dilution 1:10 in blocking solution, followed. Sections were thoroughly washed with blocking solution (5 times for 5 min) and labelled in the dark for 3 h at RT with a dilution 1:2,000 goat anti-rat IgG (H+L) secondary antibody conjugated with AlexaFluor488 (Molecular Probes) in blocking solution. Sections were then rinsed in abundant blocking solution (5 times 5 min), then with PBS, then with water. Following, it was performed a 1 min treatment with 0.8% (w/v) sodium metaperiodate (Sigma) solution and then sections were washed three times in water and once in PBS. The second exposure was performed ON at 4ºC now with the primary antibody anti-Prx at dilution 1:5 in blocking solution. Sections were thoroughly washed with blocking solution (5 times for 5 min) and labelled for 3 h at RT with 1:2,000 goat anti-rabbit IgG (H+L) secondary antibody conjugated with AlexaFluor568 (Molecular Probes) in blocking solution. Sections were then rinsed in abundant blocking solution (5 times 5 min) and then with PBS for 10 min. In order to stain the cell walls, sections were incubated for 5 min with 0.01% calcofluor in PBS and washed with water. Finally, sections were mounted in anti-fading mounting medium (Vectashield mounting medium, Vector Laboratories) and observed using a confocal microscope (Leica SP2 AOBS SE). Visualization of the fluorescence was performed using an excitation wavelength of 488 nm for AGPs and 561 nm for Prx.

II.3 Class III peroxidases and arabinogalactan proteins in *Arabidopsis thaliana*

II.3.1 Plant material and treatments

Arabidopsis thaliana of the accession Col0 plants were grown at 21ºC in a growth chamber, under a 12 h light photoperiod, using white fluorescent light at 35 µmol m^{-2} s^{-1}. Plants in growth stage 1.11 / 3.20 or in growth stage 3.70 to 3.90 according to Boyes et al. (2001). In some instances, 30 min prior to fixation, leaves were syringe infiltrated through the abaxial face with bi-distilled water and 10 mM H_2O_2 or with 2 mM KCN in 10 mM H_2O_2.

II.3.2 Protein extraction from leaves

See section II.2.2.

II.3.3 Extraction of the apoplastic fluid from leaves

See section II.2.3.

II.3.4 Isolation of protoplasts and vacuoles from leaves

Arabidopsis mesophyll protoplasts were obtained as described in Yoo et al. (2007), with some modifications. Leaves from adult plants were cut into 1 mm wide strips and transferred to an enzyme mixture of 1.5% cellulase (Onozuka R10) and 0.4% macerozyme (Onozuka R10) dissolved in 0.4 M mannitol, 20 mM KCl, 10 mM $CaCl_2.2H_2O$ and 20 mM MES, pH 5.7. The leaf strips were vacuum infiltrated for 15 min and the digestion was further allowed for 3 h, at 25ºC, in the dark. The enzyme solution containing protoplasts was filtered through a 100 µm nylon mesh and the filtrate was centrifuged at 600 rpm for 5 min at RT, with acceleration and deceleration set at the minimum. The protoplast pellet was washed with cold W5 solution (154 mM NaCl, 125 mM $CaCl_2.2H_2O$ and 5 mM KCl in 2 mM MES, pH 5.7). Following a 5 min centrifugation at 600 rpm at RT the pellet was gently ressuspended in a small volume (5 to 7 mL) of cold W5 solution. Protoplasts were counted using a haemocytometer. Protoplasts were centrifuged again and ressuspended in cold MW5 solution (320 mM mannitol in W5 solution).

Arabidopsis mesophyll vacuoles were isolated according to the method described by Hadlington and Denecke (2001). Protoplasts in MW5 solution were centrifuged at 200 *g* for 5 min at RT and the protoplasts pellet was chilled on ice for 10 min. Lysis

occurred by adding 3 mL of 42ºC pre-warmed lysis buffer (0.2 M mannitol, 10% Ficoll 400, 20 mM EDTA, 150 µg mL^{-1} BSA, 2 mM DTT and 10 µg mL^{-1} Neutral Red in 5 mM Hepes pH 8.0) and incubation at RT for 10 min. After lysis, the mixture was overlaid with a 1.5 mL layer of 5% Ficoll buffer (1:1 mixture of lysis and vacuole buffers) and one layer of 0.75 mL of vacuole buffer (10 mM Hepes pH 7.5, 0.6 M mannitol, 150 µg mL^{-1} BSA). After centrifugation at 300 *g* for 10 min at RT, vacuoles were recovered from the upper phase, in vacuole buffer.

II.3.5 Protein extraction from protoplasts and vacuoles

See section II.2.5.

II.3.6 Determination of peroxidase activity

See section II.2.6.

II.3.7 Isoelectric focusing and *in gel* Prx activity

See section II.2.7.

II.3.8 Purification of AtPrx34 from leaves

See section II.2.8.

II.3.9 Isolation of AGPs from leaves

See section II.2.9.

II.3.10 Spectrophotometric assays of the HrPrxII and AtPrx34 catalytic cycle

See section II.2.10.

II.3.11 Immunolabelling with mAbs

See section II.1.2.

II.3.12 Protein extraction for cross-linking reactions

See section II.2.11.

II.3.13 *In vitro* cross-linking in the presence of AtPrx34

The soluble and membrane fractions of proteins were incubated in the presence of 100 nM AtPrx34 and 1 mM H_2O_2 in 50 mM Tris-HCl, pH 7.0, on a final volume of 1 mL, for 1h at 25ºC. Controls either without AtPrx34 or without H_2O_2 were performed. The

membrane fractions were further treated with phospholipase C from *Bacillus cereus* for 6 h at 37ºC. The samples were then submitted to gel filtration analysis.

II.3.14 Gel filtration

See section II.2.13.

II.3.15 Dot-blot immuno analysis

See section II.2.14.

II.3.16 Immunolabelling and quantification of signal intensity

See section II.2.15.

II.3.17 Western-blot

See section II.2.17.

II.3.18 Immunolabelling with anti-Prx

Leaf sections in silane treated glass slides were incubated in 10% (w/v) sodium metaperiodate (Sigma) solution for 10 min and then sections were washed three times in water and once in PBS. Sections were incubated with blocking solution (10% goat serum in PBS), for 1 h, at RT. Exposure ON at 4ºC to the primary antibody anti-Prx at dilution 1:10 in blocking solution, followed. Sections were thoroughly washed with blocking solution (5 times for 5 min) and labelled in the dark for 3 h at RT with a dilution 1:2,000 goat anti-rabbit IgG (H+L) secondary antibody conjugated with AlexaFluor488 (Molecular Probes) in blocking solution. Sections were then rinsed in abundant blocking solution (5 times 5 min) and then with PBS for 10 min. In order to stain the cell walls, sections were incubated for 5 min with 0.01% calcofluor in PBS and washed with water. Finally, sections were mounted in anti-fading mounting medium (Vectashield mounting medium, Vector Laboratories) and observed using a confocal microscope (Leica SP2 AOBS SE). Visualization of the fluorescence was performed using an excitation wavelength of 488 nm.

II.3.19 Co-immunolabelling for confocal microscopy

See section II.2.18.

II.3.20 Co-immunolabelling for transmission electron microscopy

The co-immuno was performed as in section II.2.18, without the cell wall staining step. The primary antibodies (MAC207 and anti-Prx) were used with a dilution 1:2 and the secondary antibodies (conjugated with gold, BBInternational) were used with a dilution 1:20. The grids were observed in a transmission electron microscope Jeol JEM-1400.

II.4 Do AGPs and Prx cooperate to regulate tip growth in Arabidopsis root hairs?

II.4.1 Immunolabelling in Arabidopsis roots

After disinfection with 10% bleach and 0.02% Tween-20, seeds of *Arabidopsis thaliana* of the accession Col0 were sown in 1/2 MS medium (Duchefa) containing 1% (w/v) sucrose and 0.6% (w/v) bacto agar (BD Becton). Seeds were vernalized for 2-3 days and were transferred to the growth chamber. Seedlings were grown under continuous light for 4 days. Roots were treated in two different ways. In one way, because roots are very delicate and in order to better process and orientate the samples, some roots were mechanically fixed using 0.6% agarose, according to the method describe by Wu et al. (2012), and then cut into small pieces. These agarose pieces were then chemically fixed in 0.4% (v/v) glutaraldehyde and 3.2% (v/v) paraformaldehyde in 1% (w/v) NaPIPES (pH 7.2) for ON at 4ºC. The pieces were dehydrated in an ethanol series, infiltrated in ethanol-resin mixtures and embedded in LR White (TAAB). Semi-thin sections of roots were collected on silane treated glass slides in an area delimited with hydrophobic pen. In another way, roots were directly fixed in the same fixative, but only for 2 h at RT. These roots were then placed very gently in silane treated glass slides and delimited with hydrophobic pen. The immunolabelling elapsed as described in section II.1.2.

II.4.2 Chemical treatment of roots

Seedlings growing in 1/2 MS medium (Duchefa) containing 1% (w/v) sucrose and 0.6% (w/v) bacto agar (BD Becton) in a 12 h photoperiod for 4 days were transferred to medium supplemented with: 5 µg/mL α-Yariv, 5 µg/mL β-Yariv, 50 µM SHAM, 100 µM SHAM, 1 mM KI, 100 µM ascorbate, 1 µM H_2O_2 or 10 µM H_2O_2. Control plants were transferred to plain MS medium. Petri dishes were photographed after 10 days, and root hairs were visualized in a stereomicroscope equipped with a camera.

II.4.3 Analysis of root hair growth

After disinfection with 10% bleach and 0.02% Tween-20, seeds of *Arabidopsis thaliana* of the accession Col0 were sown in 1/4 MS medium (Duchefa) containing 1% (w/v) sucrose and 0.6% (w/v) bacto agar (BD Becton). Seeds were vernalized for 2-3 days and were transferred to the growth chamber. Seedlings were grown under continuous light for 3-4 days, and then transfered to a thin layer of medium supplemented with

different treatments covering the bottom of a well from a 6-well plate with the bottom of the wells made of a cover slip. Plates were immediately observed in an inverted microscope during 1 h and images were collected every 2 min. The treatments used were: LM2, JIM13, JIM8, JIM16, JIM14, MAC207, anti-Prx or anti-CroPrx1 (Sottomayor, 1998) with a dilution 1:2; 0.072 or 0.36 μM AtPrx34; 1 or 5 mg/mL gum arabic. All the antibodies before used were dialysed against MS medium in order to avoid the additives used to preserve the antibodies, like sodium azide.

II.5 Genetic approaches to investigate the *in vivo* interaction between Prx and AGPs

II.5.1 Plant material

Arabidopsis thaliana of the accession Col0 and *Nicotiana tabacum* (L.) cv. Petit Havana SR1 plants were grown at 21ºC in a growth chamber, under a 12 h light photoperiod, using white fluorescent light at 35 µmol m^{-2} s^{-1}.

II.5.2 Construction of AtAGP9, AtAGP58 and AtPrx34 FP fusions

The plant expression vector pMON999e35S obtained from Prof. Theodorus W. J. Gadella (University of Amsterdam) was used to clone the *AtPrx34*, *AtAGP58* and *AtAGP9* genes, with AtPrx34 corresponding to an Arabidopsis Prx with C-terminal extension and AtAGP9 and AtAGP58 corresponding to Arabidopsis classical AGPs with GPI-anchor. Both sCFP4 (mTurquoise) and sYFP3 were also obtained from Prof. Theodorus W. J. Gadella (Goedhart et al., 2010).

AtAGP9, AtAGP58 and *AtPrx34* were amplified by PCR from the cDNA clone RAFL09-72-F17 pda08713, clone RAFL04-13-J15 pda00292 and clone RAFL03-01-G07 pda13431, respectively, purchased from the Riken BioResource Center. The signal peptide (SP) sequence from the proteins was predicted using SignalP (Emanuelsson et al., 2007) and amplified using the following primers (engineered restriction sites are underlined): SP9Fw_BglII, 5'-ATTAGATCTATGGCTCGATCTTTCGCT-3', and SP9Rv_EcoRI, 5'-ATGAATTCAGCTTGACCAGTAACGC-3', for *AtAGP9*; SP58Fw_BglII, 5'-ATTAGATCTATGGCCTCTTCTTTCTCT-3', and SP58Rv_EcoRI, 5'-ATGAATTCAGCTTGAGCTAAAGAGAAAGG-3', for *AtAGP58*; SP34Fw_BglII, 5'-ATTAGATCTATGCATTTCTCTTCGTCTTC-3',and SP34Rv_EcoRI, 5'-ATGAATTCTTCTCGTACGATGTTAGTGA-3', for *AtPrx34*. The *AtAGP9*, *AtAGP58* and *AtPrx34* sequences codifying the mature protein were amplified using the following primers (engineered restriction sites are underlined): MP9Fw_SacI, 5'-TTGAGCTCCAAGCTCCGACTTCACC-3' and GPI9Rv_BamHI, 5'-TTGGATCCTTAGATCATAAACCAGACGAGA-3', for *AtAGP9*;MP58Fw_SacI, 5'-ATGAGCTCCAAGCTCCCATGATGGC-3', and GPI58Rv_BamHI, 5'-ATGGATCCTCAAACGAGGAGAAAATGGG-3', for *AtAGP58*; MP34Fw_SacI, 5'-AAGAGCTCCAACTCACCCCTACCTTCTA-3', and CTE34Rv_BamHI, 5'-ATGGATCCTCACATAGAGCTAACAAAGTCA-3', for *AtPrx34*. The amplified *AtAGP9*

SP, *AtAGP58* SP and *AtPrx34* SP were cloned in the plasmids with the fluorescent proteins (FP) using *Bgl*II/*Eco*RI, to generate e35S:SP9-FP, e35S:SP58-FP and e35S:SP34-FP, respectively. These latter were used to insert the *AtAGP9* MP-GPI, *AtAGP58* MP-GPI and *AtPrx34* MP-CTE at the 3' of the FP with *Sac*I/*Bam*HI, to finally generate the constructs e35S:SP9-FP-MP-GPI9, e35S:SP58-FP-MP-GPI58 and e35S:SP34-FP-MP-CTE34.

II.5.3 Constructions in binary vector

The FP fusions, SP9-FP-MP-GPI9, SP58-FP-MP-GPI58 and SP34-FP-MP-CTE34, from previous section, were PCR amplified using the following primers (engineered restriction sites are underlined): AGP9Fwd_AscI, 5'-ATGGCGCGCCATGGCTCGATCTTTCGCTAT-3', and AGP9Rev_NotI, 5'-ATGCGGCCGCTTAGATCATAAACCAGACGA-3', for SP9-FP-MP-GPI9; AGP58Fwd_AscI, 5'-ATGGCGCGCCATGGCCTCTTCTTTCTCTTC-3', and AGP58Rev_NotI, 5'-ATGCGGCCGCTCAAACGAGGAGAAAATGGG-3', for SP58-FP-MP-GPI58, and Prx34Fwd_AscI, 5'-ATGGCGCGCCATGCATTTCTCTTCGTCTTC-3', and Prx34Rev_NotI, 5'-ATGCGGCCGCTCACATAGAGCTAACAAAGT-3', for SP34-FP-MP-CTE34. The amplified products were cloned in the binary vector pGreenII235 (Hellens et al., 2000) downstream 35S promoter using *Asc*I/*Not*I.

II.5.4 Cloning of promoters and production of Prom:FP-fusion lines

The genomic DNA from Arabidopsis leaves was purified by the CTAB protocol described previously by Doyle and Doyle (1987). The promoter regions of *AtAGP9*, *AtAGP58* and *AtPrx34* (SAP Arabidopsis Promoterome Database; www.psb.ugent.be/promoter) were amplified by PCR, using the following primers (engineered restriction sites are underlined): Pr9Fwd_BamHI, 5'-CAGGATCCTCACCACAACCGATAGAATCAT-3', and Pr9Rev_AscI, 5'-ATGGCGCGCCTTTTGCTTTTGCTTTTTCTCTCTGT-3', for *AtAGP9* promoter; Pr58Fwd_BamHI, 5'-CAGGATCCGAGATTTGGGGGGCAAATGGAG-3', and Pr58Rev_AscI, 5'-ATGGCGCGCCGGCTATGTGTGTTTGTGTGTGGAAT-3', for *AtAGP58* promoter; and Pr34Fwd_BamHI, 5'-CAGGATCCTAAAGTCTACTTTTGGTTGGATCTGTG-3', and Pr34Rev_AscI, 5'-ATGGCGCGCCTTTTGAAAGAGGAAAAACAAAACTAG-3', for *AtPrx34* promoter. The amplified products were cloned into the binary vector pGreenII235, upstream the respective FP-fusions (see previous section), removing the 35S promoter with *Bam*HI/*Asc*I.

II.5.5 Isolation of Arabidopsis mesophyll protoplasts

For the isolation see section II.3.4. After counting the protoplasts they were left to rest on ice for 30 min. After this incubation, the protoplasts were pelleted and ressuspended to a protoplast concentration of $5x10^6$ cells mL^{-1} using the adequate volume of MMg solution (0.4 M mannitol, 15 mM $MgCl_2$ and 4 mM MES, pH 5.7). At this point, the protoplasts were ready for transformation.

II.5.6 PEG-mediated transformation of protoplasts

Polyethylene glycol-mediated transient expression of the fusion constructs was performed according to the procedure described previously by Yoo et al. (2007), with some modifications. 20 µg of DNA of FP-fusion constructs were separately mixed to 100 µL of protoplast suspension. Plasmid DNA used for protoplast transformation was isolated using the QIAGEN Plasmid Midi Kit following the manufacturer's instructions. 110 µL of a PEG solution (200 mM mannitol, 100 mM $CaCl_2.2H_2O$, and 40% (w/v) polyethylene glycol 4000) was slowly added (drop by drop) and gently blended, followed by incubation for 10 min at RT. Next, 440 µL of RT W5 solution were added drop by drop and then the protoplasts were precipitated by a 600 rpm centrifugation for 2 min, with acceleration and deceleration set at the minimum. The pellet was ressuspended in 100 µL of new W5 solution and then diluted up to 1 mL W5. Transformed protoplasts were incubated in the dark at 25ºC. For observation cells were placed on slides and fluorescence was examined using a confocal microscope (Leica SP2 AOBS SE). For visualization of CFP the excitation wavelength was 458 nm and for YFP was 514 nm.

II.5.7 *Agrobacterium*-infiltration of tobacco leaves

Agrobacterium-mediated transient expression of the binary constructs in *N. tabacum* was carried out as describe in Sparkes et al. (2006), with some modifications. Liquid LB medium supplemented with the appropriate antibiotics was inoculated with the *Agrobacterium* GV3101 clones of interest and the cultures were grown ON at 28ºC with vigorous agitation until reaching an OD_{600} = 1.5-2 (stationary phase). 1 mL of culture were centrifuged at 1,000 rpm for 10 min at RT, the supernatant was discarded, and the bacterial pellet was ressuspended in infiltration buffer (10 mM $MgCl_2$ and 10 mM MES, pH 5.6-5.8) with 100 µM acetosyringone. The bacterial suspensions were diluted with infiltration buffer to adjust the inoculum concentration to an OD_{600} = 0.1-0.3. Infiltration was done using a syringe and pressing it against the abaxial leaf epidermis

of the tobacco leaves. The infiltrated plants were incubated at 21ºC, under a 12 h photoperiod, prior to observation. The expression and localization of CFP and YFP in Agro-infiltrated leaves was monitored by observation of fresh hand-cut sections of the leaves under the confocal microscope (Leica SP2 AOBS SE).For visualization of CFP the excitation wavelength was 458 nm and for YFP was 514 nm.

II.5.8 Arabidopsis Col0 stable transformation by floral dipping

Agrobacterium-mediated stable expression of the FP fusions in binary vector in Arabidopsis was carried out as described in Zhang et al. (2006), with some modifications. An *Agrobacterium* GV3101 transformed with each construct was grown ON in 5 mL LB medium supplemented with antibiotics. 2.5 mL of this culture were diluted 1:100 in LB medium with antibiotics and grown 24 h at 28ºC. After centrifugation at 4,000 *g* during 10 min at RT, the bacteria were ressuspended in 250 mL of 5% (w/v) sucrose with 0.05% (v/v) Silwett L-77 (Lehle seeds). Healthy plants around stage 6.0 (Boyes et al., 2001) had their inflorescences gently dipped in and out several times in the *Agrobacterium* solution during 30 s and were maintained horizontally in a transparent plastic bag for ON, after which the plastic bag was open and plants were transferred to the growth chamber until seeds were collected. Transformed seeds were selected by germinating in medium supplemented with 20 μg mL^{-1} of the selection marker glufosinate-ammonium (BASTA, Sigma).

II.6 Expression profiles of *AtAGP9* and *AtAGP58* in *Arabidopsis thaliana* using FP reporter genes under the control of the endogenous promoters

II.6.1 Plant material

Arabidopsis thaliana of the accession Col0 plants were grown at 21ºC in a growth chamber, under a 12 h light photoperiod, using white fluorescent light at 35 µmol $m^{-2}s^{-1}$.

II.6.2 Expression profile of *AtAGP9* and *AtAGP58* in Arabidopsis

Plants stably transformed with the endogenous promoter CFP-fusions from section II.5.8 were observed under the confocal microscope (Leica SP2 AOBS SE). For visualization of CFP the excitation wavelength was 458 nm. Propidium iodide (PI) was used in seedlings to counterstaining the cell wall in roots. The excitation wavelength used for PI was 543 nm.

II.7 Fluorescent protein-fusion markers for vacuole and plasma membrane for transient or stable transformation in plants

II.7.1 Plant material

Arabidopsis thaliana of the accession Col0 and *Nicotiana tabacum* (L.) cv. Petit Havana SR1 plants were grown at 21ºC in a growth chamber, under a 12 h light photoperiod, using white fluorescent light at 35 µmol m^{-2} s^{-1}.

Catharanthus roseus (L.) G. Don (cv. Little Bright Eye) plants were maintained at 25ºC, in a growth chamber, under a 16 h white fluorescent light photoperiod, at 70 µmol m^{-2} s^{-1}.

Vitis vinifera (L.) Cabernet Saugvignon Berry cell culture was grown at 25ºC, in the dark, on an orbital shaker at 100 rpm.

II.7.2 Construction of FP fusion proteins

See section II.5.2.

II.7.3 Isolation of Arabidopsis mesophyll protoplasts

See section II.5.5.

II.7.4 Isolation of *C. roseus* mesophyll protoplasts

See section II.1.3.

II.7.5 Isolation of *N. tabacum* mesophyll protoplasts

The method is the same as for *C. roseus* protoplasts, only the enzyme mixture is different: 0.4% (w/v) cellulase and 0.2% (w/v) macerozyme.

II.7.6 Isolation of *Vitis vinifera* protoplasts

One day before the isolation, one week suspension cells was 5 fold diluted in fresh medium. In the following day, the cells were spun down for 1 min at 1,000 rpm at RT and the supernatant was discarded. Protoplasts were isolated as in section II.1.3.

II.7.7 PEG-mediated transformation of protoplasts

See section II.5.6.

II.7.8 Constructions in binary vector

See section II.5.3.

II.7.9 *Agrobacterium*-infiltration of tobacco leaves

See section II.5.7.

III.

RESULTS AND DISCUSSION

III.1 Cell wall and vacuolar arabinogalactan proteins are markers of cell differentiation in the leaves of the medicinal plant *Catharanthus roseus*

In order to investigate the occurrence of a possible interaction between AGPs and Prx, taking advantage of the knowledge about the main *C. roseus* leaf Prx and of the availability of a suite of monoclonal antibodies (mAbs) recognizing several AGP glycosidic epitopes, it was necessary to first characterize the labelling profile of *C. roseus* leaves with those antibodies. Furthermore, the subcellular localization of AGPs was also characterized by immunofluorescence and by cell fractionation.

III.1.1 Idioblasts and laticifers in *C. roseus* leaves

C. roseus has simple, elliptical, mesomorphic leaves (Figure III.1.1A), including an upper and lower epidermis composed of a single cell layer, and a mesophyll clearly differentiated into a single layer of elongated palisade parenchyma cells in the adaxial side, and a thicker spongy parenchyma region in the abaxial side of the leaf (Figure III.1.1B). When leaves of flowering *C. roseus* plants are observed under the fluorescence microscope, a scattered and regular pattern of idioblast cells depicting blue fluorescence can be observed, with a different distribution in the adaxial and abaxial sides of the leaves (Figures III.1.1C and D). Upon observation under the confocal microscope or using cross sections under the fluorescence microscope, it becomes clear that these blue fluorescent idioblast cells are not from the epidermis, but are either from the palisade or spongy parenchyma and are usually slightly bigger and with less chloroplasts than their counterparts (Figures III.1.1F and G). Laticifers can also be clearly observed under the confocal microscope since they depict a similar blue fluorescence to idioblasts and they are present even in small veins (Figure III.1.1E).

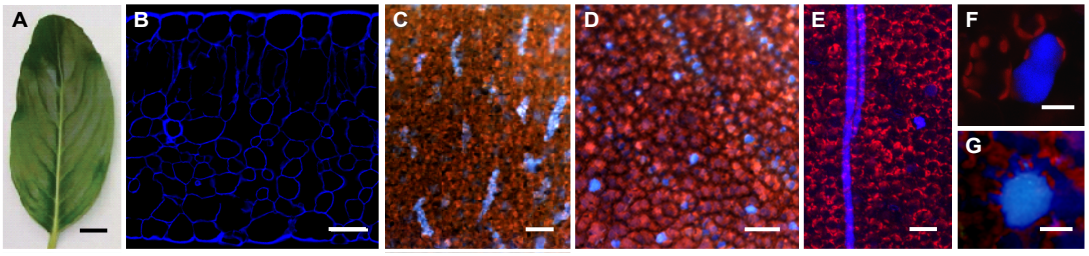

Figure III.1.1 – Different aspects of *C. roseus* leaves. (A) Fully developed leaf. (B) Leaf cross section, with cell walls counterstained in blue with calcofluor. (C) Epifluorescence microscopy image of the abaxial face of a whole mounted leaf. (D) Epifluorescence microscopy image of the adaxial face of a whole mounted leaf. (E) Confocal microscope tangential section of the palisade parenchyma showing two laticifers. (F and G) Epifluorescent microscopy images of

idioblast cells in leaf cross sections. Blue fluorescence is due to the alkaloid serpentine and reveals alkaloid containing idioblast and laticifer cells. Red fluorescence is due to chlorophyll. Scale bar for A, 0.5 cm. Scale bars for B-E, 100 µm. Scale bars for F and G, 20 µm.

III.1.2 AGP glycosidic epitopes are markers of tissue and cell differentiation in *C. roseus* leaves

In order to investigate which AGP epitopes were present in cells and tissues of *C. roseus* leaves, it was decided to use a set of monoclonal antibodies against AGP glycosidic epitopes: JIM8, JIM13, JIM14, JIM16, LM2 and MAC207. We found that all the glycosidic epitopes were present in *C. roseus* mesophyll cells, showing clearly distinct patterns (Figure III.1.2). JIM8, JIM13 and JIM14 seemed to label most types of cells in leaves, including the epidermis, stomata, palisade and spongy parenchyma, idioblasts, laticifers and vascular bundles (Figures III.1.2B-D). On the other hand, JIM16, LM2 and MAC207 showed highly specific labelling: the JIM16 epitope was specifically restricted to vascular bundles, especially in what seems to be xylem vessels (Figure III.1.2F); the LM2 epitope was exclusively localized in stomata and in vascular bundles, apparently in what seems to be vascular parenchyma (Figure III.1.2E); and, interestingly, the MAC207 epitope was specifically localized in the TIA accumulating cells, laticifers and idioblasts (Figure III.1.2A).

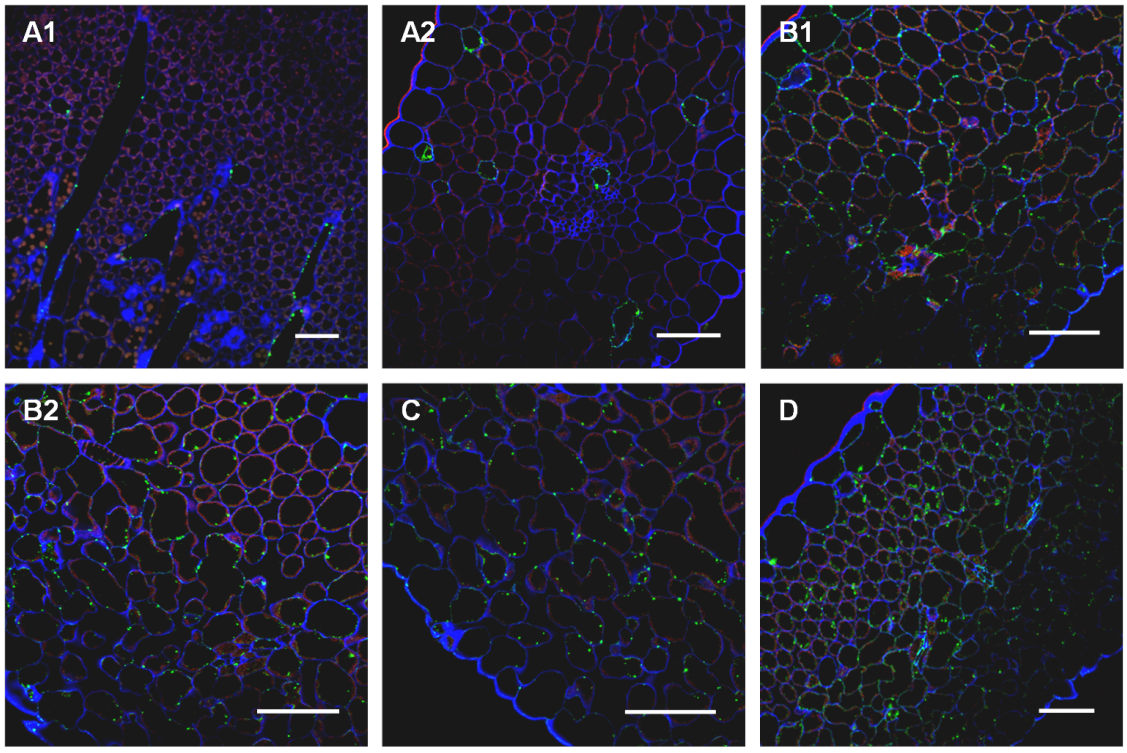

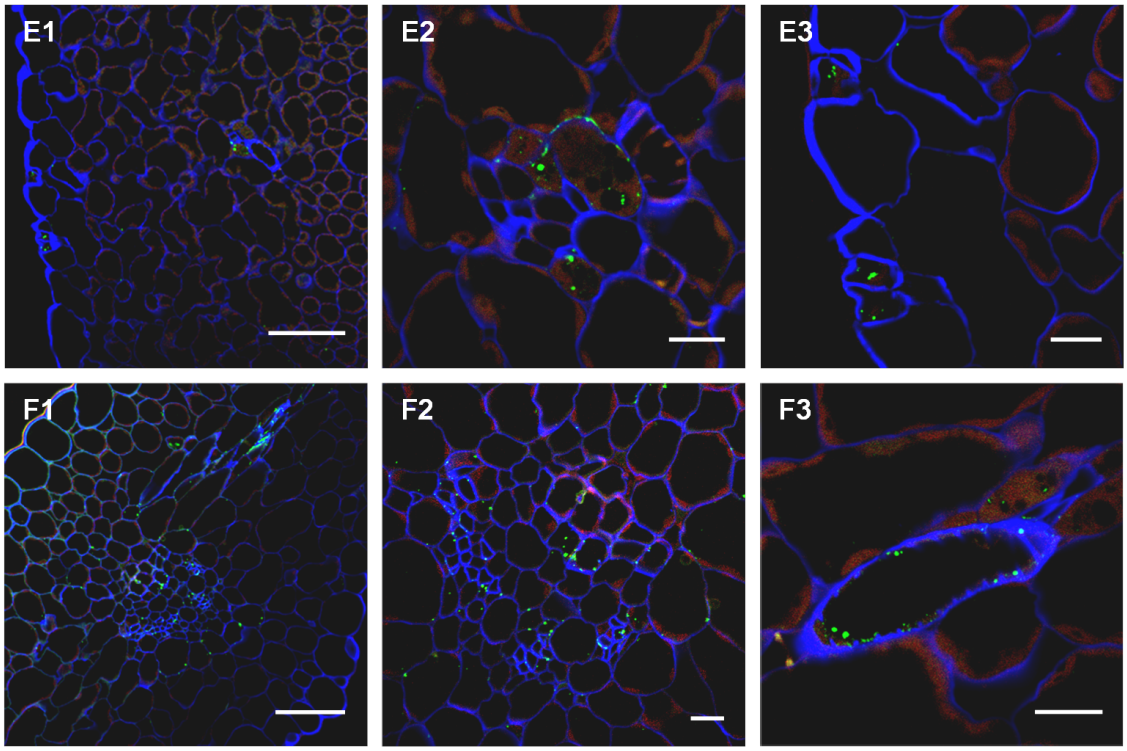

Figure III.1.2 – Green-immunofluorescence localization of AGPs in *C. roseus* leaves, using mAbs recognizing specific glycosidic epitopes. (A) MAC207. (B) JIM13. (C) JIM8. (D) JIM14. (E) LM2. (F) JIM16. Cell walls were counterstained with calcofluor (blue fluorescence). Autofluorescence of chloroplasts in red. Scale bars for A-E1 and F1, 50 µm. Scale bars for E2-E3 and F2-F3, 10 µm.

The glycosidic epitopes of AGPs recognized by mAbs have shown organ-, tissue- and cell-specific labelling patterns in many plant species, indicating that AGPs are markers of cellular identity and fate (Knox, 1997). JIM8 and JIM13 have often shown developmentally regulated labelling of specific cells during sexual reproduction and embryogenesis, and they have also been associated specifically to the phloem in roots (Pennell et al., 1991; Knox, 1997; Samaj et al., 1998; Showalter, 2001; Pereira et al., 2006; Coimbra et al., 2007). JIM13 has been further associated to differentiating xylem cells, but in the shoot apex of *Asclepias speciosa* it labelled most cells including laticifers (Casero et al., 1998; Serpe et al., 2002). MAC207 was shown to bind to the plasma membrane of all cells of the carrot root apex (Knox et al., 1989) and, although some cell-specific labelling has been sometimes referred in tissues involved in sexual reproduction, the localizations reported for this epitope are normally general, including the bulk of mesophyll cells in several plants (Showalter, 2001). On the other hand, Serpe et al. (2002) detected very low labelling by MAC207 in the laticifers of *Asclepias speciosa.* The epitope recognized by LM2 has been localized in most cells of maize roots, including vascular parenchyma, epidermal cells and pericycle cells, and it was shown to increase in embryogenic callus, being present in most of the cells, although

with more intensity in the protodermal layer of early globular-shaped embryos (Saare-Surminski et al., 2000; Samaj et al., 2000). In *Asclepias speciosa*, LM2 did not label laticifers but specifically labelled sieve tubes (Serpe et al., 2001). Our results seem to add to this complexity, since the usually specific JIM8, JIM13 and JIM14 are present in all leaf cell types of *C. roseus*, including mesophyll, epidermis, laticifers, and idioblasts. On the contrary, the usually less specific MAC207 shows a highly specific localization in the alkaloid accumulating cells of *C. roseus* leaves, the laticifers and idioblasts. LM2 and JIM16 have also a highly specific pattern in *C. roseus* leaves, with LM2 labelling only what seems to be vascular parenchyma cells and the stomata, and JIM16 labelling the vascular bundle.

Here, it is shown that the MAC207 epitope (Figures III.1.2A and III.1.3A) is an identity marker of alkaloid accumulating cells, laticifers and idioblasts, which present distinctive blue autofluorescence (Figures III.1.1C – G) and accumulate indole alkaloids (Yoder and Mahlberg, 1976; Eilert et al., 1985; Mersey and Cutler, 1986). More recently, localization of several transcripts and enzymes from the indole alkaloid biosynthetic pathway predicts that the initial biosynthetic steps occur in the epidermis, while late steps take place in laticifers and idioblasts, thus requiring the intercellular translocation of a pathway intermediate (St-Pierre et al., 1999; Guirimand et al., 2011). Nothing is known about the long distance transport of the indole alkaloids in *C. roseus*, but it is appealing to hypothesize that MAC207 epitopes may be involved in a recognition process determining uptake of the translocated alkaloid intermediates specifically into laticifers and idioblasts.

III.1.3 AGPs are localized in the cell wall and the vacuole of *C. roseus* leaf cells

Immunolocalization of the AGPs glycosidic epitopes in *C. roseus* leaves has also provided information on their subcellular localization. JIM8, JIM13, JIM14 and MAC207 all seemed to label epitopes placed both in the plasma membrane/cell wall and in the membrane of the vacuole, with a quite important proportion being present in this late location (Figure III.1.3).

In order to further characterize the unusual presence of AGPs in the vacuole observed upon immunodetection, protoplasts of *C. roseus* leaves were isolated and investigated for the presence of soluble and membrane associated total AGPs using rocket electrophoresis in Yariv-containing gels. Figure III.1.4 shows that protoplasts possess a high quantity of total soluble AGPs when compared with total soluble AGPs present in leaf extracts – more than half, when considering the concentration of AGPs

relative to the total protein in each crude extract. Since the leaf soluble protein fraction had been obtained using a low salt extraction buffer, it was hypothesized that maybe much of the cell wall soluble proteins, including AGPs, could have stayed ionically bound to the cell wall fraction discarded during extraction, leading to an underestimation of leaf soluble AGPs in Figure III.1.4, and therefore to an overestimation of the proportion of soluble AGPs in protoplasts. Hence, in a new extraction, the cell wall pellet was washed with high salt buffer and, after volume equalization, the several fractions were again analyzed by Yariv rocket electrophoresis (Figure III.1.5). In fact, there were soluble AGPs that had stayed bounded to the cell wall pellet, but this accounted only for around 10% of the total amount of soluble AGPs, indicating that the previous conclusion on the presence of a high proportion of soluble AGPs in protoplasts is valid. Soluble AGPs present in protoplasts can be understood as mainly localized in the vacuole, since the only other possible localization is within the secretory pathway, which is a transitory localization and could not account for such a big accumulation of AGPs. Therefore, these results suggest that a big part of the soluble AGPs present in the leaf extracts are actually present in vacuoles, rather than in the cell wall, indicating that this localization may have functional relevance rather than being a recycling terminus.

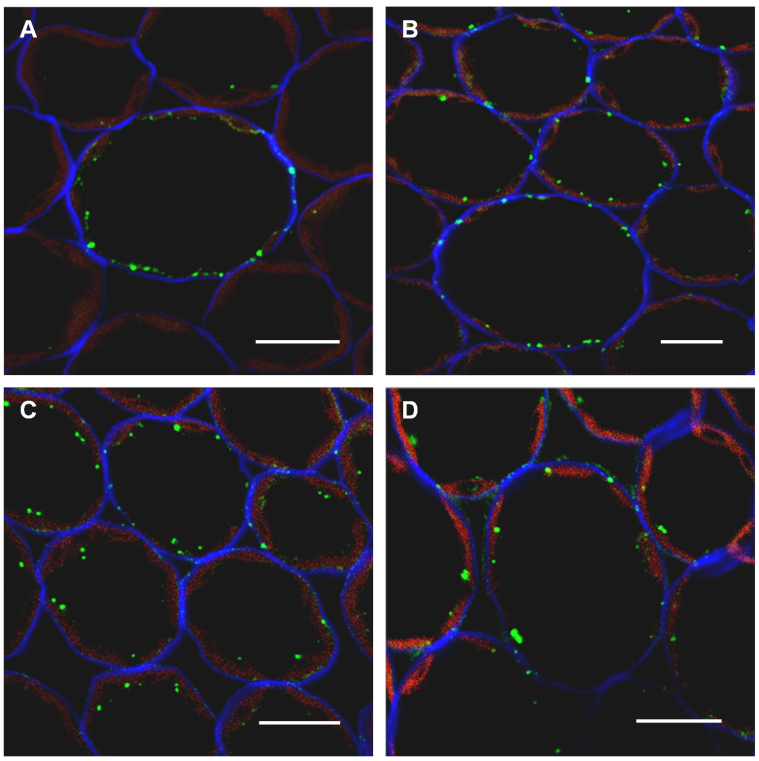

Figure III.1.3 – Green-immunofluorescence localization of AGPs in *C. roseus* leaves, using mAbs recognizing specific glycosidic epitopes. (A) MAC207. (B) JIM13. (C) JIM8. (D) JIM14. Cell walls were counterstained with calcofluor (blue fluorescence). Autofluorescence of chloroplasts in red. Scale bars, 10 µm.

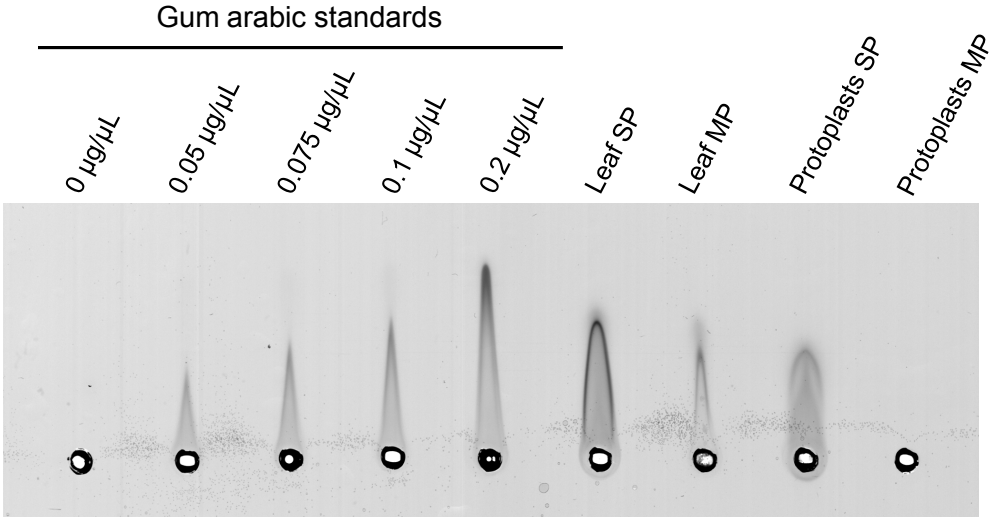

Figure III.1.4 – Yariv rocket electrophoresis of soluble proteins (SP) and membrane proteins (MP) extracted from leaves and leaf protoplasts from *C. roseus*. Wells were loaded with equal amounts of protein of each fraction, diluted to the same volume used for the standards, except for Protoplasts MP, which was loaded with 5x less protein. Concentrations calculated by densitometry were 0.40 µg/µL for Leaf SP, 0.10 µg/µL for Leaf MP and 0.24 µg/µL for Protoplasts SP.

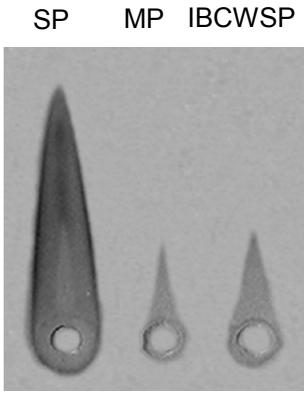

Figure III.1.5 – Rocket electrophoresis in a an agarose gel containing Yariv reagent of soluble proteins (SP), membrane proteins (MP) and soluble proteins ionically bound to the cell wall (IBCWSP) extracted from leaves. Wells were loaded with 18 µL of fractions with equalized volumes.

Immunodetection of JIM8 and JIM13 AGP epitopes in the soluble and membrane protein fractions of leaves and leaf protoplasts was also investigated and showed an intense labelling in the soluble proteins of protoplasts, similarly to the observed for total AGPs (Figure III.1.6A). Considering that the membranes present in the protoplast fraction and the leaves are the same, we can compare the results obtained for the soluble protein fractions after equalization based on the results obtained for membrane fractions. If that is done using the densitometry values measured (Figure III.1.6A), the amount of JIM8 and JIM13 soluble AGPs estimated is actually higher for protoplast than leaf extracts, what should be impossible. This may be a consequence of some kind of bias introduced by using such different biological materials as protoplasts and

whole leaves. Another interesting explanation could be that the stress induced by the preparation of protoplasts could in fact induce the biosynthesis and secretion of AGPs, which could actually be highly present inside the cells, in transit through the secretory system to the cell surface, for protection purposes and/or to the vacuoles, for unknown functions. In any case, and as before, this strongly indicates that a big part of leaf soluble AGPs are actually present in vacuoles, rather than in the cell wall.

Comparing the results obtained for the extracted protein fractions with the ones obtained for the tissue sections, it is striking that the first indicates prevalence of the AGP epitopes and total AGPs in soluble proteins (Figures III.1.4 – III.1.6), while the second shows labelling mainly associated with membranes. This seems to suggest that either soluble AGPs are loosely associated with the membranes, or that the GPI anchor mediated membrane association of AGPs to the plasma membrane or the tonoplast is broken during the extraction procedure, either by mechanical stress or by contact with otherwise inaccessible phospholipases. If this is true, the protoplast soluble AGPs could also result from *in vivo* plasma membrane bound AGPs, and not only from vacuoles as interpreted above, even if immunolabelling of tissue sections also supports the major vacuolar localization. On the other hand, since we did not perform immunolocalization in isolated protoplasts, the question remains whether these naked cells may be enriched in plasma membrane or secretory AGPs with a protection role. To clarify this, vacuoles were isolated with high purity from leaf protoplasts (Carqueijeiro, 2013), and the relative immunolabelling of soluble and membrane protein fractions of protoplasts and vacuoles was compared (Figure III.1.6B). The two samples were normalized by the total number of protoplasts and vacuoles, considering a 1:1 ratio of protoplasts:vacuoles. JIM8 and JIM13 AGP epitopes showed relatively similar labelling in the soluble proteins of both protoplasts and vacuoles (Figure III.1.6B), meaning that most of the labelling present in the soluble proteins of protoplasts is indeed present in the vacuoles and not in the secretory pathway. Furthermore, this experiment also showed the presence of a quite significant relative labelling in the membrane proteins of vacuoles, meaning that JIM13 and JIM8 AGPs are definitely present in the tonoplast with a high relative abundance (Figure III.1.6B).

As a whole, both immunolabelling and cell fractionation studies converge to indicate a quite conspicuous and organized localization of the AGP epitopes in the tonoplast, suggestive of functional relevance.

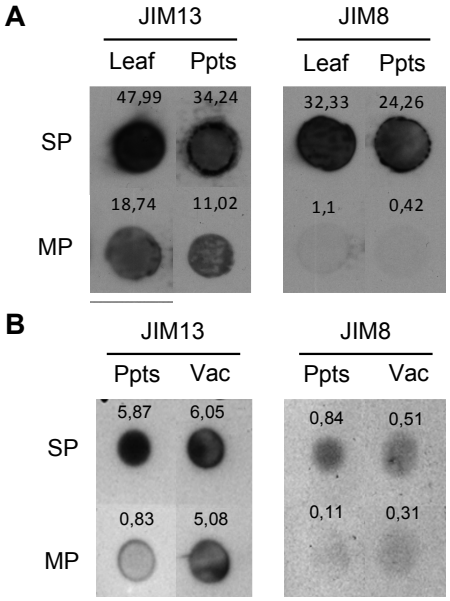

Figure III.1.6 – Immunodetection of JIM8 and JIM13 AGP epitopes in dot blots of soluble proteins (SP) and membrane proteins (MP) extracted from leaves, protoplasts and vacuoles. (A) Comparative labelling between SP and MP fractions from leaf and leaf protoplasts. The protein load was equal for the two SP fractions and for the two MP fractions, with the SP load being 2.5x the one of MP. (B) Comparative labelling between SP and MP fractions from leaf protoplasts and leaf vacuoles. Loading was normalized by the number of protoplasts and vacuoles used to obtain the extracts, considering a 1:1 ratio of protoplasts:vacuoles. Values above each dot correspond to the volume (optical density*area) of signal intensity measured by densitometry.

III.1.4 AGPs are organized in membrane microdomains

Observation of the immunodetection of AGP epitopes in *C. roseus* leaves clearly showed that these epitopes appeared as individual spots with a patchy distribution, suggesting an organization in membrane microdomains both at the level of the plasma membrane and the tonoplast (Figure III.1.3) (Sottomayor et al., 2008). The first time MAC207 was characterized, Pennell et al. (1989) observed that the plasma membrane in protoplasts from sugar beet culture cells presented a continuous labelling, but the plasma membrane of protoplasts from carrot cultured cells showed “patches” of labelled epitopes, a type of localization that has also been observed by other authors (Coimbra et al., 2007). This patched or punctuated distribution observed for AGPs correlates interestingly with the set of data indicating the existence in plant plasma membranes of microdomains, called lipid rafts. These microdomains are proposed to host GPI-anchored proteins, such as AGPs, and a subset of integral and peripheral cell surface proteins which interact to perform specific functions (Bhat and Panstruga, 2005). This particular localization may have a functional meaning, since AGPs may interact specifically with other protein co-localized in the microdomains to fulfil their functions, namely with Prxs, which are shown in the following section to co-localize in these microdomains.

III.2 Class III peroxidases and arabinogalactan proteins in *Catharanthus roseus*

In this section, the capacity of Prxs to interact *in vitro* and *in vivo* with AGPs was investigated in the leaves of *C. roseus*, taking advantage of the fact that the Prx isoenzyme complement of its leaves has been shown to be composed mainly by a single protein, CroPrx1, which has been thoroughly characterized (Sottomayor et al., 1998; Costa et al., 2008).

III.2.1 Class III peroxidases are reduced by *C. roseus* arabinogalactan proteins

In order to investigate if Prxs can interact with AGPs it was decided to use the well-characterized CroPrx1 from *C. roseus*. Investigation of the Prx profile of *C. roseus* leaves through IEF shows one major Prx isoenzyme detected using the high affinity artificial Prx substrate 4-MN that was previously characterized as CroPrx1 (Figure III.2.1) (Costa et al., 2008). IEF analysis further reveals that CroPrx1 is the major detectable Prx in the apoplastic fluid and vacuoles, confirming CroPrx1 as the main Prx in *C. roseus* leaves for the two possible subcellular localizations of Prxs. Since CroPrx1 was shown to be localized in the cell wall, where AGPs are also located, CroPrx1 was purified in order to evaluate its capacity to accept AGPs as substrates and to perform *in vitro* cross-linking assays of AGPs. For purification of CroPrx1, 300 g of leaves were used for a purification procedure involving ammonium sulfate precipitation and 4 chromatographic steps that enabled a high purification of CroPrx1 - 2067 fold (Table III.2.1)

Figure III.2.1 – Peroxidase isoenzyme profile obtained by isoelectric focusing for protein extracts of *C. roseus* leaves (Leaf), leaf cell wall fluid (CW) and leaf vacuoles (Vac).

Table III.2.1 - Purification of CroPrx1 from *C. roseus* leaves.

Purification step	Total activity (nKat)	Specific activity (nKat/mg)	Yield (%)	Purification (fold)
Crude extract	4300	1.9	100	1
> 30% $(NH_4)_2SO_4$	3919	3.8	91	2
Phenyl Sepharose	2651	13.9	62	7
Concanavalin A	1342	82.1	31	43
Sephacryl S200	1044	388.2	24	204
HitrapCaptoS	79	3927.0	2	2067

The capacity of purified *C. roseus* AGPs to reduce the catalytic intermediates of CroPrx1 and of horseradish peroxidase type II was investigated, to determine whether AGPs might function as substrates of CroPrx1 and of Prxs in general. During the catalytic cycle of Prxs, the native ferric form (Fe^{3+}) suffers a single two-electron oxidation by H_2O_2 to give compound I (CoI):

$$Fe^{3+} + H_2O_2 \xrightarrow{k_1} CoI + H_2O.$$

CoI then experiences two successive one-electron reductions by molecules working as Prx substrates, returning to the native form (Fe^{3+}) through the intermediate compound II (CoII):

$$CoI + RH \xrightarrow{k_2} CoII + R^{\bullet}$$
$$CoII + RH \xrightarrow{k_3} Fe^{3+} + R^{\bullet}.$$

These peroxidase intermediate forms (Fe^{3+}, CoI, and CoII) can be easily distinguished by their absorbance spectra (Figure III.2.2): Fe^{3+} has a maximum at 403 nm, CoI at 395 nm, and CoII has a maximum at 418 nm. Thus, the capacity of purified *C. roseus* leaf AGPs to act as substrates of CroPrx1 was investigated by following the rate of conversion between the Prx catalytic intermediates in the presence of AGPs.

H_2O_2 and AGPs purified from *C. roseus* leaves were sequentially added to CroPrx1, and consecutive absorbance spectra of the enzyme were detected in a spectrophotometer, to evaluate the interconversion between the different CroPrx1 catalytic intermediates (Figure III.2.3A). Upon addition of H_2O_2 to the native ferric form of the enzyme, the transition of the ferric form to CoI and CoII occurred, with the exclusive accumulation of CoII as the only stable intermediate (trace 1, Figure III.2.3A). Upon addition of AGPs, CoII was totally reduced to the Fe^{3+} form (trace 2-11, Figure

III.2.3A). The disappearance of CoII can be clearly correlated with Fe^{3+} reappearance/formation, proving their interconversion, and confirming the absence of CoI. Since CoI formation and decay was too fast to be detected, its conversion rates could not be estimated. On the other hand, the CoII reduction step was the limiting step during the reaction with AGPs, so the time course of CoII reduction during the reaction with AGPs was plotted as a function of time, against the control in the absence of substrate (Figure III.2.3B). The addition of AGPs significantly accelerated CoII reduction in comparison with the control, clearly indicating the capacity of AGPs to act as a CroPrx1 reducing substrate.

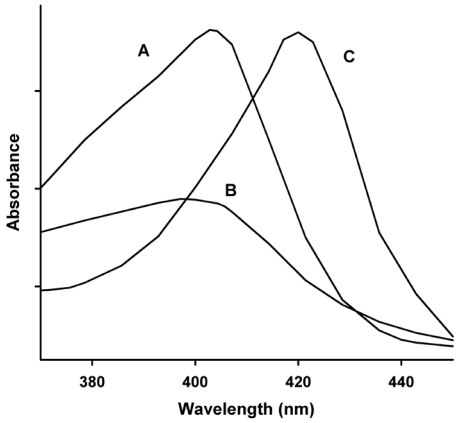

Figure III.2.2 – Visible absorption spectra of the catalytic intermediates of Prx. (A) Native ferric form. (B) Compound I. (C) Compound II. Adapted from Sottomayor (1998).

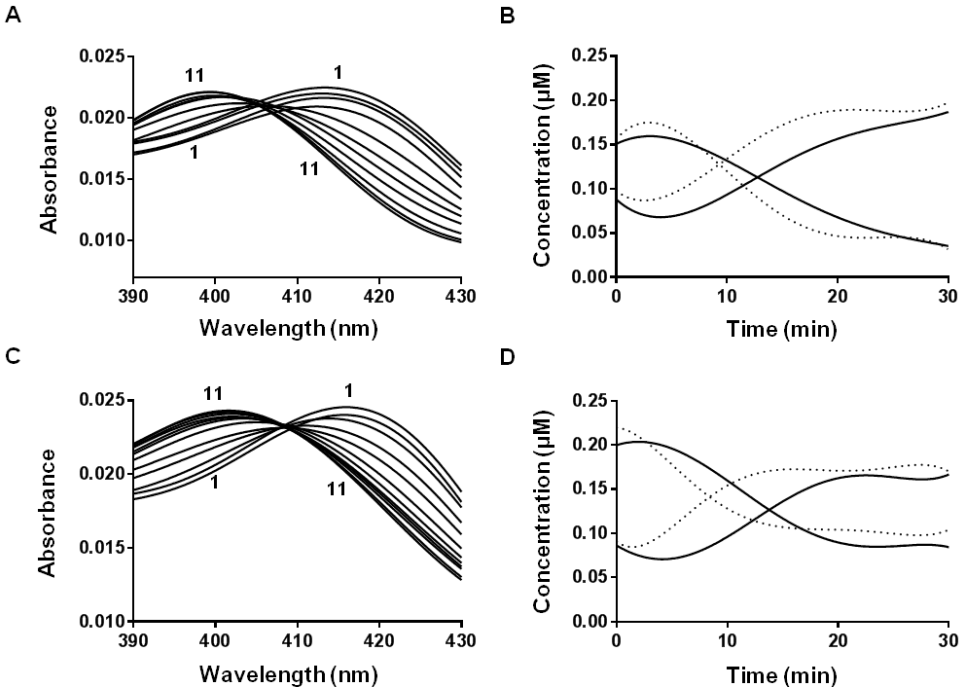

Figure III.2.3 – Reduction of Prxs by AGPs. (A) Consecutive absorbance scans of 0.25 µM CroPrx1 after the consecutive addition of 0.5 µM H_2O_2 and 20 µg ml^{-1} AGPs purified from *C. roseus* leaves. Trace 1, scan after addition of

H_2O_2. Trace 2-11, scans after addition of AGPs, measured at 2, 5, 7, 9, 13, 15, 17, 21, 27 and 31 min. (B) Time course of the evolution of CroPrx1 CoII (upper trace at 0 min) and native form (lower trace at 0 min) in the presence (·····) and absence of AGPs (——) determined for the reaction shown in A. (C) Consecutive absorbance scans of 0.25 μM horseradish peroxidase II after the consecutive addition of 0.5 μM H_2O_2 and 20 μg ml^{-1} AGPs purified from *C. roseus* leaves. Trace 1, scan after addition of H_2O_2. Trace 2-11, scans after addition of AGPs, measured at 2, 5, 7, 9, 13, 15, 17, 21, 27 and 31 min. (D) Time course of the evolution of horseradish peroxidase II CoII (upper trace at 0 min) and native form (lower trace at 0 min) in the presence (·····) and absence of AGPs (——) determined for the reaction shown in C.

In order to ascertain whether the capacity of accepting AGPs as a substrate was a specific feature of CroPrx1, or rather a general property of Prxs, the capacity of the enzyme model horseradish peroxidase to accept AGPs as substrate was investigated (Figures III.2.3C and D). Results show that CoII from horseradish peroxidase type II is also reduced by AGPs, indicating that the capacity to oxidize AGPs is a general feature of Prxs. When the K_m for AGP oxidation by CoII from both enzymes was estimated (Figure III.2.4), it was shown to be lower for CroPrx1 (0.79 μg ml^{-1}) than for horseradish peroxidase type II (1.36 μg ml^{-1}), indicating a higher affinity of CroPrx1 for AGPs coming from the same species/organ.

These results further extend the potential multifunctionality of CroPrx1, previously shown to also accept as substrates several *C. roseus* alkaloids and phenolic compounds (Costa et al., 2008; Ferreres et al., 2011), at the same time it adds a new general substrate to Prxs - AGPs. This multifunctionality and overlapping substrate profile is indeed a hallmark of Prx isoenzymes that renders quite difficult the characterization of *in planta* Prx functions (Sottomayor and Ros Barceló, 2004).

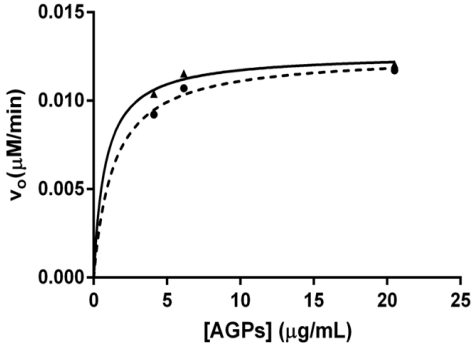

Figure III.2.4 – Michaelis-Menten plot of the rate of CoII reduction by AGPs. ·●· HrPrxII. —▲— CroPrx1.

III.2.2 CroPrx1 mediates intra and inter-molecular cross-linking of AGPs *in vitro*

In order to investigate if the oxidation of AGPs by CroPrx1 was capable of mediating cross-linking reactions, several monoclonal antibodies (mAbs) were used. These mAbs

were prepared against the glycosidic epitopes from purified AGPs of different plant sources (Pennell et al., 1989; Knox et al., 1991; Pennell et al., 1991; Smallwood et al., 1996) and have been extensively used for studies of AGP function (Pennell and Roberts, 1990; Stacey et al., 1990; Knox et al., 1991; Pennell et al., 1991; Schindler et al., 1995; Toonen et al., 1997; Samaj et al., 1998; Samaj et al., 2000; Showalter, 2001; Pereira et al., 2006; Coimbra et al., 2007). Therefore, the glycosidic epitopes they recognize are considered as representative of AGPs. The possibility that those epitopes may eventually be associated to other macromolecules cannot be ruled out, but these would also be functionally important, since it's precisely the specific localization of these epitopes that have often implicated AGPs in distinct developmental functions.

Soluble and membrane protein fractions were incubated in the presence of CroPrx1 and H_2O_2, and changes in molecular weight were investigated through gel filtration chromatography followed by immuno-dot-blot analyses of the different molecular weight sub-fractions. The rationale was that Prx could mediate inter-molecular cross-linking of AGPs, namely with other cell wall macromolecules, with the correspondent changes in molecular weight being detected as a shift in the labelling of the different gel filtration fractions. Due to the use of gel filtration, the cellular fraction referred to as membrane fraction actually enabled only the detection of membrane associated proteins. Densitometry of the fractions obtained was used to construct the graphics presented in Figure III.2.5. Incubation of the soluble fraction in the presence of CroPrx1 and H_2O_2 leads to the increase of the size of AGPs recognized by mAbs JIM8 and JIM13, suggesting the occurrence of inter-molecular cross-linking (Figures III.2.5A and C). The increase in molecular weight is very high, from 38, 76 and 180 kDa to a broad peak maxing around 580 kDa for JIM8 and around 460 kDa for JIM13. Surprisingly, the incubation in the presence of CroPrx1 and H_2O_2 also increased the intensity of labelling by both JIM8 and JIM13, meaning a higher quantity of epitopes, this effect being particularly noteworthy for the membrane associated fraction (Figures III.2.5B and D). Integration of the area of the peaks by the trapezoidal method revealed that labelling by JIM8 and JIM13 increased 4.2 and 4.8 fold respectively in the soluble fraction, and 16 and 15 fold respectively in the membrane associated fraction. This increase is not always clearly evident in Figure III.2.5 due to the logarithmic scale used for plotting the molecular weight. Although some increase in molecular weight was observed in the membrane associated fraction after the enzymatic treatment, the increase in labelling intensity was not clearly associated with an increase in size

(Figures III.2.5B and D), suggesting that the links leading to new epitopes may, at least in part, be intra-molecular.

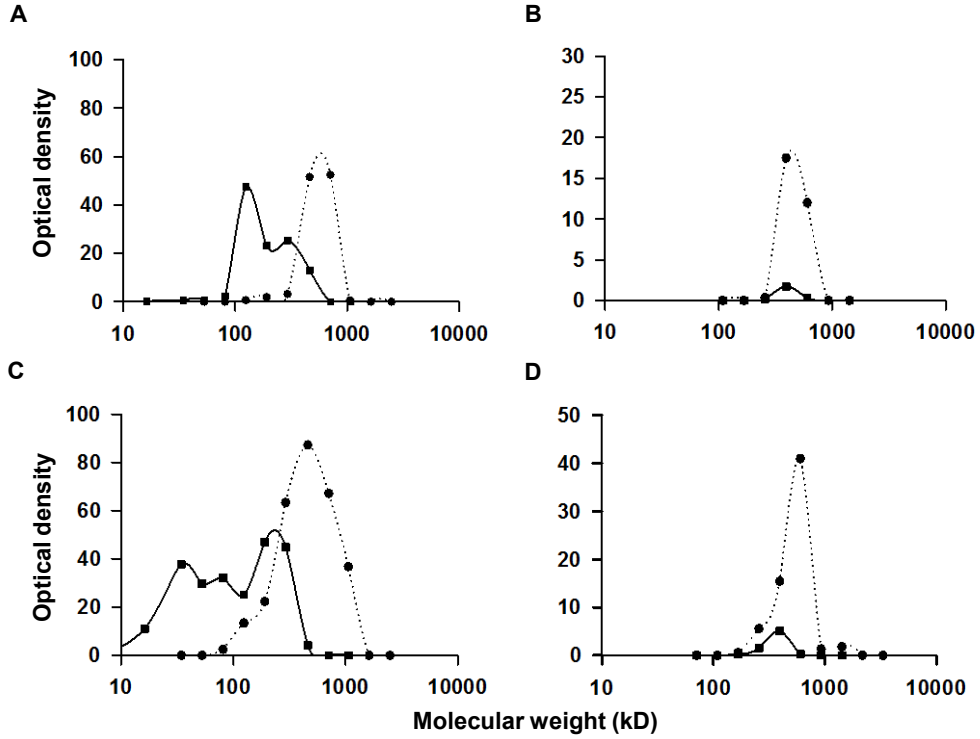

Figure III.2.5 – Changes in the molecular weight and quantity of AGPs recognized by the mAbs JIM8 and JIM13 after incubation with CroPrx1 and H_2O_2, as detected by dot-blot densitometry of fractions resulting from gel filtration. (A and B) JIM8. (C and D) JIM13. (A and C) Soluble proteins. (B and D) Membrane associated proteins. —■— Control reaction in the absence of CroPrx1 and in the presence of 1 mM H_2O_2. ···●··· Reaction in the presence of 100 nM CroPrx1 and 1 mM H_2O_2.

According to Lamport et al. (2006) the soluble fraction includes AGPs that are mainly located in the cell wall and periplasmic space, and it is conceivable that the increase in molecular weight observed may result from cross-linking reactions between different AGP molecules or with other soluble cell wall molecules present in the extracts such as pectins, a type of interaction that has been reported by Immerzeel et al. (2006) and Tan et al. (2013), and that could explain the big increase in size observed. In fact, cell wall AGPs have been suggested to act as pectin plasticizers (Lamport and Kieliszewski, 2005; Lamport et al., 2006) and their cross-linking may thus contribute to increase cell wall resistance/protection properties and inhibit cell expansion, similarly to what has been proposed for extensin (Price et al., 2003; Fry, 2004; Cannon et al., 2008). In any case, our results suggest that Prx-mediated oxidative cross-linking involving AGPs may represent a further mechanism in the dynamics and remodelling of cell wall properties, adding to the proposed roles of Prxs

in the cross-linking of extensins and cell wall polysaccharides, and in the biosynthesis of lignin and suberin.

As a whole, the *in vitro* study clearly demonstrated that CroPrx1 is capable of mediating cross-linking of AGPs originating from the same tissue and subcellular compartment, including inter-molecular cross-linking of soluble and membrane associated AGPs, and what seems to be intra-molecular cross-linking of membrane associated AGPs, leading to newly formed JIM8 and JIM13 epitopes.

III.2.3 Peroxidase-like activity mediates cross-linking of AGPs *in vivo*

CroPrx1-mediated *in vitro* reactions resulted in an increase of labelling by mAbs JIM8 and JIM13. This meant that changes in the labelling of leaf tissues with these mAbs as a result of increasing the availability of H_2O_2 to endogenous CroPrx1 or other Prxs could be investigated, delivering evidence of an *in vivo* activity. Thus, leaves were infiltrated with H_2O_2, which diffuses easily through the apoplast and across membranes to the symplast, becoming available to both cell wall and vacuolar CroPrx1, or other Prx activities present. When leaves were infiltrated with H_2O_2, a clear and quantifiable increase in the intensity of labelling by mAbs JIM8 and JIM13 was observed, indicating the possible occurrence of *in vivo* Prx-mediated links in the construction of *de novo* AGP glycosidic epitopes (Figures III.2.6A, C and D). It is evident that the labelling increase is particularly strong near the abaxial surface of the leaf, showing a decreasing gradient to the adaxial surface, certainly corresponding to the progressive decaying of H_2O_2 starting from the infiltration side. Detailed observation of the labelling suggests that this increase is happening both at the level of the cell wall and at the level of the vacuole (Figure III.2.7). Furthermore, when it was investigated what happened with the epitopes labelled by two other AGP mAbs presenting specific cell labelling in *C. roseus* leaves, LM2 and MAC207, it was observed that their labelling intensity also increased upon infiltration of leaves with H_2O_2 (Figures III.2.6B, E and F). Finally, the increase in the intensity of labelling resulting from infiltration of leaves with H_2O_2 was sensitive to the simultaneous infiltration with the Prx inhibitors KCN and NaN_3, further supporting a role for Prx in the genesis of AGP glycosidic epitopes *in planta* (Figure III.2.6). The concentration of H_2O_2 used for the infiltration of leaves was 10 mM since it produced more evident results than 1 mM and because, although high, it is within the order of magnitude of previously reported physiological concentrations (Neill et al., 2002; Cheeseman, 2006).

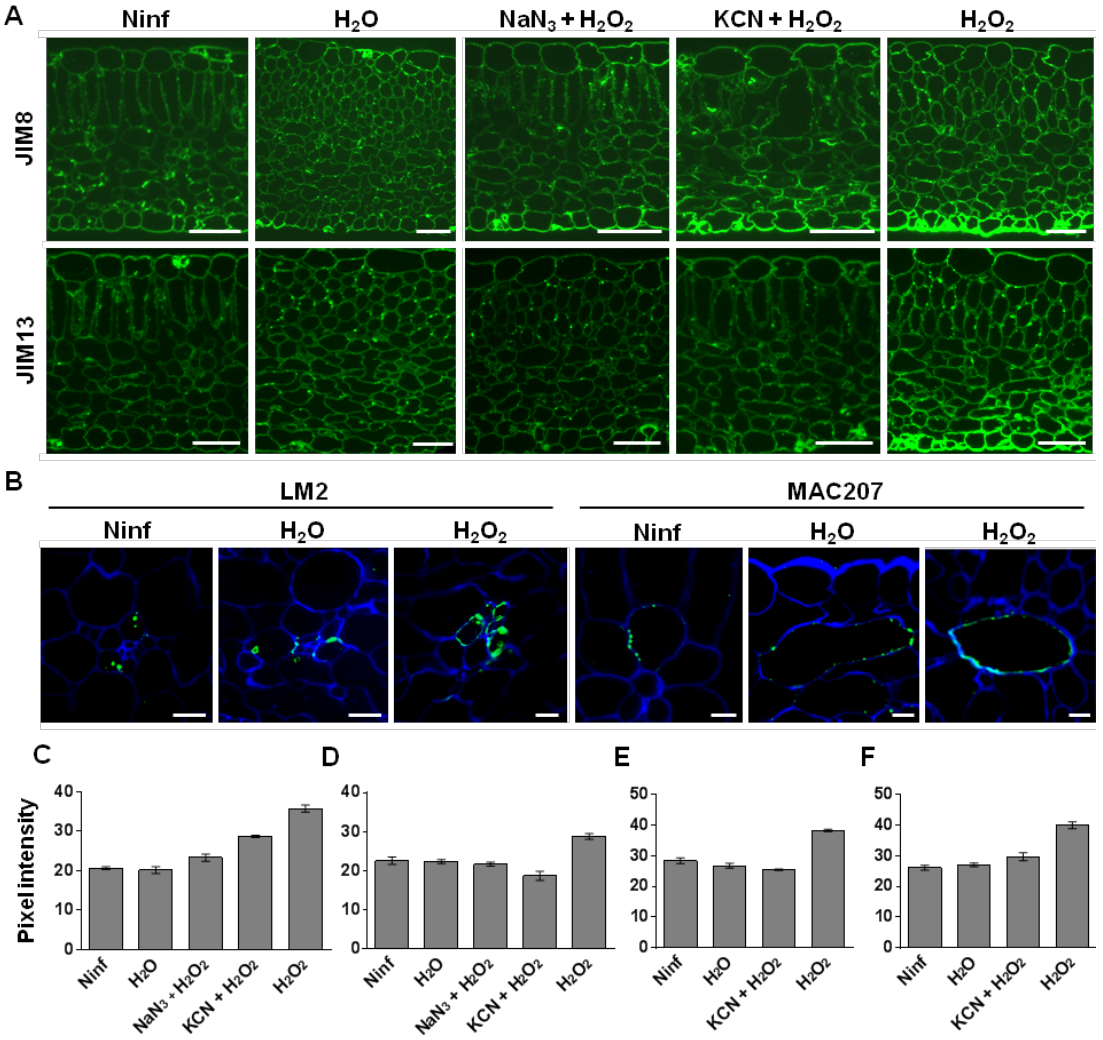

Figure III.2.6 – Green-immunofluorescence localization and intensity of AGPs recognized by several mAbs in *C. roseus* leaves infiltrated with 10 mM H_2O_2 and with 10 mM H_2O_2 plus 2 mM peroxidase inhibitors, NaN_3 and KCN. (A) Labelling with JIM8 and JIM13. (B) Labelling with LM2 and MAC207. Cell walls were counterstained with calcofluor (blue fluorescence). (C to F) Quantification of the labelling intensity obtained for the different treatments when using the several mAbs. (C) JIM8. (D) JIM13. (E) LM2. (F) MAC207. Ninf, non-infiltrated controls. H_2O, water-infiltrated controls. Scale bars for JIM8 and JIM13 images, 50 µm. Scale bars for LM2 and MAC207 images, 10 µm.

III.2.4 AGP epitopes and CroPrx1 co-localize in microdomains of the plasma membrane and the tonoplast of *C. roseus* mesophyll cells

The immunolocalization study performed during the *in vivo* cross-linking experiments also provided information on the subcellular localization of the recognized AGP epitopes. JIM8, JIM13 and MAC207 all seemed to label epitopes placed both in the plasma membrane/cell wall and in the tonoplast (Figures III.2.7, III.2.8A and B). Moreover, most of these epitopes appeared as individual spots with a patchy distribution, suggesting an organization in microdomains. These results confirmed that AGP epitopes were localized in cellular compartments where interaction with CroPrx1

would be possible, the cell wall and the vacuole. This later localization of AGP epitopes has been observed before (Pennell et al., 1989; Herman and Lamb, 1992; Samaj et al., 2000), but has been considered a consequence of AGP turnover with no functional relevance (Showalter, 2001). However, our results show a quite conspicuous and organized localization of the AGP epitopes in the tonoplast, suggestive of functional relevance. Most interestingly, the punctuated localization observed for the AGP epitopes is highly similar to the localization observed for CroPrx1 both in the tonoplast and the plasma membrane/cell wall (Figure III.2.8), and has also been observed by other authors for AGP epitopes (Coimbra et al., 2007).

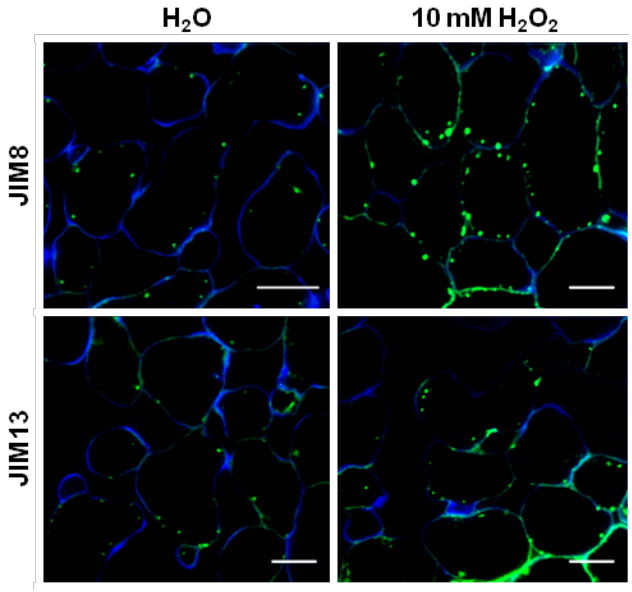

Figure III.2.7 – Green-immunofluorescence fine localization of AGPs recognized by mAbs JIM8 and JIM13 in *C. roseus* leaves infiltrated with H_2O or 10 mM H_2O_2. Cell walls were counterstained with calcofluor (blue fluorescence). Scale bars, 20 µm.

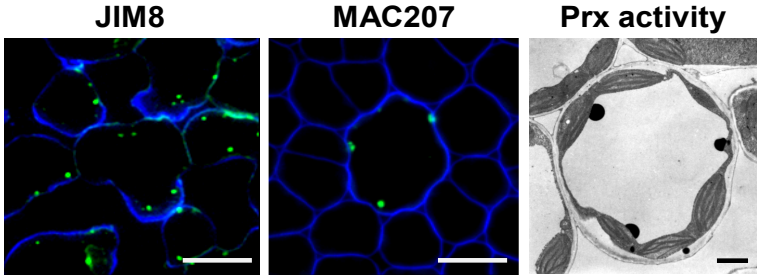

Figure III.2.8 – Green-immunofluorescence localization of AGPs recognized by mAbs JIM8 and MAC207 and cytochemical localization of peroxidase activity in *C. roseus* leaves. Cell walls were counterstained with calcofluor (blue fluorescence). Scale bar for immunofluorescence images, 20 µm. Scale bar for cytochemistry image (adapted from Sottomayor and Barceló (2003)), 5 µm.

The obvious next step was to investigate if CroPrx1 co-localized with AGP epitopes in *C. roseus* mesophyll cells. This was performed using a polyclonal antibody

that recognizes CroPrx1 with high specificity (Figure III.2.9), which was used for co-immunolocalization with the AGP mAbs. The results obtained are shown in Figure III.2.10 and it can be seen that the punctuated localization observed for the AGP epitopes largely overlaps with the localization observed for CroPrx1, both in the tonoplast and the plasma membrane/cell wall, supporting the possibility of *in vivo* interaction between the two.

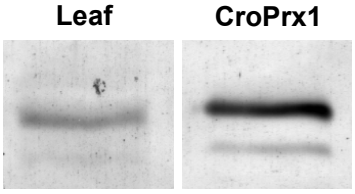

Figure III.2.9 – Western-blot of a protein extract from leaves of *C. roseus* (Leaf) and pure CroPrx1 using anti-Prx.

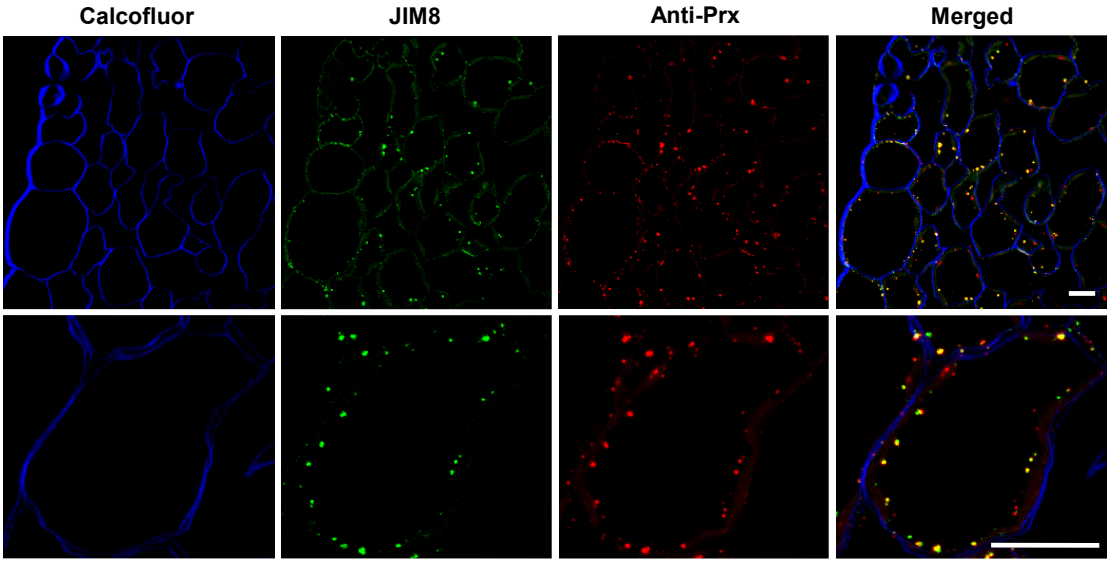

Figure III.2.10 – Immunofluorescence co-localization of Prx and AGPs recognized by mAb JIM8 in *C. roseus* leaves. Cell walls were counterstained in blue with calcofluor. Scale bars, 10 µm.

Therefore, *C. roseus* Prx is capable of mediating cross-linking of AGPs leading to *de novo* formation of the AGP epitopes both *in vitro* and *in vivo*, and the two protein groups co-localize in microdomains of the plasma membrane and the tonoplast of *C. roseus* leaf cells. These results suggest that Prx and AGPs may interact *in vivo* in a reaction dependent on H_2O_2. It is tempting to hypothesize that this interaction may function as a signalling platform responsive to H_2O_2, which has been shown to work as a signal molecule involved in several environmental and developmental processes. This hypothesis is discussed and presented in more detail below, in the last chapter of the thesis.

III.3 Class III peroxidases and arabinogalactan proteins in *Arabidopsis thaliana*

The results of the previous section suggest that Prxs are involved in the construction of AGP glycosidic epitopes and implicate Prxs in the developmental and cell physiology functions attributed to AGPs, with H_2O_2 as an important regulatory molecule. In order to investigate if this putative Prx-AGP interaction is a general feature of plants, and to investigate the physiological meaning of such interaction, the study proceeded to the model plant *Arabidopsis thaliana*.

Therefore, in this section, the capacity of Prxs to interact *in vitro* and *in vivo* with Arabidopsis AGPs was investigated, namely taking advantage of the fact that the Prx isoenzyme complement of Arabidopsis leaves has been shown to be composed mainly by a single protein, AtPrx34 (Figueiredo, 2011).

III.3.1 Class III peroxidases are reduced by Arabidopsis arabinogalactan proteins

In order to investigate if AGPs are a substrate of Prxs in Arabidopsis, it was decided to use AtPrx34, previously characterized in our lab (Figueiredo, 2011). Investigation of the Prx profile of Arabidopsis leaves through IEF shows one major Prx isoenzyme detected using the high affinity artificial Prx substrate 4-MN that was previously characterized as AtPrx34 (Figueiredo, 2011) (Figure III.3.1). IEF analysis reveals that AtPrx34 is the major detectable Prx in the apoplastic fluid and vacuoles of Arabidopsis leaves, confirming AtPrx34 as the main Prx in Arabidopsis leaves for the two possible subcellular localizations of Prxs.

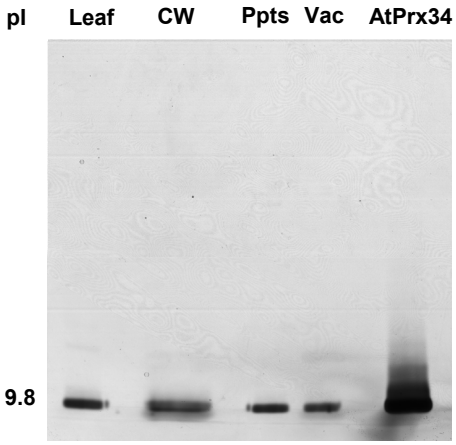

Figure III.3.1 – Peroxidase isoenzyme profile obtained by isoelectric focusing for protein extracts of Arabidopsis leaves (Leaf), leaf cell wall fluid (CW), leaf protoplasts (Ppts), leaf vacuoles (Vac) and AtPrx34 purified from leaves.

Therefore, AtPrx34 was purified in order to evaluate its capacity to accept Arabidopsis AGPs as substrates and to perform *in vitro* cross-linking assays of AGPs. For purification of AtPrx34, 300 g of leaves were used for a purification procedure involving ammonium sulfate precipitation and 4 chromatographic steps that enabled a high purification of AtPrx34 - 1430 fold (Table III.3.1).

Table III.3.1 - Purification of AtPrx34 from Arabidopsis leaves.

Purification step	Total activity (nKat)	Specific activity (nKat/mg)	Yield (%)	Purification (fold)
Crude extract	13800	5.8	100	1
> 30% $(NH_4)_2SO_4$	16550	5.9	119	1
Phenyl Sepharose	10187	11.0	73	2
Concananvalin A	4503	100.1	32	17
Sephacryl S200	5079	769.6	36	132
Hitrap Capto S	1211	8295.9	9	1430

The capacity of AGPs purified from Arabidopsis leaves to reduce the catalytic intermediates of AtPrx34 and of horseradish peroxidase type II was investigated, to determine whether Arabidopsis AGPs might function as substrates of AtPrx34 and of Prxs in general. For an explanation of the Prx catalytic intermediates and how they can be detected, see section III.2.1. As for *C. roseus* Prx1 and horseradish peroxidase type II, the addition of H_2O_2 to the native ferric form of AtPrx34 led to the exclusive accumulation of CoII. Therefore, the time course of CoII reduction during the reaction of AtPrx34 with Arabidopsis AGPs was plotted as a function of time, against the control in the absence of substrate (Figure III.3.2A). The addition of AGPs accelerated CoII reduction quite significantly in comparison with the control, clearly indicating the capacity of Arabidopsis AGPs to act as a reducing substrate of AtPrx34. When the same experiment was performed with horseradish peroxidase type II, it was observed that CoII of this enzyme was also reduced by Arabidopsis AGPs (Figure III.3.2B), as had been observed for *C. roseus* AGPs in section III.2.1.

The K_m for oxidation of Arabidopsis AGPs by horseradish peroxidase type II was estimated to be 60.06 µg ml^{-1}, showing that the affinity of this horseradish peroxidase for Arabidopsis leaf AGPs is quite lower than for *C. roseus* leaf AGPs (K_m = 1.36 µg mL^{-1}), indicating that different species produce different AGPs in what concerns their capacity to reduce Prxs. When the kinetic behaviour of AtPrx34 was investigated, it was observed that the oxidation of AGPs by this Prx did not follow a typical Michaelis-

Menten kinetics but rather displayed a sigmoidal kinetics indicative of an allosteric behaviour (Figure III.3.3).

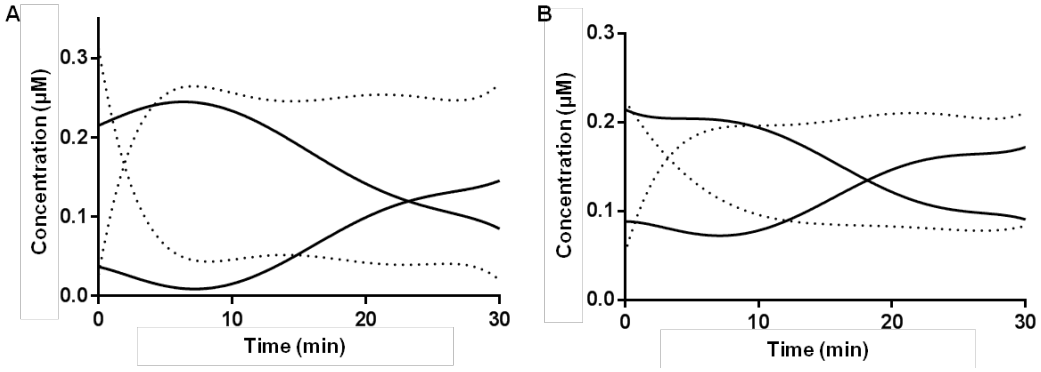

Figure III.3.2 – Reduction of Prxs by Arabidopsis AGPs. (A) Time course of the evolution of AtPrx34 CoII (upper trace at 0 min) and native form (lower trace at 0 min) in the presence (·····) and absence of AGPs (——). (B) Time course of the evolution of horseradish peroxidase II CoII (upper trace at 0 min) and native form (lower trace at 0 min) in the presence (·····) and absence of AGPs (——).

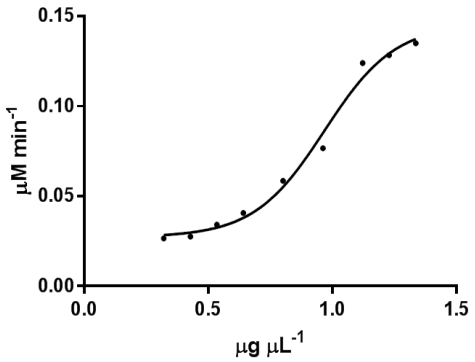

Figure III.3.3 – Rate of AtPrx34 CoII reduction by Arabidopsis AGPs.

Since Prxs are known to contain one single active site and are not reported to associate in complexes with several subunits (Veitch, 2004), this behaviour cannot be explained by substrate binding cooperativity. A similar behaviour was observed for the oxidation of scopoletin by horseradish peroxidase type VI and tobacco tissue culture isoperoxidase A3 (Reigh and Smith, 1977). At the time, this was suggested to be the result of scopoletin binding not only to the peroxidase active site but also to an ”oxidase site” whose existence was not confirmed by later structural studies of Prxs (Veitch, 2004). However, it is possible that Prxs may have regulatory binding sites distinct from the active site, where heteroallosteric effectors may bind to modulate enzyme activity. The results observed for AGPs and AtPrx34 would then suggest that some of the AGPs present in the Arabidopsis AGP extract could bind to AtPrx34 and influence positively its activity. Alternatively, since Prx activity is dependent on and modulated by

Ca^{2+} (Rasmussen et al., 1998; Veitch, 2004), and AGPs have been proposed to functions as Ca^{2+} capacitors (Lamport and Várnai, 2013), it is possible that increasing AGPs concentration will lead to an increase in Ca^{2+} concentration that may determine the sigmoidal kinetics. In any case, Arabidopsis AGPs were shown to be good substrates of both horseradish peroxidase type II and AtPrx34, further supporting the conclusion from section III.3.2 that AGPs are an important substrate of Prxs in plants.

III.3.2 MAC207, JIM14, JIM16 and LM2 AGP epitopes are present in Arabidopsis leaves

In order to investigate the possibility of occurrence of an AGP-Prx interaction in Arabidopsis using experimental approaches equivalent to the ones applied to *C. roseus*, it was necessary to find out if any of the AGP glycosidic epitopes recognized by available mAbs was present in Arabidopsis leaves. Therefore, a set of AGP mAbs was screened against Arabidopsis leaves: JIM8, JIM13, JIM14, JIM16, LM2 and MAC207. Four of these glycosidic epitopes, JIM14, MAC207, JIM16 and LM2, were present in Arabidopsis leaves, while JIM8 and JIM13 AGP glycosidic epitopes were completely absent from Arabidopsis leaves (Figure III.3.4). JIM14 and MAC207 labelled most types of cells in Arabidopsis leaves, including the mesophyll, epidermal cells and vascular bundles (Figures III.3.4A and B). On the other hand, JIM16 and LM2 epitopes were specifically localized in vascular bundles (Figures III.3.4C and D).

The glycosidic epitopes of AGPs recognized by mAbs have shown organ-, tissue and cell-specific labelling patterns indicating that AGPs are markers of cellular identity and fate (Knox, 1997). In Arabidopsis leaves, possible examples of AGPs pattern formation during differentiation, reflecting in cell fate, are the localization of LM2 and JIM16 in vascular bundles (Figures III.3.4C and D). AGPs have been shown to be present on the secondary-wall thickenings of cells destined to undergo programmed cell death (PCD), producing xylem (Schindler et al., 1995). Thus, one possibility is that these AGP epitopes mark cells that are committed to PCD. The immunolocalization experiments in Arabidopsis leaves have also provided information on the subcellular localization of the recognized AGP epitopes. JIM14 and MAC207 seem to label epitopes placed both in the plasma membrane/cell wall and in the tonoplast, with a quite important proportion being present in this late location (Figures III.3.4A2 – B2). Moreover, these two epitopes appeared as individual spots with a patchy distribution, suggesting an organization in microdomains. This punctuated localization in plasma membrane and tonoplast microdomains has already been discussed in sections III.1 and III.2. It has, namely, been proposed that GPI-anchored AGPs localized in plasma

membrane or tonoplast microdomains may mediate signalling in plants through interaction with other signalling proteins co-localized in the microdomain.

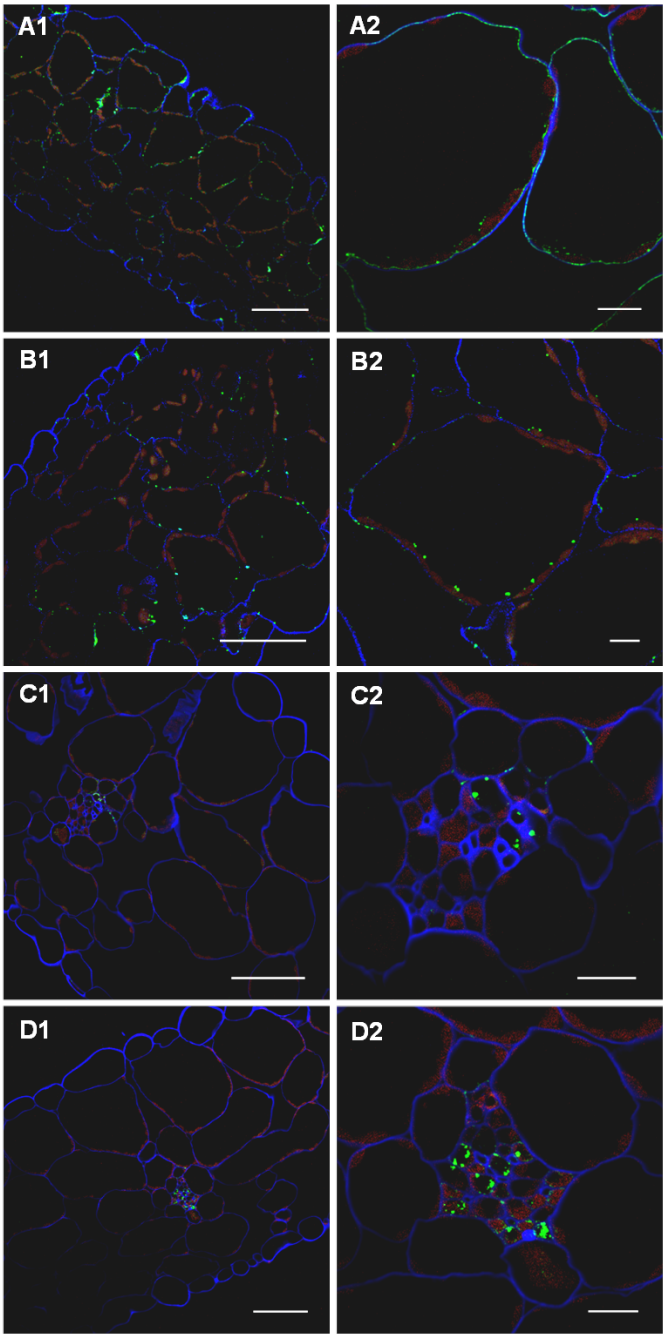

Figure III.3.4 – Green-immunofluorescence localization of AGPs in *A. thaliana* leaves, using mAbs recognizing specific glycosidic epitopes. (A) JIM14 labels all cell types. (B) MAC207 labels all cell types. (C) JIM16 labels specific cells from the vascular bundles. (D) LM2 labels specific cells from the vascular bundles. Cell walls were counterstained with calcofluor (blue fluorescence). Autofluorescence of chloroplasts in red. Scale bars for A1-D1, 50 µm. Scale bars for A2-D2, 10 µm.

Comparing the labelling patterns obtained in Arabidopsis leaves with the ones obtained for *C. roseus* leaves in section III.1, it is obvious that AGP epitope

localizations are also species-specific. Interestingly, the MAC207 epitope is localized in all types of cells in Arabidopsis leaves but in *C. roseus* leaves it marks specifically idioblasts, cells specialized in alkaloid accumulation. On the other hand, JIM8 and JIM13 profusely mark all cell types of *C. roseus* leaves and are completely absent from Arabidopsis leaves. The fact that specific AGPs do not bear the same morphogenetic identity in different species has been repeatedly acknowledged, and it has even been suggested that their distribution may have taxonomic significance (Knox, 1997). However, the meaning of this disparity is not understood.

III.3.3 AtPrx34 mediates changes in the molecular weight and abundance of AGP epitopes *in vitro*

Using a similar approach to the one applied in section III.2, the capacity of AtPrx34 to mediate oxidative cross-linking of AGPs was investigated by examining changes in AGPs molecular weight upon incubation of leaf protein fractions with AtPrx34 and H_2O_2. This was performed by analyses of the reaction products through gel filtration chromatography followed by dot-blot analyses of the different molecular weight sub-fractions using mAbs against AGP glycosidic epitopes. The leaf protein extracts were fractionated in soluble and membrane proteins, which were analysed independently. Due to the use of gel filtration, the use of the membrane fraction without any treatment enabled only the detection of membrane associated proteins. However, this time, experiments also involved the treatment of the membrane fraction with phospholipase C*,* commonly used for the release of GPI anchored proteins from the membrane. This treatment enabled the release of true membrane AGPs and their analysis by gel filtration. Densitometry of the dot blot results obtained for the MAC207 AGP epitope, highly abundant in Arabidopsis leaves (Figure III.3.4B), was used to construct the graphics presented in Figure III.3.5. Contrary to the observed for *C. roseus*, where CrPrx1 action resulted in a clear increase of the molecular weight of AGPs recognized by mAbs and sometimes of labelling intensity as well, the results obtained for Arabidopsis were more elusive (Figure III.3.5). For soluble proteins, two new peaks appeared for higher molecular weights, while two from lower molecular weights disappeared (Figure III.3.5A). This may be explained by cross-linking of the MAC207 AGPs from the low molecular weight peaks with other molecules to generate the peaks with higher molecular weight. However, the results obtained for membrane proteins are less easy to understand. For this protein fraction, which included the GPI anchored proteins released by treatment of phospholipase C, there was a prominent low

molecular weight peak appearing *de novo*, and a decrease in the labelling intensity of a high molecular weight peak (Figure III.3.5C).

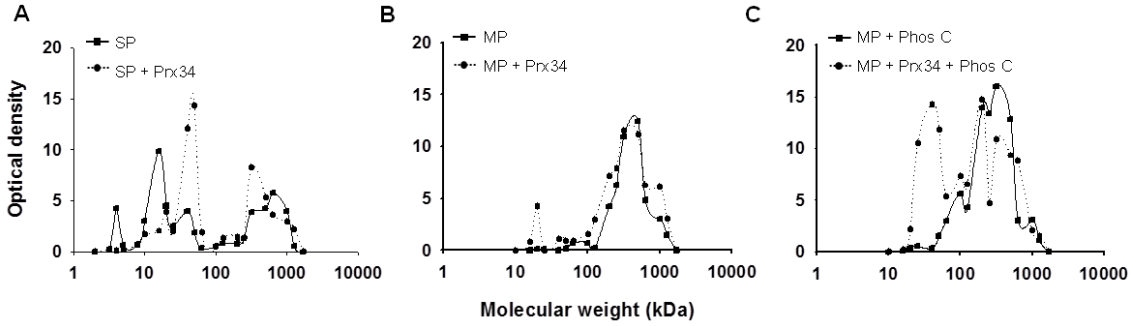

Figure III.3.5 - Changes in the molecular weight and quantity of AGPs recognized by the mAb MAC207 after incubation with AtPrx34 and H_2O_2, as detected by dot-blot densitometry of fractions resulting from gel filtration. (A) Soluble proteins. (B and C) Membrane associated proteins.

In section III.2, the increase of labelling intensity of one AGP peak without any other change occurring, was interpreted as intra-molecular cross-linking of AGPs leading to *de novo* formation of the glycosidic epitopes being detected, in this case, the MAC207 epitopes. Here, besides an increase in MAC207 epitopes, a new situation occurs where decrease of labelling happens, without the concomitant increase of labelling at higher molecular weights that could have explained that decrease (resulting from cross-linking of AGPs with other molecules). The only obvious explanation for this maybe that, the same way some cross-linking reactions may lead to conformational changes leading to the formation of a particular glycosidic epitope, other additional cross-linking reactions may lead to further conformational changes or molecular associations that abolish or mask the same epitope. It is interesting to note that, in soluble proteins from Arabidopsis leaves, the major effect observed upon Prx oxidation may be explained by AGP inter-molecular cross-linking leading to an increase in molecular weight, as was observed for the same protein fraction from *C. roseus* leaves. Conversely, the changes in labelling intensity not explained by molecular weight changes were observed in the membrane or membrane associated protein fractions from the two species. Moreover, when comparing the changes observed for the membrane proteins of Arabidopsis resulting from treatment with phospholipase C with the controls without phospholipase C (Figures III.3.5B and C), it can be seen that the big new peak of low molecular weight resulting from the action of AtPrx34 appears only in the fraction treated with phospholipase C, meaning that this set of AGPs for which Prx action resulted in intra-molecular cross-linking were bound to the membrane by a GPI anchor. Actually, this was also observed for the JIM8 epitope, which was absent

from leaf sections, but labelled a big peak of AGPs that appeared only after incubation of Arabidopsis leaf membrane proteins with AtPrx34 + H_2O_2 and only in the protein fraction released by phospholipase C (Figure III.3.6).

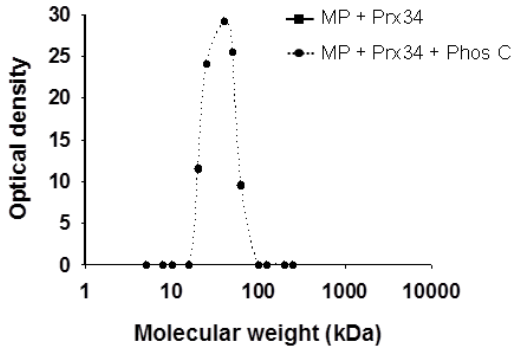

Figure III.3.6 - Changes in the molecular weight and quantity of membrane AGPs recognized by the mAb JIM8 after incubation with AtPrx34 and H_2O_2 and phospholipase C, as detected by dot-blot densitometry of fractions resulting from gel filtration.

The data above suggests that AGP glycosidic epitopes may be highly dynamic *in planta*, possibly fluctuating depending on stress conditions or other conditions that lead to generation of H_2O_2. Overall, the results from this section indicate that, in the model plant Arabidopsis, Prx may mediate reactions leading to inter- and/or intra-molecular cross-linking of AGPs, potentially contributing to the remodelling of AGP glycosidic epitopes *in planta* and implicating Prxs in the signalling and/or structural functions attributed to AGPs.

III.3.4 Peroxidase-like activity mediates changes in abundance of AGP epitopes *in vivo*

AtPrx34-mediated *in vitro* reactions seemed to result in an overall increase of labelling by MAC207 (Figure III.3.5), even if not as prominent as was observed for JIM8 and JIM13 in *C. roseus* (see section III.2). This meant again that changes in the labelling of leaf tissues with MAC207 could occur and be investigated by increasing the availability of H_2O_2 to endogenous AtPrx34 or other Prxs, delivering evidence of *in vivo* activity. Therefore, leaves from Arabidopsis in two different developmental stages (Figure III.3.7) were infiltrated with H_2O_2, which diffuses easily through the apoplast and across membranes to the symplast, becoming available to both cell wall and vacuolar AtPrx34, or other Prx activities present (Figure III.3.8).

When Arabidopsis leaves were infiltrated with H_2O_2, a clear and quantifiable increase in the intensity of labelling by MAC207 was observed, indicating the

occurrence of *in vivo* Prx-mediated links that resulted in the appearance of new MAC207 AGP glycosidic epitopes (Figure III.3.8). This was observed both in young Arabidopsis plants with a small rosette (Figure III.3.8A), and in more mature plants (Figure III.3.8B). In some leaf sections, in areas close to the infiltration spot, it is evident that the labelling increase is particularly strong near the abaxial surface of the leaf, showing a decreasing gradient to the adaxial surface, certainly corresponding to the progressive decaying of H_2O_2 starting from the infiltration side (Figure III.3.8B). The observed increase in the intensity of labelling resulting from infiltration of leaves with H_2O_2 was sensitive to the simultaneous infiltration with the Prx inhibitor KCN further supporting a role for Prx in the genesis of the MAC207 AGP glycosidic epitope *in planta*. The concentration of H_2O_2 used for infiltration of leaves was 10 mM as used for *C. roseus,* since it produced more evident results than 1 mM and because, although high, it is within the order of magnitude of previously reported physiological concentrations (Neill et al., 2002; Cheeseman, 2006).

Figure III.3.7 – Plants of Arabidopsis used for H_2O_2 infiltration of leaves. (A) Young plants in growth stage 1.11 / 3.20 of Boyes et al. (2001), corresponding to rosettes with 11 leaves and with around 20% of its final size. (B) Plants in growth stage 3.70 to 3.90 of Boyes et al. (2001), corresponding to rosettes with around 70-100% of its final size but with no detectable inflorescence emergence. Scale bar, 1 cm.

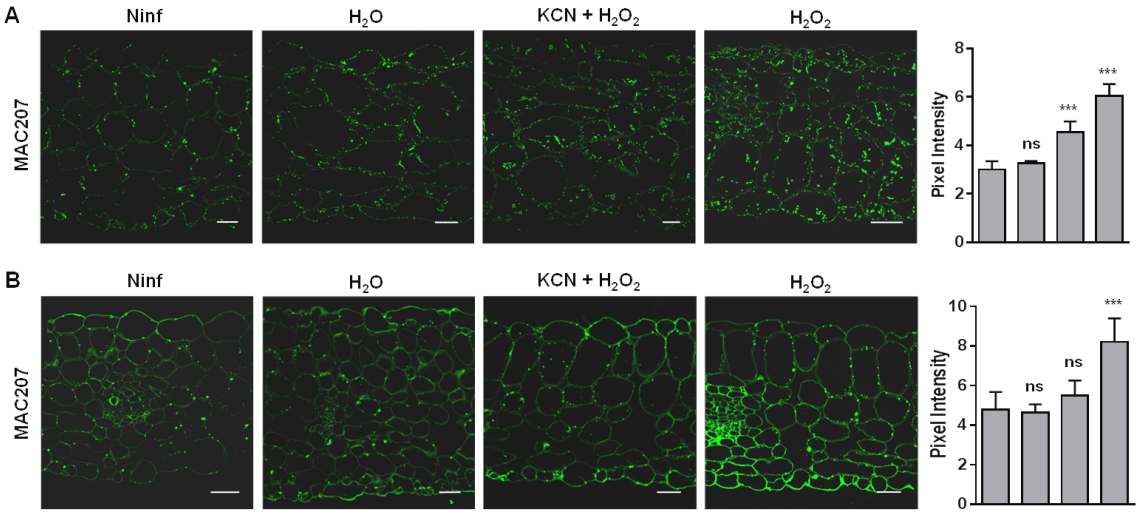

Figure III.3.8 – Green-immunofluorescence localization and intensity of MAC207 AGP epitope in Arabidopsis leaves infiltrated with 10 mM H_2O_2 and with 10 mM H_2O_2 plus 2 mM peroxidase inhibitor KCN. (A) Young plants. (B) Mature

plants. Ninf – non-infiltrated controls. H_2O – water-infiltrated controls. Values are means ± SE of $n \geq 10$ for young plants and $n \geq 5$ for mature plants. (ns) mean differences are not statistically significant, (***) $p<0.001$, one way ANOVA, with multiple comparisons. Scale bars, 25 µm.

III.3.5 AGP epitopes and Prx co-localize in microdomains of the plasma membrane and the tonoplast of Arabidopsis mesophyll cells

The occurrence of an *in vivo* interaction between AGPs and Prx implies that they are co-localized in the cell. The immunolocalization study described above in section III.3.2 showed that JIM14 and MAC207 labelled individual spots with a patchy distribution (Figure III.3.4), indicating that AGPs are likely localized in microdomains as observed for *C. roseus* in sections III.1 and III.2. Likewise, it should be expected that Prx co-localize with AGPs in those microdomains. Therefore, the localization of Prx in Arabidopsis leaves was investigated using the Prx polyclonal antibody from section III.2, since it was shown to also recognize AtPrx34, the main Prx from Arabidopsis leaves (Figure III.3.9). Immunolabelling of Arabidopsis leaf sections using the anti-Prx showed that Prx proteins indeed presented a similar punctuated localization, both in the tonoplast and the plasma membrane/cell wall (Figure III.3.10).

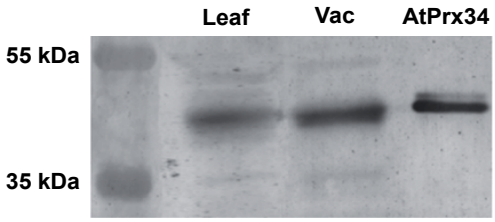

Figure III.3.9 – Western-blot of a protein extract from leaves of Arabidopsis (Leaf) and from vacuoles (Vac), and pure AtPrx34 using anti-Prx.

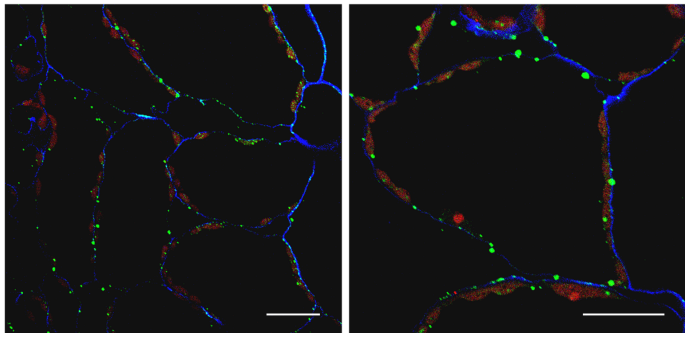

Figure III.3.10 – Green-immunofluorescence localization of Prxs in *A. thaliana* leaves using the anti-Prx. Cell walls were counterstained with calcofluor (blue fluorescence). Autofluorescence of chloroplasts in red. Scale bars, 20 µm.

The obvious next step was to perform co-immunolocalization for Prx and the MAC207 AGP epitope. The results obtained are shown in Figure III.3.11 and it is

possible to observe that the punctuated localization observed for the AGP epitopes is highly similar and greatly overlaps with the localization observed for Prx both in the tonoplast and the plasma membrane/cell wall, strongly supporting the possibility of *in vivo* interaction between the two protein families. This result was further confirmed by electron microscopy, by which it was possible to detect overlap/high proximity of AGP and Prx labelling in some domains of the plasma membrane (Figure III.3.12).

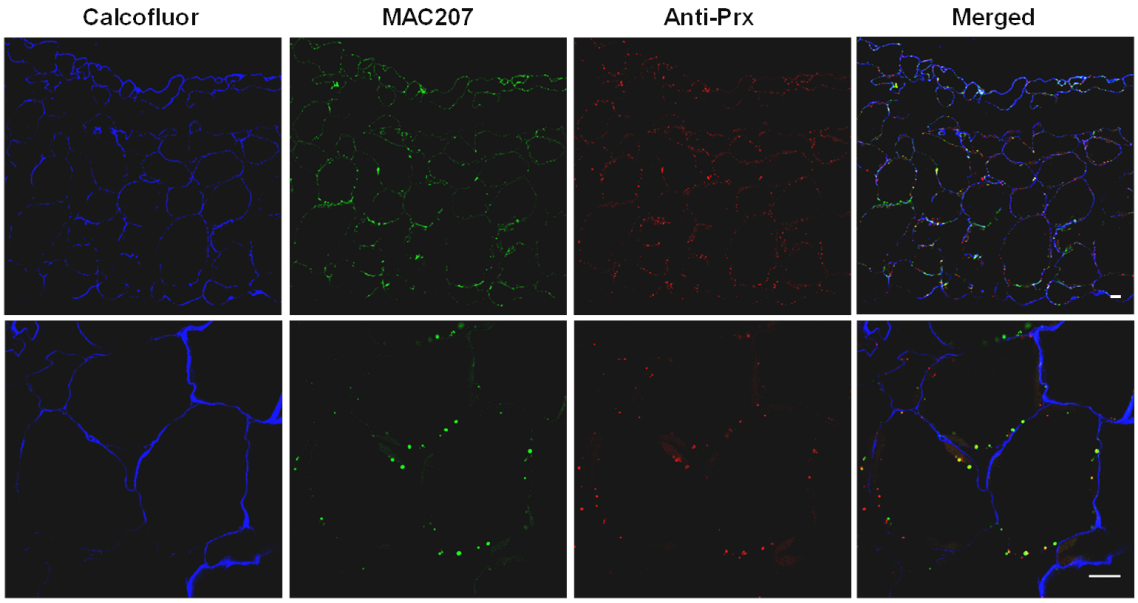

Figure III.3.11 – Immunofluorescence co-localization of Prx and AGPs in *A. thaliana* leaves. Scale bars, 10 µm.

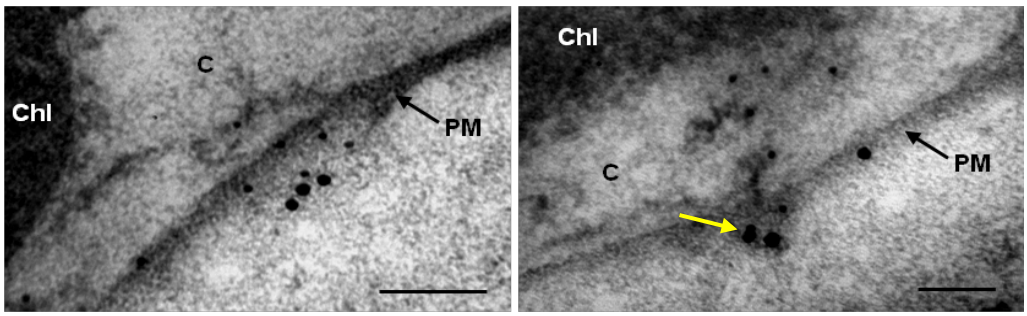

Figure III.3.12 – Co-immunogold cytochemistry using MAC207 and anti-Prx antibodies in *A. thaliana* leaves. Gold particles with 10 nm label AGPs and gold particles with 15 nm label Prx. C – cytosol. Chl – chloroplast. PM – plasma membrane. Yellow arrow indicates two gold particles of different size overlapping. Scale bars, 100 nm.

This punctuated distribution and co-localization observed for AGPs and Prx in Arabidopsis mesophyll cells correlates with the results obtained for *C. roseus* (sections III.1 and III.2). This reinforces the idea that GPI-anchored AGPs localized in detergent-resistant microdomains may mediate signalling in plants through interaction with other signalling proteins co-localized in the microdomains, namely with Prxs. In fact, all the data obtained for *C. roseus* and here for Arabidopsis strongly support the hypothesis of

in vivo interaction between Prx and AGPs. This Prx-AGP interaction suggest that Prx and H_2O_2 may be important regulators of the developmental and signalling functions attributed to AGPs, and establish a direct link between AGPs functions/signalling and H_2O_2 signalling. This hypothesis is discussed and presented in more detail below, in the last chapter of the thesis.

III.4 Do AGPs and Prx cooperate to regulate tip growth in Arabidopsis root hairs?

The possibility that AGPs suffer oxidative cross-linking by Prx may have structural consequences in the cell wall, but, most certainly, will also affect their signalling properties. In fact, an interaction between Prx and AGPs could function as a cell surface signalling switch in which H_2O_2 production triggered by stress or developmental cues could be used by Prx to perform cross-linking of AGPs, leading to changes on their interaction with other proteins, ultimately resulting in activation of intracellular signalling (see discussion in chapter IV). The model situation selected to test this hypothesis was cell expansion during the localized growth of root hairs. In fact, the characterization of the NADPH oxidase mutant *rhd2* (*root hair defective*) has implicated ROS in the regulation of cell expansion in root hairs (Foreman et al., 2003; Takeda et al., 2008) and, on the other hand, the AGP function-blocker Yariv reagent was shown to inhibit the root epidermal cell expansion necessary for root hair growth (Ding and Zhu, 1997). Additionally, Velasquez et al. (2011) reported that *O*-glycosylated cell wall proteins are essential in root hair growth, with AGPs as possible candidates. Finally, previous work in our lab has shown that several Prx inhibitors inhibited root hairs differentiation, also implicating these enzymes in the process (Figueiredo, 2011). For all these reasons, focal cell expansion during the tip growth of root hairs seems to be a good candidate model to test the hypothesis that the interaction Prx-AGP may function as a signalling platform responsive to H_2O_2.

Root hairs are long, thin tubular outgrowths from epidermal cells that are produced in the differentiating zone of the root and are important for the uptake of minerals and water from the soil (Figure III.4.1). In Arabidopsis, the trichoblasts (hair-forming cells) and atrichoblasts (non-hair cells) are arranged in alternating files along the root surface (Carol and Dolan, 2002). Root hairs are formed at the basal region of trichoblasts, where a single polarized outgrowth appears and will continue to grow by what is called tip growth – an extreme type of polarized growth in which elongation is focused on a single specialized region, the apex. It is known that the stable maintenance of this focal growth site is dependent from the localized production of ROS by the RHD2 NADPH oxidase mentioned above, which stimulates a Ca^{2+} influx into the cytoplasm that is required for root hair growth (Foreman et al., 2003; Takeda et al., 2008). Therefore, the application of our H_2O_2-Prx-AGP hypothesis to root hair tip growth postulates that the H_2O_2 resulting from the activity of RHD2 will be used by Prx to oxidase AGPs, triggering a signal that will result in the stimulation of the Ca^{2+} influx. To test this hypothesis, roots and root hairs were submitted to a range of treatments

potentially impairing Prxs or AGPs, including targeted treatments with the mAbs recognizing AGP glycosidic epitopes. Therefore, previously to these treatments, the presence and distribution in Arabidopsis roots of different AGP glycosidic epitopes was investigated. The presence of Prx was also investigated using the Prx polyclonal antibody from sections III.2 and III.3, but no results were obtained. This may be because root Prxs are not recognized by this antibody.

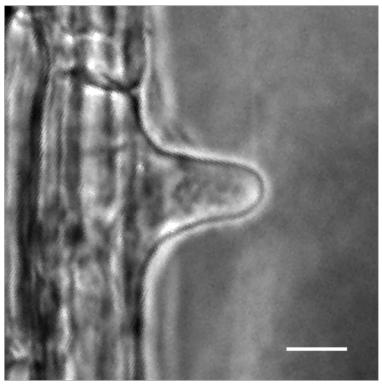

Figure III.4.1 – Bright field image of an Arabidopsis root hair. Scale bar, 10 µm.

III.4.1 AGP epitopes recognized by several mAbs are present in Arabidopsis roots

Roots from Arabidopsis seedlings were fixed and either immediately processed for immunofluorescence, or dehydrated, included and sectioned longitudinally or transversally before processing for immunofluorescence. Figure III.4.2 depicts the anatomy of Arabidopsis roots in the differentiating zone to help in the interpretation of the labelling results.

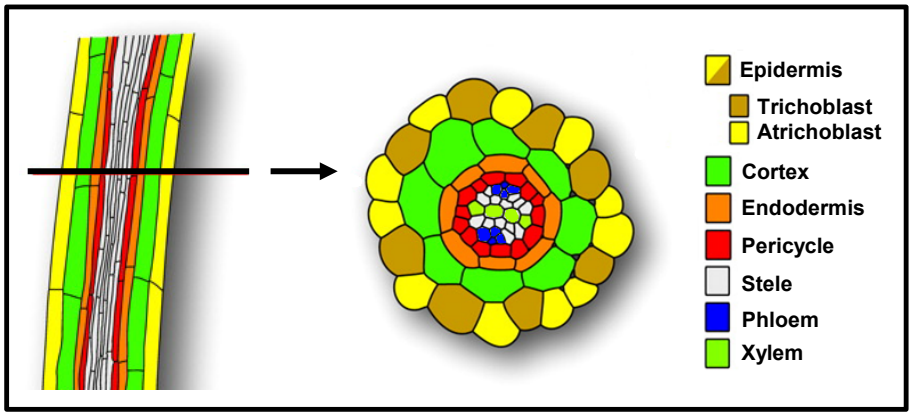

Figure III.4.2 – Schematic representation of the anatomy of Arabidopsis root. Adapted from Overvoorde et al. (2010).

JIM14 labelled intensely the transition from the apical meristem to the elongation zone and the root hair tips (Figure III.4.3A). Transversal sections from the root hair zone revealed that JIM14 labelled all types of cells in this area, with a lower intensity in the epidermis (Figure III.4.3B2). MAC207 epitopes were also localized in all types of cells, except in xylem cells, but with a higher labelling in epidermis, pericycle and phloem, and clearly labelling root hairs (Figure III.4.4). JIM16 was specifically localized at the surface of root hairs and in the outer surface of epidermal cells, forming a conspicuous layer around the root cap and the epidermal cells from the root apex (Figure III.4.5). LM2 labelled specific epidermal cells in the root hair zone but it did not label root hairs (Figure III.4.6). Finally, JIM8 and JIM13 labelled specifically xylem and procambium cells, and the xylem-pole pericycle cells (Figures III.4.7 and III.4.8).

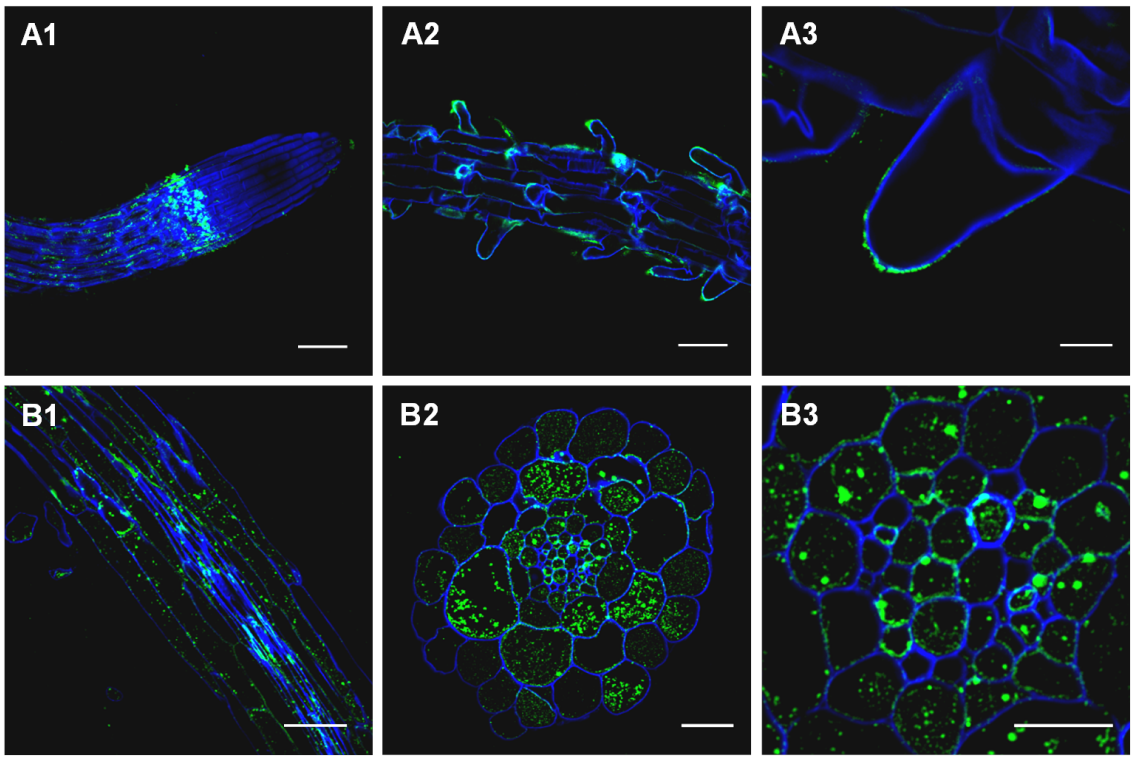

Figure III.4.3 – Green-immunofluorescence localization of JIM14 AGPs epitope in Arabidopsis roots. (A) Whole mount roots. (B) LR White-embedded and sectioned roots. Cell walls were counterstained with calcofluor (blue fluorescence). Scale bar for A1-2 and B1, 50 µm. Scale bar for B2, 20 µm. Scale bar for A3 and B3, 10 µm.

Comparing the labelling patterns in Arabidopsis root with the labelling patterns in Arabidopsis leaf, only JIM14 and MAC207 epitopes are general, being localized in almost all types of cells in these two organs (Figure III.3.4 from section III.3 and Figures III.4.3 and III.4.4). Moreover, another thing in common in both organs is the fact that the JIM4 epitope is completely absent. The other mAbs tested have all labelled different tissues or cells in leaf and root, indicating that the AGPs with those

epitopes are likely associated with different functions in both organs. Even if JIM14 and MAC207 label all types of cells in roots, the fact that JIM14 labelling is stronger in cortex cells (Figure III.4.3B2) and MAC207 labelling is stronger in epidermal cells (Figure III.4.4B2) may indicate that these epitopes have additional specific functions in these tissues. The localization of the LM2 epitope in specific cells in root epidermis is quite interesting, because these cells are probably trichoblasts, the cells that differentiate root hairs (Figure III.4.6B). Since the LM2 epitope is not present in root hairs, this means that AGPs with the LM2 epitope may be important for root epidermal cell fate specification, preceding differentiation of trichoblasts into root hair cells.

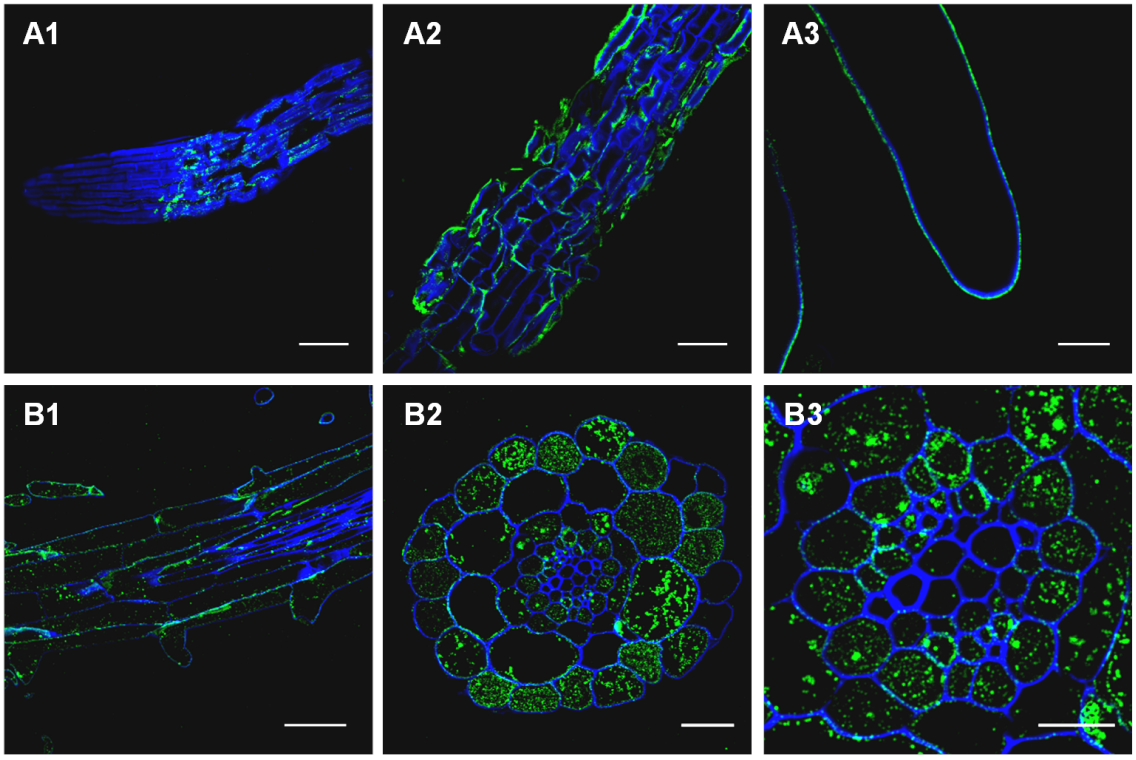

Figure III.4.4 – Green-immunofluorescence localization of MAC207 AGPs epitope in Arabidopsis roots. (A) Whole mounted roots. (B) LR White-embedded and sectioned roots. Cell walls were counterstained with calcofluor (blue fluorescence). Scale bar for A1-2 and B1, 50 µm. Scale bar for B2, 20 µm. Scale bar for A3 and B3, 10 µm.

The localization of the JIM16 epitope at the surface of root hairs and in the outer surface of root epidermal cells is also an interesting result (Figure III.4.5). This may indicate that AGPs with the JIM16 epitope are one of the components of Arabidopsis root wax/exudates. Little is known about the nature, biosynthesis and role of root waxes, but they are probably involved in water and gas exchange and in defence, like the cuticles found in leaves (Li et al., 2007). To our knowledge, the presence of AGPs in root waxes has never been reported before. In theory, specific root-secreted enzymes involved in degradation and remodelling of cell wall glycoproteins and

polysaccharides (Wen et al., 2007) could release specific oligosaccharides from AGPs in the root surface, which could act as signals in defence.

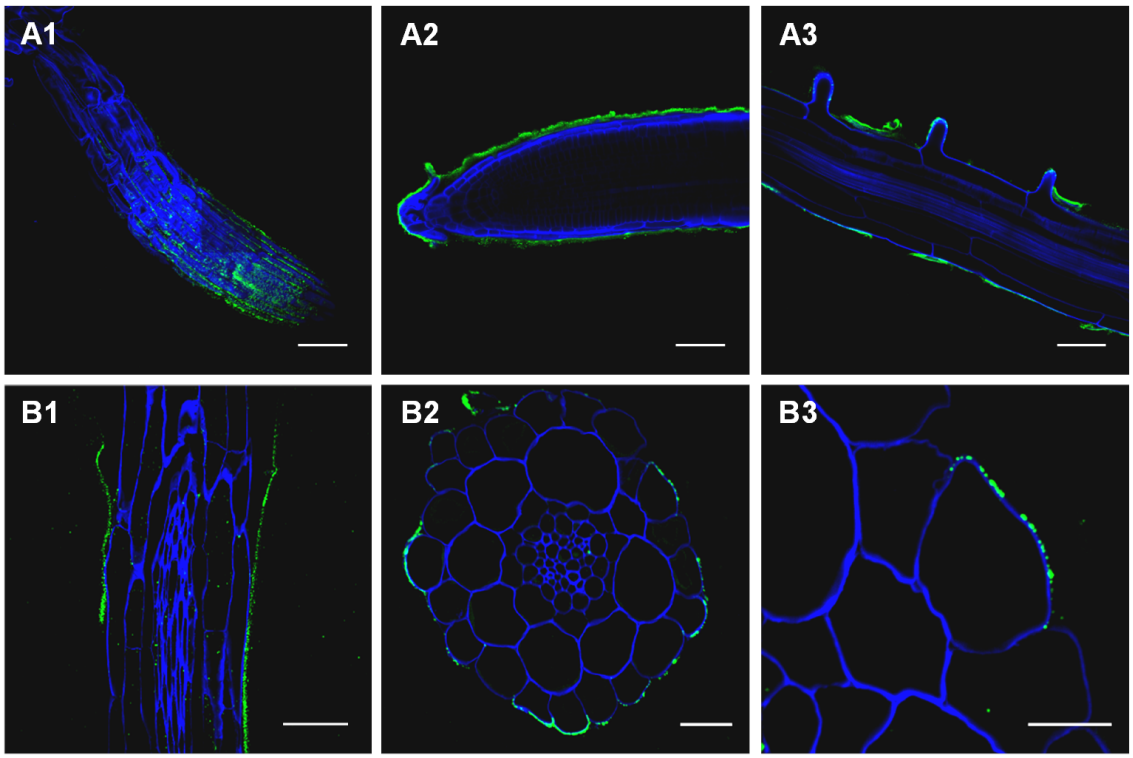

Figure III.4.5 – Green-immunofluorescence localization of JIM16 AGPs epitope in Arabidopsis roots. (A) Whole mounted roots. (B) LR White-embedded and sectioned roots. Cell walls were counterstained with calcofluor (blue fluorescence). Scale bar for A1-3 and B1, 50 µm. Scale bar for B2, 20 µm. Scale bar for B3, 10 µm.

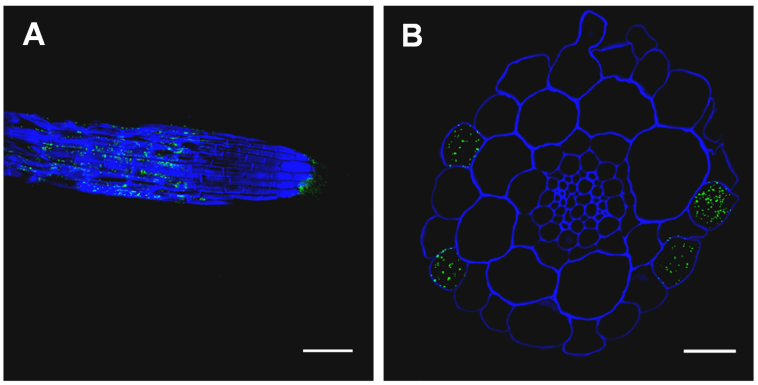

Figure III.4.6 – Green-immunofluorescence localization of LM2 AGPs epitope in Arabidopsis roots. (A) Whole mounted root. (B) LR White-embedded and sectioned root. Cell walls were counterstained with calcofluor (blue fluorescence). Scale bar for A, 50 µm. Scale bar for B, 20 µm.

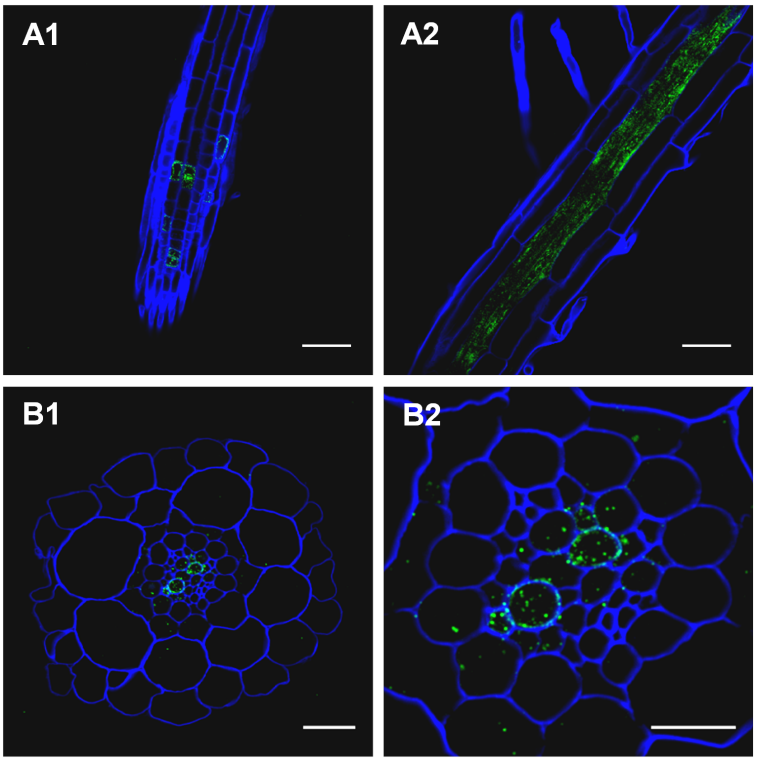

Figure III.4.7 – Green-immunofluorescence localization of JIM8 AGPs epitope in Arabidopsis roots. (A) Whole mounted roots. (B) LR White-embedded and sectioned roots. Cell walls were counterstained with calcofluor (blue fluorescence). Scale bar for A1-2, 50 µm. Scale bar for B1, 20 µm. Scale bar for B2, 10 µm.

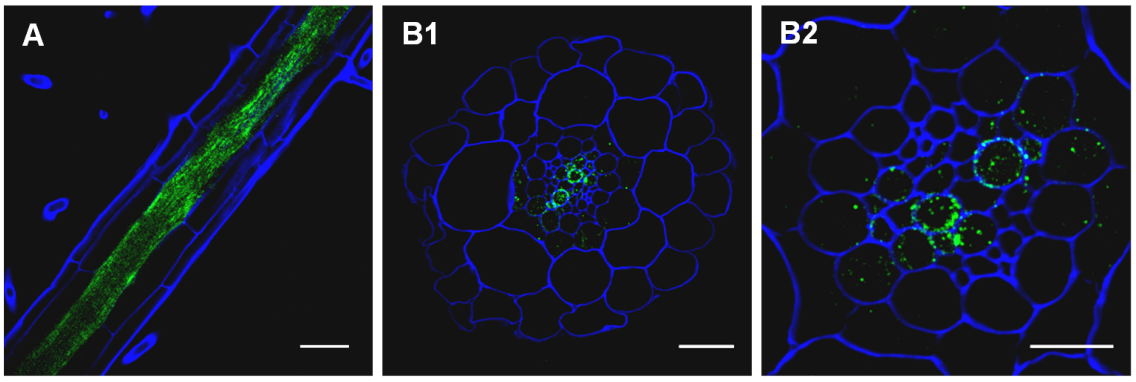

Figure III.4.8 – Green-immunofluorescence localization of JIM13 AGPs epitope in Arabidopsis roots. (A) Whole mounted roots. (B) LR White-embedded and sectioned roots. Cell walls were counterstained with calcofluor (blue fluorescence). Scale bar for A, 50 µm. Scale bar for B1, 20 µm. Scale bar for B2, 10 µm.

Together, these observations indicate that AGP-associated epitopes are developmentally regulated in plant roots and that modulation of AGP expression occurs during cell development and positioning of cells within the root.

III.4.2 The development of Arabidopsis roots and root hairs is sensitive to factors interfering with AGPs, Prx and ROS

In order to evaluate the hypothesis that Prx and AGPs might cooperate to mediate transduction of the ROS signal produced by NADPH oxidase during tip growth of root hairs, Arabidopsis roots and root hairs were submitted to a range of treatments potentially impairing Prxs, AGPs or ROS. In a first set of experiments, the growth behaviour of roots and root hairs was analyzed in seedlings of Arabidopsis growing in vertical Petri dishes in the presence of various substances for 10 days. In a second set of experiments (following section), the effect in the growth rate of root hairs of a range of antibodies, Prxs, and AGPs was evaluated.

In order to confirm the results obtained by Ding and Zhu (1997), the effect of Yariv reagents in root hairs was investigated. Root growth and the formation and elongation of root hairs were profoundly affected in Arabidopsis seedlings growing in the presence of the AGP function-blocker β-Yariv reagent (Figure III.4.9). Roots had a slow and abnormal growth compared with the seedlings growing on media without additives, with roots presenting curling and branching, and the general structure resembling more a fibrous root than the normal tap root of Arabidopsis (Figure III.4.9A). Significantly, the differentiation of root hairs was completely inhibited, with epidermal cells sometimes presenting bulging (Figure III.4.9B), as previously observed by Ding and Zhu (1997). For comparison, no root phenotype or root hair inhibition was observed in seedlings grown in media containing α-Yariv reagent, which does not bind to AGPs (Figure III.4.9). Our results indeed confirmed the previous observations of Ding and Zhu (1997), indicating a role of AGPs in root hair differentiation. This is also supported by the study of the Arabidopsis mutant *reb1-1* (*root epidermal bulger*), for which the absence of a subpopulation of AGPs normally present in wild-type root is associated with a root hair phenotype similar to the β-Yariv treatment (Ding and Zhu, 1997). Furthermore, Andème-Onzighi et al. (2002) reported that the swelling phenotype of this mutant is restricted to trichoblasts and that the AGP mAbs LM2 and JIM14 stained all epidermal cells in the wild type, preferentially trichoblasts, while in *reb1-1* they stained the atrichoblasts only. However, our results with labelling of Arabidopsis roots with the same mAbs are somewhat different, at least in what concerns the wild type (same Columbia background as Andème-Onzighi et al. (2002)). We have observed that JIM14 stained almost all root cells, with a labelling intensity weaker in the epidermis than the cortex, and with no noticeable difference between trichoblasts and atrichoblasts (Figure III.4.3). On the other hand, JIM14 conspicuously labelled the tip of

the root hairs, something that is not mentioned by Andème-Onzighi et al. (2002). Concerning LM2, we observed that its epitopes were localized exclusively in what seemed to be the trichoblasts (Figure III.4.6), being completely absent from other epidermal cells. In any case, our results also point to an involvement of AGPs in the differentiation fate of trichoblasts and the tip growth of root hairs.

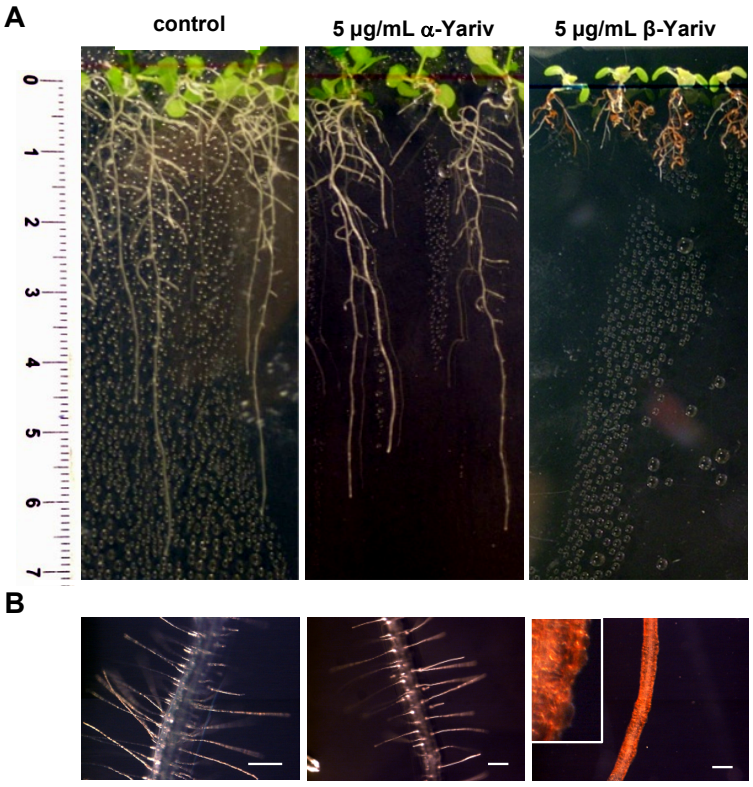

Figure III.4.9 – Root phenotype of Arabidopsis seedlings growing in the presence of Yariv reagents for 10 days. (A) Overall aspect of Arabidopsis seedlings and roots in the Petri dishes. (B) Magnification of the root hair zone from a representative root. Scale bars, 100 µm.

Recently, it was shown that the *REB1-1* gene encodes an enzyme that converts D-glucose into D-galactose, providing galactose to AGPs and xyloglucans, and supporting a link between the normal carbohydrate structure of AGPs and the control of cell expansion (Nguema-Ona et al., 2006).

Previously, Figueiredo (2011) showed that the Prx inhibitors KCN and DTT completely abolished the differentiation of root hairs in Arabidopsis roots. These inhibitors are not specific for Prxs, but they act through different mechanisms - KCN attaches to the Prx heme iron ion and prevents electron transport while DTT reduces the Prx disulfide bonds. However, the induction of a common effect in root hairs was considered suggestive of Prx mediation. Here, a third Prx inhibitor was used, salicylhydroxamic acid (SHAM), which has still a different mechanism of action on Prxs

- it competes to the H_2O_2-binding site (Davies and Edwards, 1989). It can be seen in Figure III.4.10 that the low concentration of SHAM used was sufficient to reduce root growth and root hair density and size. These effects were even more evident when the concentration of SHAM was increased to 100 µM, which is still a low concentration. Therefore, these results further support a role of Prxs in the differentiation and growth of root hairs. Moreover, this study also indicates that Prxs are involved in root growth, as previously suggested by Dunand et al. (2007) and Tsukagoshi et al. (2010).

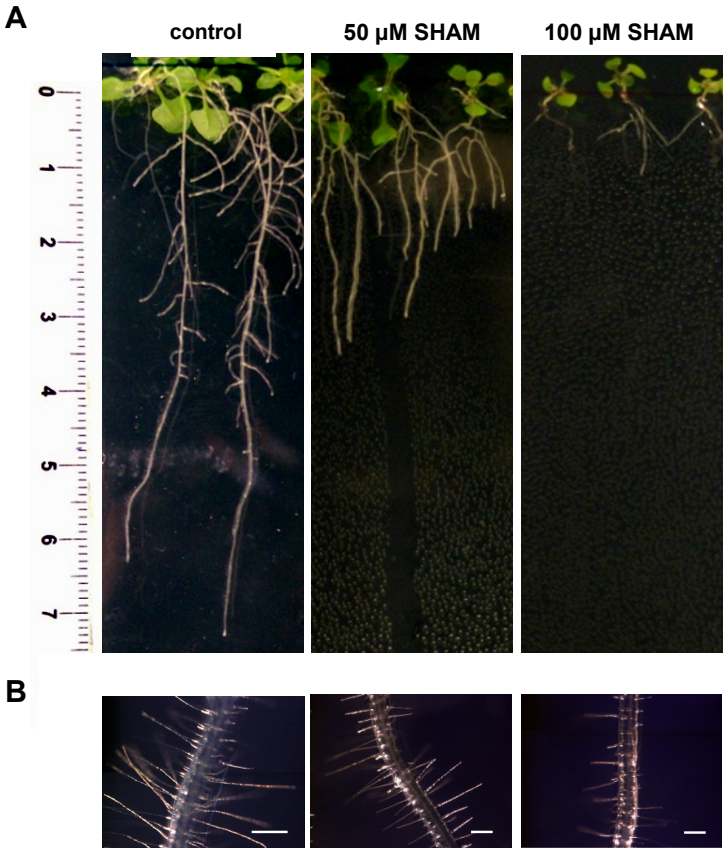

Figure III.4.10 – Root phenotype of Arabidopsis seedlings growing in the presence of SHAM for 10 days. (A) Overall aspect of Arabidopsis seedlings and roots in the Petri dishes. (B) Magnification of the root hair zone from a representative root. Scale bars, 100 µm.

In order to further confirm the involvement of ROS, namely of H_2O_2, in the growth of root hairs, Arabidopsis seedlings were also treated with ROS scavengers. Roots of seedlings grown in the presence of KI, an efficient scavenger of H_2O_2, had no hairs, what means that the H_2O_2 is important for the development of root hairs (Figure III.4.11). In fact, ROS have been implicated in the growth of root hairs, which have also been shown to accumulate H_2O_2 in the tip (Foreman et al., 2003; Dunand et al., 2007). On the other hand the roots treated with KI had sizes similar to control roots, suggesting that H_2O_2 is not necessary for root elongation. However, some roots

presented some curling bearing resemblances with the Yariv treatment above, suggesting that H_2O_2 may be important for the orientation of root growth, possibly in association with AGPs. Ascorbate, a general ROS scavenger, induced a significant decrease of root growth and of root hair density and size (Figure III.4.11). This suggests that other ROS than H_2O_2 are important for root growth. In fact, it has been previously reported that the superoxide anion and, indeed the balance superoxide anion / H_2O_2, is important for the transition from proliferation to differentiation in the root (Tsukagoshi et al., 2010).

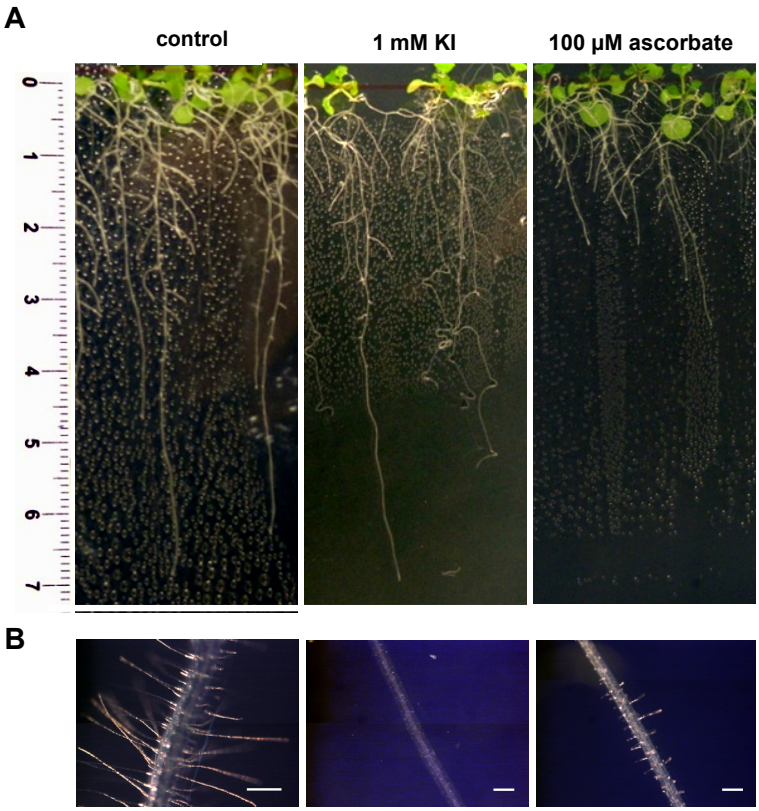

Figure III.4.11 – Root phenotype of Arabidopsis seedlings growing in the presence of ROS scavengers for 10 days. (A) Overall aspect of Arabidopsis seedlings and roots in the Petri dishes. (B) Magnification of the root hair zone from a representative root. Scale bars, 100 µm.

Finally, seedlings were grown in the presence of H_2O_2 to investigate the effect of this signal molecule in the development of root hairs (Figure III.4.12). In the presence of 1 µM H_2O_2, roots and root hairs were significantly smaller than the control. However, root hair density looked similar. In the presence of 10 µM H_2O_2, the seedlings arrested growth completely and some of them became white (data not shown). Taking in account the putative role of H_2O_2 in root hair growth (results with KI above and Foreman et al. (2003)), it was expected to see bigger root hairs in the seedlings treated with H_2O_2, but it was just the opposite that occurred (Figure III.4.12). On the one hand,

it is possible that seedlings being exposed to the signal molecule H_2O_2 for several days may induce several levels of effects in the seedlings, namely systemic responses, some of which eventually affect negatively the tip growth of root hairs, but not their differentiation. On the other hand, it is possible that a generalized overabundance of H_2O_2, contrary to a highly localized physiological production, may induce cross-linking of cell wall components by other Prxs than the ones co-localized with AGPs, increasing the rigidity of the cell wall and counteracting tip growth.

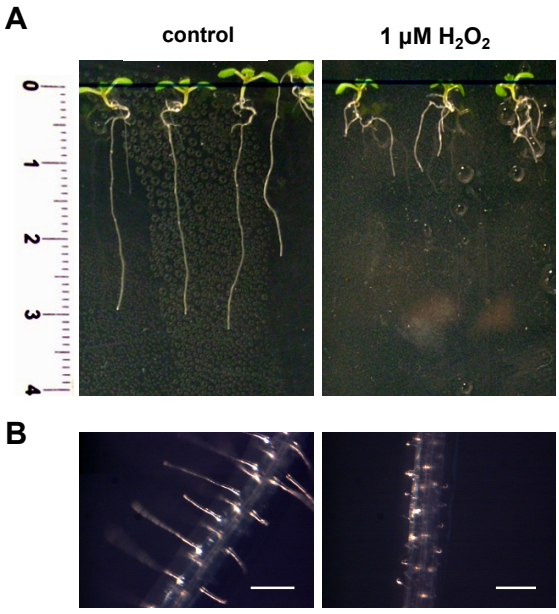

Figure III.4.12 – Root phenotype of Arabidopsis seedlings growing in the presence of H_2O_2 for 6 days. (A) Overall aspect of Arabidopsis seedlings and roots in the Petri dishes. (B) Magnification of the root hair zone from a representative root. Scale bars, 100 µm.

III.4.3 The tip growth of root hairs is affected by AGPs, Prx, anti-AGPs and anti-Prx

In order to avoid secondary and systemic effects in seedlings due to prolonged exposure to treatments (as done in the previous section), a second set of experiments was designed where the tip growth rate was specifically monitored, immediately after transference of 3-4 days old seedlings to medium with different treatments. This medium was in a thin layer, covering the bottom of a well made of a cover slip, thus enabling the observation of the root hairs in an inverted microscope (Figure III.4.13). This time, the influence of factors specifically binding to AGPs or Prx was investigated. Thus, the seedlings were incubated in the presence of different mAbs recognizing root AGP epitopes (section III.4.1), and of two anti-Prx polyclonal sera: the anti-Prx used in previous sections, recognizing CroPrx1 and AtPrx34, and an anti-CroPrx1 produced

against two peptides of CroPrx1. Additionally, seedlings were also exposed to two different concentrations of AtPrx34 and gum arabic. The measurement of the elongation rate was always made in root hairs that had around 25 µm as starting size, in order to measure them in similar growth phases. The results obtained are presented in Figure III.4.14.

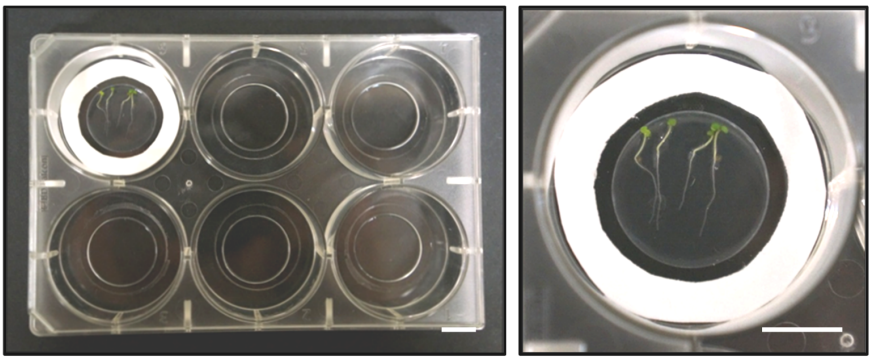

Figure III.4.13 – 6-well plate with the bottom of the wells made of a cover slip for the observation in an inverted microscope. Scale bars, 1 cm.

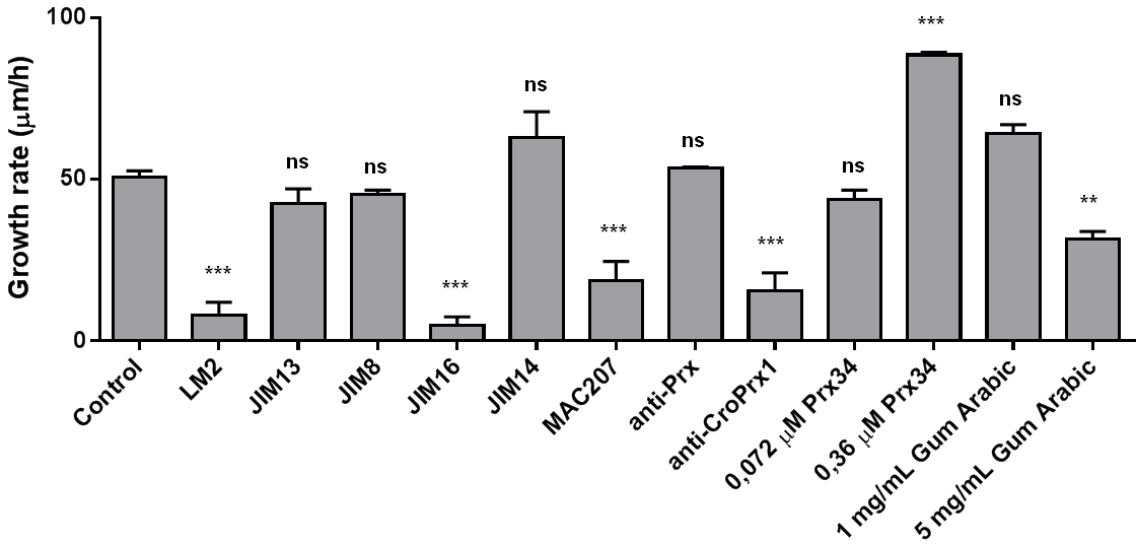

Figure III.4.14 – Growth rate of Arabidopsis root hairs in the presence of different treatments. Values are means ± SE. (ns) mean differences are not statistically significant, (***) $p< 0.001$, (**) $p< 0.01$, one way ANOVA, multiple comparisons.

In our experimental setup, the control root hairs had a medium elongation rate of 0.85 µm per minute, near the maximum values reported of 1 to 2 µm per minute (Duckett et al., 1994). The AGP mAbs JIM8 and JIM13 did not affect root hair elongation, in line with the fact that they did not label root hairs or trichoblasts (Figures III.4.7 and III.4.8), and confirming the absence of any unspecific effect due to the contact of the hairs with the mAbs. Interestingly, JIM14 did not significantly affect

elongation too, although it was shown to strongly label root hairs (Figure III.4.3). Therefore, it seems that AGPs with this epitope, although present in root hairs, are not essential for their elongation. Inversely, JIM16, LM2 and MAC207 significantly inhibited the elongation of root hairs, suggesting the participation of AGPs with these epitopes in the process. In agreement, MAC207 and JIM16 both labelled strongly root hairs (Figures III.4.4 and III.4.5) but, curiously, LM2 did not (Figure III.4.6). LM2 specifically labelled what seemed to be trichoblasts, but was absent from root hairs as far as we could detect. These results suggest that maybe some AGPs with LM2 epitopes indeed persist in root hairs, in levels that enable them to have an important function, but that are below the immunofluorescence detection level of the technique used. The anti-Prx used in previous sections for immunolocalization of Prx in *C. roseus* and Arabidopsis leaves (sections III.2 and III.3) did not affect the growth of root hairs (Figure III.4.14), in line with the absence of labelling found for roots and root hairs. However, when anti-CroPrx1 was used, a significant inhibition of the growth of root hairs was observed (Figure III.4.14). This antibody was prepared by immunization of rabbits with two surface peptides from CroPrx1 and it is possible that they recognize several Arabidopsis Prxs that share 5 aminoacids epitopes with those peptides. Significantly, this antibody clearly labelled Arabidopsis root hairs tip (Figure III.4.15). Therefore, it may be concluded that Prx is involved in elongation of Arabidopsis root hairs.

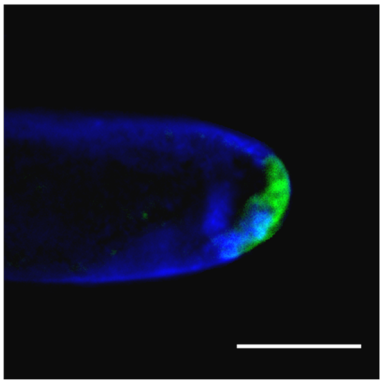

Figure III.4.15 – Green-immunofluorescence localization of Prx in Arabidopsis root hair using the anti-CroPrx1 antibody. Cell walls were counterstained with calcofluor (blue fluorescence). Scale bar, 10 μm.

In order to further investigate this involvement of AGPs and Prx in root hair elongation, the effect of the addition of AtPrx34 and gum arabic were also investigated. The presence of a low concentration of AtPrx34 did not affect the growth of the root hairs, but the presence of 0.36 μM significantly increased the elongation rate (Figure III.4.14). These results match well with the explanation based in the H_2O_2-Prx-AGP hypothesis that an excess of Prx will use the H_2O_2 produced by NADPH oxidase more

efficiently to induce a higher cross-linking of AGPs, and therefore a higher triggering of the signalling resulting in Ca^{2+} spiking and elongation. Conversely, the presence of gum arabic had a significant inhibitory effect in root hair elongation (Figure III.4.14), what could be explained by competition of gum arabic with the root hair endogenous AGPs for Prx, resulting in a lower cross-linking of the endogenous AGPs and therefore in a lower level of signalling triggering.

Overall, the results of this section all support a role for Prx and AGPs in the elongation of Arabidopsis root hairs, namely through an interaction between them. This interaction could fit in the present knowledge about tip growth in the following way: the H_2O_2 resulting from the tip localized activity of RHD2 NADPH oxidase (Foreman et al., 2003; Takeda et al., 2008) would be used by Prx localized at the tip (Figure III.4.15) to oxidise closely located AGPs (Figures III.4.3 – III.4.5), who would in turn trigger a signal resulting in the stimulation of the Ca^{2+} influx necessary for tip growth.

III.5 Genetic approaches to investigate the *in vivo* interaction between Prx and AGPs

The results of the previous sections all suggested the occurrence of a potentially functional interaction between Prx and AGPs in the medicinal plant *Catharanthus roseus* and the model plant *Arabidopsis thaliana*. In order to further investigate this interaction hypothesis *in vivo* it was decided to use a strategy involving fusions with fluorescent proteins (FPs) and Förster resonance energy transfer (FRET). The investigation of protein-protein interaction by FRET involves the fusion of each of the two potentially interacting proteins with a different and appropriate FP, in which one FP is excited by its specific wavelength and works as a donor of resonance energy to the second FP, which works as an acceptor and will emit light of its specific emission wavelength (Figure III.5.1). The most common pair of fluorophores used for this end is the cyan fluorescent protein (CFP) – yellow fluorescent protein (YFP) pair. When the CFP donor and YFP acceptor are in proximity (1–10 nm) due to the interaction of the two fused proteins, the donor CFP emission will decrease and the acceptor YFP emission will increase, because of the intermolecular FRET from the donor to the acceptor.

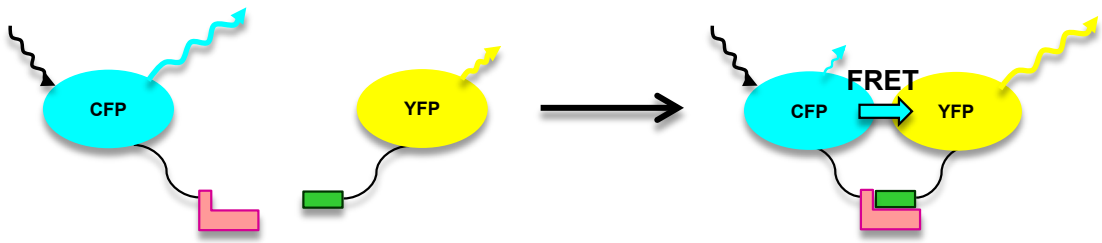

Figure III.5.1 – Image illustrating the occurrence of FRET when using the pair CFP-YFP to investigate protein-protein interaction.

To investigate the possible *in vivo* interaction Prx-AGP by FRET it was necessary to select specific Arabidopsis Prx and AGP gene(s). It was decided to use AtPrx34 for FRET studies, together with the AGPs more expressed in Arabidopsis leaves. The reasons to select AGPs and Prx from leaves were: i) all the work from section III.3 had been performed with Arabidopsis leaves, ii) the main Prx of Arabidopsis leaves (AtPrx34) had already been characterized and cloned in our lab, and iii) transient expression in protoplasts from Arabidopsis leaves, that was well established in our lab, is an easy and fast method to test FRET. Therefore, the AGPs more expressed in Arabidopsis leaves were selected by an *in silico* search, their cDNAs were ordered,

and the necessary FP fusion constructs were generated. Due to the difficulty in obtaining conclusive results, the selected AGP and Prx genes were used successively for transient and stable transformation of Arabidopsis, using both the strong, constitutive 35S promoter, and the respective endogenous promoters. In parallel, a preliminary analysis of the knock-outs and overexpressors of the selected AGP genes was performed.

III.5.1 *In silico* search for highly expressed classical AGP genes in Arabidopsis leaves

In order to select the main leaf AGPs in Arabidopsis, the microarray database GENEVESTIGATOR (www.genevestigator.ethz.ch) (Hruz et al., 2008; Hruz et al., 2011) was used to screen the expression levels of all Arabidopsis AGP genes. The GENEVESTIGATOR data provides absolute expression levels computed from numerous microarrays studies, indicating broad expression patterns over distinct organs, developmental stages and experimental conditions. Since GENEVESTIGATOR enables only the expression analysis of 10 genes at a time, several rounds of analysis were performed for the 22 classical AGP genes identified in Arabidopsis (Showalter et al., 2010), always selecting the genes with higher expression in leaves, based on the absolute expression values. Figure III.5.2 shows the 10 more highly expressed Arabidopsis classical AGP genes in leaves of Arabidopsis excluding *AGP6* and *AGP11*. These two extensively studied AGPs in Arabidopsis for their importance in reproduction, not being among the first 3 genes in leaves, were not selected for this analysis since they reach an expression level in flowers much higher than all the other Arabidopsis AGP genes, what would make all the differences between the other genes difficult to observe if they were plotted together in the same graph. Figure III.5.2 clearly shows that *AtAGP9* and *58* are the more transcriptionally abundant AGPs in Arabidopsis, especially in leaves. *AtAGP9* is also highly expressed in roots and *AtAGP58* is highly expressed in seedlings, particularly in cotyledons. In order to compare in more detail the expression profiles of *AtAGP9* and *58*, it was performed an analysis only with these two genes, which confirmed the strong expression of both genes in leaves (Figure III.5.3). However, the expression of *AtAGP58* was higher than *AtAGP9*. *AtAGP58* presented also a higher expression in seedlings. On the other hand, *AtAGP9* exhibited a higher expression in roots, siliques and flowers (Figure III.5.3).

In sum, transcriptomic analysis using the microarray database GENEVESTIGATOR identified *AtAGP58* and *AtAGP9* as classical AGP genes with

high global expression in Arabidopsis, being the most expressed in the leaves, the focus of this work. Consequently, these genes were selected for further studies.

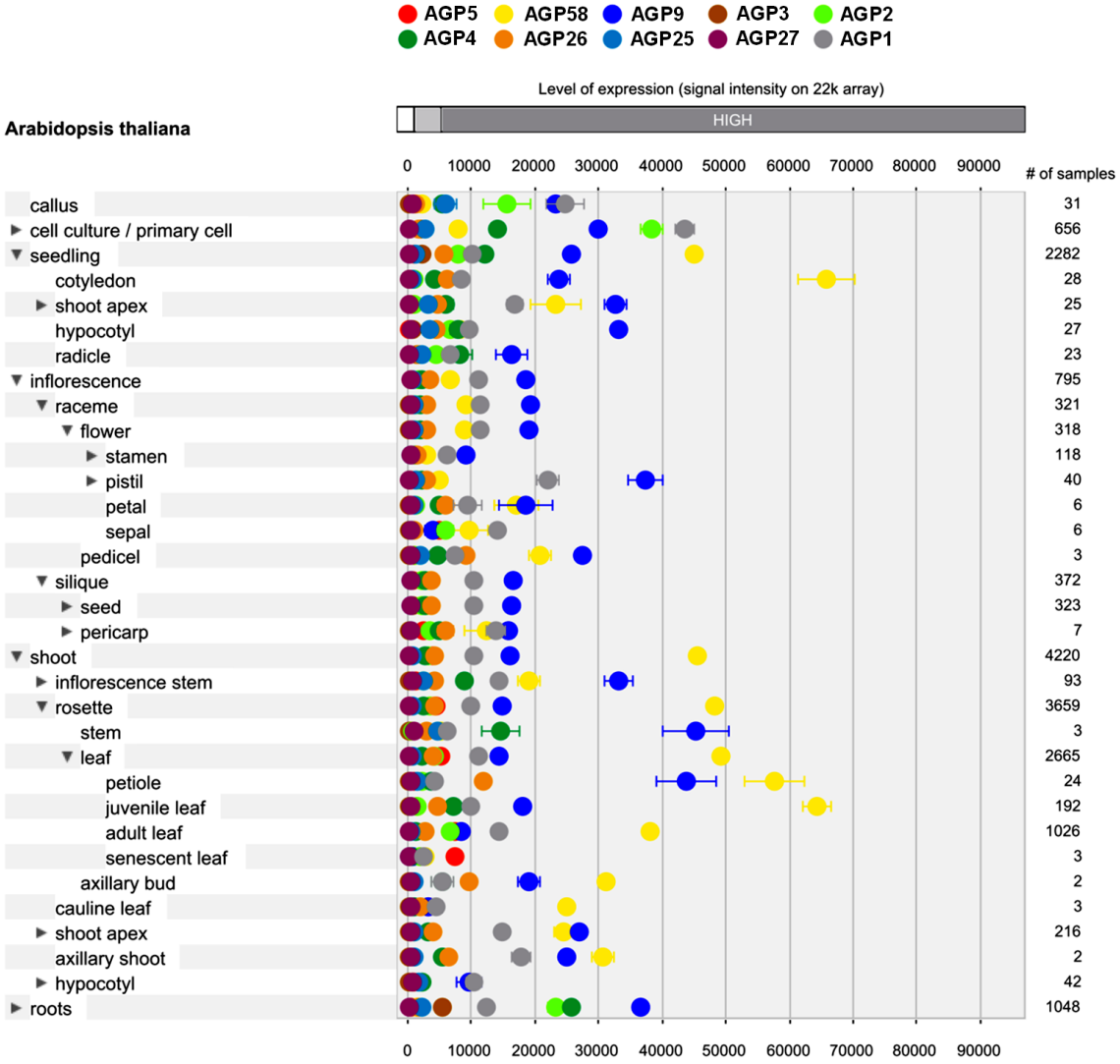

Figure III.5.2 – *In silico* characterization using GENEVESTIGATOR of the expression profile in different Arabidopsis organs of the 10 classical Arabidopsis *AGP* genes with higher expression in leaves, excluding *AGP6* and *11*. Data represent compiled Arabidopsis microarray experiments as reported by GENEVESTIGATOR, with the number of microarray experiments used to compute the expression values represented on the right as number of samples.

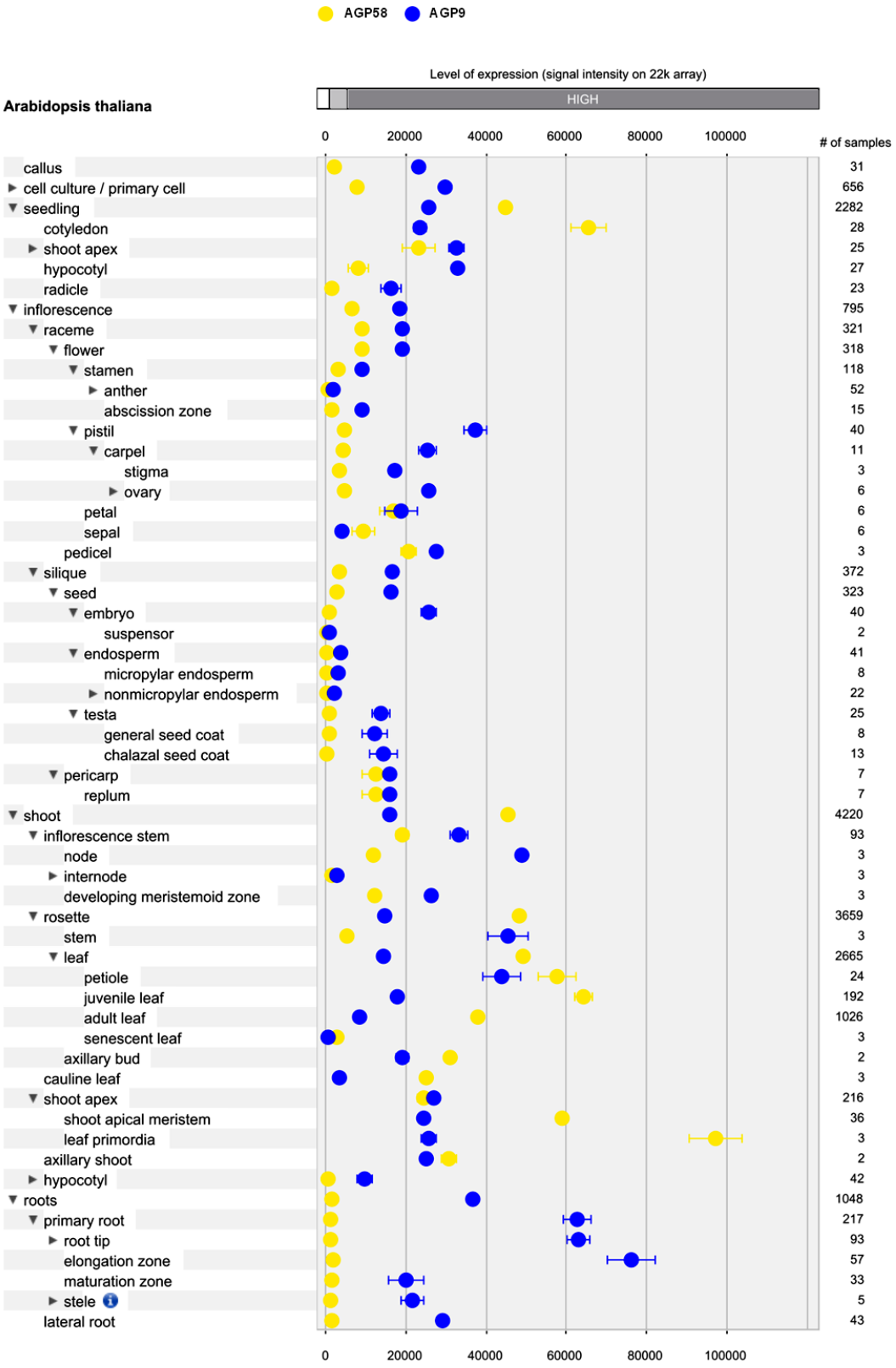

Figure III.5.3 – *In silico* characterization using GENEVESTIGATOR of the expression profile of *AtAGP9* and *58* in different Arabidopsis organs. Data represent compiled Arabidopsis microarray experiments as reported by GENEVESTIGATOR, with the number of microarray experiments used to compute the expression values represented on the right as number of samples.

III.5.2 Transient expression and co-expression of FP fusions with *AtPrx34* and *AtAGP9* or *58*

With the final aim of performing FRET, the cDNAs of *AtPx34*, *AtAGP9* and *58* were used to generate fusion constructs of each gene with both YFP and CFP, in order to be sure of generating the best possible conditions for the occurrence of FRET. A newer optimized version of CFP was used, the sCFP4 or mTurquoise, since it is brighter and more photostable than other CFP variants, at the same time it has a lifetime among the highest reported for fluorescent protein variants so far (Goedhart et al., 2010). These features make this CFP an excellent FRET donor for protein-protein interaction studies (Goedhart et al., 2010). The constructs were cloned in the plant expression vector pMON999 under the control of the strong constitutive promoter e35S, a version of the 35S promoter from cauliflower mosaic virus enhanced by a complete duplication. For AtPrx34, the major Prx present in Arabidopsis leaves (Figueiredo, 2011), two types of constructs were performed: i) one set with the ER signal peptide (SP) at the N-terminus of the FP and the mature protein (MP) plus the C-terminal extension (CTE) constituting a vacuolar sorting signal at the C-terminus of the FP, and ii) a second set in which the CTE as not present, in order to obtain a protein fusion that will be secreted (Figure III.5.4A). In this way, expression of the two constructs should result in a Prx protein sorted to the vacuole in the first case (vPrx34), and a Prx protein secreted to the extracellular space in the second case (sPrx34), that potentially would be able to associate with the plasma membrane AGPs (as observed by co-immunolocalization in Figure III.3.11 from section III.3). In the case of AGPs, the fusions were performed including each AGP SP at the N-terminus of the FP, and the remainder AGP sequence, including the C-terminal GPI signal, at the C-terminus of the FP (Figure III.5.4B).

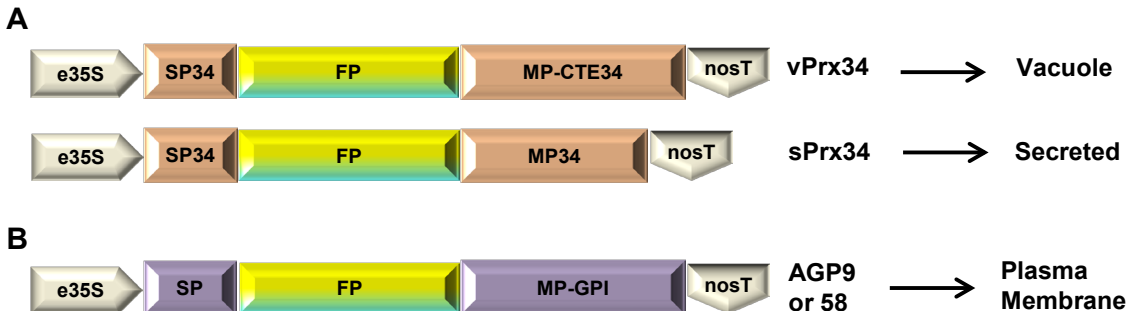

Figure III.5.4 – Schematic representation of the FP-fusions. (A) Scheme of the FP-fusions for AtPrx34. (B) Scheme of the FP-fusions for AtAGP9 and 58. FP – fluorescent protein. e35S – double 35S promoter. SP – signal peptide. MP – mature protein. MP-CTE – mature protein with C-terminal extension. MP-GPI – mature protein with GPI-signal sequence. nosT – *nos* terminator.

The rationale of the strategy followed here was that each Prx and AGP fusion with the respective FP would be sorted to membrane microdomains similarly to the observed with both cytochemical and immunolocalization studies in the previous sections for Prx and AGPs. The possible interaction between Prx and AGPs in those microdomains could then be evaluated by the occurrence or not of FRET. However, when the Prx and AGP fusions were transiently expressed in Arabidopsis leaf protoplasts, the observed fluorescence never appeared organized in microdomains (Figures III.5.5 and III.5.6). The vPrx34 fusions profusely labelled the entire content of the vacuoles, while the sPrx34 fusions labelled the ER and possibly the Golgi, but never seemed to label the plasma membrane, maybe because they were secreted to the medium and did not remain attached to the plasma membrane (Figure III.5.5). On their turn, the fusions of AtAGP9 and 58 clearly labelled intensely the plasma membrane in a continuous way, as can be seen in Figure III.5.6, where fluorescence appears as a thin continuous line outside the chloroplasts, unequivocally identified as the plasma membrane. A co-transformation of an YFP-fusion of sPrx34 with a CFP-fusion of AtAGP58 was tried but was inconclusive (Figure III.5.7): the Prx fusion yellow fluorescence appeared in the ER and did not show any overlapping with the blue fluorescence of the AtAGP58 fusion, which appeared in the plasma membrane with a continuous localization. It was reasoned that this absence of organization of the protein fusions in membrane associated microdomains, like expected, could either result from: i) the use of a very strong promoter resulting in high and saturating protein levels that invaded the whole plasma membrane or vacuolar compartment instead of remaining restricted to membrane associated microdomains, or ii) the loss of a typical plasma membrane organization due to the absence of cell wall in protoplasts. Therefore, three successive strategies were essayed to try to circumvent these possible artefacts: i) the use of the native promoters to obtain an equilibrated expression level, ii) the use of transient expression in tobacco leaf epidermis to use a natural plant cell environment with a cell wall, and iii) the generation of stable transformants of Arabidopsis.

Therefore, the promoter regions of *AtAGP9* and *58* were identified using the SAP Arabidopsis Promoterome Database (www.psb.ugent.be/promoter), and they were amplified and cloned, together with the *AtPrx34* promoter previously isolated in our lab (Figueiredo, 2011), upstream the previously generated FP fusions, in the binary vector pGreenII235. Transient expression in Arabidopsis leaf protoplasts of the *AtAGP58* fusion with CFP under the control of the endogenous promoter showed that fluorescence still appeared as a continuous line in the plasma membrane (Figure III.5.8), thus, no more transformations were performed with this expression system.

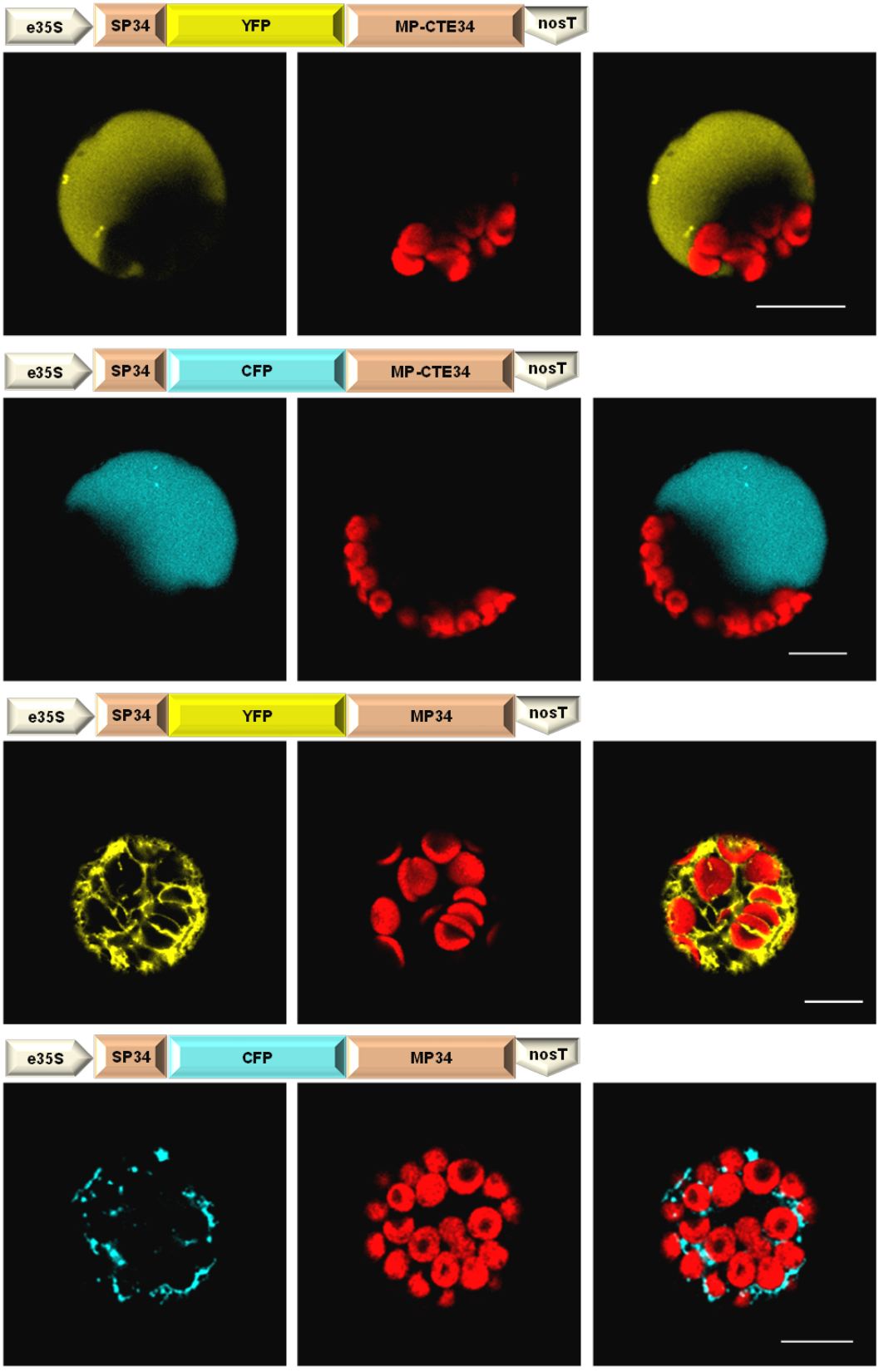

Figure III.5.5 – Transient transformation of *A. thaliana* mesophyll protoplasts with AtPrx34 FP-fusions. Images on the left – YFP or CFP channel. Images in the middle – red channel showing chloroplast autofluorescence. Images on the right – merged images. The schematic representation of each construct used for transformation is depicted right above the respective set of confocal images. Scale bars, 10 µm.

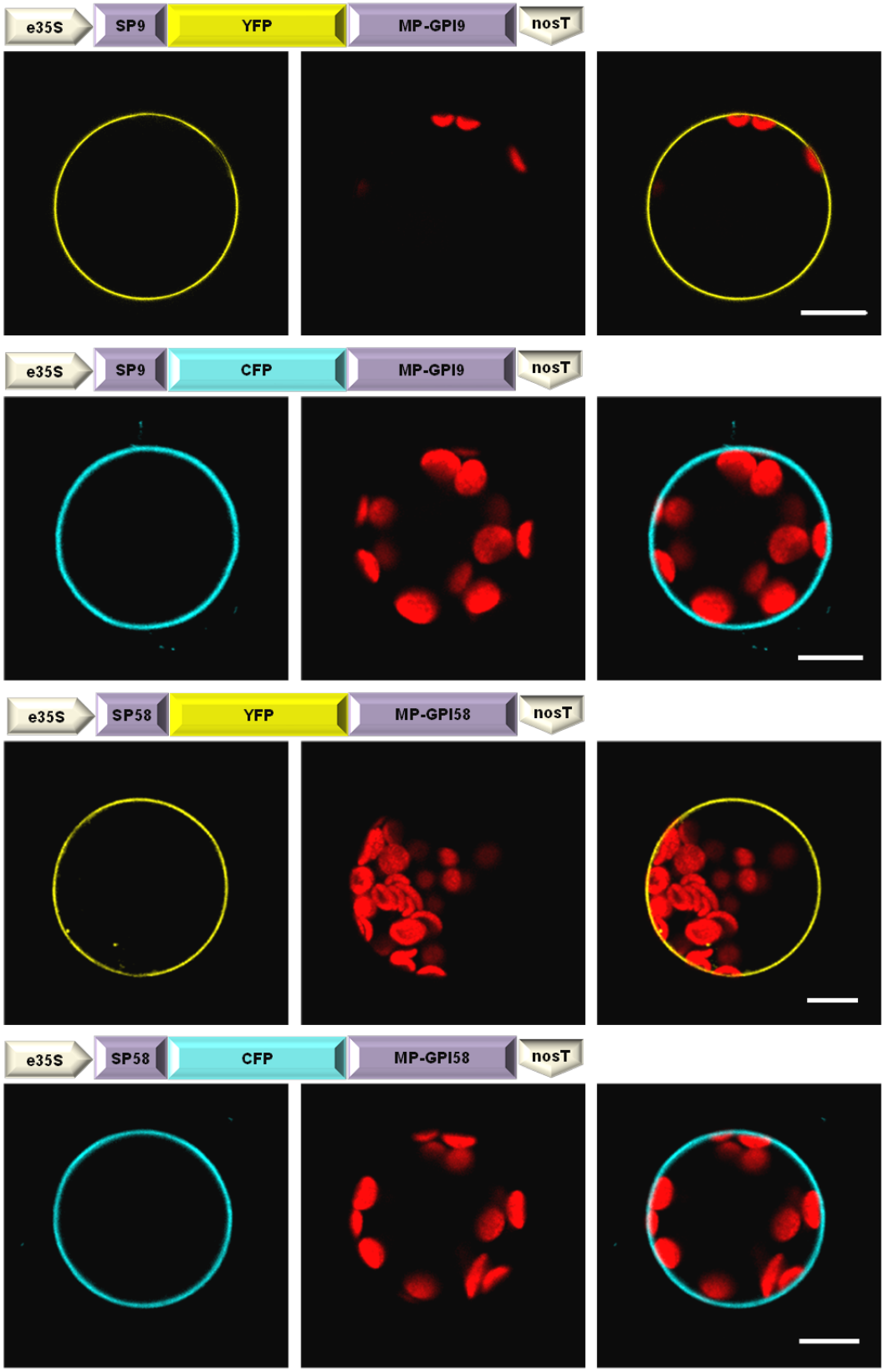

Figure III.5.6 – Transient transformation of *A. thaliana* mesophyll protoplasts with AtAGP9 and 58 FP-fusions. Images on the left – YFP or CFP channel. Images in the middle – red channel showing chloroplast autofluorescence. Images on the right – merged images. The schematic representation of each construct used for transformation is depicted right above the respective set of confocal images. Scale bars, 10 µm.

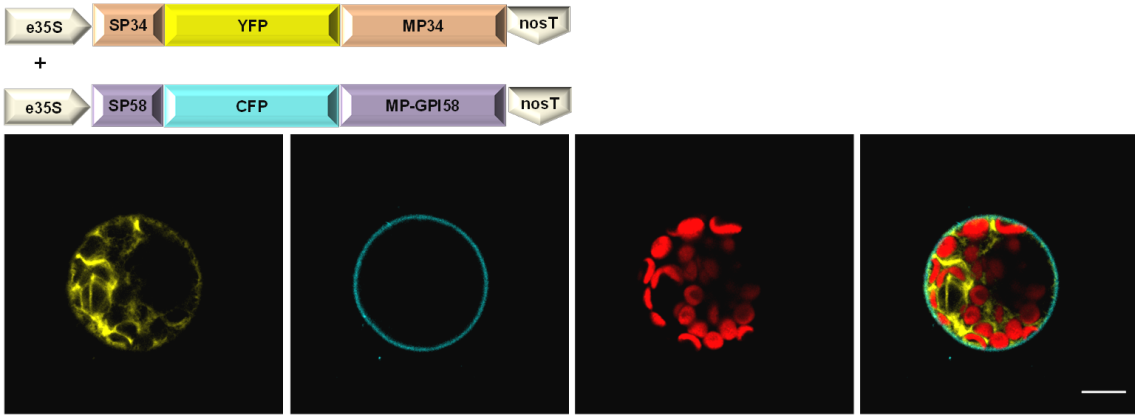

Figure III.5.7 – Transient co-transformation of *A. thaliana* mesophyll protoplasts with sPrx34 YFP-fusion and AtAGP58 CFP-fusion. First image – YFP channel. Second image – CFP channel. Third image – red channel showing chloroplast autofluorescence. Last image – merged image. The schematic representation of each construct used for co-transformation is depicted right above the confocal images. Scale bar, 10 µm.

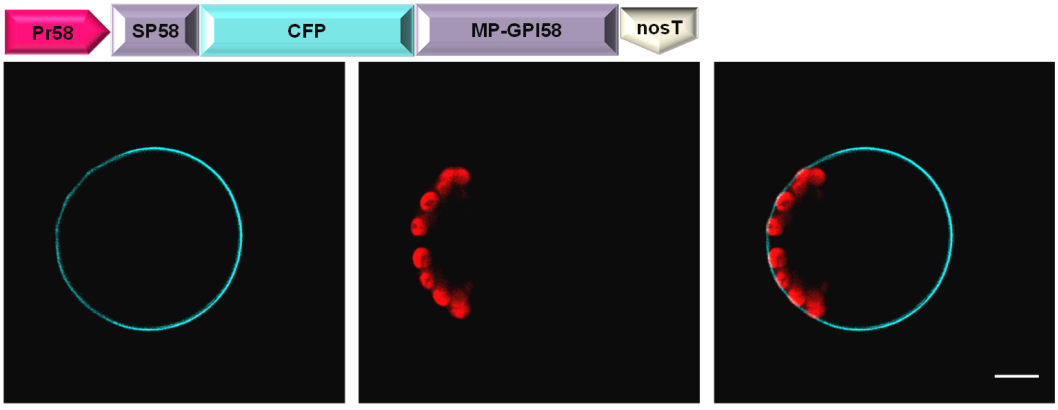

Figure III.5.8 – Transient transformation of *A. thaliana* mesophyll protoplasts with AtAGP58 CFP-fusion under the control of the endogenous promoter. Image on the left – CFP channel. Image in the middle – red channel showing chloroplast autofluorescence. Image on the right – merged image. The schematic representation of the construct used for transformation is depicted right above the confocal images. Scale bar, 10 µm.

Next, the constructs under the control of the 35S promoter were used for transient expression in tobacco leaf epidermis (Figures III.5.9 – III.5.11). The vPrx34 fusion with CFP appeared again occupying the entire vacuole, and not associated to tonoplast microdomains (Figure III.5.9). For the correspondent fusion with YFP it was not possible to obtain results. Curiously, the FP fusions of sPrx34 presented behaviours somewhat different when CFP or YFP were used (Figure III.5.9). For the YFP fusion, the fluorescence appeared in the ER, presenting sometimes a discontinuous peripheral distribution, which was not clear if it corresponded to the ER from a thin layer of cytoplasm or the plasma membrane. On the contrary, for the CFP equivalent fusion, fluorescence was never detected in the ER, and it seemed to label continuously the plasma membrane. This meant that the presence of a different FP in a

fusion seemed to influence at least the efficiency of the transit of the fusion throughout the secretory pathway, and raised concerns about the validity of this strategy/system.

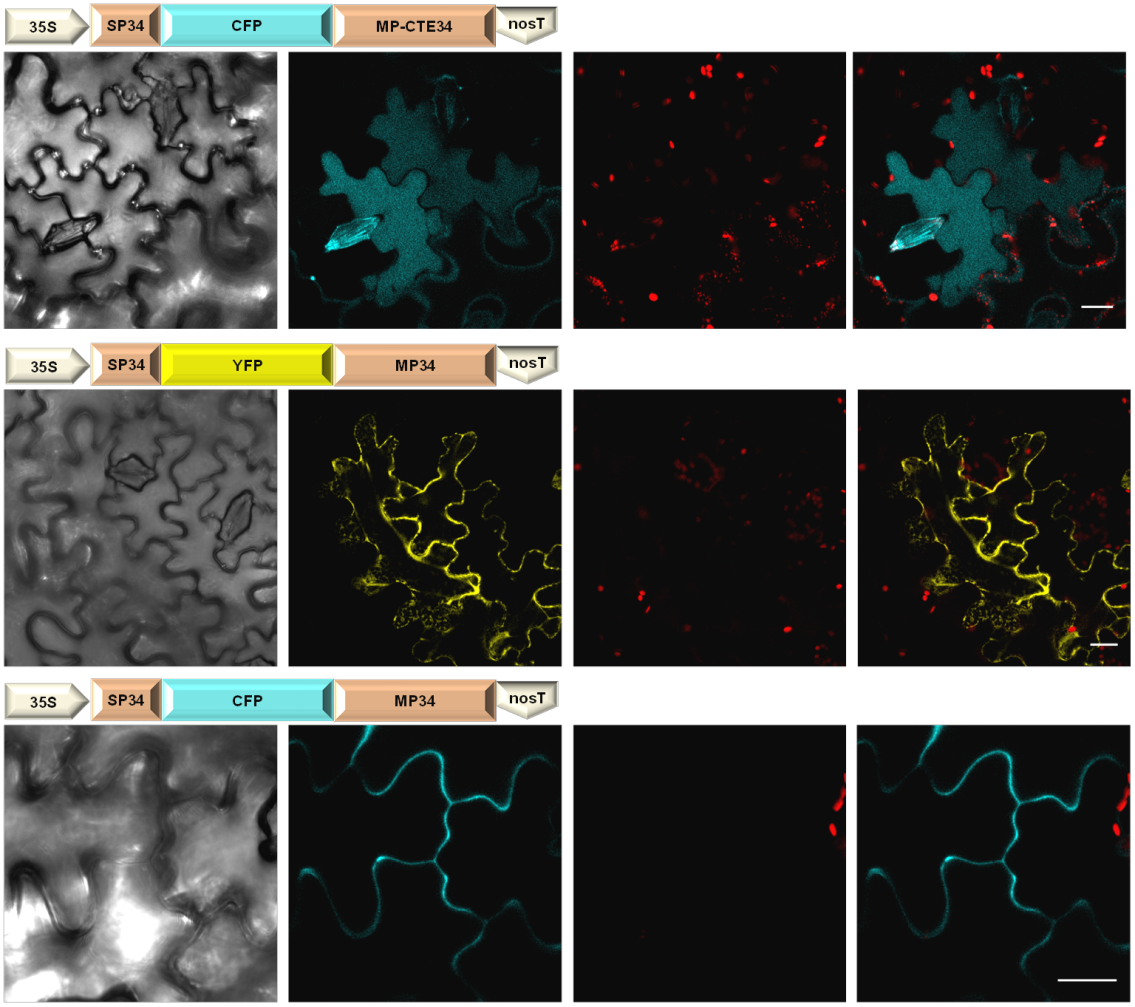

Figure III.5.9 – Confocal images of tobacco epidermal cells transiently expressing the vPrx34 and sPrx34 FP-fusions. First column – bright field images. Second column – YFP or CFP channel. Third column – red channel showing chloroplasts autofluorescence. Last column – merged images. The schematic representation of each construct used for transformation is depicted right above the respective set of confocal images. Scale bars, 20 μm.

For the fusions of AtAGP9 and 58 with both CFP and YFP, the results were similar among them and with the previously obtained for expression in Arabidopsis leaf protoplasts – continuous labelling of the plasma membrane (Figure III.5.10). Co-transformation of tobacco leaf epidermis with the CFP fusion of vPrx34 and the YFP fusion of AtAGP58 reproduced the individual transformation labelling, with the AtPrx34 fusion blue fluorescence filling the vacuole and the AtAGP58 fusion yellow fluorescence labelling the plasma membrane (Figure III.5.11). When the YFP fusion of sPrx34 was used for co-transformation with the CFP fusion of AtAGP9 and 58, the yellow fluorescence of the AtPrx34 fusion always seemed to localize inside the blue

fluorescence of the AGP fusions, suggesting that, in fact, the YFP fusions of sPrx34 localized mainly at the ER or other cytoplasmic components of the secretory pathway, and not at the plasma membrane (Figure III.5.11). Finally, individual transformations were performed using the endogenous promoters instead of 35S (Figures III.5.12 and III.5.13). Since the results were quite similar to the ones observed when using the 35S promoter (Figures III.5.9 and III.5.10), and it was still not possible to observe any clear organization in membrane microdomains, no co-transformations were performed.

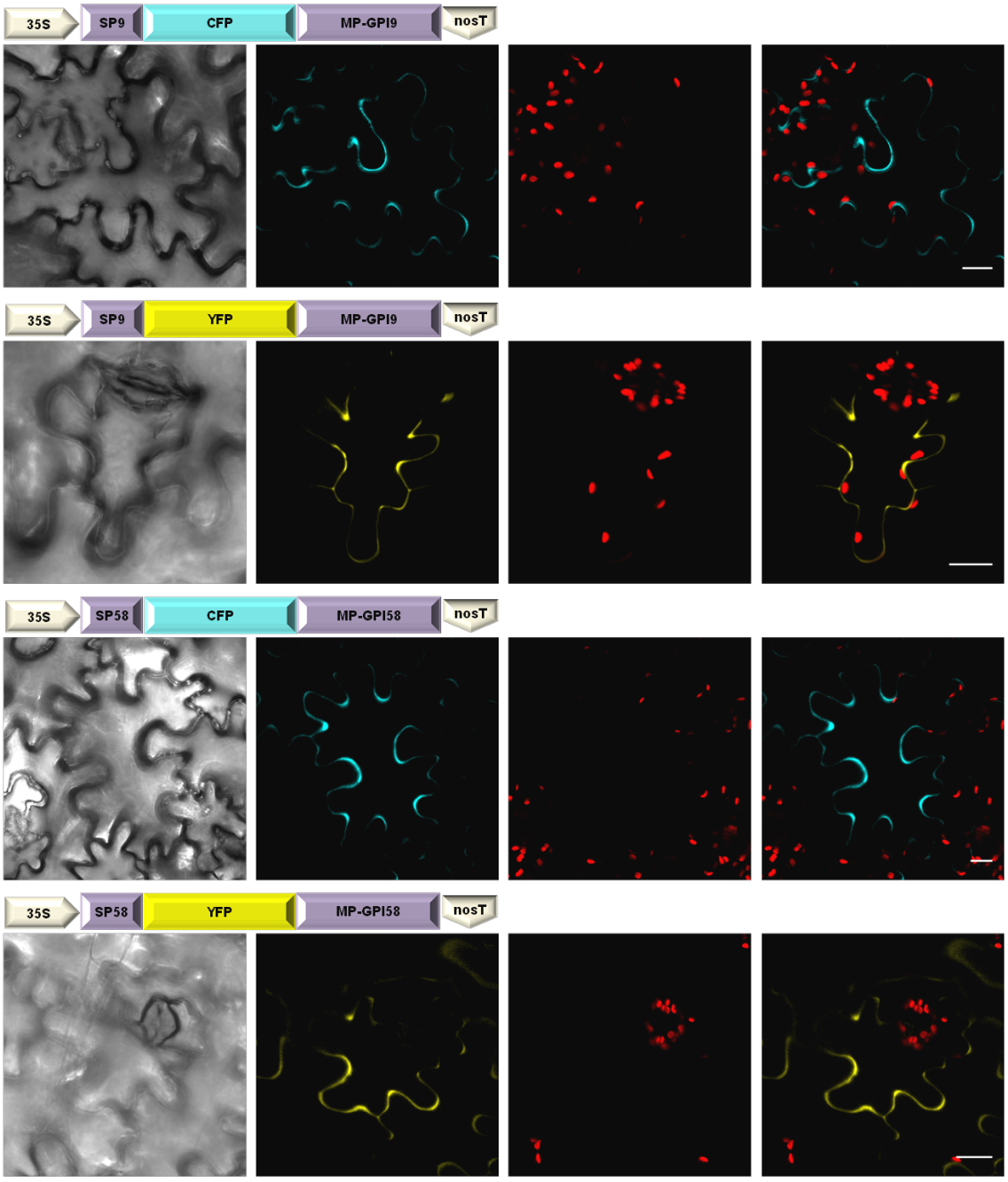

Figure III.5.10 – Confocal images of tobacco epidermal cells transiently expressing the AtAGP9 and 58 FP-fusions. First column – bright field images. Second column – YFP or CFP channel. Third column – red channel showing chloroplasts

autofluorescence. Last column – merged images. The schematic representation of each construct used for transformation is depicted right above the respective set of confocal images. Scale bars, 20 μm.

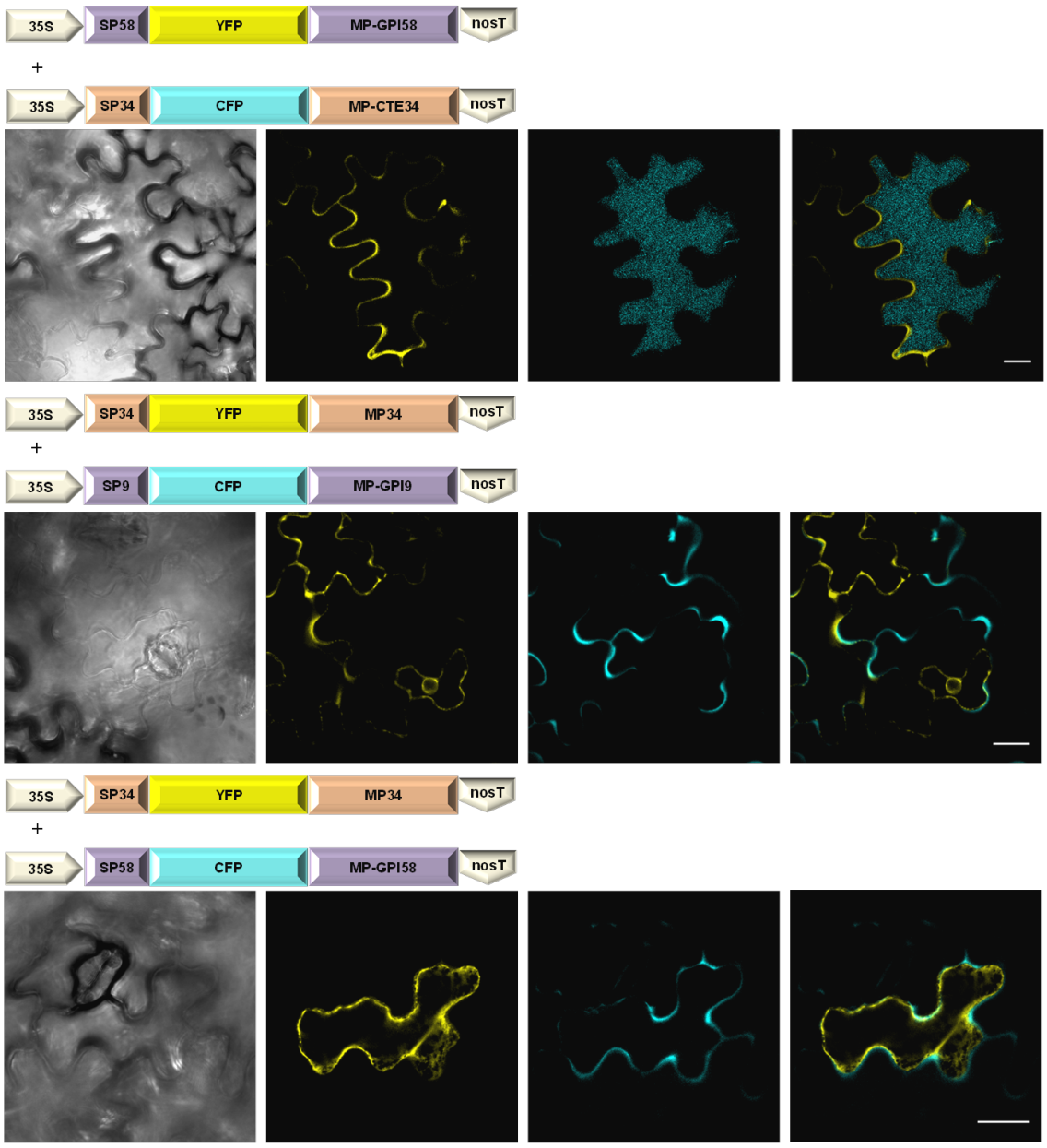

Figure III.5.11 – Confocal images of tobacco epidermal cells transiently co-expressing Prx and AGPs FP-fusions. First column – bright field images. Second column – YFP channel. Third column –CFP channel. Last column – merged images. The schematic representation of each construct used for co-transformation is depicted right above the respective set of confocal images. Scale bars, 20 μm.

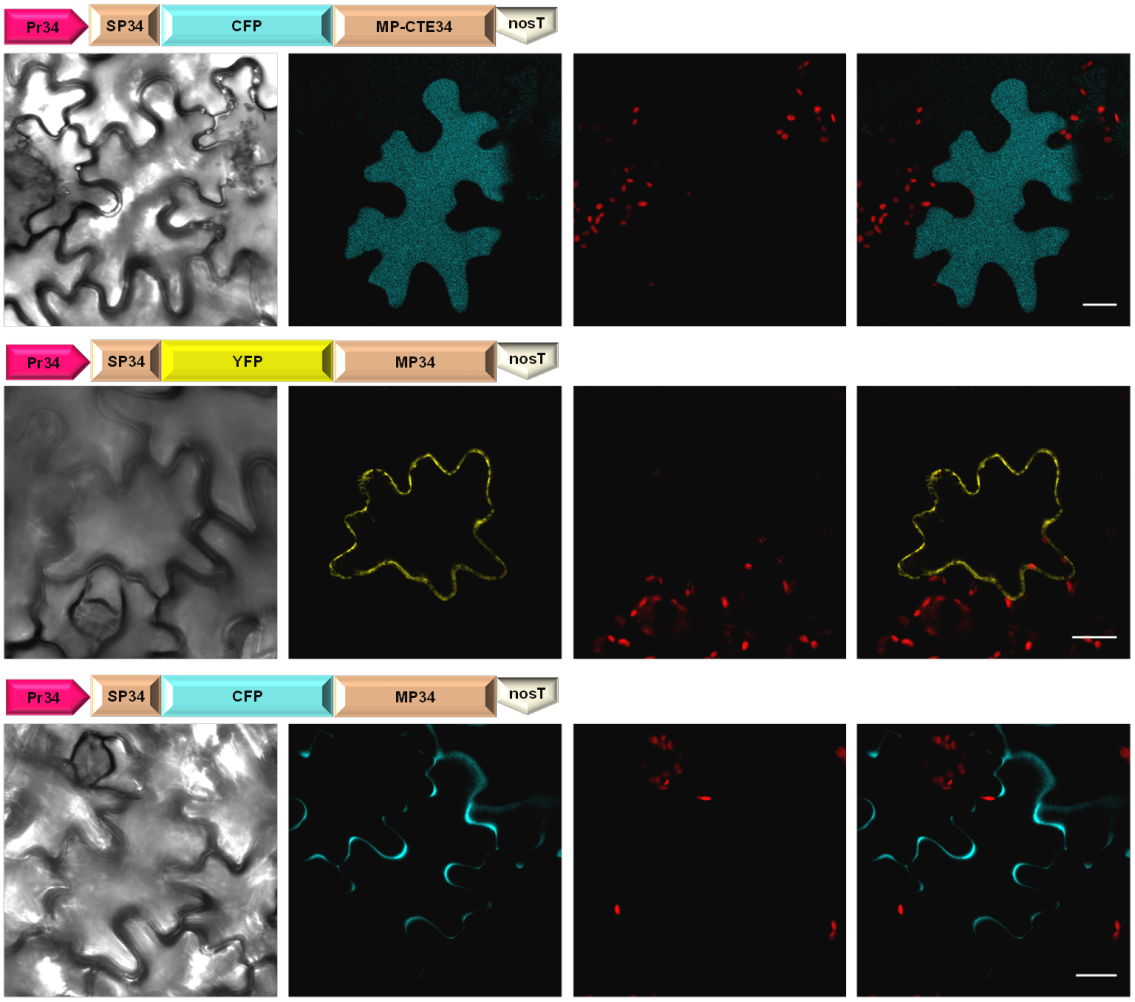

Figure III.5.12 – Confocal images of tobacco epidermal cells transiently expressing the AtPrx34 FP-fusion under the control of the endogenous promoter. First column – bright field images. Second column – CFP or YFP channel. Third column – red channel showing chloroplasts autofluorescence. Last column – merged images of the two channels. The schematic representation of each construct used for transformation is depicted right above the respective set of confocal images. Scale bars, 20 μm.

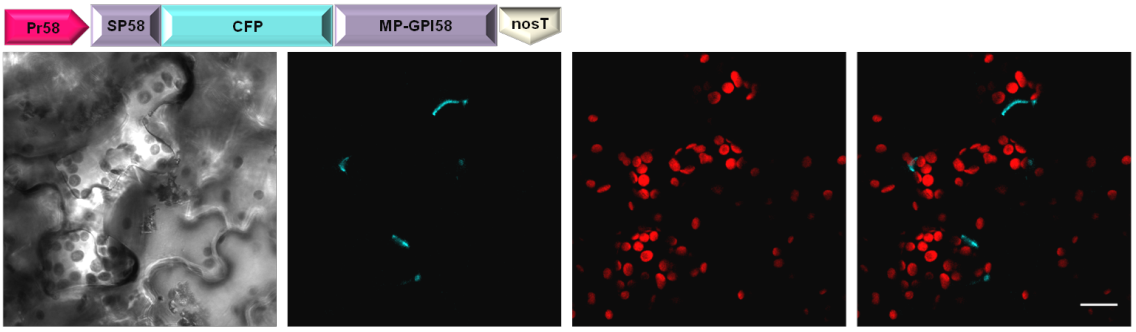

Figure III.5.13 – Confocal images of tobacco epidermal cells transiently expressing the AtAGP58 CFP-fusion under the control of the endogenous promoter. First image – bright field image. Second image – CFP channel. Third image – red channel showing chloroplasts autofluorescence. Last image – merged image. The schematic representation of the construct used for transformation is depicted right above the confocal images. Scale bar, 20 μm.

III.5.3 Stable expression and co-expression with AtPrx34 YFP-fusions and AtAGP9/58 CFP-fusions

Since expression in tobacco leaf epidermis was still not the ideal system to investigate the exact fine cellular organization and potential interaction of Prx and AGPs codified by Arabidopsis genes, a final strategy was tried that consisted in the stable transformation and co-transformation of Arabidopsis plants. Therefore, Arabidopsis plants were transformed by floral dipping, stable transformants were obtained, and the fluorescence pattern observed in the epidermal cells of leaves was investigated using confocal microscopy. The Arabidopsis leaf epidermis stably expressing the fusion of vPrx34 under the control of the 35S promoter showed fluorescence in all cells, which was present as a faint fluorescence filling the vacuole and more strongly in a thin peripheral layer that was somewhat discontinuous in some zones (Figure III.5.14A). When sPrx34 was used, fluorescence seemed to appear in the plasma membrane, also presenting a somewhat discontinuous pattern (Figure III.5.14B), even if not organized in isolated spot-like domains like observed with immunolocalization (see section III.3). Similarly, *AtAGP9* and *58* under the control of the 35S promoter seemed to label the plasma membrane in a less continuous way than the observed for tobacco leaf epidermis (Figure III.5.15). When co-transformation of AtAGP58 with sPrx34, both under the control of 35S, was performed, the two labellings largely overlapped when labelling was more or less continuous, but overlapped less when discontinuities were observed (Figure III.5.16).

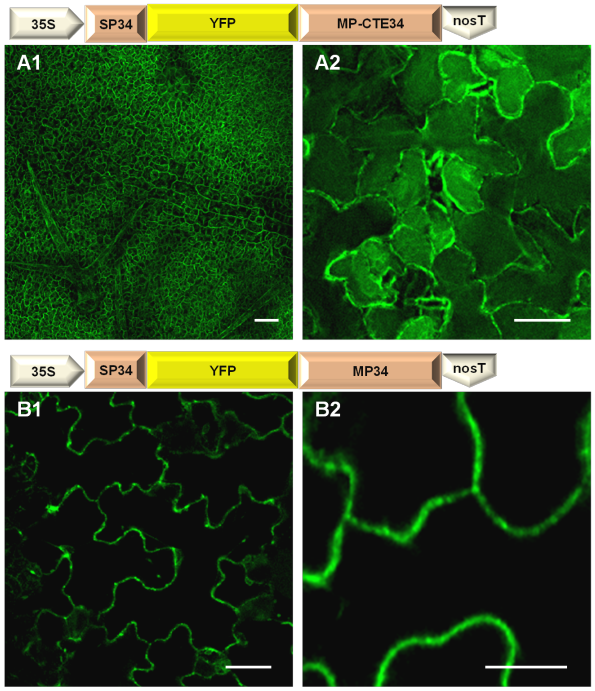

Figure III.5.14 - Confocal images of Arabidopsis leaf from plants stably expressing *vPrx34* or *sPrx34* under the control of the 35S promoter. (A) vPrx34. (B) sPrx34. The schematic representation of the constructs used in the stable transformation is depicted right above the confocal images. Scale bars for A and B1, 50 µm. Scale bar for B2, 20 µm.

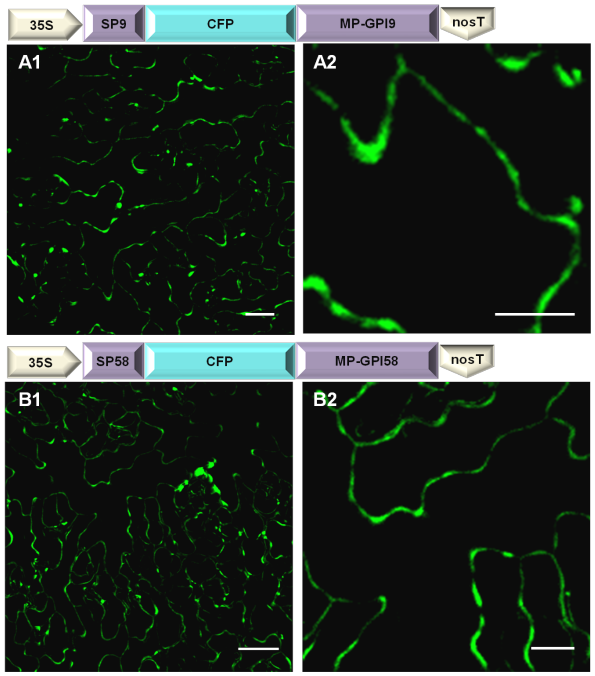

Figure III.5.15 – Confocal images of Arabidopsis leaf from plants stably expressing *AtAGP9* or *58* under the control of the 35S promoter. (A) AtAGP9. (B) AtAGP58. The schematic representation of the constructs used in the stable transformation is depicted right above the confocal images. Scale bars for A1 and B1, 50 µm. Scale bars for A2 and B2, 20 µm.

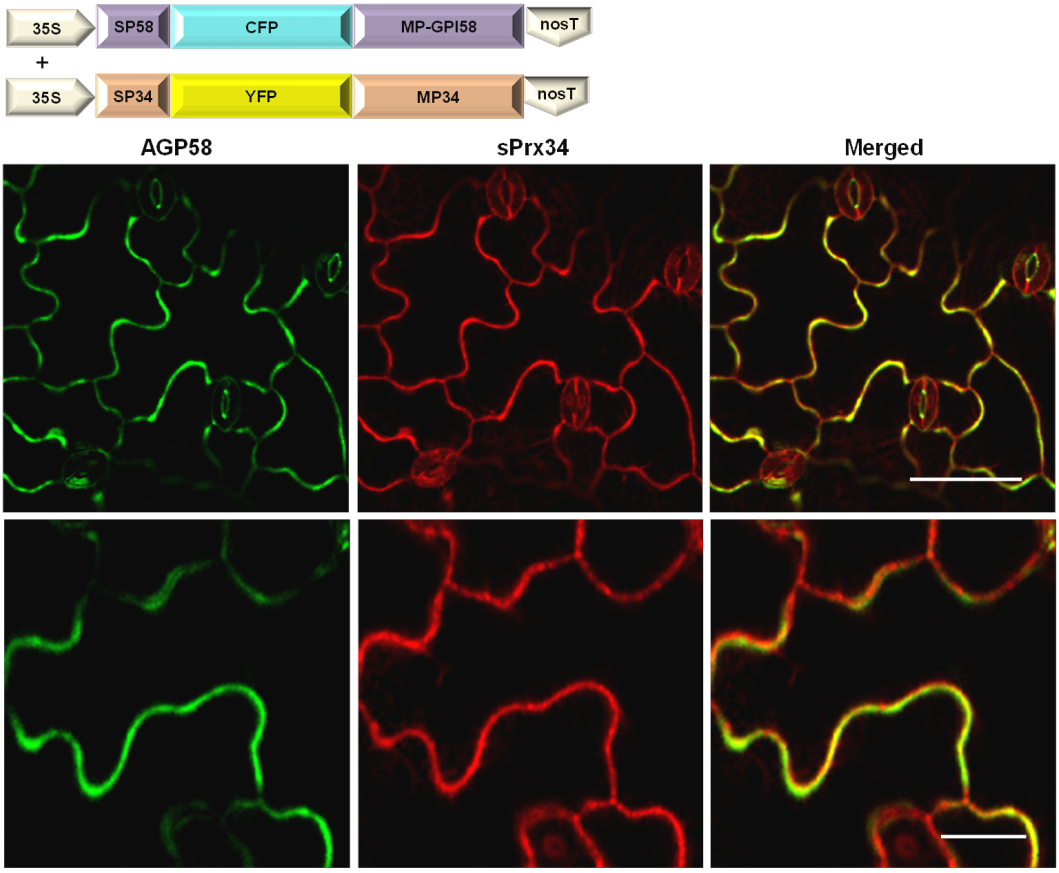

Figure III.5.16 – Confocal images of Arabidopsis leaf from plants stably co-expressing *AtAGP58* and *sPrx34* under the control of the 35S promoter. The schematic representation of the constructs used in the stable co-transformation is depicted right above the confocal images. Scale bars for upper images, 50 µm. Scale bars for bottom images, 20 µm.

When the endogenous promoter of *AtAGP58* was used, the fluorescence in leaf epidermal cells appeared in the plasma membrane with a relatively clear discontinuous pattern (Figure III.5.17). However, co-transformation with either the vPrx34 or the sPrx34 under the control of the respective endogenous promoter showed no significant overlapping of fluorescences (Figures III.5.17 and III.5.18). The fluorescence of vPrx34 fusion appeared mostly in the vacuole and also in the plasma membrane very faintly, but this labelling did not seem to clearly overlap with the labelling of AtAGP58 (Figure III.5.17). Curiously, the fluorescence of sPrx34 fusion could not be detected in the leaf epidermis, but only in some areas of the cell wall of the palisade parenchyma cells (Figure III.5.18), presenting only marginal overlap with the plasma membrane fluorescence of the AtAGP58 fusion protein. Screening of the fluorescence of AtAGP9 and sPrx34 in different organs of Arabidopsis plants co-transformed with the two under the control of the respective promoters never detected any significant overlapping of fluorescence, on the contrary, the fluorescence patterns were always divergent,

sometimes because the two genes were actually expressed in different cell types (Figure III.5.19).

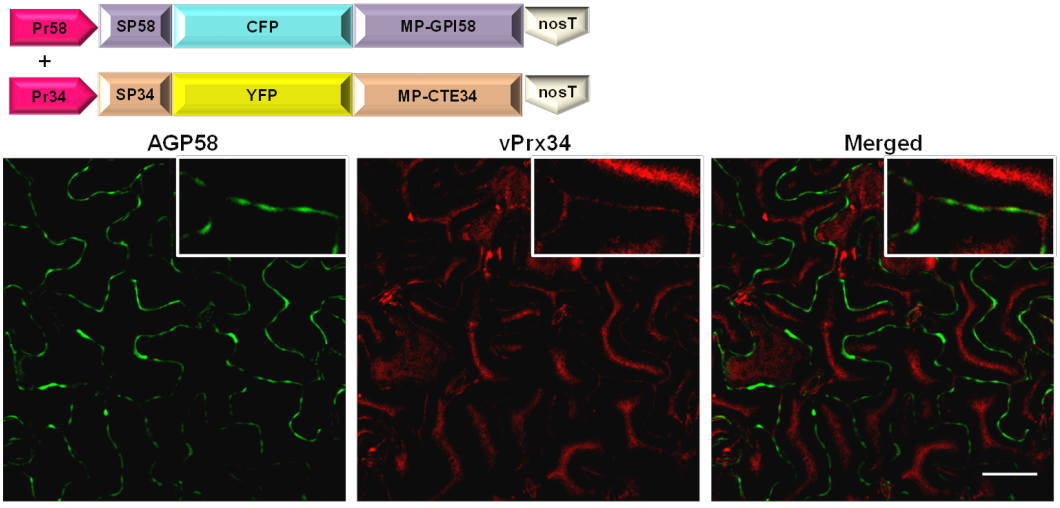

Figure III.5.17 – Confocal images of Arabidopsis leaf from plants stably co-expressing *AtAGP58* and *vPrx34* under the control of the endogenous promoters. The schematic representation of the constructs used in the stable co-transformation is depicted right above the confocal images. Scale bar, 50 µm.

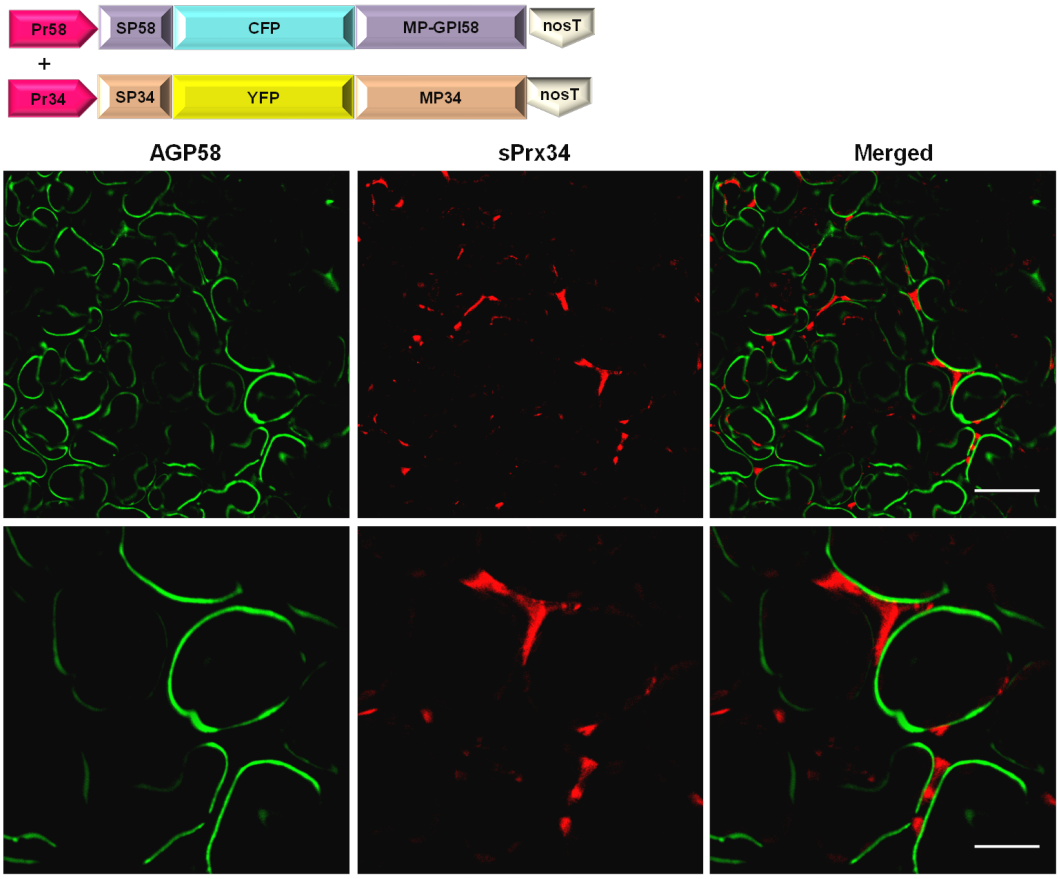

Figure III.5.18 – Confocal images of Arabidopsis leaf from plants stably co-expressing *AtAGP58* and *sPrx34* under the control of the endogenous promoters. The schematic representation of the constructs used in the stable co-

transformation is depicted right above the confocal images. Scale bars for upper images, 50 µm. Scale bars for down images, 20 µm.

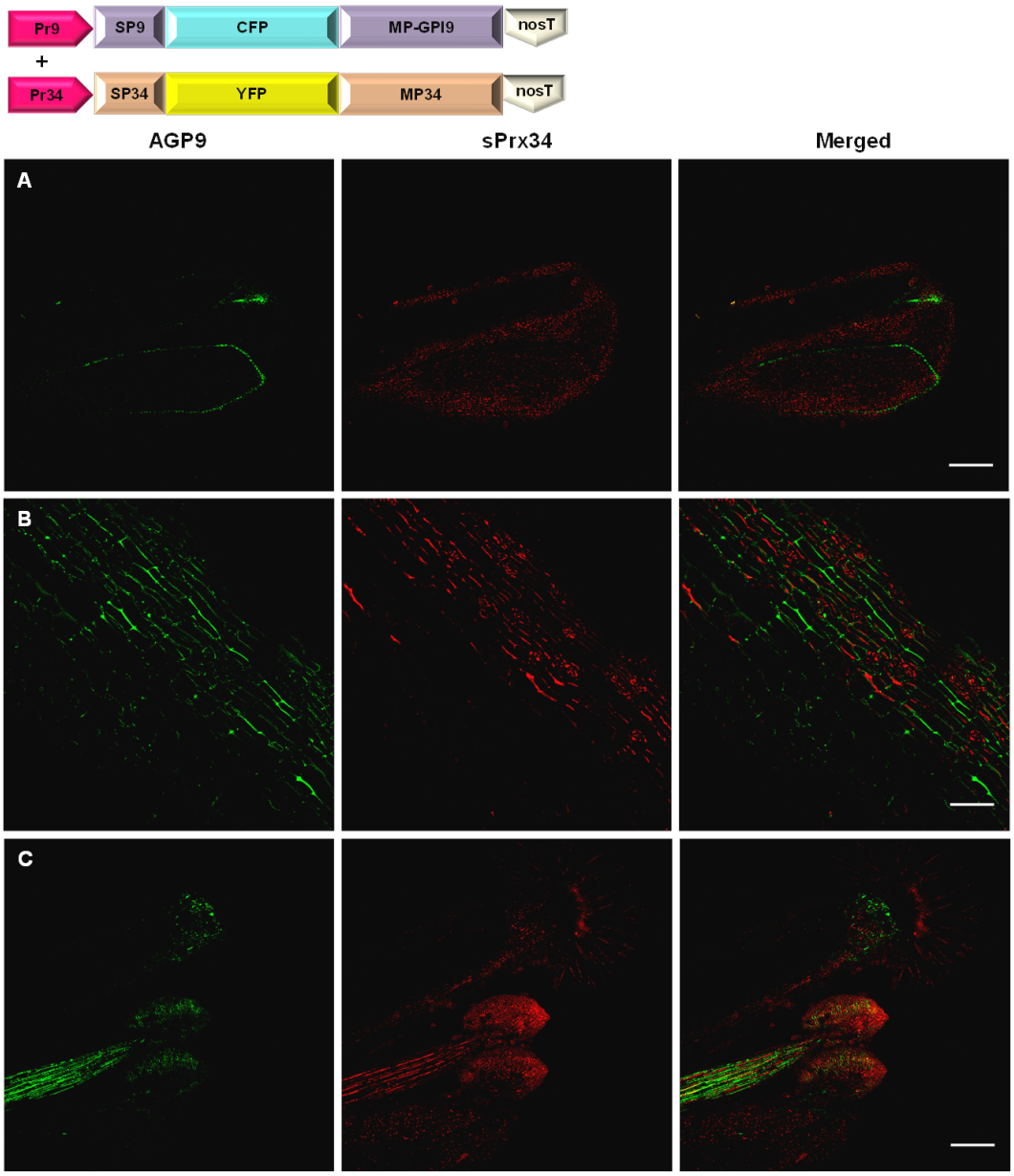

Figure III.5.19 – Confocal images of Arabidopsis plants stably co-expressing *AtAGP9* and *sPrx34* under the control of the endogenous promoters. (A) Petal. (B) Leaf midrib. (C) Stamen and carpel. Scale bars, 200 µm.

III.5.4 Preliminary characterization of overexpression lines for AtAGP9 and AtAGP58

The Arabidopsis lines generated in the previous section, with the AtAGP9 and 58 FP-fusions under the control of the promoter 35S, are overexpressing lines for AtAGP9 and 58 and were therefore analysed for the presence of a phenotype. All throughout development, these lines did not show any morphological phenotype in comparison

with the wild-type, neither did the AtAGP9 and 58 knock-out lines ordered from NASC – The European Arabidopsis Stock Center (data not shown). However, when the rate of root hair growth was measured in these lines and compared with the wild type, it could be seen that overexpression of AtAGP9 and 58 induced an increase in the elongation rate of root hairs of about 45 and 30% respectively (Figure III.5.20A). Moreover, observation of the root hairs under the confocal microscope confirmed that in these lines, the AtAGP9 and 58 FP-fusions were indeed present in the plasma membrane of root hairs (Figures III.5.20B and C).

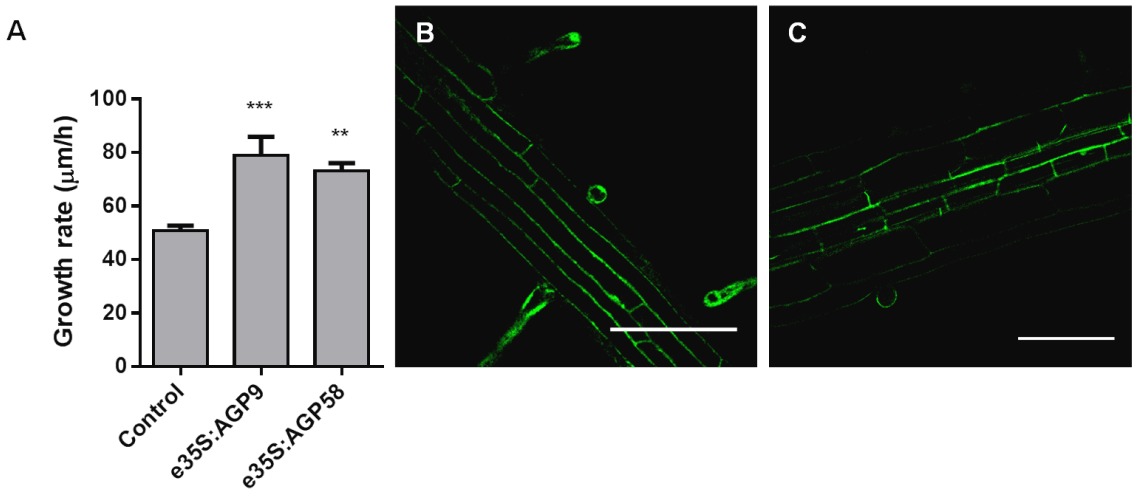

Figure III.5.20 – Growth rate of root hairs and CFP fluorescent pattern of *AtAGP9* and *58* under the control of the 35S promoter in Arabidopsis roots. (B) *AtAGP9*. (C) *AtAGP58*. (***) $p< 0.001$, (**) $p< 0.01$, t-test. Scale bar for B, 100µm. Scale bar for C, 50µm.

III.5.5 Conclusions

In conclusion, transient and stable expression of Prx and AGP fusions with FP proteins in different systems, including the whole plant homologous expression system, were inconclusive in what concerns the possibility of protein-protein interaction between Prx and AGPs. Neither was it possible to confirm whether AGPs or Prx are indeed targeted to membrane microdomains, although some images obtained when using the endogenous promoter of *AtAGP58* controlling the respective FP-gene fusion are suggestive of an organization in membrane patches (Figure III.5.17). One of the reasons for this failure may be that the genes used do not codify the right Prx and/or AGPs that are indeed interacting, and were detected by the antibodies used in section III.3. Another reason may be that the fusions with the FPs somehow disrupt the targeting of Prx and AGPs to the membrane microdomains where they are normally localized. There may still be the problem that although those microdomains are detected by immunolabelling, they may be more difficult to detect in a live dynamic

membrane, where movements of the domains will mask their existence in fluorescence confocal detection. In fact, the depth of field that can be obtained with the confocal microscope itself may also limit the possibility of detection of the microdomains, since the fluorescence of domains localized at different depths may coalesce in the captured image to yield a continuous signal.

However, an interesting result was obtained in this section, since it was observed that the ectopic accumulation of AtAGP9 and 58 both increased the rate of elongation of root hairs, supporting a role of AGPs in root hair tip growth, our model hypothesis for a functional role of H_2O_2-Prx-AGPs as a signalling platform (see section III.4).

III.6 Expression profiles of *AtAGP9* and *AtAGP58* in *Arabidopsis thaliana* using FP reporter genes under the control of the endogenous promoters

In the previous section, stable transformants of *Arabidopsis thaliana* expressing *AtAGP9* and *AtAGP58* FP-fusions under the control of the respective endogenous promoters were generated in order to investigate the putative co-localization of the codified proteins. These lines also constitute a very useful tool to investigate the overall expression profile of those genes in the plants of Arabidopsis, with this description being an important step towards understanding the function of a gene. Therefore, those Arabidopsis lines were carefully screened under the confocal microscope to determine the expression profile of *AtAGP9* and *AtAGP58* throughout development and in different plant organs. A similar study was already performed for *AtPrx34* by Figueiredo (2011).

III.6.1 Expression profile in the adult plant

The AGP-CFP expression profile driven by the promoters of *AtAGP58* (Figure III.6.1) and *9* (Figure III.6.2) genes was first examined in the aerial parts of Arabidopsis adult plants, including fully developed leaves, flowers and siliques.

The AtAGP58 lines provided undeniable evidence that *AtAGP58* was strongly expressed in leaves, being detected in the whole leaf, including in trichomes (Figures III.6.1C-D). These results confirm the GENEVESTIGATOR data (see section III.5.1). The expression of *AtAGP58* in trichomes may be associated with the cell expansion process. In fact, in cotton fibers, which are trichomes with a lot of structural and genetic similarities with Arabidopsis trichomes, AGPs are involved in fiber initiation and elongation phenomena (Li et al., 2010; Huang et al., 2013). *AtAGP58* was highly expressed in sepals (Figure III.6.1B) and it was also present in the style (Figure III.6.1A). GENEVESTIGATOR data indicated a higher expression of *AtAGP58* in petals than in sepals. However, in these lines it was observed a strong expression in sepals and no expression in petals. The presence of AtAGP58 in the style could explain the expression level in the pistil indicated by GENEVESTIGATOR (see section III.5.1). AGPs are one of the prominent transmitting tract components in styles from many species, which has led to the suggestion that they might serve as nutrients for pollen tube growth, play a role in the control of water balance, serve as an adhesive matrix that facilitates pollen tube growth, or function in cell to cell interaction (Sommer-

Knudsen et al., 1997; Cheung and Wu, 1999; Showalter, 2001). For instance, tobacco AGPs, TTS1 and TTS2, are highly localized in the transmitting tract of the style and have been implicated in pollen tube growth guidance (Cheung et al., 1995). LeAGP1 is also abundant in stylar transmitting tissues, with putative roles in guiding and nourishing pollen tube growth. These among other observations have led to the hypothesis that pistil AGPs function in recognition, adhesion, pollen tube nutrition, pollen tube guidance, and other similar roles.

The AtAGP9 lines showed a strong expression in the style and the stamen (Figures III.6.2A-D), supporting the GENEVESTIGATOR data, which presented AtAGP9 as the AGP, within the set of 10 selected classical AGPs, with the highest expression in flowers, particularly in the stamen and the pistil (see section III.5.1). This means that AtAGP9 can be involved, like AtAGP58, in pollen tube guidance through the stylar transmitting tissues. Additionally, the presence in the anthers indicates that AtAGP9 may be involved in pollen development. In petals, sepals and leaves, AtAGP9 was only localized along the veins (Figures III.6.2E-F and I-J). This explains the lower expression in leaves of *AtAGP9* comparing with *AtAGP58* in GENEVESTIGATOR data (see section III.5.1). Similar to *AtAGP9*, many other AGP genes show vascular-specific or –preferential expression patterns. For instance, *in situ* hybridization demonstrated that *ZeFLA11*, a FLA gene from *Zinnia*, is specifically expressed in stem vascular tissue (Dahiya et al., 2006). Moreover, xylogen, a chimeric AGP, is also expressed in vascular tissues in *Zinnia* (Motose et al., 2001), and a double xylogen mutant in Arabidopsis presents discontinuous leaf venation patterns (Motose et al., 2004). Therefore, this consistent association of the *AtAGP9* promoter activity with the vascular tissues throughout plant organs, implicate AtAGP9 in vascular development. As in AtAGP58 lines, AtAGP9 was also present in trichomes (Figure III.6.2K). *AtAGP9* was also highly expressed in siliques (Figure III.6.2G). In immature seeds, the *AtAGP9* expression was confined to the funiculus and what might be the chalazal seed coat or the embryo (Figure III.6.2H), although by comparing with the GENEVESTIGATOR data (see section III.5.1) it is more likely to be the embryo.

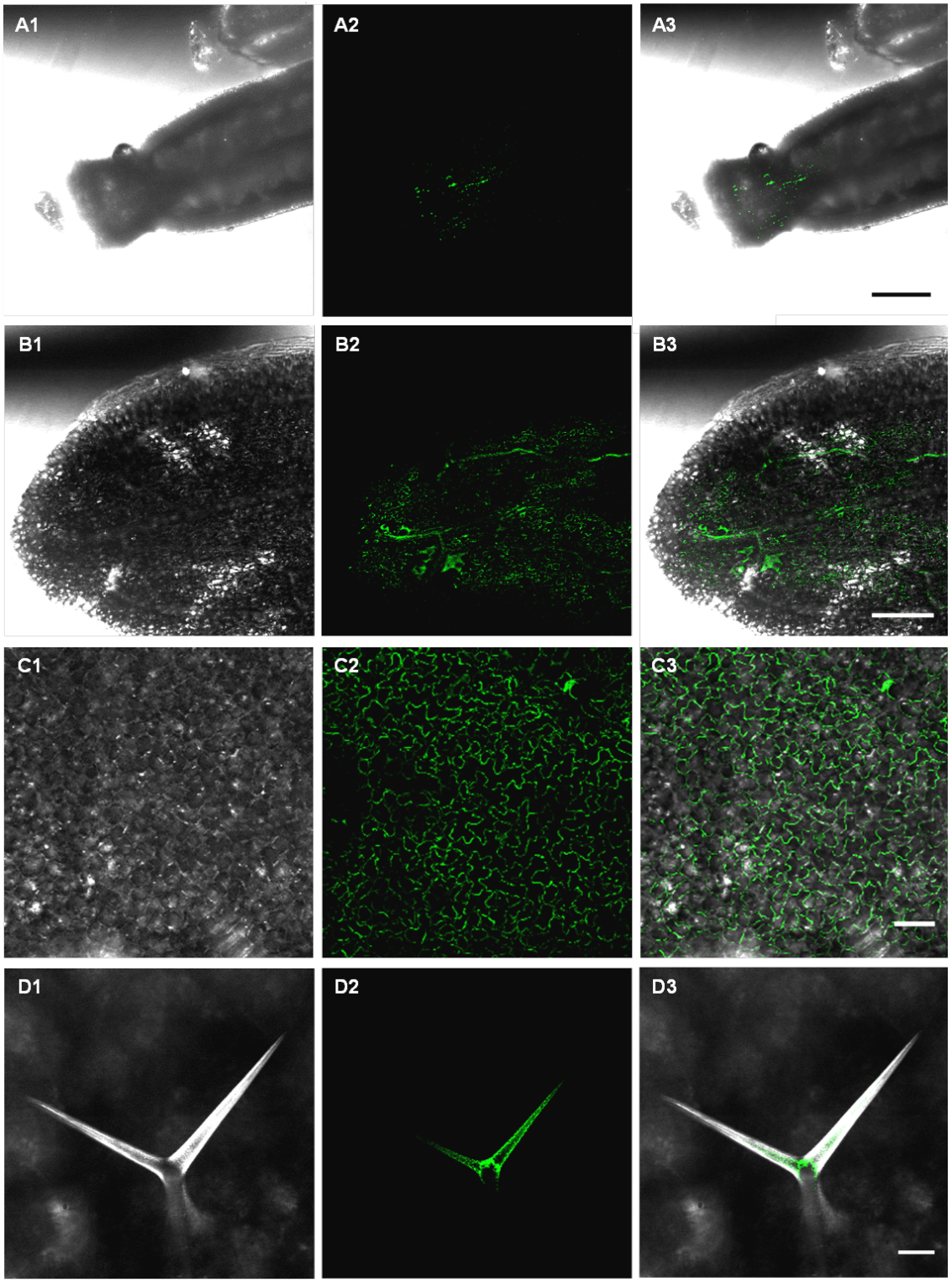

Figure III.6.1 – Expression pattern of *AtAGP58* driven by the endogenous promoter in adult plants. (A1-D1) Bright field images. (A2-D2) CFP fluorescence images. (A3-D3) Merged images. (A) Carpel. (B) Sepal. (C) Leaf. (D) Trichome. Scale bar for A-B 200 µm, for C 100 µm, for D 50 µm.

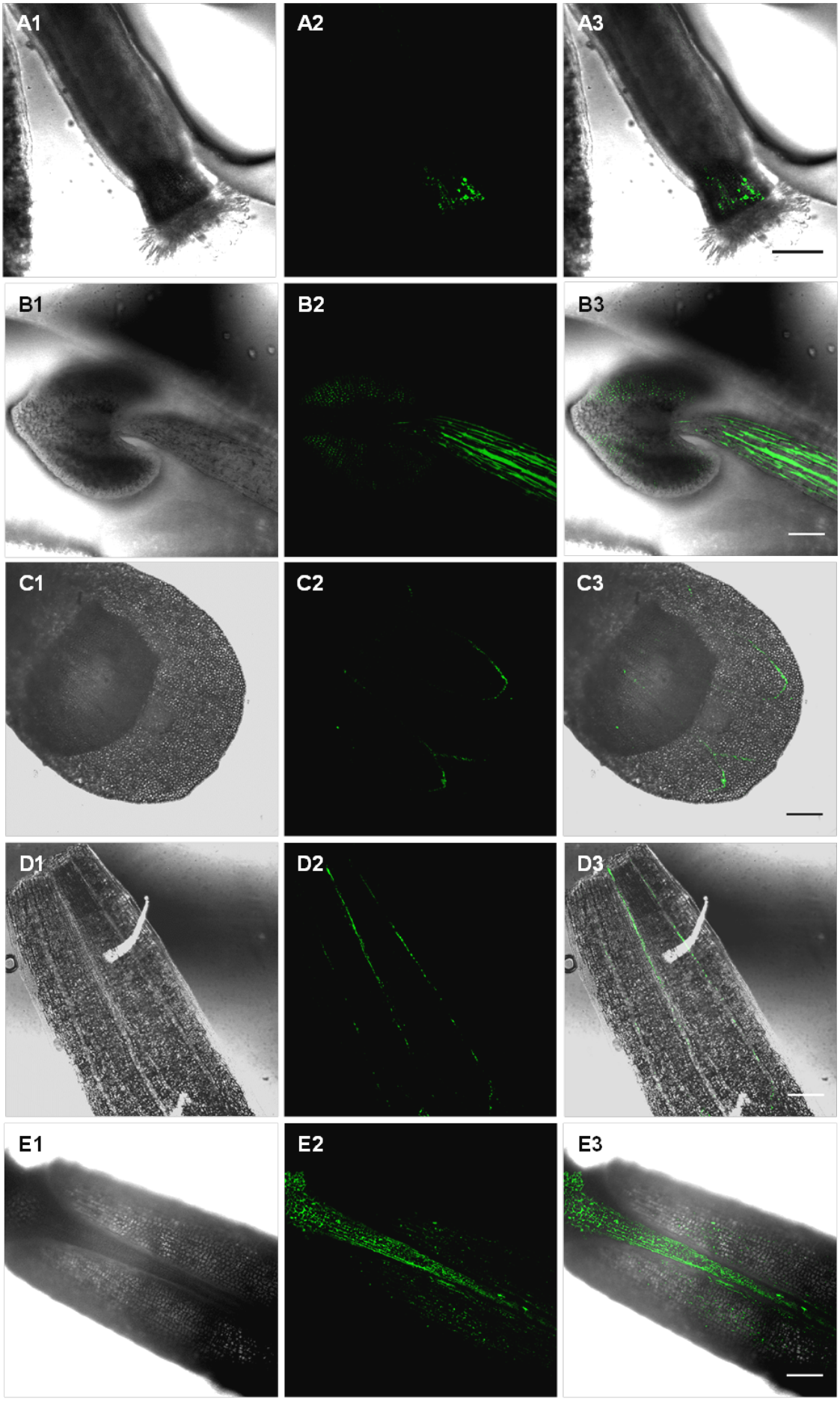
A1
A2
A3
B1
B2
B3
C1
C2
C3
D1
D2
D3
E1
E2
E3

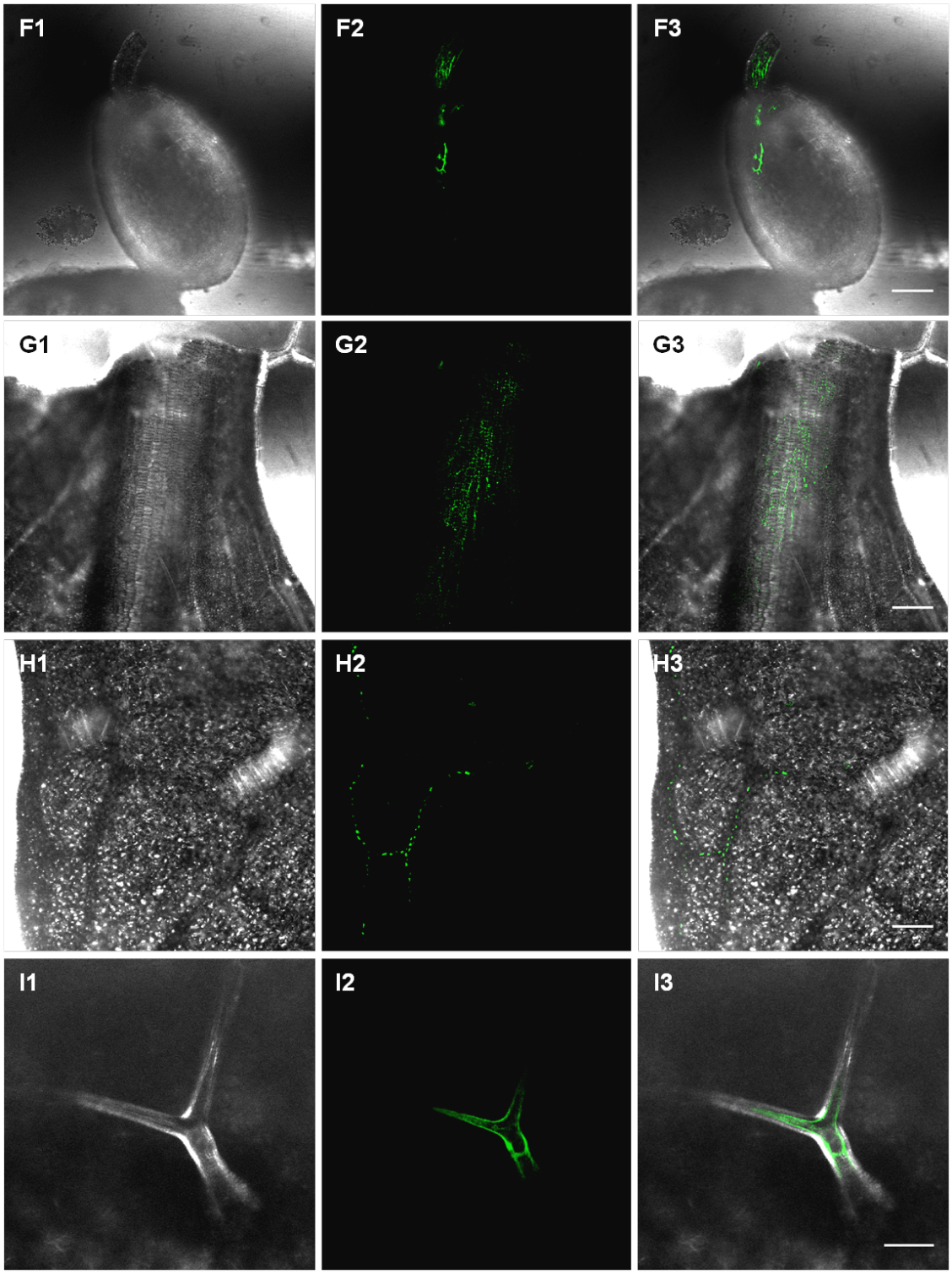

Figure III.6.2 – Expression pattern of *AtAGP9* driven by the endogenous promoter in adult plants. (A1-I1) Bright field images. (A2-I2) CFP fluorescence images. (A3-I3) Merged images. (A) Carpel. (B) Stamen. (C) Petal. (D) Sepal. (E) Silique. (F) Seed. (G-H) Leaf. (I) Trichome. Scale bars for A, C-E, G and H, 200 µm. Scale bars for B and F, 100 µm. Scale bar for I, 50 µm.

III.6.2 Expression profile in seedlings

In AtAGP58 transgenic seedlings (Figure III.6.3), a strong expression was observed in cotyledons, as expected from the GENEVESTIGATOR analysis, and a high expression in leaf primordia and in hypocotyl was also observed (Figures III.6.3A – C). Relating these observations with the ones from the two previous sections led to the conclusion that the *AtAGP58* promoter drives expression characteristically in green organs, both in adult plants and in seedlings.

In AtAGP9 transgenic seedlings (Figure III.6.4), the expression in cotyledons was lower than in AtAGP58 lines and no expression was detected in the leaf primordia (Figures III.6.4A and B). However, the expression in hypocotyls was higher than in AtAGP58 lines (Figure III.6.4C). This high expression of *AtAGP9* in hypocotyls indicates that AtAGP9 may be involved in hypocotyl elongation. Hypocotyl elongation is governed by cell division and cell elongation, two processes in which AGPs have been implicated. A classical AGP from cucumber, CsAGP1, is a gibberellin-responsive gene and is involved in hypocotyl elongation (Park et al., 2003). A mutant of AtAGP19, one of the lysine-rich AGPs from Arabidopsis, shows shorter hypocotyls, among other abnormalities, and it was proved by Yang et al. (2007) that this AGP is essential for cell division and expansion.

III.6.3 Expression profile in roots

In AtAGP58 transgenic roots (Figure III.6.3D), the *AtAGP58* expression was very low and erratic along the root, being totally absent from the root hairs, elongation zone and apex, which is in agreement with GENEVESTIGATOR data (see section III.5.1).

In roots, AtAGP9 was present all over the root, except in root hairs (Figures III.6.4D and E). The higher expression was observed in the maturation zone (Figure III.6.4E). These results support the GENEVESTIGATOR analysis, which showed a strong expression of *AtAGP9* in roots. In fact, a number of studies have shown that AGPs are important for root development. Van Hengel and Roberts (2003) demonstrated that AtAGP30, a histidine-rich AGP, is specifically expressed in roots and plays two roles in root development: a role in ABA perception during germination and a role in root regeneration from cell cultures. AtFLA1 is a FLA expressed in the mature vasculature of lateral roots and the elongation zone of the primary root, which has recently been shown to play a role in lateral root development and shoot regeneration from root tissues (Johnson et al., 2011). The function of AtFLA1 is unclear but one possibility is to be involved in regulating cell differentiation and expansion in the newly formed lateral roots but may also have a role in defining cell fate and identity,

a role of AGPs that has been already discussed in previous sections based on differential expression of specific AGP-associated epitopes as markers of cell fate. The strong expression of *AtAGP9* all over the root, including in the root apex, may indicate a function in root development.

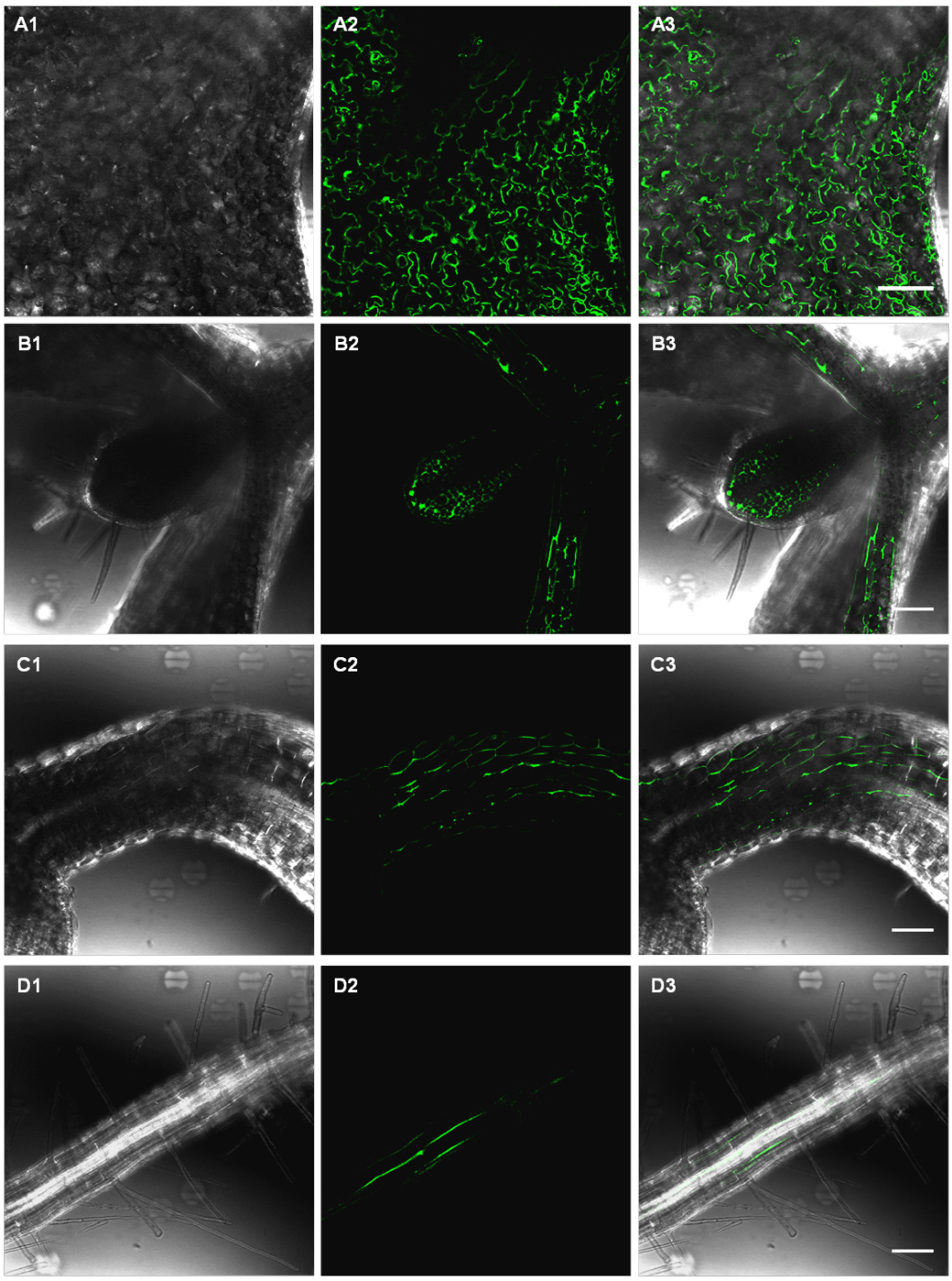

Figure III.6.3 – Expression pattern of *AtAGP58* driven by the endogenous promoter in seedlings. (A1-D1) Bright field images. (A2-D2) CFP fluorescence images. (A3-D3) Merged images. (A) Cotyledon. (B) Leaf primordia. (C) Hypocotyl. (D) Root. Scale bars, 100 µm.

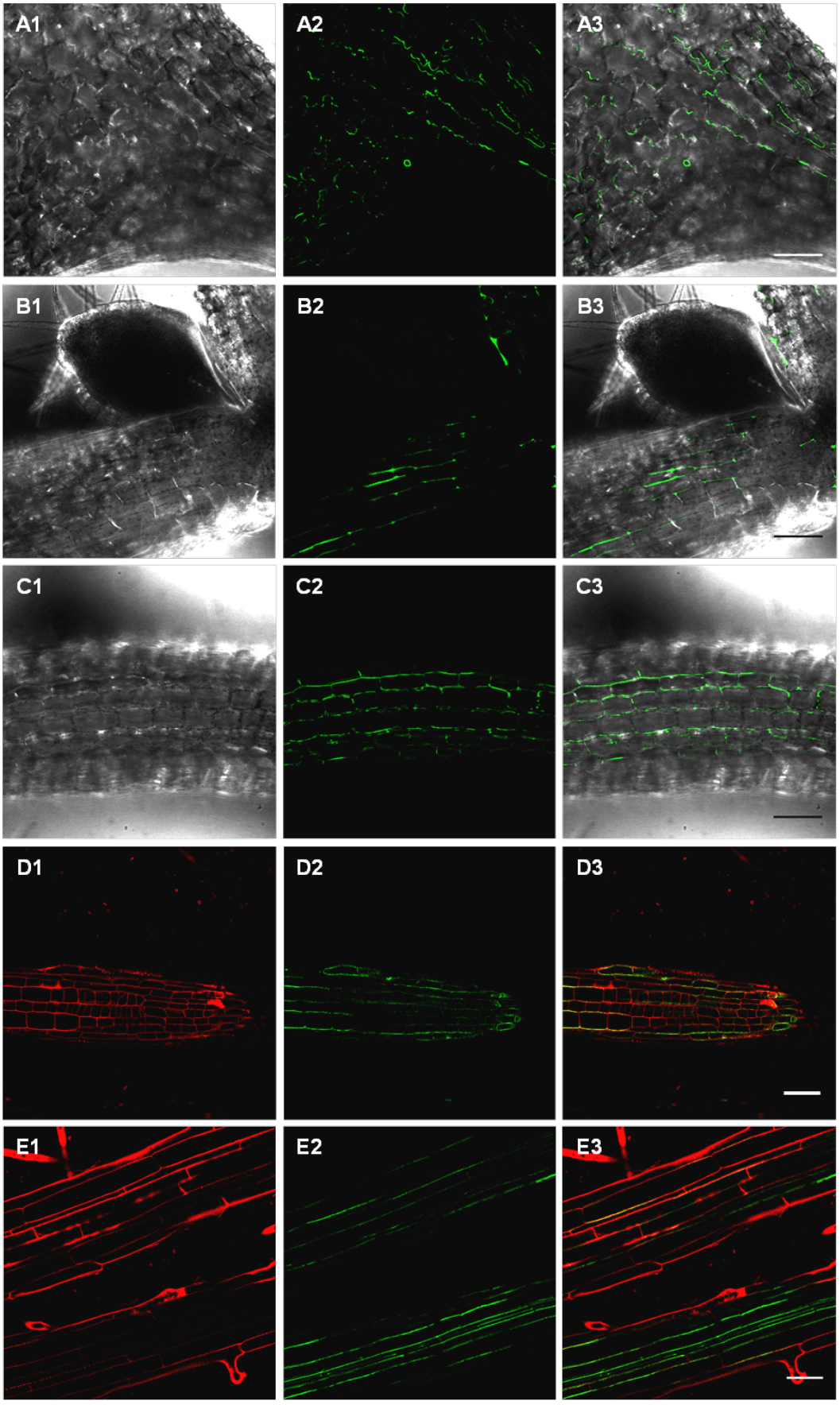
A1
A2
A3
B1
B2
B3
C1
C2
C3
D1
D2
D3
E1
E2
E3

Figure III.6.4 – Expression pattern of *AtAGP9* driven by the endogenous promoter in seedlings. (A1-C1) Bright-field images. (A2-E2) CFP fluorescence images. (D1-E1) Propidium iodide fluorescence counterstaining the cell wall. (A3-E3) Merged images. (A) Cotyledon. (B) Leaf primordia. (C) Hypocotyl. (D-E) Root. Scale bars for A-C, 100 µm. Scale bars for D-E, 50 µm.

III.6.4 AtAGP9 and AtAGP58 in *Arabidopsis thaliana*

A summary of the expression profile driven by the promoters of *AtAGP9* and *AtAGP58* is represented in Figure III.6.5. Both AtAGP9 and 58 are present in quite diverse developmental stages and plant organs, indicating either the involvement in an array of different functions and/or the involvement in some basic function important for many cell types and developmental stages. Overall, both AtAGP9 and 58 may be important for pollen tube guidance or feeding in the style, trichome differentiation and seedling development. AtAGP58 seems to be important in sepals and leaves, while AtAGP9 is important for vascular bundles, stamens, siliques and seeds. Whether some of the functions of these AGPs may relate with specific Prx partners through a signalling mechanism as proposed in this thesis is always an hypothesis. It is also unknown how much of the functions of AGPs may be related with their glycosidic moiety and whether this moiety (including highly specific epitopes recognized by mAbs) is specific to a given AGP aminoacid sequence, or may be added to different AGP polypeptide backbones, being dependent on the differentiation and environmental status of a cell.

Although the studies with promoter-fusions enable to anticipate some of the functions of AtAGP9 and AtAGP58, further analyses of the respective mutants needs to be done in order to try to clarify their specific function, even if the expected redundancy of AGPs may difficult the production of phenotypes.

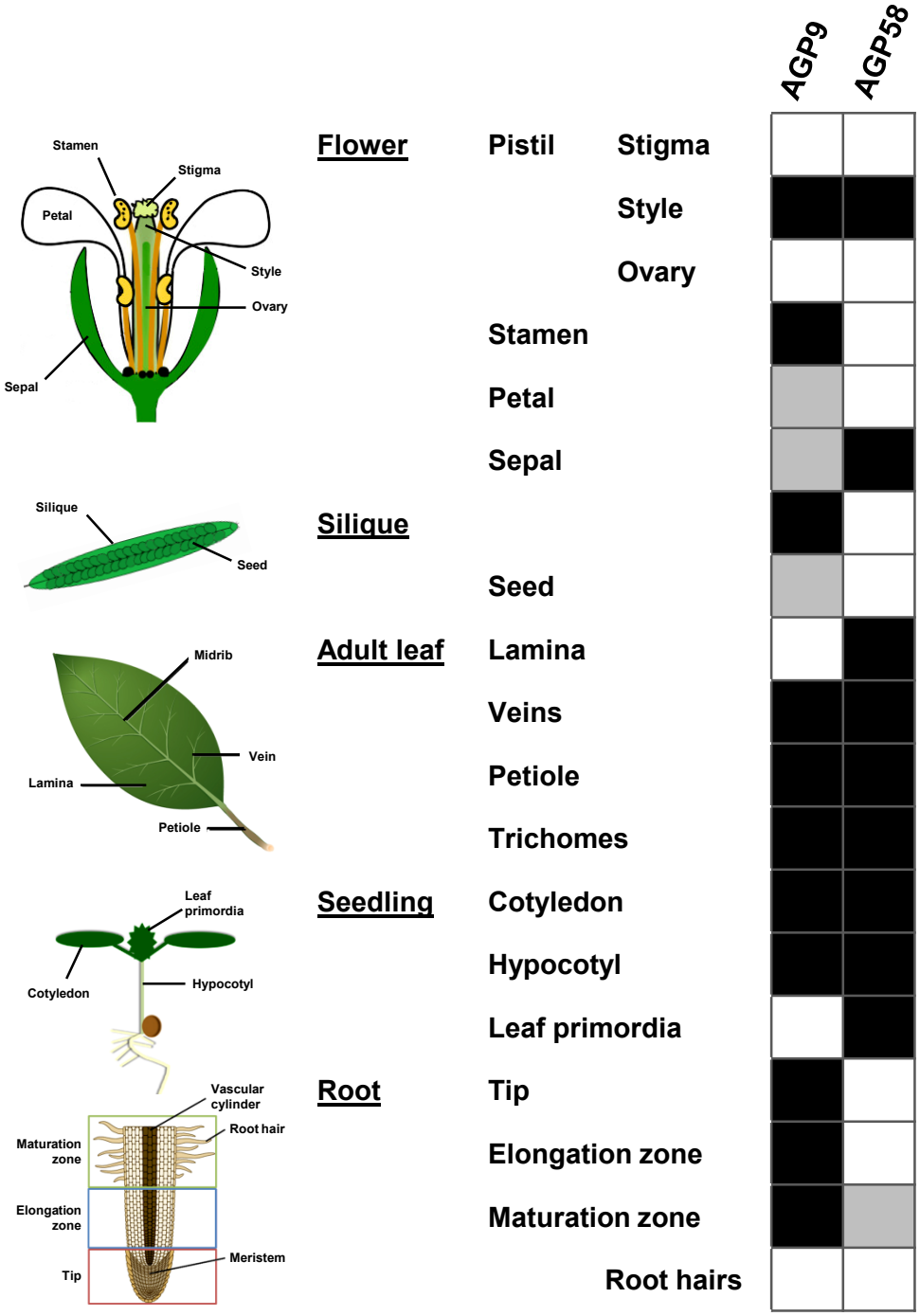

Figure III.6.5 – Schematic representation of the expression profile of *AtAGP9* and *AtAGP58* in Arabidopsis, as determined by transformation with promoter fusions. White – absence, grey – low expression, black – high expression.

III.7 Fluorescent protein fusions with an AGP and a Prx as plasma membrane and vacuole markers for live plant cell imaging

Nowadays, one of the major challenges for biologists is to assign functions to the countless number of candidate genes identified by genome and transcriptome projects. A central determinant of protein function is the subcellular localization, which can be assayed by several methods, such as analysis of fixed tissue specimens or fractionated cellular constituents. However, these methods are often technically challenging, time-consuming and laborious, and give insufficient information. More representative sets of information allowing the observation of cellular structures and the dynamics of a protein in their native states can be obtained from live cell imaging. When investigating the localization of newly characterized proteins within the cell by live imaging, it is desirable to confirm the exact subcellular localization by co-expression with known fluorescent subcellular markers. As plant cells have a variety of endomembrane compartments, one of the major factors influencing the success of colocalization studies is the availability and diversity of specific organellar markers.

In this section, FP fusions with AtAGP58 and AtPrx34 from Arabidopsis generated in section III.5 are shown to work as species independent subcellular markers for the plasma membrane and the vacuole of plant cells, respectively. These fusions were successfully tested by protoplast transient expression in four plant models, *Arabidopsis thaliana*, *Nicotiana tabacum*, *Catharanthus roseus* and *Vitis vinifera*. The respective FP fusions in a binary vector were also successfully tested by agroinfiltration of *N. tabacum* leaves.

III.7.1 AtAGP58 and AtPrx34 FP-fusions

AtAGP58 from *A. thaliana* is a classical AGP (Showalter et al., 2010) highly expressed in leaves (see previous sections) and analysis of its predicted aminoacid sequence by SignalP (Emanuelsson et al., 2007) predicts the presence of an ER signal peptide (SP) with 25 aminoacids, while Plant big-PI predictor (Eisenhaber et al., 2003) indicates the presence of a C-terminal GPI-anchor signal sequence with 27 aminoacids (Figure III.7.1). The presence of this GPI-anchor signal indicates that this AGP should be attached to a membrane, most likely the plasma membrane, since AGPs are considered cell wall, extracellular proteins (Ellis et al., 2010).

MASSFSSQAFFLLTLSMVLIPFSLAQAPMMAPSGSMSMPPMSSGGGSSVPPPVMSPMPMMTPPPMPM
TPPPMPMTPPPMPMAPPPMPMASPPMMPMTPSTSPSPLTVPDMPSPPMPSGMESSPSPGPMPPAMAA
SPDSGAFNVRNNVVTLSCVVGVVAAHFLLV

Figure III.7.1 – Predicted aminoacid sequence of classical AtAGP58 from *A. thaliana*. The signal peptide is underlined and was predicted by SignalP (http://www.cbs.dtu.dk/services/SignalP/). The putative GPI-anchor signal sequence is shown in pink and was predicted by Plant big-PI predictor (http://mendel.imp.ac.at/gpi/plant_server.html).

AtPrx34 is the most abundant Prx in Arabidopsis leaves and it has been extensively studied in our group (Figueiredo, 2011). Analysis by SignalP predicts the presence of an ER signal peptide (SP) with 30 aminoacids, and the alignment with other well characterized Prxs shows the presence of a C-terminal extension (CTE) with 18 aminoacids (Figure III.7.2), responsible for directing the protein to the vacuole (Figueiredo, 2011).

MHFSSSSTSSTWTILITLGCLMLHASLSAAQLTPTFYDRSCPNVTNIVRETIVNELRSDPRIA
ASILRLHFHDCFVNGCDASILLDNTTSFRTEKDAFGNANSARGFPVIDRMKAAVERACPRTVS
CADMLTIAAQQSVTLAGGPSWRVPLGRRDSLQAFLELANANLPAPFFTLPQLKASFRNVGLDR
PSDLVALSGGHTFGKNQCQFILDRLYNFSNTGLPDPTLNTTYLQTLRGLCPLNGNRSALVDFD
LRTPTVFDNKYYVNLKERKGLIQSDQELFSSPNATDTIPLVRAYADGTQTFFNAFVEAMNRMG
NITPTTGTQGQIRLNCRVVNSNSLLHDVVDIVDFVSSM

Figure III.7.2 – Predicted aminoacid sequence of AtPrx34 from *A. thaliana*. The signal peptide is underlined and was predicted by SignalP (http://www.cbs.dtu.dk/services/SignalP/). The C-terminal extension is shown in pink and was predicted in an alignment with other Prxs performed by Welinder et al. (2002).

AtAGP58 and AtPrx34 were fused to a newer optimized version of the CFP, the sCFP4 or mTurquoise, which is brighter and more photostable than other CFP variants, at the same time it has a lifetime among the highest reported for fluorescent protein variants so far (Goedhart et al., 2010). The FP fusions were cloned in two different vectors: an expression vector, pMON999, for the transient expression in protoplasts, and a binary vector, pGreenII235, for agroinfiltration of *N. tabacum* leaves.

The sCFP4 was first cloned in the pMON999 vector to generate the expression vector pMON999:sCFP4 (Figure III.7.3A).The complete AtAGP58 and AtPrx34 cDNAs were then used as template to amplify the signal peptide (SP) and the mature protein codifying regions by PCR, with primers including restriction sites for directional cloning (Figures III.7.3B and C). For both fusions, the respective SP codifying region was cloned in frame at the N-terminus codifying region of sCFP4. Next, the DNA sequences corresponding to the mature protein with the GPI-signal sequence of AtAGP58 (MP-GPI58) and the mature protein with the C-terminal extension of AtPrx34 (MP-CTE34) were cloned at the C-terminus codifying region of sCFP4 to generate the constructs pMON999:SP58-sCFP4-MP-GPI58 and pMON999:SP34-sCFP4-MP-CTE34 (Figures

III.7.3B and C). These fusions were then amplified and cloned in the binary vector pGreenII235.

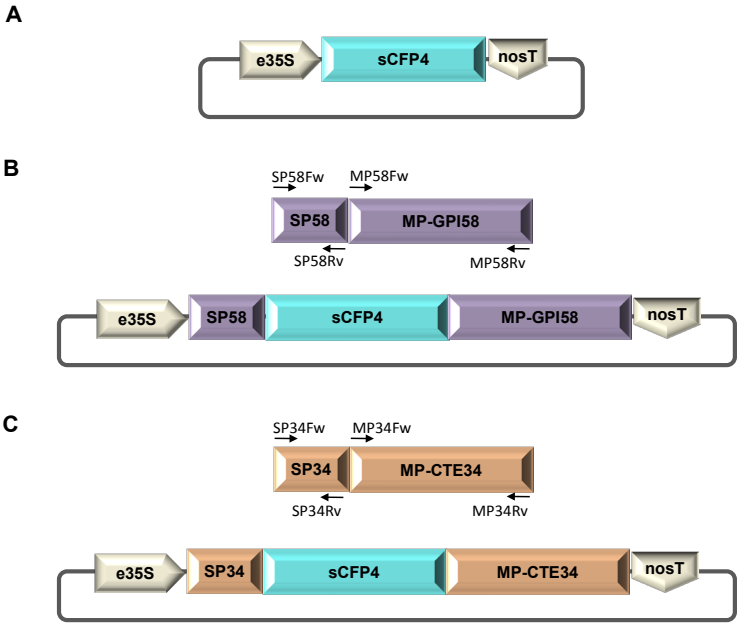

Figure III.7.3 – Schematic representation of the cloning strategy followed to obtain the FP-fusions. (A) Representation of pMON999-sCFP4, depicting the double 35S promoter, sCFP4 and the *nos* terminator regions. (B) Scheme of the domains of AtAGP58 and the primers used for their amplification (top). The SP region of AtAGP58 was cloned in frame into pMON999-sCFP4 upstream sCFP4 (bottom). The MP-GPI region of AtAGP58 was cloned downstream sCFP4 (bottom). (C) Representation of the different domains of AtPrx34 and the primers used for their amplification (top). The SP region of AtPrx34 was cloned in frame into pMON999-sCFP4 upstream sCFP4 (bottom). The MP-CTE region of AtPrx34 was cloned downstream sCFP4 (bottom). e35S – double 35S promoter. SP – signal peptide. MP-GPI – mature protein with GPI-signal sequence. MP-CTE – mature protein with C-terminal extension. nosT – *nos* terminator.

III.7.2 AtAGP58 and AtPrx34 fusions with CFP mark the plasma membrane and the vacuole of Arabidopsis leaf cells

PEG-mediated transformation of protoplasts is a very simple and efficient technique, widely used to study the subcellular localization of proteins. In this study, this procedure was used to test the subcellular fate of the AtAGP58 and AtPrx34 CFP fusions in Arabidopsis leaf cells. In order to prove the efficiency of the PEG-mediated technique of transient expression in protoplasts, the cells were also transformed with a construct only with free (untargeted) sCFP4 (Figures III.7.4 - III.7.7, C).The localization of fluorescence was monitored from 24 to 72 h after transformation and the results are shown in Figure III.7.4. Protoplasts transformed with free (untargeted) sCFP4 showed a strong fluorescence in the cytosol. Because of its small size, sCFP can enter nuclear pores, so a conspicuous blue fluorescence was also observed in the nucleus (Figure III.7.4C). In protoplasts transformed with the AtAGP58 fusion, fluorescence appeared

like a perfectly defined circumference line at the surface of the cells, completely external to chloroplasts, indicating an unmistakable localization in the plasma membrane (Figure III.7.4D). Finally, in protoplasts transformed with the AtPrx34 fusion, fluorescence accumulated clearly in the large central vacuole of the cell, since it occupied a big volume of the cell and was excluded from the regions with chloroplasts or the nucleus (Figure III.7.4E). Comparing with other vacuolar fusion markers using GFP (Figueiredo, 2011), the fluorescence of the AtPrx34 fusion used in this work was superior, possibly due to a higher stability of sCFP in the acidic/proteolytic environment of the vacuole.

The time-course of transient expression and the peak of sCFP4 accumulation/fluorescence depended on the construct, possibly as a consequence of the different protein pathways and destination compartments involved. Thus, free sCFP4 and the AtAGP58 fusion already appeared with a strong fluorescent signal in a lot of protoplasts, 24 h after transformation, with the number of fluorescent protoplasts continuing to increase until at least 72 h after transformation. On the other hand, the AtPrx34 fusion was not visible at all at 24 h, becoming well noticeable in the vacuole at 48 h (Figure III.7.4). However, the fluorescence observed for the AtPrx34 fusion in the vacuole was lower than the one observed in the cytosol for free sCFP or in the plasma membrane for the AtAGP58 fusion, possibly due to the dilution effect in such a big compartment, to the influence of its acid pH or to some sCFP sensitivity to vacuolar proteases (Tamura et al., 2003).

As a whole, these results indicated that the AtAGP58 and AtPrx34 fusions with sCFP are good markers for the plasma membrane and the vacuole that may be used for live cell imaging in the Arabidopsis model species.

III.7.3 AtAGP58 and AtPrx34 fusions with CFP mark the plasma membrane and the vacuole of cells from *Nicotiana tabacum*, *Catharanthus roseus* and *Vitis vinifera*

In order to investigate if the AtAGP58 and AtPrx34 fusions could also be used as plasma membrane and vacuole markers in other plant species, leaf protoplasts from *N. tabacum* and *C. roseus*, and protoplasts from *V. vinifera* cell cultures were also transiently transformed with the constructs from Figure III.7.3. As can be seen in Figures III.7.5 – III.7.7, the AtAGP58 fusion clearly labelled the plasma membrane in the cells of all three species, while the AtPrx34 fusions conspicuously labelled the vacuole of all three species as well. As had been previously observed for Arabidopsis,

free sCFP4 and the AtAGP58 fusion already appeared with a strong fluorescent signal in a lot of protoplasts after 24 h, while the fluorescence of the AtPrx34 fusion took longer to appear, being clearly visible only at 48h. Likewise, the fluorescence observed in the vacuole for the AtPrx34 fusion was not as strong as the one observed in the cytosol for free sCFP or in the plasma membrane for the AtAGP58 fusion.

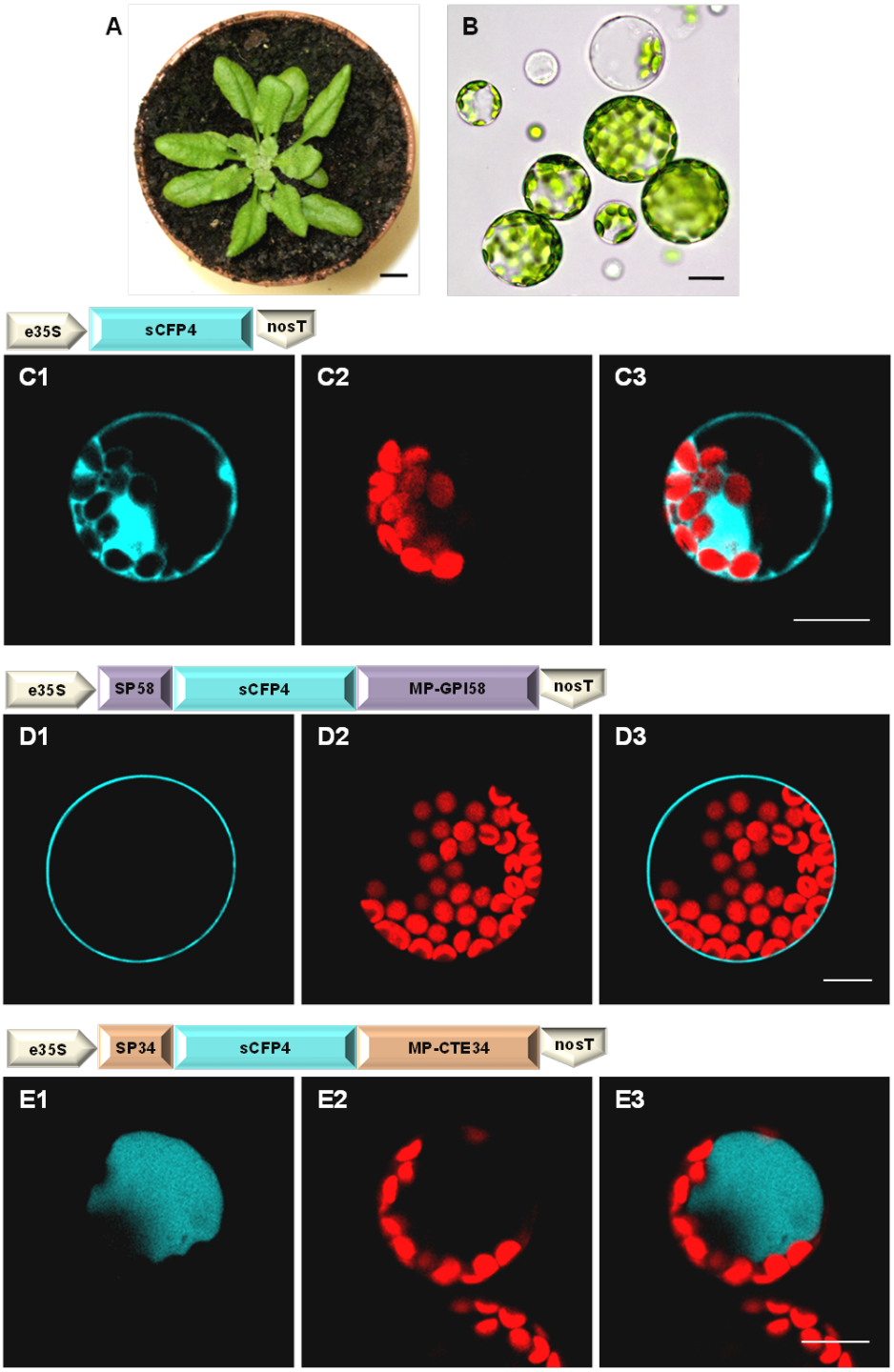

Figure III.7.4 – Transient transformation of *A. thaliana* mesophyll protoplasts with CFP-fusions. (A) *A. thaliana* plant. (B) Bright field image of *A. thaliana* mesophyll protoplasts. (C-E) Confocal images of protoplasts transformed with CFP-

fusions. The schematic representation of each construct used for transformation is depicted right above the respective set of confocal images. (C1-E1) CFP channel. (C2-E2) Red channel showing chloroplast autofluorescence. (C3-E3) Merged images. Scale bar for A, 1 cm. Scale bar for B, 20 µm. Scale bars for C-E, 10 µm.

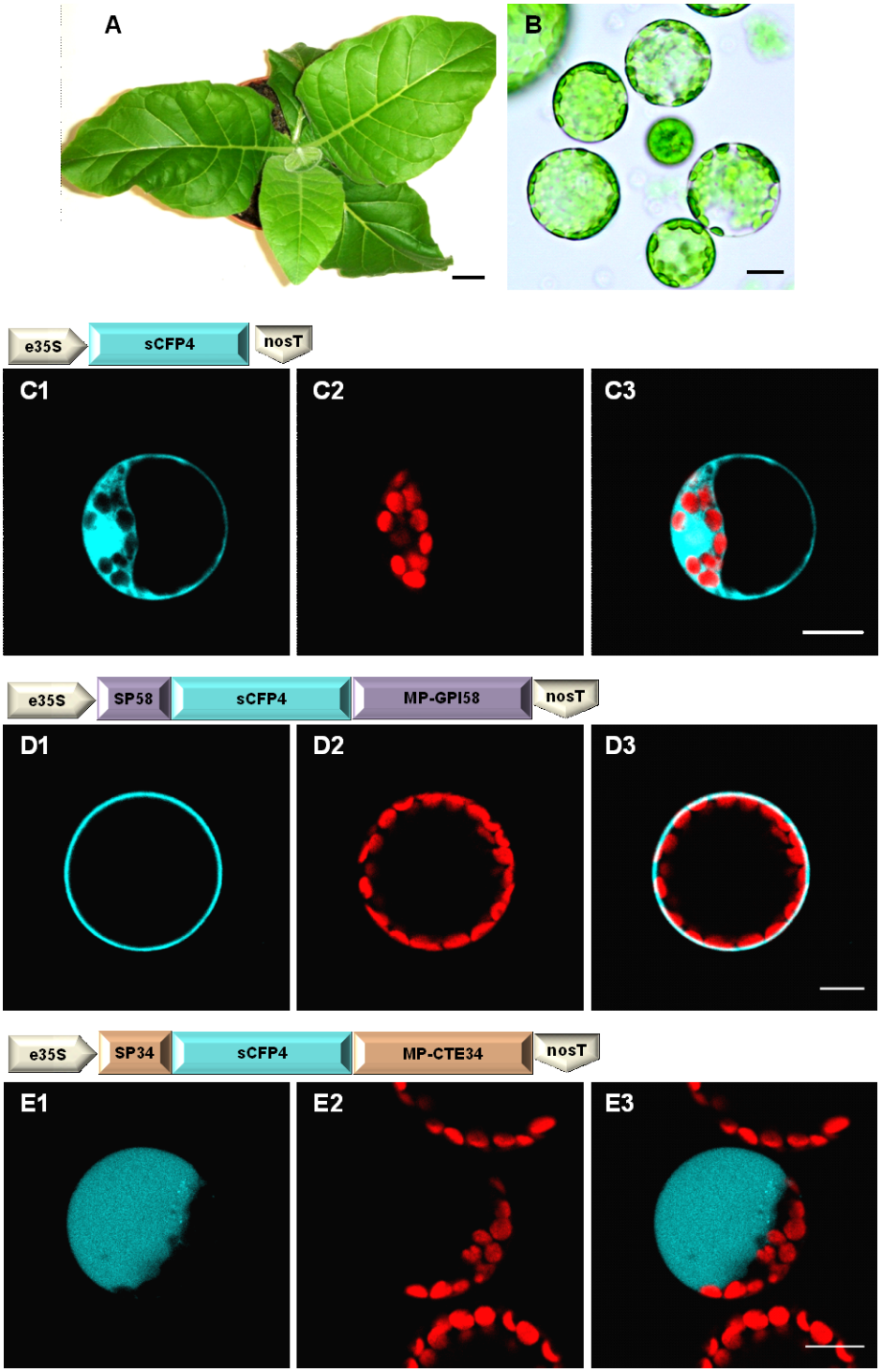

Figure III.7.5 - Transient transformation of *N. tabacum* mesophyll protoplasts with CFP-fusions. (A) *N. tabacum* plant. (B) Bright field image of *N. tabacum* mesophyll protoplasts. (C-E) Confocal images of protoplasts transformed with CFP-fusions. The schematic representation of each construct used for transformation is depicted right above the respective set of confocal images. (C1-E1) CFP channel. (C2-E2) Red channel showing chloroplast autofluorescence. (C3-E3) Merged images. Scale bar for A, 3 cm. Scale bar for B, 20 µm. Scale bars for C-E, 10 µm.

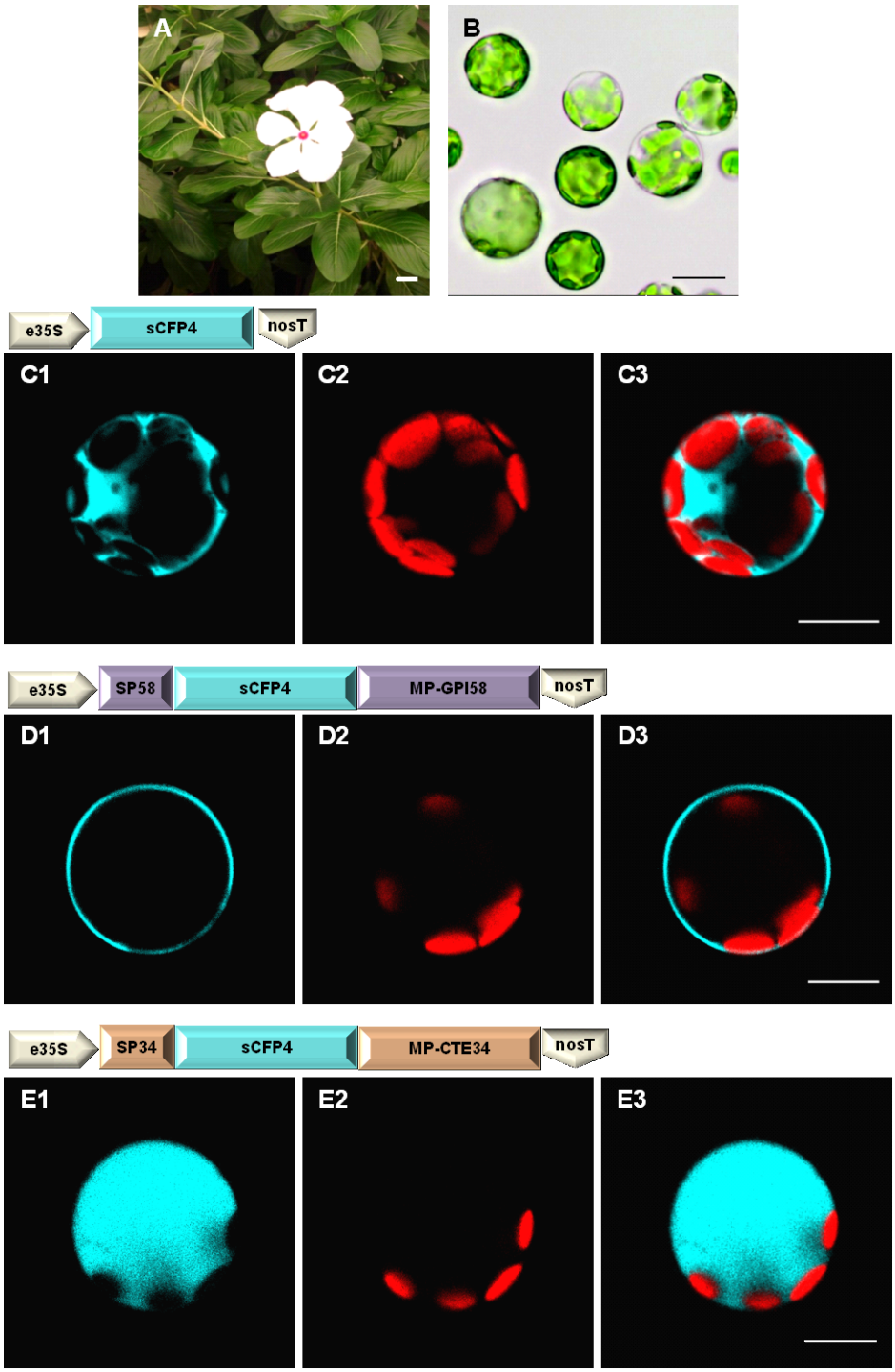

Figure III.7.6 - Transient transformation of *C. roseus* mesophyll protoplasts with CFP-fusions. (A) *C. roseus* plant. (B) Bright field image of *C. roseus* mesophyll protoplasts. (C-E) Confocal images of protoplasts transformed with CFP-fusions. The schematic representation of each construct used for transformation is depicted right above the respective set of confocal images. (C1-E1) CFP channel. (C2-E2) Red channel showing chloroplast autofluorescence. (C3-E3) Merged images. Scale bar for A, 5 cm. Scale bar for B, 20 µm. Scale bars for C-E, 10 µm.

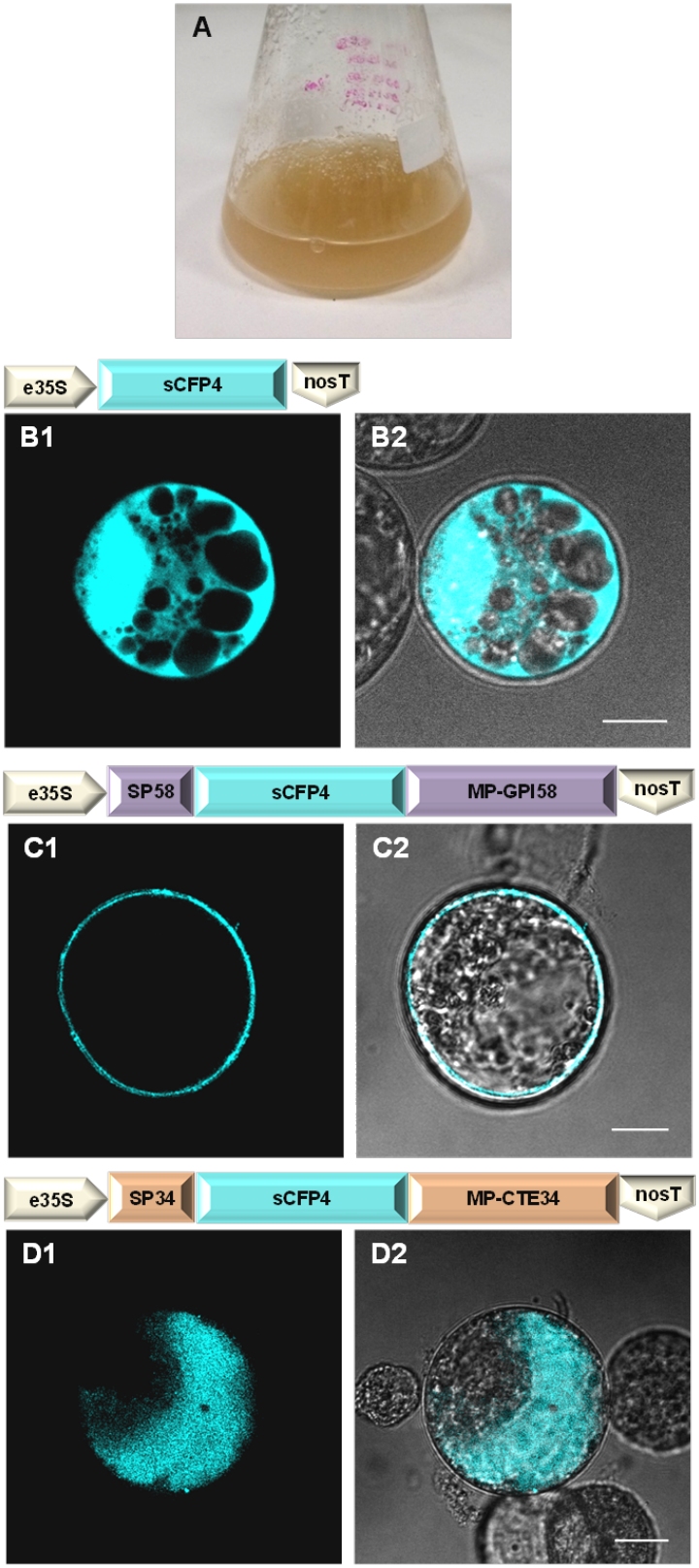

Figure III.7.7 - Transient transformation of *V. vinifera* protoplasts with CFP-fusions. (A) *V. vinifera* cell culture. (B-D) Confocal images of *V. vinifera* protoplasts transformed with CFP-fusions. The schematic representation of each construct used for transformation is depicted right above the respective set of confocal images. (B1-D1) CFP channel. (B2-D2) Merged images of CFP channel and bright field images. Scale bars, 10 µm.

III.7.4 AtAGP58 and AtPrx34 fusions with CFP mark the plasma membrane and the vacuole from leaf epidermal cells of *N. tabacum* upon agroinfiltration

Agroinfiltration of *N. tabacum* leaf epidermis is often used for live cell imaging of plant proteins (Pereira et al., 2013), and therefore, the validity of the AtAGP58 and AtPrx34 fusions as subcellular markers were also tested in this system. The fusions were subcloned in a binary vector and were then tested by transient transformation of tobacco leaf epidermal cells by agroinfiltration. This is an easy and non-invasive technique that simply requires the infiltration of a suspension of bacteria carrying the construct into the plant material. This methodology has been widely used in *N. tabacum*, with high levels of transgene expression, mainly because the size of the leaves of this plant allows testing multiple constructs/combination of constructs in a single leaf (Sparkes et al., 2006). Both constructs were successfully expressed in tobacco leaves, with high transformation efficiency (Figure III.7.8). The AtAGP58 fusion was located clearly at the surface of the cells (Figures III.7.8A and B) and the AtPrx34 fusion accumulated unquestionably in the central vacuole (Figures III.7.8C and D), as foreseen. This means that these constructs also work well as markers in Agrobacterium-mediated transformation techniques.

III.7.5 AtAGP58 and AtPrx34 fusions with CFP are excellent species independent markers for the plasma membrane and the vacuole of plant cells

Fusion of GFP coding sequence to coding regions of proteins of unknown cellular location has become an extremely valuable tool for determining directly and non-invasively where a protein, and consequently a biochemical or regulatory process, resides within the plant cell. Numerous fluorescent proteins have been developed and cover nearly the entire visible spectrum, from deep blue to deep red, providing a wide choice of genetically encoded fluorescent markers. The development of these fluorescent proteins with different excitation and emission wavelengths has enabled researchers to visualize multiple proteins simultaneously to gain information regarding not only localization and dynamics, but also interactions in living cells. An important tool for taking rigorous and full advantage from live cell imaging is the availability of FP fusions working as reliable markers of subcellular compartments.

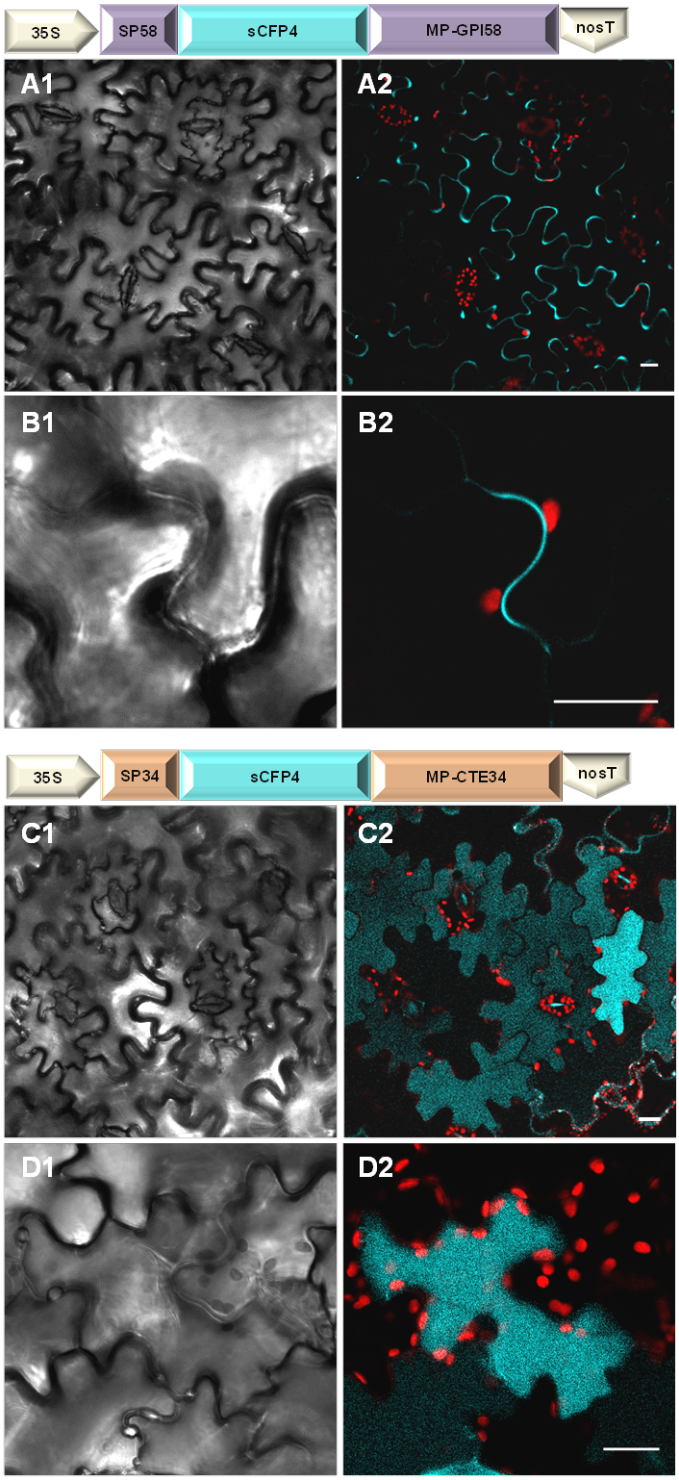

Figure III.7.8 – Confocal images of tobacco epidermal cells transiently expressing the CFP-fusions, 48 to 64 h after infiltration with Agrobacterium. (A1-D1) Bright field images. (A2-D2) Merged images of two channels: CFP channel, and red channel showing chloroplasts autofluorescence. The schematic representation of each construct used for transformation is depicted right above the respective set of confocal images. Scale bars, 20 µm.

The transformation method used here to evaluate the usefulness of AtAGP58 and AtPrx34 fusions as subcellular markers was PEG mediated transient expression in protoplasts. Live imaging of FP fusions can be investigated by both transient and stable

expression methods. Stable transformation has the advantage that many different cell types can be examined in which the fluorescent protein fusion is expressed. Moreover, because of the damage that may occur during DNA incorporation in transient assays and the variability in amount of gene delivered and FP transcript produced with this method, analysis of healthy stable transformants may sometimes be more reliable. However, transient assays are extremely simple, cheap and fast, making them particularly suited for the evaluation of a high number of candidate genes or different experimental conditions, and is therefore the more usual method of choice for live cell imaging.

In this study, carefully designed fusions of sCFP with AtAGP58 and AtPrx34 from *Arabidopsis thaliana* were shown to consistently mark respectively the plasma membrane and the vacuole of cells from four different plant species, including cells from leaves and suspension cultures. The two constructs yielded a high transformation and a strong fluorescence signal, when using either PEG mediated protoplast transformation or leaf epidermis agroinfiltration. Importantly, tobacco leaf cells transformed by agroinfiltration can be used to generate stable plant lines, by simply tissue culturing the transformed region. Moreover, Agrobacterium-mediated transformation can also be used to generate stably transformed Arabidopsis plants using the floral-dipping technique. Stably transformed Arabidopsis lines offer advantages in terms of homologous expression and the option of further genetic manipulation owing to the large resource base for this species.

The AtAGP58 fusion accumulates in the plasma membrane of transformed cells 24 h after transformation and exhibits a strong fluorescence, revealing to be an excellent plasma membrane marker. The AtPrx34 fusion takes longer to produce a fluorescent signal, but it yields a significant fluorescence in the big vacuolar compartment that is stronger than the one observed with other GFP fusions targeted to the vacuole (Figueiredo, 2011), also indicating that the AtPrx34 fusion with sCFP is a good marker for this organelle. Overall, the results obtained in this study demonstrate that the AtAGP58 and AtPrx34 fusions can be used as plasma membrane and vacuole markers for investigating the sorting of uncharacterized proteins and/or the dynamics of these cellular structures and of the respective protein sorting pathways. Furthermore, the equal sCFP4 fluorescence patterns observed for the expression of the two fusions in the homologous system *A. thaliana* and the heterologous systems *N. tabacum*, *C. roseus* and *V. vinifera* suggest the existence of conserved mechanisms of sorting and signal recognition among plant species for AGPs and Prxs.

IV.

FINAL DISCUSSION AND FUTURE PERSPECTIVES

Understanding the dynamics and modifications experienced by AGPs should help to explain their functioning and, therefore, should help to explain the important aspects of plant development and cell-cell communication in which these proteoglycans have been implicated. Previously, in a single report, it has been proposed that plasma membrane AGPs may suffer cross-linking mediated by Prx (Kjellbom et al., 1997). The possibility that AGPs could be cross-linked by Prx raised interesting hypothesis since such an event could have not only structural consequences, but could also affect or even determine the signalling properties of AGPs. Therefore, in this thesis, the main objective was to investigate the occurrence of an interaction between AGPs and Prxs and the physiological importance of such interaction, using the model plants *C. roseus* and Arabidopsis. The results obtained, their interpretation, and their integration with the data reported in the literature, enabled to unravel important information concerning several aspects of AGPs and Prx biology.

AGPs and cell differentiation

Cell differentiation, the process by which a cell becomes specialized and different from its original kind, lies at the heart of the development of complex organisms. This process is far from being understood, and more so in plants, where apart from genetic determination, development is highly affected by environmental clues (Alberts et al., 2007). Among molecules implicated in cell differentiation, AGPs are considered to be particularly important, and have consistently been observed as markers of cellular identity and fate (Seifert and Roberts, 2007; Ellis et al., 2010). The complex carbohydrate epitopes present in the AGP glycan moiety have been shown to exhibit a highly specific spatial and temporal dynamics throughout development and cell differentiation, namely during root and shoot development, xylem differentiation, embryogenesis, and male and female gametogenesis (Stacey et al., 1990; Knox et al., 1991; Schindler et al., 1995; Toonen et al., 1997; Samaj et al., 1998; Samaj et al., 2000; Showalter, 2001; Pereira et al., 2006; Coimbra et al., 2007). Therefore, AGPs are confirmed markers of cellular identity and fate (Pennell et al., 1989; Pennell and Roberts, 1990; Pennell et al., 1991), and in some instances their direct role in cellular differentiation as morphogens has been proved (Motose et al., 2004).

Here, as a necessary step to investigate the putative interaction between Prx and AGPs, a thorough characterization of the labelling by mAbs recognizing an array of AGP glycosidic epitopes was performed for *C. roseus* and Arabidopsis, revealing specific patterns that further implicate AGPs in cell differentiation.

In *C. roseus* leaves, the AGP glycosidic epitopes LM2, JIM16 and MAC207 were revealed to be markers of cell identity, while JIM8, JIM13 and JIM14 were present in all types of leaf cells. In Arabidopsis, JIM14 was also present all over the leaves and roots, with MAC207 presenting a similar general distribution, contrary to *C. roseus*, where it labelled only laticifers and idioblasts. The labelling pattern of JIM16 and LM2 in Arabidopsis showed similarities with *C. roseus* since they specifically labelled the vascular bundles from leaves of both species. In Arabidopsis roots, JIM16 specifically labelled the surface of all epidermal cells, while LM2 labelled what seemed to be trichoblasts, the cells differentiating root hairs. Additionally, JIM8 and JIM13 labelled the xylem cells in roots, with these epitopes being absent from leaves. This data clearly shows that several AGP epitopes are cell- and tissue-specific, being cell identity markers both in *C. roseus* and Arabidopsis. Moreover, the labelling by MAC207, JIM8 and JIM13 was clearly distinct between the two species analysed, adding to the already known intriguing fact that the localization of AGP epitopes does not bear the same morphogenetic identity in different species. In fact, it has even been suggested that the localization of AGP epitopes may have taxonomic significance (Knox, 1997).

The specific labelling of laticifers and idioblasts by MAC207 in *C. roseus* leaves is particularly interesting. In fact, *C. roseus* leaf laticifers and idioblasts have been shown to be actively involved in TIA biosynthesis and accumulation, and are likely to be the single site in the plant where the biosynthesis of the medicinal anticancer TIAs is completed (Mahroug et al., 2007). Therefore, understanding the distinct nature of these specific cell types can pave the way for a future manipulation of plants concerning their valuable secondary metabolism.

The meaning / function of the observed specific patterns of AGP epitopes is still an open question. In a few instances, it has been shown that these epitopes precede differentiation being sometimes essential for the process, while other epitopes have been shown to be embryogenesis-inhibiting or –promoting (reviewed in Rumyantseva (2005) and in Seifert and Roberts (2007)). Most of the times, however, the AGP epitopes have appeared basically as markers of morphogenesis and development with unknown function.

AGPs and subcellular localization

The AGP epitopes in *C. roseus* and Arabidopsis, besides presenting the expected localization at the cell wall/plasma membrane, were also clearly detected in the tonoplast. Moreover, cell fractionation studies confirmed the presence of high levels of both soluble and membrane AGPs in the vacuoles of *C. roseus* mesophyll cells.

Previous reports using mAbs have shown the localization of AGPs in the tonoplast of root and leaf cells, and in multivesicular bodies localized both in the cytoplasm and the vacuole, which were interpreted as an endocytic pathway for vacuolar disposal of periplasmic matrix components (Pennell et al., 1989; Herman and Lamb, 1992; Samaj et al., 2000). Actually, vacuolar localization has been repeatedly considered just a consequence of AGP turnover with no functional relevance (Showalter, 2001). However, the vacuolar conspicuous localization observed here is suggestive of functional relevance in the vacuole. Moreover, in *C. roseus* leaves, both the AGP epitopes and total AGPs show an abundant, possibly major localization in the tonoplast/vacuole, indicating that the paradigm of AGPs as cell wall proteoglycans may need to be reconsidered.

Furthermore, the AGP epitopes presented a punctuated distribution suggesting a possible localization in membrane microdomains, both at the cell surface and the tonoplast. Actually, recent proteomic studies have detected the presence of AGPs in microdomains of certain tissues and it has been specifically suggested that GPI-anchored AGPs localized in microdomains may mediate signalling in plants through interaction with other signalling proteins co-localized in the microdomain (Mongrand et al., 2004; Borner et al., 2005; Sardar et al., 2006; Lefebvre et al., 2007; Sardar and Showalter, 2007; Zhang et al., 2011; Yoshida et al., 2013). Our results suggest that the tonoplast membrane may also be organized in microdomains, and that GPI-anchored AGPs are localized in such microdomains, both in the tonoplast and the plasma membrane. In fact, very recently, the presence of detergent-resistant membrane microdomains was detected for the first time in tonoplast membranes (Ozolina et al., 2013). Most importantly, Prx was observed to co-localize with AGPs in those membrane microdomains, clearly indicating a possible *in vivo* interaction important for signalling (discussed below).

The Prx-AGPs interaction and its physiological meaning – the H_2O_2 connection

In this thesis, it was shown that AGPs from *C. roseus* and Arabidopsis are good substrates for Prxs in general, adding a new family of compounds to the long list of Prx substrates. Moreover, it was shown that, *in vitro*, the major Prxs from the leaves of *C. roseus* and Arabidopsis mediated reactions that resulted in changes of the molecular weight and abundance of the glycosidic epitopes from the respective AGPs, compatible with the occurrence of inter and/or intra-molecular cross-linking. These reactions seemed to also occur *in vivo*, since infiltration of leaves with H_2O_2 resulted in the

increase in the intensity of AGPs labelling, likely mediated by Prx. Finally, immunolabelling studies revealed that Prx and AGPs co-localized in membrane microdomains, further supporting an *in planta* interaction.

This Prx-AGP interaction and co-localization observed both in *C. roseus* and Arabidopsis suggest that Prx and H_2O_2 may be important regulators of the developmental and signalling functions attributed to AGPs, and establish a direct link between AGPs functions/signalling and H_2O_2 signalling. Therefore, a model is proposed here for the functional relevance of the Prx-AGP interaction, in which these two protein families are co-localized in plasma membrane microdomains, where they may function as a cell surface signalling switch/gateway between the apoplast and the symplast (Figure IV.1): as soon as an H_2O_2 signal is triggered by wounding, infection or other type of stress, namely resulting from the activity of a potentially co-localized NADPH oxidase, Prx will perform intra- and/or inter-molecular cross-linking of the associated AGPs, leading to a change in the interaction of AGPs with other signalling proteins in the membrane microdomain, or to changes in their interaction with the cytoskeleton, ultimately resulting in the launch of an intracellular signalling pathway. In brief, the Prx-AGP interaction may constitute an H_2O_2 sensor. On the other hand, H_2O_2 could also lead to Prx-mediated cross-linking of the abundant soluble AGPs, putatively located in the periplasmic space or within the cell wall, leading to the formation of high molecular weight aggregates influencing the properties of the cell wall. The model proposed may also apply to the patches of AGPs and Prx observed in the membrane of the vacuole, where the Prx-AGP system could also assume signalling functions, such as the detection and response to changes in turgor pressure. Meaningfully, NADPH oxidase has also been detected in the vacuole proteome (Carter et al., 2004).

It is actually conceivable that the steric consequences of the cross-linking of AGPs by Prx may sometimes mimic the AGP cross-linking effect of the Yariv reagent, which has been shown to induce several types of cellular responses as a consequence of its interaction with AGPs, including PCD, changes in cellular expansion, etc (Showalter, 2001; Chaves et al., 2002; Seifert and Roberts, 2007). Guan and Nothnagel (2004) have observed that the gene expression profile induced by Yariv treatment of Arabidopsis suspension cell cultures is most similar to that induced by wounding, which in turn has been reported to induce H_2O_2 production, Prx, and oxidative cross-linking of AGPs (Kjellbom et al., 1997; Orozco-Cardenas and Ryan, 1999; Bernards et al., 2004).

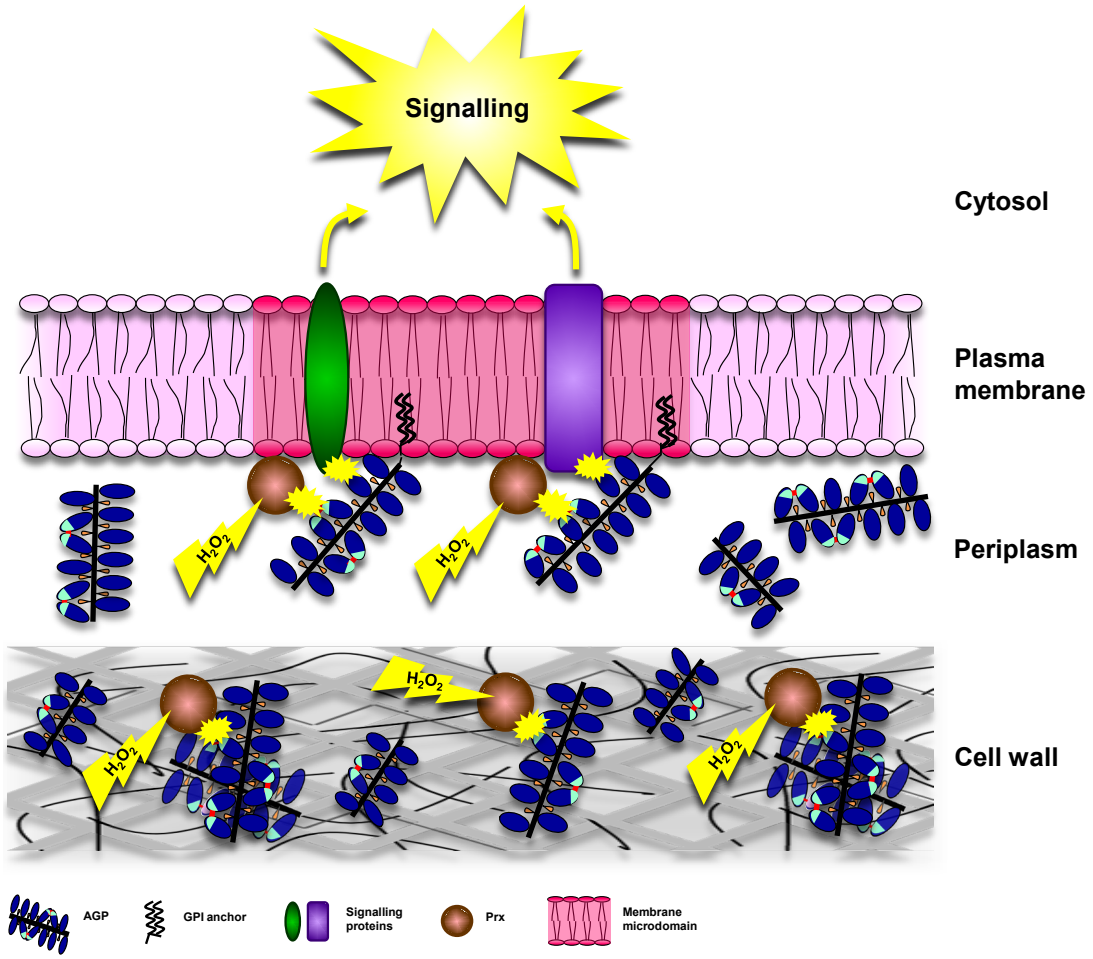

Figure IV.1 – Model proposed for the functional importance of the interaction between Prxs and AGPs at the plant cell surface. H_2O_2 resulting from stress will trigger Prx-mediated cross-linking of AGPs co-located in plasma membrane microdomains, resulting in steric changes in AGPs that will propagate to transmembrane signalling proteins also present at the microdomain, ultimately leading to the activation of intracellular signalling. Additional intra-molecular and/or inter-molecular cross-linking may also occur at the level of the periplasmic space and the cell wall, affecting cell wall properties.

In order to confirm if the model proposed in Figure IV.1 is indeed present in plant cells, the importance of the pair Prx-AGPs during the focal expansion of Arabidopsis root hairs was investigated in this thesis. The AGP blocker Yariv and the Prx inhibitor SHAM both had a negative impact in the number and size of root hairs in Arabidopsis seedlings, as well as the ROS scavengers KI and ascorbate. Moreover, the growth rate of root hairs was significantly impaired by AGP and Prx antibodies labelling root hairs or trichoblasts (LM2, JIM16, MAC207 and anti-CroPrx1). Additionally, AtPrx34 stimulated root hair growth rate, while gum arabic inhibited growth. All these results support a role of ROS, AGPs and Prx in tip growth of root hairs that fit well with the application of the Prx-AGP H_2O_2-sensor model to this physiological process as depicted in Figure IV.2: i) NADPH oxidase active at the root tip (Foreman et al., 2003;

Takeda et al., 2008) produces superoxide anion that spontaneously or enzymatically dismutates to H_2O_2; ii) this signal molecule is then used by Prx localized at the tip to cross-link closely located AGPs that will interact with other co-located proteins, ultimately activating Ca^{2+} channels and leading to the Ca^{2+} influx necessary for tip growth (Foreman et al., 2003; Takeda et al., 2008). Alternatively or even additionally, it may be conceived that the Prx-mediated cross-linking of AGPs may lead to localized Ca^{2+} release from the AGP glycan moiety, contributing decisively to the necessary Ca^{2+} gradient, since AGPs have been proposed to act as Ca^{2+} capacitors (Lamport and Várnai, 2013). Therefore, the observed stimulation of root hair growth by AtPrx34 could be explained by a more active cross-linking of AGPs resulting in an increase of signal intensity, while inhibition by gum arabic could be explained by its competition with endogenous AGPs for Prx. Further important support to a role of AGPs in tip growth was the result that the ectopic expression of *AtAGP9* and *58* in root hairs both increased the rate of their elongation.

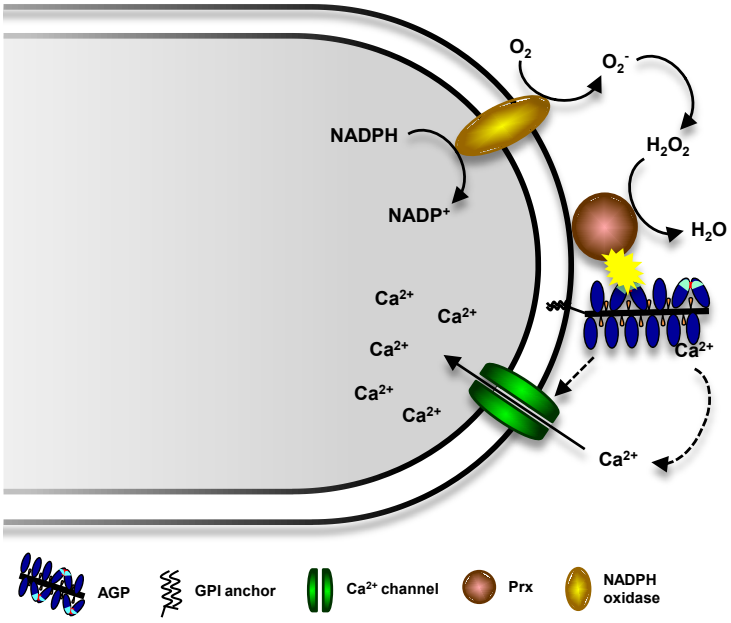

Figure IV.2 – Model proposed for the interaction between Prxs and AGPs during tip growth in root hairs. H_2O_2 resulting from NADPH oxidase activity will trigger Prx-mediated cross-linking of AGPs co-localized at the tip of the root hair, resulting in the activation of Ca^{2+} channels and leading to the Ca^{2+} influx necessary for tip growth. Alternatively or even additionally, the Prx-mediated cross-linking of AGPs will lead to localized Ca^{2+} release from the AGP glycan moiety, contributing decisively to the necessary Ca^{2+} gradient.

Future perspectives

The logical next step is to investigate if there are AGP or Prx mutants that show a root hair phenotype. This may be done by focusing first in the mutants of the genes shown to be highly expressed in the root hair zone in GENEVESTIGATOR. It could then be

investigated whether the addition of Prx would complement any of the knock-outs, for functional confirmation, and to determine the direction of the interaction: if the addition of Prx complements the Prx knock-out, but not an AGP knock-out, this means that if there is a cooperation between the two, the AGP is down-stream Prx in the pathway. The AGP and Prx genes showing a root hair phenotype could then be used for *in vivo* interaction studies using FRET or BiFC. The use of Arabidopsis lines expressing the Ca^{2+} sensor Cameleon YC3.6 (Monshausen et al., 2007) is also planned, in order to investigate whether inhibition of Prx and AGPs interferes with Ca^{2+} influx as predicted.

In this thesis, the knock-outs of *AtAGP9* and *AtAGP58* were investigated and did not have any phenotype, namely concerning root hairs. This is understandable, since these genes were selected due to a high expression in leaves, when work was focused in the leaves. However, in the leaves, ABA-mediated stomata closure has been shown to involve H_2O_2 signalling and activation of Ca^{2+} influx (Pei et al., 2000; Desikan et al., 2004), similarly to root hair tip growth, and is therefore a candidate process for regulation by the Prx-AGP interaction. Thus, it would be interesting to investigate whether the *AtAGP9* and *AtAGP58* mutants will show a phenotype if submitted to drought.

A remaining open question concerning the Prx-AGP interaction proposed here and the observed fact that AGPs are substrates of Prx, is the identity of the chemical group(s) in AGPs that may be oxidised by Prx. In fact, the precise identity of the chemical groups involved in the Prx-mediated cross-linking of cell wall glycoproteins and polysaccharides remains a matter of debate, but several lines of data point to the participation of phenolic side-chains, including feruloyl residues of wall polysaccharides such as pectins, or tyrosine residues of cell wall glycoproteins such as extensin (Fry, 2004; Held et al., 2004; Abdel-Massih et al., 2007). In AGPs, it is not likely that Tyr residues will be exposed for cross-linking, the most reasonable hypothesis being the cross-linking of feruloyl residues putatively esterified in the glycan chains. In fact, feruloyl- and *p*-coumaroyl-arabinogalactans have been detected in beet and spinach, new crossed-hydroxycinnamate dimers, trimers and tetramers continue to be found in the cell wall, and gum arabic AGPs were shown to include di-ferulates, supporting the hypothesis that AGPs might also be feruloylated (Fry, 1982; Colquhoun et al., 1994; Fry, 2004; Renard et al., 2006; Bunzel, 2010). During the work of this thesis, the presence of Prx-reactive feruloyl residues in AGPs from Arabidopsis, gum arabic and *Brassica* was submitted to a preliminary survey (see Annex). Results were still inconclusive, but it was possible to detect the presence of feruloyl residues in gum arabic and *Brassica* AGPs, suggesting that the glycosidic chains of AGPs may be

feruloylated. Such residues may thus function as good Prx substrates that, upon oxidation, will form radicals that will react to form cross-links. This line of research has to be further investigated using increased levels of isolated AGPs and improved analysis methods such as the ones cited by Bunzel (2010).

An interesting result also obtained in this thesis was the fact that AtPrx34 presented a sigmoidal kinetics in the presence of growing concentrations of Arabidopsis leaf AGPs, indicative of heteroallosteric activation (see section III.3.1). This regulation should be further characterized, namely if AGPs can modulate the activity of AtPrx34 against common Prx phenolic substrates, and if this modulation is dependent on changes in Ca^{2+}. Moreover, the binding of AGPs to AtPrx34 could be characterized by thermal shift assays (Differential Scanning Fluorimetry) and Isothermal Titration Calorimetry, to determine whether there is binding to two sites (the active site and a regulatory one). Finally, subfractionation of AGPs could eventually allow to determine if it is the same AGP or different AGPs functioning as substrate and regulatory effector. An allosteric behaviour for class III peroxidases has been reported only a few times and was never extensively characterized (Reigh and Smith, 1977; Srivastava and Van Huystee, 1977; Gafert et al., 1995; Zatón and Ochoa de Aspuru, 1995; Pintus et al., 2008), but it may be extremely important *in vivo*, since Ferreres et al. (2011) has suggested that Prx activity should be under tight regulatory control in plant cells. Meaningfully, Veitch (2004) refers that a distinctive structural feature of Prxs relative to class I and II peroxidases is the presence of several *α*–helices, with two of them showing high variability among plant Prxs. Regulation of Prx activity through binding of specific effectors to this variable region could be used to determine *in vivo* specific functions for different Prx isoenzymes, in spite of their broad and overlapping substrate profile *in vitro*.

In conclusion, the results obtained in the course of this thesis contributed with important data concerning the localization and functions of AGPs, and have provided novel information regarding a potentially physiological interaction between AGPs and Prxs, two important families of cell wall proteins. Most importantly, many new questions were raised for the future.

V.

LITERATURE CITED

Abdel-Massih RM, Baydoun EAH, Waldron KW, Brett CT (2007) Effects of partial enzymic degradation of sugar beet pectin on oxidative coupling of pectin-linked ferulates *in vitro*. Phytochemistry **68:** 1785-1790

Acosta-Garcia G, Vielle-Calzada JP (2004) A classical arabinogalactan protein is essential for the initiation of female gametogenesis in Arabidopsis. Plant Cell **16:** 2614-2628

Alberts B, Johnson A, Lewis J, Raff M, Roberts K, Walter P (2007) Molecular Biology of the Cell. Garland Pub. Inc., New York

Almagro L, Gómez Ros LV, Belchi-Navarro S, Bru R, Ros Barceló A, Pedreño MA (2009) Class III peroxidases in plant defence reactions. Journal of Experimental Botany **60:** 377-390

Anand S, Tyagi A (2010) Characterization of a pollen-preferential gene OSIAGP from rice (Oryza sativa L. subspecies indica) coding for an arabinogalactan protein homologue, and analysis of its promoter activity during pollen development and pollen tube growth. Transgenic Research **19:** 385-397

Andème-Onzighi C, Sivaguru M, Judy-March J, Baskin T, Driouich A (2002) The reb1-1 mutation of Arabidopsis alters the morphology of trichoblasts, the expression of arabinogalactan-proteins and the organization of cortical microtubules. Planta **215:** 949-958

Baldwin TC, McCann MC, Roberts K (1993) A Novel Hydroxyproline-Deficient Arabinogalactan Protein Secreted by Suspension-Cultured Cells of Daucus carota (Purification and Partial Characterization). Plant Physiology **103:** 115-123

Baluška F, Busti E, Dolfini S, Gavazzi G, Volkmann D (2001) Lilliputian Mutant of Maize Lacks Cell Elongation and Shows Defects in Organization of Actin Cytoskeleton. Developmental Biology **236:** 478-491

Baluška F, Šamaj J, Wojtaszek P, Volkmann D, Menzel D (2003) Cytoskeleton-Plasma Membrane-Cell Wall Continuum in Plants. Emerging Links Revisited. Plant Physiology **133:** 482-491

Barceló AR, Pomar F, Lopez-Serrano M, Pedreño MA (2003) Peroxidase: a multifunctional enzyme in grapevines. Functional Plant Biology **30:** 577-591

Bassham DC, Brandizzi F, Otegui MS, Sanderfoot AA (2008) The secretory system of Arabidopsis. The Arabidopsis book / American Society of Plant Biologists **6:** e0116

Bernal MA, Pedreno MA, Calderon AA, Munoz R, Barceló AR, Merino de Caceres F (1993) The subcellular localization of isoperoxidases in Capsicum annuum leaves and their different expression in vegetative and flowered plants, Vol 72. Academic Press, London, ROYAUME-UNI

Bernards M, Summerhurst DK, Razem F (2004) Oxidases, peroxidases and hydrogen peroxide: The suberin connection. Phytochemistry Reviews **3:** 113-126

Bhat RA, Panstruga R (2005) Lipid rafts in plants. Planta **223:** 5-19

Bindschedler LV, Dewdney J, Blee KA, Stone JM, Asai T, Plotnikov J, Denoux C, Hayes T, Gerrish C, Davies DR, Ausubel FM, Paul Bolwell G (2006) Peroxidase-dependent apoplastic oxidative burst in Arabidopsis required for pathogen resistance. The Plant Journal **47:** 851-863

Birecka H, Catalfamo J (1976) Cell isoperoxidases in sweet potato plants in relation to mechanical injury and ethylene. Plant Physiol **57:** 74-79

Bolwell GP, Wojtaszek P (1997) Mechanisms for the generation of reactive oxygen species in plant defence – a broad perspective. Physiological and Molecular Plant Pathology **51:** 347-366

Borner GHH, Lilley KS, Stevens TJ, Dupree P (2003) Identification of Glycosylphosphatidylinositol-Anchored Proteins in Arabidopsis. A Proteomic and Genomic Analysis. Plant Physiology **132:** 568-577

Borner GHH, Sherrier DJ, Stevens TJ, Arkin IT, Dupree P (2002) Prediction of Glycosylphosphatidylinositol-Anchored Proteins in Arabidopsis. A Genomic Analysis. Plant Physiology **129:** 486-499

Borner GHH, Sherrier DJ, Weimar T, Michaelson LV, Hawkins ND, MacAskill A, Napier JA, Beale MH, Lilley KS, Dupree P (2005) Analysis of Detergent-Resistant Membranes in Arabidopsis. Evidence for Plasma Membrane Lipid Rafts. Plant Physiology **137:** 104-116

Bosch M, Knudsen JS, Derksen J, Mariani C (2001) Class III Pistil-Specific Extensin-Like Proteins from Tobacco Have Characteristics of Arabinogalactan Proteins. Plant Physiology **125:** 2180-2188

Boyes DC, Zayed AM, Ascenzi R, McCaskill AJ, Hoffman NE, Davis KR, Görlach J (2001) Growth Stage–Based Phenotypic Analysis of Arabidopsis: A Model for High Throughput Functional Genomics in Plants. The Plant Cell Online **13:** 1499-1510

Bradley DJ, Kjellbom P, Lamb CJ (1992) Elicitor- and wound-induced oxidative cross-linking of a proline-rich plant cell wall protein: A novel, rapid defense response. Cell **70:** 21-30

Bradley DJ, Wood EA, Larkins AP, Galfre G, Butcher GW, Brewin NJ (1988) ISOLATION OF MONOCLONAL-ANTIBODIES REACTING WITH PERIBACTEROID MEMBRANES AND OTHER COMPONENTS OF PEA ROOT-NODULES CONTAINING RHIZOBIUM-LEGUMINOSARUM. Planta **173:** 149-160

Breton C, Bettler E, Joziasse DH, Geremia RA, Imberty A (1998) Sequence-Function Relationships of Prokaryotic and Eukaryotic Galactosyltransferases. Journal of Biochemistry **123:** 1000-1009

Bringmann M, Landrein B, Schudoma C, Hamant O, Hauser M-T, Persson S (2012) Cracking the elusive alignment hypothesis: the microtubule–cellulose synthase nexus unraveled. Trends in Plant Science **17:** 666-674

Brisson LF, Tenhaken R, Lamb C (1994) Function of Oxidative Cross-Linking of Cell Wall Structural Proteins in Plant Disease Resistance. The Plant Cell Online **6:** 1703-1712

Brooker RJ, Widmaier EP, Graham LE, Stiling PD (2010) Biology, Ed 2nd edition. McGraw-Hill

Brown S, Renaudin JP, Prevot C, Guern J (1984) Flow cytometry and sorting of plant protoplasts: technical problems and physiological results from a study of pH and alkaloids in *Catharanthus roseus*. Physiologie vegetale **22:** 541-554

Buchanan-Wollaston V, Page T, Harrison E, Breeze E, Lim PO, Nam HG, Lin J-F, Wu S-H, Swidzinski J, Ishizaki K, Leaver CJ (2005) Comparative transcriptome analysis reveals significant differences in gene expression and signalling pathways between developmental and dark/starvation-induced senescence in Arabidopsis. The Plant Journal **42:** 567-585

Buchanan B, Gruissem W, Jones R (2002) Biochemistry & Molecular Biology of Plants. Wiley

Bunzel M (2010) Chemistry and occurrence of hydroxycinnamate oligomers. Phytochemistry Reviews **9:** 47-64

Burnette WN (1981) "Western Blotting": Electrophoretic transfer of proteins from sodium dodecyl sulfate-polyacrylamide gels to unmodified nitrocellulose and radiographic detection with antibody and radioiodinated protein A. Analytical Biochemistry **112:** 195-203

Butowt R, Niklas A, Rodriguez-Garcia MI, Majewska-Sawka A (1999) Involvement of JIM13- and JIM8-Responsive Carbohydrate Epitopes in Early Stages of Cell Wall Formation. Journal of Plant Research **112:** 107-116

Caffall KH, Mohnen D (2009) The structure, function, and biosynthesis of plant cell wall pectic polysaccharides. Carbohydrate Research **344:** 1879-1900

Cannesan MA, Durand C, Burel C, Gangneux C, Lerouge P, Ishii T, Laval K, Follet-Gueye M-L, Driouich A, Vicré-Gibouin M (2012) Effect of Arabinogalactan Proteins from the Root Caps of Pea and Brassica napus on Aphanomyces euteiches Zoospore Chemotaxis and Germination. Plant Physiology **159:** 1658-1670

Cannon MC, Terneus K, Hall Q, Tan L, Wang Y, Wegenhart BL, Chen L, Lamport DTA, Chen Y, Kieliszewski MJ (2008) Self-assembly of the plant cell wall requires an extensin scaffold. Proceedings of the National Academy of Sciences of the United States of America **105:** 2226-2231

Carol RJ, Dolan L (2002) Building a hair: tip growth in Arabidopsis thaliana root hairs. Philosophical Transactions of the Royal Society of London. Series B: Biological Sciences **357:** 815-821

Carqueijeiro I (2013) Unravelling the metabolism and transmembrane transport of the highly valuable medicinal alkaloids from *Catharanthus roseus*. Universidade do Porto, Faculdade de Ciências

Carter C, Pan SQ, Jan ZH, Avila EL, Girke T, Raikhel NV (2004) The vegetative vacuole proteome of *Arabidopsis thaliana* reveals predicted and unexpected proteins. Plant Cell **16:** 3285-3303

Casero PJ, Casimiro I, Knox JP (1998) Occurrence of cell surface arabinogalactan-protein and extensin epitopes in relation to pericycle and vascular tissue development in the root apex of four species. Planta **204:** 252-259

Cervone F, Hahn MG, De Lorenzo G, Darvill A, Albersheim P (1989) Host-Pathogen Interactions: XXXIII. A Plant Protein Converts a Fungal Pathogenesis Factor into an Elicitor of Plant Defense Responses. Plant Physiology **90:** 542-548

Chaves I, Regalado AP, Chen M, Ricardo CP, Showalter AM (2002) Programmed cell death induced by (β-d-galactosyl)3 Yariv reagent in Nicotiana tabacum BY-2 suspension-cultured cells. Physiologia Plantarum **116:** 548-553

Cheeseman JM (2006) Hydrogen peroxide concentrations in leaves under natural conditions. Journal of Experimental Botany **57:** 2435-2444

Chen CG, Pu ZY, Moritz RL, Simpson RJ, Bacic A, Clarke AE, Mau SL (1994) Molecular cloning of a gene encoding an arabinogalactan-protein from pear (Pyrus communis) cell suspension culture. Proceedings of the National Academy of Sciences **91:** 10305-10309

Chen S-x, Schopfer P (1999) Hydroxyl-radical production in physiological reactions. European Journal of Biochemistry **260:** 726-735

Cheung AY, Wang H, Wu H-m (1995) A floral transmitting tissue-specific glycoprotein attracts pollen tubes and stimulates their growth. Cell **82:** 383-393

Cheung AY, Wu HM (1999) Arabinogalactan proteins in plant sexual reproduction. Protoplasma **208:** 87-98

Clarke AE, Anderson RL, Stone BA (1979) Form and function of arabinogalactans and arabinogalactan-proteins. Phytochemistry **18:** 521-540

Classen B, Thude S, Blaschek W, Wack M, Bodinet C (2006) Immunomodulatory effects of arabinogalactan-proteins from Baptisia and Echinacea. Phytomedicine **13:** 688-694

Coimbra S, Almeida J, Junqueira V, Costa ML, Pereira LG (2007) Arabinogalactan proteins as molecular markers in *Arabidopsis thaliana* sexual reproduction. Journal of Experimental Botany **58:** 4027-4035

Coimbra S, Costa M, Jones B, Mendes MA, Pereira LG (2009) Pollen grain development is compromised in Arabidopsis agp6 agp11 null mutants. Journal of Experimental Botany **60:** 3133-3142

Coimbra S, Costa M, Mendes M, Pereira A, Pinto J, Pereira L (2010) Early germination of Arabidopsis pollen in a double null mutant for the arabinogalactan protein genes AGP6 and AGP11. Sexual Plant Reproduction **23:** 199-205

Cole RA, Fowler JE (2006) Polarized growth: maintaining focus on the tip. Current Opinion in Plant Biology **9:** 579-588

Colquhoun IJ, Ralet MC, Thibault JF, Faulds CB, Williamson G (1994) Structure identification of feruloylated oligosaccharides from sugar-beet pulp by nmr-spectroscopy. Carbohydrate Research **263:** 243-256

Cosgrove DJ (2005) Growth of the plant cell wall. Nat Rev Mol Cell Biol **6:** 850-861

Cosio C, Dunand C (2009) Specific functions of individual class III peroxidase genes. Journal of Experimental Botany **60:** 391-408

Costa M, Nobre MS, Becker JD, Masiero S, Amorim MI, Pereira LG, Coimbra S (2013) Expression-based and co-localization detection of arabinogalactan protein 6 and arabinogalactan protein 11 interactors in Arabidopsis pollen and pollen tubes. Bmc Plant Biology **13**

Costa MMR, Hilliou F, Duarte P, Pereira LG, Almeida I, Leech M, Memelink J, Barcelo AR, Sottomayor M (2008) Molecular cloning and characterization of a vacuolar class III peroxidase involved in the metabolism of anticancer alkaloids in *Catharanthus roseus*. Plant Physiology **146:** 403-417

Coutinho PM, Deleury E, Davies GJ, Henrissat B (2003) An Evolving Hierarchical Family Classification for Glycosyltransferases. Journal of Molecular Biology **328:** 307-317

Cruz-Garcia F, Nathan Hancock C, Kim D, McClure B (2005) Stylar glycoproteins bind to S-RNase in vitro. The Plant Journal **42:** 295-304

Dahiya P, Findlay K, Roberts K, McCann M (2006) A fasciclin-domain containing gene, ZeFLA11, is expressed exclusively in xylem elements that have reticulate wall thickenings in the stem vascular system of Zinnia elegans cv Envy. Planta **223:** 1281-1291

Dardelle F, Lehner A, Ramdani Y, Bardor M, Lerouge P, Driouich A, Mollet J-C (2010) Biochemical and Immunocytological Characterizations of Arabidopsis Pollen Tube Cell Wall. Plant Physiology **153:** 1563-1576

Davies B, Edwards SW (1989) Inhibition of myeloperoxidase by salicylhydroxamic acid. The Biochemical journal **258:** 801-806

Davies DR, Bindschedler LV, Strickland TS, Bolwell GP (2006) Production of reactive oxygen species in *Arabidopsis thaliana* cell suspension cultures in response to an elicitor from *Fusarium oxysporum*: implications for basal resistance. Journal of Experimental Botany **57:** 1817-1827

De Gara L, Locato V, Dipierro S, de Pinto MC (2010) Redox homeostasis in plants. The challenge of living with endogenous oxygen production. Respiratory Physiology & Neurobiology **173, Supplement:** S13-S19

de Graaf BHJ, Knuiman BA, Derksen J, Mariani C (2003) Characterization and localization of the transmitting tissue-specific PELPIII proteins of Nicotiana tabacum. Journal of Experimental Botany **54:** 55-63

Demesa-Arévalo E, Vielle-Calzada J-P (2013) The Classical Arabinogalactan Protein AGP18 Mediates Megaspore Selection in Arabidopsis. The Plant Cell Online

Desikan R, Cheung M, Clarke A, Golding S, Sagi M, Fluhr R, Rock C, Hancock J, Neill S (2004) Hydrogen peroxide is a common signal for darkness- and ABA-induced stomatal closure in Pisum sativum. Functional Plant Biology **31:** 913-920

Díaz J, Pomar F, Bernal A, Merino F (2004) Peroxidases and the metabolism of capsaicin in Capsicum annuum L. Phytochemistry Reviews **3:** 141-157

Ding L, Zhu JK (1997) A role for arabinogalactan-proteins in root epidermal cell expansion. Planta **203:** 289-294

Doblin MS, Pettolino F, Bacic A (2010) Plant cell walls: the skeleton of the plant world. Functional Plant Biology **37:** 357-381

Dolan L, Linstead P, Roberts K (1995) An AGP epitope distinguishes a central metaxylem initial from other vascular initials in theArabidopsis root. Protoplasma **189:** 149-155

Dong C-H, Xia G-X, Hong Y, Ramachandran S, Kost B, Chua N-H (2001) ADF Proteins Are Involved in the Control of Flowering and Regulate F-Actin Organization, Cell Expansion, and Organ Growth in Arabidopsis. The Plant Cell Online **13:** 1333-1346

Douroupi TG, Papassideri IS, Stravopodis DJ, Margaritis LH (2005) Molecular cloning and tissue-specific transcriptional regulation of the first peroxidase family member, Udp1, in stinging nettle (Urtica dioica). Gene **362:** 57-69

Doyle JJ, Doyle JL (1987) A rapid DNA isolation procedure for small quantities of fresh leaf tissue. Phytochemical Bulletin **19:** 11-15

Driouich A, Follet-Gueye M-L, Vicré-Gibouin M, Hawes M (2013) Root border cells and secretions as critical elements in plant host defense. Current Opinion in Plant Biology

Du H, Clarke AE, Bacic A (1996) Arabinogalactan-proteins: a class of extracellular matrix proteoglycans involved in plant growth and development. Trends in Cell Biology **6:** 411-414

Duckett CM, Grierson C, Linstead P, Schneider K, Lawson E, Dean C, Poethig S, Roberts K (1994) Clonal relationships and cell patterning in the root epidermis of Arabidopsis. Development **120:** 2465-2474

Dunand C, Crèvecoeur M, Penel C (2007) Distribution of superoxide and hydrogen peroxide in Arabidopsis root and their influence on root development: possible interaction with peroxidases. New Phytologist **174:** 332-341

Dunand C, De Meyer M, Crèvecoeur M, Penel C (2003) Expression of a peroxidase gene in zucchini in relation with hypocotyl growth. Plant Physiology and Biochemistry **41:** 805-811

Dunford HB (1982) Peroxidases. Adv. Inorg. Biochem. **4:** 41-68

Duroux L, Welinder K (2003) The Peroxidase Gene Family in Plants: A Phylogenetic Overview. Journal of Molecular Evolution **57:** 397-407

Egelund J, Ellis M, Doblin M, Qu Y, Bacic A (2010) Genes and Enzymes of the GT31 Family: Towards Unravelling the Function(s) of the Plant Glycosyltransferase Family Members. *In* Annual Plant Reviews. Wiley-Blackwell, pp 213-234

Eilert U, Nesbitt LR, Constabel F (1985) Laticifers and latex in fruits of periwinkle, *Catharanthus roseus*. Canadian Journal of Botany-Revue Canadienne De Botanique **63:** 1540-1546

Eisenhaber B, Wildpaner M, Schultz CJ, Borner GHH, Dupree P, Eisenhaber F (2003) Glycosylphosphatidylinositol Lipid Anchoring of Plant Proteins. Sensitive Prediction from Sequence- and Genome-Wide Studies for Arabidopsis and Rice. Plant Physiology **133:** 1691-1701

Ellis M, Egelund J, Schultz CJ, Bacic A (2010) Arabinogalactan-Proteins: Key Regulators at the Cell Surface? Plant Physiology **153:** 403-419

Emanuelsson O, Brunak S, von Heijne G, Nielsen H (2007) Locating proteins in the cell using TargetP, SignalP and related tools. Nature Protocols **2:** 953-971

Estévez JM, Kieliszewski MJ, Khitrov N, Somerville C (2006) Characterization of Synthetic Hydroxyproline-Rich Proteoglycans with Arabinogalactan Protein and Extensin Motifs in Arabidopsis. Plant Physiology **142:** 458-470

Fang G, Li J (2007) Preparation method for compound arabinogalactan film coated tablets. *In* CFIPI Center, ed, Vol CN101053588 (A)

Ferguson C, Bacic A, Anderson MA, Read SM (1999) Subcellular distribution of arabinogalactan proteins in pollen grains and tubes as revealed with a monoclonal antibody raised against stylar arabinogalactan proteins. Protoplasma **206:** 105-117

Ferrer MA, Calderón AA, Muñoz R, Ros Barceló A (1990) 4-Methoxy-α-naphthol as a specific substrate for kinetic, zymographic and cytochemical studies on plant peroxidase activities. Phytochemical Analysis **1:** 63-69

Ferreres F, Figueiredo R, Bettencourt S, Carqueijeiro I, Oliveira J, Gil-Izquierdo A, Pereira DM, Valentão P, Andrade PB, Duarte P, Barceló AR, Sottomayor M (2011) Identification of phenolic compounds in isolated vacuoles of the medicinal plant Catharanthus roseus and their interaction with vacuolar class III peroxidase: an H2O2 affair? Journal of Experimental Botany **62:** 2841-2854

Figueiredo R (2011) Functions of Class III Peroxidases in higher plants: multiple approaches using the medicinal plant *Catharanthus roseus* and the mo del plant *Arabidopsis thaliana*. Universidade do Porto

Fincher GB, Stone BA, Clarke AE (1983) Arabinogalactan-Proteins: Structure, Biosynthesis, and Function. Annual Review of Plant Physiology **34:** 47-70

Foreman J, Demidchik V, Bothwell JHF, Mylona P, Miedema H, Angel Torres M, Linstead P, Costa S, Brownlee C, Jones JDG, Davies JM, Dolan L (2003) Reactive oxygen species produced by NADPH oxidase regulate plant cell growth. Nature **422:** 442-446

Foster A (1956) Plant idioblasts: Remarkable examples of cell specialization. Protoplasma **46:** 184-193

Fry SC (1982) Phenolic components of the primary-cell wall - feruloylated disaccharides of D-galactose and L-arabinose from spinach polysaccharide. Biochemical Journal **203:** 493-504

Fry SC (2004) Oxidative coupling of tyrosine and ferulic acid residues: Intra- and extra-protoplasmic occurrence, predominance of trimers and larger products, and possible role in inter-polymeric cross-linking. Phytochemistry Reviews **3:** 97-111

Fry SC, Aldington S, Hetherington PR, Aitken J (1993) Oligosaccharides as Signals and Substrates in the Plant Cell Wall. Plant Physiology **103:** 1-5

Führs H, Behrens C, Gallien S, Heintz D, Van Dorsselaer A, Braun H-P, Horst WJ (2010) Physiological and proteomic characterization of manganese sensitivity and tolerance in rice (Oryza sativa) in comparison with barley (Hordeum vulgare). Annals of Botany **105:** 1129-1140

Gabaldón C, López-Serrano M, Pedreño MA, Barceló AR (2005) Cloning and Molecular Characterization of the Basic Peroxidase Isoenzyme from Zinnia elegans, an Enzyme Involved in Lignin Biosynthesis. Plant Physiology **139:** 1138-1154

Gafert J, Friedrich J, Vanderkooi JM, Fidy J (1995) Structural Changes and Internal Fields in Proteins: A Hole-Burning Stark Effect Study of Horseradish Peroxidase. The Journal of Physical Chemistry **99:** 5223-5227

Gane AM, Craik D, Munro SLA, Howlett GJ, Clarke AE, Bacic A (1995) Structural analysis of the carbohydrate moiety of arabinogalactan-proteins from stigmas and styles of Nicotiana alata. Carbohydrate Research **277:** 67-85

Gao M, Kieliszewski MJ, Lamport DTA, Showalter AM (1999) Isolation, characterization and immunolocalization of a novel, modular tomato arabinogalactan-protein corresponding to the LeAGP-1 gene. The Plant Journal **18:** 43-55

Gao M, Showalter AM (1999) Yariv reagent treatment induces programmed cell death in Arabidopsis cell cultures and implicates arabinogalactan protein involvement. Plant Journal **19:** 321-331

Garcia-Florenciano E, Claderon AA, Pedreno MA, Munoz R, Ros Barceló A (1991) The vacuolar localization of basic isoperoxidases in grapevine suspension cell cultures and its significance in indole-3-acetic acid catabolism, Vol 10. Springer, Dordrecht, PAYS-BAS

Gaspar Y, Johnson K, McKenna J, Bacic A, Schultz C (2001) The complex structures of arabinogalactan-proteins and the journey towards understanding function. Plant Molecular Biology **47:** 161-176

Gaspar YM, Nam J, Schultz CJ, Lee L-Y, Gilson PR, Gelvin SB, Bacic A (2004) Characterization of the Arabidopsis Lysine-Rich Arabinogalactan-Protein AtAGP17 Mutant (rat1) That Results in a Decreased Efficiency of Agrobacterium Transformation. Plant Physiology **135:** 2162-2171

Gilson P, Gaspar YM, Oxley D, Youl JJ, Bacic A (2001) NaAGP4 is an arabinogalactan protein whose expression is suppressed by wounding and fungal infection inNicotiana alata. Protoplasma **215:** 128-139

Goedhart J, van Weeren L, Hink MA, Vischer NOE, Jalink K, Gadella TWJ (2010) Bright cyan fluorescent protein variants identified by fluorescence lifetime screening. Nature Methods **7:** 137-U174

Goodrum LJ, Patel A, Leykam JF, Kieliszewski MJ (2000) Gum arabic glycoprotein contains glycomodules of both extensin and arabinogalactan-glycoproteins. Phytochemistry **54:** 99-106

Gorres KL, Raines RT (2010) Prolyl 4-hydroxylase. Crit Rev Biochem Mol Biol **45:** 106-124

Graaf BJ, Knuiman B, Bosch MM, Mariani C (2000) The Class III Pistil-Specific Extensin-Like Proteins of Nicotiana tabacum Show Arabinogalactan-Protein-Like Characteristics and are Non-Specifically Translocated Through Pollen Tube Walls In Vivo. *In* E Nothnagel, A Bacic, A Clarke, eds, Cell and Developmental Biology of Arabinogalactan-Proteins. Springer US, pp 283-284

Griffith OH, Ryan M (1999) Bacterial phosphatidylinositol-specific phospholipase C: structure, function, and interaction with lipids. Biochimica et Biophysica Acta (BBA) - Molecular and Cell Biology of Lipids **1441:** 237-254

Guan Y, Nothnagel EA (2004) Binding of arabinogalactan proteins by Yariv phenylglycoside triggers wound-like responses in Arabidopsis cell cultures. Plant Physiology **135:** 1346-1366

Guirimand G, Guihur A, Ginis O, Poutrain P, Héricourt F, Oudin A, Lanoue A, St-Pierre B, Burlat V, Courdavault V (2011) The subcellular organization of strictosidine biosynthesis in Catharanthus roseus epidermis highlights several trans-tonoplast translocations of intermediate metabolites. FEBS Journal **278:** 749-763

Hadlington JL, Denecke J (2001) Transient expression, a tool to address questions in plant cell biology. *In* C Hawes, B Jeunemaitre, eds, In Plant Cell Biology: A Practical Approach. Oxford University Press, Oxford, UK, pp 107–125

Hagel JM, Yeung EC, Facchini PJ (2008) Got milk? The secret life of laticifers. Trends in Plant Science **13:** 631-639

Hahn MG, Lerner DR, Fitter MS, Norman PM, Lamb CJ (1987) Characterization of monoclonal antibodies to protoplast membranes of Nicotiana tabacum identified by an enzyme-linked immunosorbent assay. Planta **171:** 453-465

Hawes MC, Gunawardena U, Miyasaka S, Zhao X (2000) The role of root border cells in plant defense. Trends in Plant Science **5:** 128-133

Held MA, Tan L, Kamyab A, Hare M, Shpak E, Kieliszewski MJ (2004) Di-isodityrosine is the intermolecular cross-link of isodityrosine-rich extensin analogs cross-linked *in vitro*. Journal of Biological Chemistry **279:** 55474-55482

Hellens R, Edwards EA, Leyland N, Bean S, Mullineaux P (2000) pGreen: a versatile and flexible binary Ti vector for Agrobacterium-mediated plant transformation. Plant Molecular Biology **42:** 819-832

Herman EM, Lamb CJ (1992) Arabinogalactan-rich glycoproteins are localized on the cell-surface and in intravacuolar multivesicular bodies. Plant Physiology **98:** 264-272

Hieta R, Myllyharju J (2002) Cloning and Characterization of a Low Molecular Weight Prolyl 4-Hydroxylase from Arabidopsis thaliana : EFFECTIVE HYDROXYLATION OF PROLINE-RICH, COLLAGEN-LIKE, AND HYPOXIA-INDUCIBLE TRANSCRIPTION FACTOR α-LIKE PEPTIDES. Journal of Biological Chemistry **277:** 23965-23971

Hiraga S, Sasaki K, Ito H, Ohashi Y, Matsui H (2001) A Large Family of Class III Plant Peroxidases. Plant and Cell Physiology **42:** 462-468

Holst Christensen J, Overney S, Rohde A, Ardiles Diaz W, Bauw G, Simon P, Van Montagu M, Boerjan W (2001) The syringaldazine-oxidizing peroxidase PXP 3-4 from poplar xylem: cDNA isolation, characterization and expression. Plant Molecular Biology **47:** 581-593

Hruz T, Laule O, Szabo G, Wessendorp F, Bleuler S, Oertle L, Widmayer P, Gruissem W, Zimmermann P (2008) Genevestigator V3: A Reference Expression Database for the Meta-Analysis of Transcriptomes. Advances in Bioinformatics **2008:** 5

Hruz T, Wyss M, Docquier M, Pfaffl M, Masanetz S, Borghi L, Verbrugghe P, Kalaydjieva L, Bleuler S, Laule O, Descombes P, Gruissem W, Zimmermann P (2011) RefGenes: identification of reliable and condition specific reference genes for RT-qPCR data normalization. BMC Genomics **12:** 156

Hu Y, Qin Y, Zhao J (2006) Localization of an arabinogalactan protein epitope and the effects of Yariv phenylglycoside during zygotic embryo development of Arabidopsis thaliana. Protoplasma **229:** 21-31

Huang GQ, Gong SY, Xu WL, Li W, Li P, Zhang CJ, Li DD, Zheng Y, Li FG, Li XB (2013) A Fasciclin-Like Arabinogalactan Protein, GhFLA1, Is Involved in Fiber Initiation and Elongation of Cotton. Plant Physiology **161:** 1278-1290

Immerzeel P, Eppink MM, de Vries SC, Schols HA, Voragen AGJ (2006) Carrot arabinogalactan proteins are interlinked with pectins. Physiologia Plantarum **128:** 18-28

Jackson PAP, Galinha CIR, Pereira CS, Fortunato A, Soares NC, Amâncio SBQ, Ricardo CPP (2001) Rapid Deposition of Extensin during the Elicitation of Grapevine Callus Cultures Is Specifically Catalyzed by a 40-Kilodalton Peroxidase. Plant Physiology **127:** 1065-1076

Jansen MAK, Elfstrand M, Heggie L, Sitbon F, Dix PJ, Thorneley RNF (2004) Over-expression of phenol-oxidising peroxidases alters the UV-susceptibility of transgenic Nicotiana tabacum. New Phytologist **163:** 585-594

Jauh G, Lord E (1996) Localization of pectins and arabinogalactan-proteins in lily (Lilium longiflorum L.) pollen tube and style, and their possible roles in pollination. Planta **199:** 251-261

Jermyn M, Yeow Y, Woods E (1975) A Class of Lectins Present in the Tissues of Seed Plants. Functional Plant Biology **2:** 501-531

Jermyn MA (1978) Isolation From the Flowers of Dryandra praemorsa of a Flavonol Glycoside That Reacts With β-Lectins. Australian Journal of Plant Physiology **5:** 697-705

Johansson A, Rasmussen S, Harthill J, Welinder K (1992) cDNA, amino acid and carbohydrate sequence of barley seed-specific peroxidase BP 1. Plant Molecular Biology **18:** 1151-1161

Johnson KL, Jones BJ, Bacic A, Schultz CJ (2003) The Fasciclin-Like Arabinogalactan Proteins of Arabidopsis. A Multigene Family of Putative Cell Adhesion Molecules. Plant Physiology **133:** 1911-1925

Johnson KL, Kibble NAJ, Bacic A, Schultz CJ (2011) A Fasciclin-Like Arabinogalactan-Protein (FLA) Mutant of Arabidopsis thaliana, fla1, Shows Defects in Shoot Regeneration. Plos One **6**

Jones MA, Raymond MJ, Smirnoff N (2006) Analysis of the root-hair morphogenesis transcriptome reveals the molecular identity of six genes with roles in root-hair development in Arabidopsis. The Plant Journal **45:** 83-100

Kawamoto T, Noshiro M, Shen M, Nakamasu K, Hashimoto K, Kawashima-Ohya Y, Gotoh O, Kato Y (1998) Structural and phylogenetic analyses of RGD-CAP/βig-h3, a fasciclin-like adhesion protein expressed in chick chondrocytes. Biochimica et Biophysica Acta (BBA) - Gene Structure and Expression **1395:** 288-292

Kawamura Y, Wakabayashi K, Hoson T, Yamamoto R, Kamisaka S (2000) Stress-relaxation Analysis of Submerged and Air-grown Rice Coleoptiles: Correlations with Cell Wall Biosynthesis and Growth. Journal of Plant Physiology **156:** 689-694

Kawano T (2003) Roles of the reactive oxygen species-generating peroxidase reactions in plant defense and growth induction. Plant Cell Reports **21:** 829-837

Keegstra K (2010) Plant Cell Walls. Plant Physiology **154:** 483-486

Kelly J, Jarrell H, Millar L, Tessier L, Fiori LM, Lau PC, Allan B, Szymanski CM (2006) Biosynthesis of the N-Linked Glycan in Campylobacter jejuni and Addition onto Protein through Block Transfer. Journal of Bacteriology **188:** 2427-2434

Keren-Keiserman A, Tanami Z, Shoseyov O, Ginzberg I (2004) Peroxidase activity associated with suberization processes of the muskmelon (Cucumis melo) rind. Physiologia Plantarum **121:** 141-148

Kieliszewski MJ, Kamyab A, Leykam JF, Lamport DTA (1992) A Histidine-Rich Extensin from Zea mays Is an Arabinogalactan Protein. Plant Physiology **99:** 538-547

Kieliszewski MJ, Lamport DTA (1994) Extensin: repetitive motifs, functional sites, post-translational codes, and phylogeny. The Plant Journal **5:** 157-172

Kieliszewski MJ, Shpak E (2001) Synthetic genes for the elucidation of glycosylation codes for arabinogalactan-proteins and other hydroxyproline-rich glycoproteins. Cellular and Molecular Life Sciences **58:** 1386-1398

Kinoshita T, Fujita M, Maeda Y (2008) Biosynthesis, Remodelling and Functions of Mammalian GPI-anchored Proteins: Recent Progress. Journal of Biochemistry **144:** 287-294

Kitazawa K, Tryfona T, Yoshimi Y, Hayashi Y, Kawauchi S, Antonov L, Tanaka H, Takahashi T, Kaneko S, Dupree P, Tsumuraya Y, Kotake T (2013) β-Galactosyl Yariv Reagent Binds to the β-1,3-Galactan of Arabinogalactan Proteins. Plant Physiology **161:** 1117-1126

Kjellbom P, Snogerup L, Stohr C, Reuzeau C, McCabe PF, Pennell RI (1997) Oxidative cross-linking of plasma membrane arabinogalactan proteins. Plant Journal **12:** 1189-1196

Kleeff J, Ishiwata T, Kumbasar A, Friess H, xFc, chler MW, Lander AD, Korc M (1998) The cell-surface heparan sulfate proteoglycan glypican-1 regulates growth factor action in pancreatic carcinoma cells and is overexpressed in human pancreatic cancer. The Journal of Clinical Investigation **102:** 1662-1673

Knox JP (1997) The use of antibodies to study the architecture and developmental regulation of plant cell walls. *In* International Review of Cytology - a Survey of Cell Biology, Vol 171, Vol 171. Academic Press Inc, San Diego, pp 79-120

Knox JP (2008) Revealing the structural and functional diversity of plant cell walls. Current Opinion in Plant Biology **11:** 308-313

Knox JP, Day S, Roberts K (1989) A set of cell surface glycoproteins forms an early marker of cell position, but not cell type, in the root apical meristem of *Daucus carota* L. Development **106:** 47-56

Knox JP, Linstead PJ, Peart J, Cooper C, Roberts K (1991) Developmentally regulated epitopes of cell-surface arabinogalactan proteins and their relation to root-tissue pattern-formation. Plant Journal **1:** 317-326

Kohorn BD (2000) Plasma Membrane-Cell Wall Contacts. Plant Physiology **124:** 31-38

Kreuger M, Holst G-J (1993) Arabinogalactan proteins are essential in somatic embryogenesis of Daucus carota L. Planta **189:** 243-248

Kreuger M, Holst G-J (1995) Arabinogalactan-protein epitopes in somatic embryogenesis of Daucus carota L. Planta **197:** 135-141

Kreuger M, Holst G-J (1996) Arabinogalactan proteins and plant differentiation. Plant Molecular Biology **30:** 1077-1086

Kumari M, Taylor G, Deyholos M (2008) Transcriptomic responses to aluminum stress in roots of Arabidopsis thaliana. Molecular Genetics and Genomics **279:** 339-357

Kwasniewski M, Janiak A, Mueller-Roeber B, Szarejko I (2010) Global analysis of the root hair morphogenesis transcriptome reveals new candidate genes involved in root hair formation in barley. Journal of Plant Physiology **167:** 1076-1083

Lagrimini LM, Gingas V, Finger F, Rothstein S, Liu T (1997) Characterization of Antisense Transformed Plants Deficient in the Tobacco Anionic Peroxidase. Plant Physiology **114:** 1187-1196

Lagrimini* LM, Joly R, Dunlap J, Liu T-T (1997) The consequence of peroxidase overexpression in transgenic plants on root growth and development. Plant Molecular Biology **33:** 887-895

Lalanne E, Honys D, Johnson A, Borner GHH, Lilley KS, Dupree P, Grossniklaus U, Twell D (2004) SETH1 and SETH2, Two Components of the Glycosylphosphatidylinositol Anchor Biosynthetic Pathway, Are Required for Pollen Germination and Tube Growth in Arabidopsis. The Plant Cell Online **16:** 229-240

Lallemand-Breitenbach V, Quesnoit M, Braun V, El Marjou A, Poüs C, Goud B, Perez F (2004) CLIPR-59 Is a Lipid Raft-associated Protein Containing a Cytoskeleton-associated Protein Glycine-rich Domain (CAP-Gly) That Perturbs Microtubule Dynamics. Journal of Biological Chemistry **279:** 41168-41178

Lally D, Ingmire P, Tong H-Y, He Z-H (2001) Antisense Expression of a Cell Wall–Associated Protein Kinase, WAK4, Inhibits Cell Elongation and Alters Morphology. The Plant Cell Online **13:** 1317-1332

Lamport DTA, Kieliszewski MJ (2005) Stress upregulates periplasmic arabinogalactan-proteins. Plant Biosystems **139:** 60-64

Lamport DTA, Kieliszewski MJ, Showalter AM (2006) Salt stress upregulates periplasmic arabinogalactan proteins: using salt stress to analyse AGP function. New Phytologist **169:** 479-492

Lamport DTA, Várnai P (2013) Periplasmic arabinogalactan glycoproteins act as a calcium capacitor that regulates plant growth and development. New Phytologist **197:** 58-64

Langan K, Nothnagel E (1997) Cell surface arabinogalactan-proteins and their relation to cell proliferation and viability. Protoplasma **196:** 87-98

Larkin PJ (1977) Plant protoplast agglutination and membrane-bound beta-lectins. Journal of Cell Science **26:** 31-46

Larkin PJ (1978) Plant protoplast agglutination by artificial carbohydrate antigens. Journal of Cell Science **30:** 283-292

Laus MC, Logman TJ, Lamers GE, Van Brussel AAN, Carlson RW, Kijne JW (2006) A novel polar surface polysaccharide from Rhizobium leguminosarum binds host plant lectin. Molecular Microbiology **59:** 1704-1713

Lease K, Ingham E, Walker JC (1998) Challenges in understanding RLK function. Current Opinion in Plant Biology **1:** 388-392

Lee KJD, Sakata Y, Mau S-L, Pettolino F, Bacic A, Quatrano RS, Knight CD, Knox JP (2005) Arabinogalactan Proteins Are Required for Apical Cell Extension in the Moss Physcomitrella patens. The Plant Cell Online **17:** 3051-3065

Lefebvre B, Furt F, Hartmann M-A, Michaelson LV, Carde J-P, Sargueil-Boiron F, Rossignol M, Napier JA, Cullimore J, Bessoule J-J, Mongrand S (2007) Characterization of Lipid Rafts from Medicago truncatula Root Plasma Membranes: A Proteomic Study Reveals the Presence of a Raft-Associated Redox System. Plant Physiology **144:** 402-418

Leidich SD, Kostova Z, Latek RR, Costello LC, Drapp DA, Gray W, Fassler JS, Orlean P (1995) Temperature-sensitive Yeast GPI Anchoring Mutants gpi2 and gpi3 Are Defective in the Synthesis of N-Acetylglucosaminyl Phosphatidylinositol.: CLONING OF THE GPI2 GENE. Journal of Biological Chemistry **270:** 13029-13035

Levitin B, Richter D, Markovich I, Zik M (2008) Arabinogalactan proteins 6 and 11 are required for stamen and pollen function in Arabidopsis. The Plant Journal **56:** 351-363

Li Y-Q, Faleri C, Geitmann A, Zhang H-Q, Cresti M (1995) Immunogold localization of arabinogalactan proteins, unesterified and esterified pectins in pollen grains and pollen tubes ofNicotiana tabacum L. Protoplasma **189:** 26-36

Li Y, Beisson F, Ohlrogge J, Pollard M (2007) Monoacylglycerols Are Components of Root Waxes and Can Be Produced in the Aerial Cuticle by Ectopic Expression of a Suberin-Associated Acyltransferase. Plant Physiology **144:** 1267-1277

Li Y, Liu D, Tu L, Zhang X, Wang L, Zhu L, Tan J, Deng F (2010) Suppression of GhAGP4 gene expression repressed the initiation and elongation of cotton fiber. Plant Cell Reports **29:** 193-202

Lim PO, Kim HJ, Gil Nam H (2007) Leaf Senescence. Annual Review of Plant Biology **58:** 115-136

Lind JL, Bacic A, Clarke AE, Anderson MA (1994) A style-specific hydroxyproline-rich glycoprotein with properties of both extensins and arabinogalactan proteins. The Plant Journal **6:** 491-502

Lind JL, Bonig I, Clarke AE, Anderson MA (1996) A style-specific 120-kDa glycoprotein enters pollen tubes of Nicotiana alata in vivo. Sexual plant reproduction **9:** 75-86

Liszkay A, Kenk B, Schopfer P (2003) Evidence for the involvement of cell wall peroxidase in the generation of hydroxyl radicals mediating extension growth. Planta **217:** 658-667

López-Serrano M, Fernández MD, Pomar F, Pedreño MA, Ros Barceló A (2004) Zinnia elegans uses the same peroxidase isoenzyme complement for cell wall lignification in both single-cell tracheary elements and xylem vessels. Journal of Experimental Botany **55:** 423-431

Ma H, Zhao J (2010) Genome-wide identification, classification, and expression analysis of the arabinogalactan protein gene family in rice (Oryza sativa L.). Journal of Experimental Botany **61:** 2647-2668

MacAdam J, Grabber J (2002) Relationship of growth cessation with the formation of diferulate cross-links and p-coumaroylated lignins in tall fescue leaf blades. Planta **215:** 785-793

Magliano TMA, Casal JJ (1998) In vitro cross-linking of extensin precursors by mustard extracellular isoforms of peroxidase that respond either to phytochrome or to wounding. Journal of Experimental Botany **49:** 1491-1499

Mahendran T, Williams PA, Phillips GO, Al-Assaf S, Baldwin TC (2008) New Insights into the Structural Characteristics of the Arabinogalactan−Protein

(AGP) Fraction of Gum Arabic. Journal of Agricultural and Food Chemistry **56:** 9269-9276

Mahroug S, Burlat V, St-Pierre B (2007) Cellular and sub-cellular organisation of the monoterpenoid indole alkaloid pathway in Catharanthus roseus. Phytochemistry Reviews **6:** 363-381

Majewska-Sawka A, Nothnagel EA (2000) The multiple roles of arabinogalactan proteins in plant development. Plant Physiology **122:** 3-9

Malainine ME (2007) An arabinogalactan protein having the property of absorbing fats and method for obtaining this arabinogalactan protein. *In* WIP Organization, ed, Vol WO/2007/100236 (A2)

Mathé C, Barre A, Jourda C, Dunand C (2010) Evolution and expression of class III peroxidases. Archives of Biochemistry and Biophysics **500:** 58-65

Matile P, Hörtensteiner S, Thomas H (1999) CHLOROPHYLL DEGRADATION. Annual Review of Plant Physiology and Plant Molecular Biology **50:** 67-95

Matsui T, Tabayashi A, Iwano M, Shinmyo A, Kato K, Nakayama H (2011) Activity of the C-terminal-Dependent Vacuolar Sorting Signal of Horseradish Peroxidase C1a is Enhanced by its Secondary Structure. Plant and Cell Physiology **52:** 413-420

Matthysse A, Kijne J (1998) Attachment of Rhizobiaceae to Plant Cells. *In* H Spaink, A Kondorosi, PJ Hooykaas, eds, The Rhizobiaceae. Springer Netherlands, pp 235-249

Mau S-L, Chen C-G, Pu Z-Y, Moritz RL, Simpson RJ, Bacic A, Clarke AE (1995) Molecular cloning of cDNAs encoding the protein backbones of arabinogalactan-proteins from the filtrate of suspension-cultured cells of Pyrus communis and Nicotiana alata. The Plant Journal **8:** 269-281

McCabe PF, Valentine TA, Forsberg LS, Pennell RI (1997) Soluble Signals from Cells Identified at the Cell Wall Establish a Developmental Pathway in Carrot. The Plant Cell Online **9:** 2225-2241

Mersey BG, Cutler AJ (1986) Differential distribution of specific indole alkaloids in leaves of Catharanthus roseus Canadian Journal of Botany-Revue Canadienne De Botanique **64:** 1039-1045

Mika A, Minibayeva F, Beckett R, Lüthje S (2004) Possible functions of extracellular peroxidases in stress-induced generation and detoxification of active oxygen species. Phytochemistry Reviews **3:** 173-193

Moller I, Marcus S, Haeger A, Verhertbruggen Y, Verhoef R, Schols H, Ulvskov P, Mikkelsen J, Knox JP, Willats W (2008) High-throughput screening of monoclonal antibodies against plant cell wall glycans by hierarchical clustering of their carbohydrate microarray binding profiles. Glycoconjugate Journal **25:** 37-48

Mollet J-C, Kim S, Jauh G-Y, Lord EM (2002) Arabinogalactan proteins, pollen tube growth, and the reversible effects of Yariv phenylglycoside. Protoplasma **219:** 89-98

Mongrand S, Morel J, Laroche J, Claverol S, Carde JP, Hartmann MA, Bonneu M, Simon-Plas F, Lessire R, Bessoule JJ (2004) Lipid rafts in higher plant cells: Purification and characterization of triton X-100-insoluble microdomains from tobacco plasma membrane. Journal of Biological Chemistry **279:** 36277-36286

Monshausen GB, Bibikova TN, Messerli MA, Shi C, Gilroy S (2007) Oscillations in extracellular pH and reactive oxygen species modulate tip growth of Arabidopsis root hairs. Proceedings of the National Academy of Sciences **104:** 20996-21001

Morita Y, Mikami B, Yamashita H, Lee JY, Aibara S, Sato M, Katsube Y, Tanaka N (1991) Primary and crystal structure of horseradish peroxidase isozyme E5. *In* J Lobarzewski, H Greppin, C Penel, T Gaspar, eds, Biochemical, molecular and physiological aspects of plant peroxidases. University of Geneva, Geneva

Motose H, Fukuda H, Sugiyama M (2001) Involvement of local intercellular communication in the differentiation of zinnia mesophyll cells into tracheary elements. Planta **213:** 121-131

Motose H, Sugiyama M, Fukuda H (2001) An Arabinogalactan Protein(s) is a Key Component of a Fraction that Mediates Local Intercellular Communication Involved in Tracheary Element Differentiation of Zinnia Mesophyll Cells. Plant and Cell Physiology **42:** 129-137

Motose H, Sugiyama M, Fukuda H (2004) A proteoglycan mediates inductive interaction during plant vascular development. Nature **429:** 873-878

Munnik T, Irvine RF, Musgrave A (1998) Phospholipid signalling in plants. Biochimica et Biophysica Acta (BBA) - Lipids and Lipid Metabolism **1389:** 222-272

Neill S, Desikan R, Hancock J (2002) Hydrogen peroxide signalling. Current Opinion in Plant Biology **5:** 388-395

Nguema-Ona E, Andème-Onzighi C, Aboughe-Angone S, Bardor M, Ishii T, Lerouge P, Driouich A (2006) The reb1-1 Mutation of Arabidopsis. Effect on the Structure and Localization of Galactose-Containing Cell Wall Polysaccharides. Plant Physiology **140:** 1406-1417

Nguema-Ona E, Bannigan A, Chevalier L, Baskin TI, Driouich A (2007) Disruption of arabinogalactan proteins disorganizes cortical microtubules in the root of *Arabidopsis thaliana*. Plant Journal **52:** 240-251

Nguema-Ona E, Coimbra S, Vicre-Gibouin M, Mollet JC, Driouich A (2012) Arabinogalactan proteins in root and pollen-tube cells: distribution and functional aspects. Annals of Botany **110:** 383-404

Nguema-Ona E, Vicré-Gibouin M, Cannesan M-A, Driouich A (2013) Arabinogalactan proteins in root–microbe interactions. Trends in Plant Science **18:** 440-449

Nielsen KL, Indiani C, Henriksen A, Feis A, Becucci M, Gajhede M, Smulevich G, Welinder KG (2001) Differential Activity and Structure of Highly Similar Peroxidases. Spectroscopic, Crystallographic, and Enzymatic Analyses of Lignifying Arabidopsis thaliana Peroxidase A2 and Horseradish Peroxidase A2†,‡. Biochemistry **40:** 11013-11021

Norman PM, Wingate VPM, Fitter MS, Lamb CJ (1986) Monoclonal antibodies to plant plasma-membrane antigens. Planta **167:** 452-459

Normanly J (1997) Auxin metabolism. Physiologia Plantarum **100:** 431-442

Nosáľová G, Prisenžňáková L, Paulovičová E, Capek P, Matulová M, Navarini L, Liverani FS (2011) Antitussive and immunomodulating activities of instant coffee arabinogalactan-protein. International Journal of Biological Macromolecules **49:** 493-497

Nothnagel EA (1997) Proteoglycans and Related Components in Plant Cells. *In* WJ Kwang, ed, International Review of Cytology, Vol Volume 174. Academic Press, pp 195-291

Nothnagel EA, Lyon JL (1986) Structural Requirements for the Binding of Phenylglycosides to the Surface of Protoplasts. Plant Physiology **80:** 91-98

Oka T, Saito F, Shimma Y-i, Yoko-o T, Nomura Y, Matsuoka K, Jigami Y (2010) Characterization of Endoplasmic Reticulum-Localized UDP-d-Galactose: Hydroxyproline O-Galactosyltransferase Using Synthetic Peptide Substrates in Arabidopsis. Plant Physiology **152:** 332-340

Orlean P, Menon AK (2007) Thematic review series: Lipid Posttranslational Modifications. GPI anchoring of protein in yeast and mammalian cells, or: how we learned to stop worrying and love glycophospholipids. Journal of Lipid Research **48:** 993-1011

Orozco-Cardenas M, Ryan CA (1999) Hydrogen peroxide is generated systemically in plant leaves by wounding and systemin via the octadecanoid pathway.

Proceedings of the National Academy of Sciences of the United States of America **96:** 6553-6557

Østergaard L, Teilum K, Mirza O, Mattsson O, Petersen M, Welinder K, Mundy J, Gajhede M, Henriksen A (2000) Arabidopsis ATP A2 peroxidase. Expression and high-resolution structure of a plant peroxidase with implications for lignification. Plant Molecular Biology **44:** 231-243

Overvoorde P, Fukaki H, Beeckman T (2010) Auxin Control of Root Development. Cold Spring Harbor Perspectives in Biology **2**

Oxley D, Bacic A (1999) Structure of the glycosylphosphatidylinositol anchor of an arabinogalactan protein from *Pyrus communis* suspension-cultured cells. Proceedings of the National Academy of Sciences of the United States of America **96:** 14246-14251

Ozaki S, Kitamura S (2005) Novel arabinogalactan, substance with antidiabetic activity and method of use thereof. *In* WIPOPNW (A1), ed,

Ozolina N, Nesterkina I, Kolesnikova E, Salyaev R, Nurminsky V, Rakevich A, Martynovich E, Chernyshov M (2013) Tonoplast of Beta vulgaris L. contains detergent-resistant membrane microdomains. Planta **237:** 859-871

Paquette SM, Bak S, Feyereisen R (2000) Intron-exon organization and phylogeny in a large superfamily, the paralogous cytochrome P450 genes of Arabidopsis thaliana. DNA and cell biology **19:** 307-317

Paredez AR, Somerville CR, Ehrhardt DW (2006) Visualization of Cellulose Synthase Demonstrates Functional Association with Microtubules. Science **312:** 1491-1495

Park MH, Suzuki Y, Chono M, Knox JP, Yamaguchi I (2003) CsAGP1, a Gibberellin-Responsive Gene from Cucumber Hypocotyls, Encodes a Classical Arabinogalactan Protein and Is Involved in Stem Elongation. Plant Physiology **131:** 1450-1459

Passardi F, Cosio C, Penel C, Dunand C (2005) Peroxidases have more functions than a Swiss army knife. Plant Cell Reports **24:** 255-265

Passardi F, Longet D, Penel C, Dunand C (2004) The class III peroxidase multigenic in land plants family in rice and its evolution. Phytochemistry **65:** 1879-1893

Passardi F, Penel C, Dunand C (2004) Performing the paradoxical: how plant peroxidases modify the cell wall. Trends in Plant Science **9:** 534-540

Passardi F, Tognolli M, De Meyer M, Penel C, Dunand C (2006) Two cell wall associated peroxidases from Arabidopsis influence root elongation. Planta **223:** 965-974

Pattathil S, Avci U, Baldwin D, Swennes AG, McGill JA, Popper Z, Bootten T, Albert A, Davis RH, Chennareddy C, Dong R, O'Shea B, Rossi R, Leoff C, Freshour G, Narra R, O'Neil M, York WS, Hahn MG (2010) A Comprehensive Toolkit of Plant Cell Wall Glycan-Directed Monoclonal Antibodies. Plant Physiology **153:** 514-525

Paul KG (1986) Peroxidases: historical background. *In* H Greppin, C Penel, T Gaspar, eds, Molecular and Physiological Aspects of Plant Peroxidases. University of Geneva, Geneva

Paulick MG, Bertozzi CR (2008) The Glycosylphosphatidylinositol Anchor: A Complex Membrane-Anchoring Structure for Proteins†. Biochemistry **47:** 6991-7000

Pedreira J, Herrera MT, Zarra I, Revilla G (2011) The overexpression of AtPrx37, an apoplastic peroxidase, reduces growth in Arabidopsis. Physiologia Plantarum **141:** 177-187

Pei Z-M, Murata Y, Benning G, Thomine S, Klusener B, Allen GJ, Grill E, Schroeder JI (2000) Calcium channels activated by hydrogen peroxide mediate abscisic acid signalling in guard cells. Nature **406:** 731-734

Peles E, Nativ M, Lustig M, Grumet M, Schilling J, Martinez R, Plowman GD, Schlessinger J (1997) Identification of a novel contactin-associated

transmembrane receptor with multiple domains implicated in protein-protein interactions. EMBO J **16:** 978-988

Pennell RI, Janniche L, Kjellbom P, Scofield GN, Peart JM, Roberts K (1991) Developmental Regulation of a Plasma Membrane Arabinogalactan Protein Epitope in Oilseed Rape Flowers. The Plant Cell Online **3:** 1317-1326

Pennell RI, Knox JP, Scofield GN, Selvendran RR, Roberts K (1989) A family of abundant plasma-membrane associated glycoproteins related to the arabinogalactan proteins is unique to flowering plants. Journal of Cell Biology **108:** 1967-1977

Pennell RI, Roberts K (1990) Sexual development in the pea is presaged by altered expression of arabinogalactan protein. Nature **344:** 547-549

Pereira C, Pereira S, Satiat-Jeunemaitre B, Pissarra J (2013) Cardosin A contains two vacuolar sorting signals using different vacuolar routes in tobacco epidermal cells. The Plant Journal **76:** 87-100

Pereira L, Coimbra S, Oliveira H, Monteiro L, Sottomayor M (2006) Expression of arabinogalactan protein genes in pollen tubes of Arabidopsis thaliana. Planta **223:** 374-380

Pilarska M, Knox JP, Konieczny R (2013) Arabinogalactan-protein and pectin epitopes in relation to an extracellular matrix surface network and somatic embryogenesis and callogenesis in Trifolium nigrescens Viv. Plant Cell, Tissue and Organ Culture (PCTOC)**:** 1-10

Pintus F, Mura A, Bellelli A, Arcovito A, Spanò D, Pintus A, Floris G, Medda R (2008) Allosteric modulation of Euphorbia peroxidase by nickel ions. FEBS Journal **275:** 1201-1212

Poon S, Heath RL, Clarke AE (2012) A Chimeric Arabinogalactan Protein Promotes Somatic Embryogenesis in Cotton Cell Culture. Plant Physiology **160:** 684-695

Potters G, Pasternak TP, Guisez Y, Jansen MAK (2009) Different stresses, similar morphogenic responses: integrating a plethora of pathways. Plant, Cell & Environment **32:** 158-169

Pourcel L, Routaboul J-M, Cheynier V, Lepiniec L, Debeaujon I (2007) Flavonoid oxidation in plants: from biochemical properties to physiological functions. Trends in Plant Science **12:** 29-36

Price NJ, Pinheiro C, Soares CM, Ashford DA, Ricardo CP, Jackson PA (2003) A biochemical and molecular characterization of LEP1, an extensin peroxidase from lupin. Journal of Biological Chemistry **278:** 41389-41399

Putoczki T, Pettolino F, Griffin MW, Möller R, Gerrard J, Bacic A, Jackson S (2007) Characterization of the structure, expression and function of Pinus radiata D. Don arabinogalactan-proteins. Planta **226:** 1131-1142

Qi W, Fong C, Lamport DTA (1991) Gum Arabic Glycoprotein Is a Twisted Hairy Rope: A New Model Based on O-Galactosylhydroxyproline as the Polysaccharide Attachment Site. Plant Physiology **96:** 848-855

Qin Y, Chen D, Zhao J (2007) Localization of arabinogalactan proteins in anther, pollen, and pollen tube of Nicotiana tabacum L. Protoplasma **231:** 43-53

Qin Y, Zhao J (2006) Localization of arabinogalactan proteins in egg cells, zygotes, and two-celled proembryos and effects of β-D-glucosyl Yariv reagent on egg cell fertilization and zygote division in Nicotiana tabacum L. Journal of Experimental Botany **57:** 2061-2074

Qu Y, Egelund J, Gilson P, Houghton F, Gleeson P, Schultz C, Bacic A (2008) Identification of a novel group of putative Arabidopsis thaliana β-(1,3)-galactosyltransferases. Plant Molecular Biology **68:** 43-59

Quiroga M, Guerrero C, Botella MA, Barceló A, Amaya I, Medina Mal, Alonso FJ, de Forchetti SM, Tigier H, Valpuesta V (2000) A Tomato Peroxidase Involved in the Synthesis of Lignin and Suberin. Plant Physiology **122:** 1119-1128

Ralph J, Bunzel M, Marita J, Hatfield R, Lu F, Kim H, Schatz P, Grabber J, Steinhart H (2004) Peroxidase-dependent cross-linking reactions of p-hydroxycinnamates in plant cell walls. Phytochemistry Reviews **3:** 79-96

Ralph J, Bunzel M, Marita JM, Hatfield RD, Lu F, Kim H, Schatz PF, Grabber JH, Steinhart H (2004) Peroxidase-dependent cross-linking reactions of p-hydroxycinnamates in plant cell walls. Phytochemistry Reviews **3:** 79-96

Rasmussen CB, Hiner ANP, Smith AT, Welinder KG (1998) Effect of Calcium, Other Ions, and pH on the Reactions of Barley Peroxidase with Hydrogen Peroxide and Fluoride: CONTROL OF ACTIVITY THROUGH CONFORMATIONAL CHANGE. Journal of Biological Chemistry **273:** 2232-2240

Reigh D, Smith EC (1977) Effect of indole-3-acetic acid on the kinetics of horseradish peroxidase catalyzed scopoletin oxidation. Experientia **33:** 1451-1452

Renard D, Lavenant-Gourgeon L, Ralet M-C, Sanchez C (2006) Acacia senegal Gum: Continuum of Molecular Species Differing by Their Protein to Sugar Ratio, Molecular Weight, and Charges. Biomacromolecules **7:** 2637-2649

Resta R, Yamashita Y, Thompson LF (1998) Ecto-enzyme and signaling functions of lymphocyte CD73. Immunological reviews **161:** 95-109

Robert S, Zouhar J, Carter C, Raikhel N (2007) Isolation of intact vacuoles from Arabidopsis rosette leaf-derived protoplasts. Nat. Protocols **2:** 259-262

Ros Barceló A (2000) Peroxidase and H_2O_2 production by plant cells: truth and clues. Current Topics in Phytochemistry **3:** 197-202

Ros Barceló A, Ferrer MA, García-Florenciano E, Muñoz R (1991) The tonoplast localization of two basic isoperoxidases of high pI in Lupinus. Botanica Acta **104:** 272-278

Ros Barceló A, Gómez Ros LV, Gabaldón C, López-Serrano M, Pomar F, Carrión JS, Pedreño MA (2004) Basic peroxidases: The gateway for lignin evolution? Phytochemistry Reviews **3:** 61-78

Ros Barceló A, Muñoz R (2000) Metabolic plasticity of plant peroxidases. *In* In: Hemantaranjan A (ed) Advances in Plant Physiology, Vol 3. Scientific Publishers (India), Jodhpur, pp 71-92

Rosti V (2000) The molecular basis of paroxysmal nocturnal hemoglobinuria. Haematologica **85:** 82-87

Roy SJ, Holdaway-Clarke TL, Hackett GR, Kunkel JG, Lord EM, Hepler PK (1999) Uncoupling secretion and tip growth in lily pollen tubes: evidence for the role of calcium in exocytosis. The Plant Journal **19:** 379-386

Rumyantseva NI (2005) Arabinogalactan proteins: Involvement in plant growth and morphogenesis. Biochemistry-Moscow **70:** 1073-1085

Saare-Surminski K, Preil W, Knox JP, Lieberei R (2000) Arabinogalactan proteins in embryogenic and non-embryogenic callus cultures of *Euphorbia pulcherrima*. Physiologia Plantarum **108:** 180-187

Šamaj J, Baluška F, Bobák M, Volkmann D (1999) Extracellular matrix surface network of embryogenic units of friable maize callus contains arabinogalactan-proteins recognized by monoclonal antibody JIM4. Plant Cell Reports **18:** 369-374

Samaj J, Baluska F, Volkmann D (1998) Cell-specific expression of two arabinogalactan protein epitopes recognized by monoclonal antibodies JIM8 and JIM13 in maize roots. Protoplasma **204:** 1-12

Šamaj J, Braun M, Baluška F, Ensikat H-J, Tsumuraya Y, Volkmann D (1999) Specific Localization of Arabinogalactan-Protein Epitopes at the Surface of Maize Root Hairs. Plant and Cell Physiology **40:** 874-883

Šamaj J, Salaj T, Matúšová R, Salaj J, Takáč T, Šamajová Og, Volkmann D (2008) Arabinogalactan-protein epitope Gal4 is differentially regulated and localized in cell lines of hybrid fir (Abies alba × Abies cephalonica) with different embryogenic and regeneration potential. Plant Cell Reports **27:** 221-229

Samaj J, Samajova O, Peters M, Baluska F, Lichtscheidl I, Knox JP, Volkmann D (2000) Immunolocalization of LM2 arabinogalactan protein epitope associated with endomembranes of plant cells. Protoplasma **212:** 186-196

Sánchez-Fernández Ro, Davies TGE, Coleman JOD, Rea PA (2001) The Arabidopsis thaliana ABC Protein Superfamily, a Complete Inventory. Journal of Biological Chemistry **276:** 30231-30244

Sanchez C, Schmitt C, Kolodziejczyk E, Lapp A, Gaillard C, Renard D (2008) The Acacia Gum Arabinogalactan Fraction Is a Thin Oblate Ellipsoid: A New Model Based on Small-Angle Neutron Scattering and Ab Initio Calculation. Biophysical Journal **94:** 629-639

Sanchez M, Pena MJ, Revilla G, Zarra I (1996) Changes in Dehydrodiferulic Acids and Peroxidase Activity against Ferulic Acid Associated with Cell Walls during Growth of Pinus pinaster Hypocotyl. Plant Physiology **111:** 941-946

Sang S, Yang C, Ho C-T (2004) Peroxidase-mediated oxidation of catechins. Phytochemistry Reviews **3:** 229-241

Sardar HS, Showalter AM (2007) A cellular networking model involving interactions among glycosyl-phosphatidylinositol (GPI)-anchored plasma membrane arabinogalactan proteins (AGPs), microtubules and F-actin in tobacco BY-2 cells. Plant Signaling & Behavior **2:** 8-9

Sardar HS, Yang J, Showalter AM (2006) Molecular interactions of arabinogalactan proteins with cortical microtubules and F-actin in bright yellow-2 tobacco cultured cells. Plant Physiology **142:** 1469-1479

Schindler T, Bergfeld R, Schopfer P (1995) Arabinogalactan proteins in maize coleoptiles: developmental relationship to cell death during xylem differentiation but not to extension growth†. The Plant Journal **7:** 25-36

Schloß P, Walter C, Mäder M (1987) Basic peroxidases in isolated vacuoles of nicotiana tabacum L. Planta **170:** 225-229

Schnabelrauch LS, Kieliszewski M, Upham BL, Alizedeh H, Lamport DTA (1996) Isolation of pl 4.6 extensin peroxidase from tomato cell suspension cultures and identification of Val—Tyr—Lys as putative intermolecular cross-link site. The Plant Journal **9:** 477-489

Schnell J, Han S, Miki B, Johnson D (2010) Soybean peroxidase propeptides are functional signal peptides and increase the yield of a foreign protein. Plant Cell Reports **29:** 987-996

Schultz C, Gilson P, Oxley D, Youl J, Bacic A (1998) GPI-anchors on arabinogalactan-proteins: implications for signalling in plants. Trends in Plant Science **3:** 426-431

Schultz C, Harrison M (2008) Novel plant and fungal AGP-like proteins in the Medicago truncatula–Glomus intraradices arbuscular mycorrhizal symbiosis. Mycorrhiza **18:** 403-412

Schultz C, Hauser K, Lind J, Atkinson A, Pu Z-y, Anderson M, Clarke A (1997) Molecular characterisation of a cDNA sequence encoding the backbone of a style-specific 120 kDa glycoprotein which has features of both extensins and arabinogalactan proteins. Plant Molecular Biology **35:** 833-845

Schultz CJ, Johnson KL, Currie G, Bacic A (2000) The Classical Arabinogalactan Protein Gene Family of Arabidopsis. The Plant Cell Online **12:** 1751-1767

Schultz CJ, Rumsewicz MP, Johnson KL, Jones BJ, Gaspar YM, Bacic A (2002) Using Genomic Resources to Guide Research Directions. The Arabinogalactan Protein Gene Family as a Test Case. Plant Physiology **129:** 1448-1463

Scott Gens J, Fujiki M, Pickard B (2000) Arabinogalactan protein and wall-associated kinase in a plasmalemmal reticulum with specialized vertices. Protoplasma **212:** 115-134

Seifert GJ, Roberts K (2007) The biology of arabinogalactan proteins. Annual Review of Plant Biology **58:** 137-161

Serpe M, Nothnagel E (1994) Effects of Yariv phenylglycosides onRosa cell suspensions: Evidence for the involvement of arabinogalactan-proteins in cell proliferation. Planta **193:** 542-550

Serpe MD, Muir AJ, Driouich A (2002) Immunolocalization of beta-D-glucans, pectins, and arabinogalactan-proteins during intrusive growth and elongation of nonarticulated laticifers in *Asclepias speciosa* Torr. Planta **215:** 357-370

Serpe MD, Muir AJ, Keidel AM (2001) Localization of cell wall polysaccharides in nonarticulated laticifers of *Asclepias speciosa* Torr. Protoplasma **216:** 215-226

Shi H, Kim Y, Guo Y, Stevenson B, Zhu J-K (2003) The Arabidopsis SOS5 Locus Encodes a Putative Cell Surface Adhesion Protein and Is Required for Normal Cell Expansion. The Plant Cell Online **15:** 19-32

Shibaya T, Sugawara Y (2009) Induction of multinucleation by β-glucosyl Yariv reagent in regenerated cells from Marchantia polymorpha protoplasts and involvement of arabinogalactan proteins in cell plate formation. Planta **230:** 581-588

Shimizu M, Igasaki T, Yamada M, Yuasa K, Hasegawa J, Kato T, Tsukagoshi H, Nakamura K, Fukuda H, Matsuoka K (2005) Experimental determination of proline hydroxylation and hydroxyproline arabinogalactosylation motifs in secretory proteins. The Plant Journal **42:** 877-889

Showalter AM (2001) Arabinogalactan-proteins: structure, expression and function. Cellular and Molecular Life Sciences **58:** 1399-1417

Showalter AM, Keppler B, Lichtenberg J, Gu D, Welch LR (2010) A Bioinformatics Approach to the Identification, Classification, and Analysis of Hydroxyproline-Rich Glycoproteins. Plant Physiology **153:** 485-513

Shpak E, Barbar E, Leykam JF, Kieliszewski MJ (2001) Contiguous Hydroxyproline Residues Direct Hydroxyproline Arabinosylation in Nicotiana tabacum. Journal of Biological Chemistry **276:** 11272-11278

Shpak E, Leykam JF, Kieliszewski MJ (1999) Synthetic genes for glycoprotein design and the elucidation of hydroxyproline-O-glycosylation codes. Proceedings of the National Academy of Sciences of the United States of America **96:** 14736-14741

Simons K, Toomre D (2000) Lipid rafts and signal transduction. Nat Rev Mol Cell Biol **1:** 31-39

Smallwood M, Yates EA, Willats WGT, Martin H, Knox JP (1996) Immunochemical comparison of membrane-associated and secreted arabinogalactan-proteins in rice and carrot. Planta **198:** 452-459

Sommer-Knudsen J, Clarke AE, Bacic A (1996) A galactose-rich, cell-wall glycoprotein from styles of Nicotiana alata. The Plant Journal **9:** 71-83

Sommer-Knudsen J, Clarke AE, Bacic A (1997) Proline- and hydroxyproline-rich gene products in the sexual tissues of flowers. Sexual Plant Reproduction **10:** 253-260

Sottomayor M (1998) Synthesis of α–3',4'-anhydrovinblastine in *Catharanthus roseus* (L.) G. Don. Universidade do Porto, Faculdade de Ciências

Sottomayor M, Barceló AR (2003) How to address the function of a member of a prolific gene family encoding a multifunctional enzyme? The case of a *Catharanthus roseus* class III peroxidase involved in alkaloid biosynthesis. *In* Proceedings of the Xii International Confress on Genes, Gene Families, and Isozymes. Medimond Publishing Co, Bologna, pp 217-221

Sottomayor M, De Pinto MC, Salema R, DiCosmo F, Pedreño MA, Ros Barcelo A (1996) The vacuolar localization of a basic peroxidase isoenzyme responsible for the synthesis of α-3',4'-anhydrovinblastine in *Catharanthus roseus* (L.) G. Don leaves. Plant Cell Environm. **19:** 761-767

Sottomayor M, Duarte P, Figueiredo R, Barceló AR (2008) A vacuolar class III peroxidase and the metabolism of anticancer indole aklaloids in

Catharanthus roseus: Can peroxidases, secondary metabolites and arabinogalactan proteins be partners in microcompartmentation of cellular reactions? Plant Signaling & Behavior **3:** 899-901

Sottomayor M, Lopes Cardoso I, Pereira LG, Ros Barceló A (2004) Peroxidase and the biosynthesis of terpenoid indole alkaloids in the medicinal plant Catharanthus roseus (L.) G. Don. Phytochemistry Reviews **3:** 159-171

Sottomayor M, Lopez-Serrano M, DiCosmo F, Ros Barceló A (1998) Purification and characterization of alpha-3',4'-anhydrovinblastine synthase (peroxidase-like) from *Catharanthus roseus* (L.) G. Don. FEBS Lett **428:** 299-303

Sottomayor M, Ros Barceló A (2004) Plant peroxidases and phytochemistry, Ed M Sottomayor
A Ros Barceló. Springer Netherlands

Sparkes IA, Runions J, Kearns A, Hawes C (2006) Rapid, transient expression of fluorescent fusion proteins in tobacco plants and generation of stably transformed plants. Nat. Protocols **1:** 2019-2025

Srivastava OP, Van Huystee RB (1977) Iaa oxidase and polyphenol oxidase activities of peanut peroxidase isozymes. Phytochemistry **16:** 1527-1530

St-Pierre B, Vazquez-Flota FA, De Luca V (1999) Multicellular compartmentation of *Catharanthus roseus* alkaloid biosynthesis predicts intercellular translocation of a pathway intermediate. Plant Cell **11:** 887-900

Stacey N, Roberts K, Knox JP (1990) Patterns of expression of the JIM4 arabinogalactan-protein epitope in cell cultures and during somatic embryogenesis in Daucus carota L. Planta **180:** 285-292

Stacey NJ, Roberts K, Carpita NC, Wells B, McCann MC (1995) Dynamic changes in cell surface molecules are very early events in the differentiation of mesophyll cells from Zinnia elegans into tracheary elements. The Plant Journal **8:** 891-906

Steffan W, Kovácč P, Albersheim P, Darvill AG, Hahn MG (1995) Characterization of a monoclonal antibody that recognizes an arabinosylated (1 → 6)-β-d-galactan epitope in plant complex carbohydrates. Carbohydrate Research **275:** 295-307

Strasser R, Bondili JS, Vavra U, Schoberer J, Svoboda B, Glössl J, Léonard R, Stadlmann J, Altmann F, Steinkellner H, Mach L (2007) A Unique β1,3-Galactosyltransferase Is Indispensable for the Biosynthesis of N-Glycans Containing Lewis a Structures in Arabidopsis thaliana. The Plant Cell Online **19:** 2278-2292

Sun W, Kieliszewski MJ, Showalter AM (2004) Overexpression of tomato LeAGP-1 arabinogalactan-protein promotes lateral branching and hampers reproductive development. The Plant Journal **40:** 870-881

Suzuki Y, Kitagawa M, Knox JP, Yamaguchi I (2002) A role for arabinogalactan proteins in gibberellin-induced α-amylase production in barley aleurone cells. The Plant Journal **29:** 733-741

Svetek J, Yadav MP, Nothnagel EA (1999) Presence of a Glycosylphosphatidylinositol Lipid Anchor on Rose Arabinogalactan Proteins. Journal of Biological Chemistry **274:** 14724-14733

Takahama U (2004) Oxidation of vacuolar and apoplastic phenolic substrates by peroxidase: Physiological significance of the oxidation reactions. Phytochemistry Reviews **3:** 207-219

Takeda S, Gapper C, Kaya H, Bell E, Kuchitsu K, Dolan L (2008) Local Positive Feedback Regulation Determines Cell Shape in Root Hair Cells. Science **319:** 1241-1244

Tams JW, Welinder KG (1998) Glycosylation and thermodynamic versus kinetic stability of horseradish peroxidase. FEBS Letters **421:** 234-236

Tamura K, Shimada T, Ono E, Tanaka Y, Nagatani A, Higashi S-i, Watanabe M, Nishimura M, Hara-Nishimura I (2003) Why green fluorescent fusion proteins

have not been observed in the vacuoles of higher plants. The Plant Journal **35:** 545-555

Tan L, Eberhard S, Pattathil S, Warder C, Glushka J, Yuan C, Hao Z, Zhu X, Avci U, Miller JS, Baldwin D, Pham C, Orlando R, Darvill A, Hahn MG, Kieliszewski MJ, Mohnen D (2013) An Arabidopsis Cell Wall Proteoglycan Consists of Pectin and Arabinoxylan Covalently Linked to an Arabinogalactan Protein. The Plant Cell Online

Tan L, Qiu F, Lamport DTA, Kieliszewski MJ (2004) Structure of a hydroxyproline (Hyp)-arabinogalactan polysaccharide from repetitive Ala-Hyp expressed in transgenic Nicotiana tabacum. Journal of Biological Chemistry **279:** 13156-13165

Thom M, Maretzki A, Komor E (1982) Vacuoles from Sugarcane Suspension Cultures: I. ISOLATION AND PARTIAL CHARACTERIZATION. Plant Physiology **69:** 1315-1319

Tiainen P, Myllyharju J, Koivunen P (2005) Characterization of a Second Arabidopsis thaliana Prolyl 4-Hydroxylase with Distinct Substrate Specificity. Journal of Biological Chemistry **280:** 1142-1148

Tognolli M, Penel C, Greppin H, Simon P (2002) Analysis and expression of the class III peroxidase large gene family in *Arabidopsis thaliana*. Gene **288:** 129-138

Toonen MAJ, Schmidt EDL, van Kammen A, de Vries SC (1997) Promotive and inhibitory effects of diverse arabinogalactan proteins on Daucus carota L. somatic embryogenesis. Planta **203:** 188-195

Tsukagoshi H, Busch W, Benfey PN (2010) Transcriptional Regulation of ROS Controls Transition from Proliferation to Differentiation in the Root. Cell **143:** 606-616

Vaknin H, Bar-Akiva A, Ovadia R, Nissim-Levi A, Forer I, Weiss D, Oren-Shamir M (2005) Active anthocyanin degradation in Brunfelsia calycina (yesterday–today–tomorrow) flowers. Planta **222:** 19-26

Valério L, De Meyer M, Penel C, Dunand C (2004) Expression analysis of the Arabidopsis peroxidase multigenic family. Phytochemistry **65:** 1331-1342

van Buuren ML, Maldonado-Mendoza IE, Trieu AT, Blaylock LA, Harrison MJ (1999) Novel Genes Induced During an Arbuscular Mycorrhizal (AM) Symbiosis Formed Between Medicago truncatula and Glomus versiforme. Molecular Plant-Microbe Interactions **12:** 171-181

van der Heijden R, Jacobs DI, Snoeijer W, Hallard D, Verpoorte R (2004) The Catharanthus Alkaloids:Pharmacognosy and Biotechnology Current Medicinal Chemistry **11:** 607-628

Van Hengel AJ, Roberts K (2003) AtAGP30, an arabinogalactan-protein in the cell walls of the primary root, plays a role in root regeneration and seed germination. The Plant Journal **36:** 256-270

van Hengel AJ, Tadesse Z, Immerzeel P, Schols H, van Kammen A, de Vries SC (2001) N-Acetylglucosamine and Glucosamine-Containing Arabinogalactan Proteins Control Somatic Embryogenesis. Plant Physiology **125:** 1880-1890

van Loon LC, Rep M, Pieterse CMJ (2006) Significance of Inducible Defense-related Proteins in Infected Plants. Annual Review of Phytopathology **44:** 135-162

VandenBosch KA, Bradley DJ, Knox JP, Perotto S, Butcher GW, Brewin NJ (1989) Common components of the infection thread matrix and the intercellular space identified by immunocytochemical analysis of pea nodules and uninfected roots. EMBO J **8:** 335-342

Veitch N (2004) Structural determinants of plant peroxidase function. Phytochemistry Reviews **3:** 3-18

Veitch NC (2004) Horseradish peroxidase: a modern view of a classic enzyme. Phytochemistry **65:** 249

Velasquez SM, Ricardi MM, Dorosz JG, Fernandez PV, Nadra AD, Pol-Fachin L, Egelund J, Gille S, Harholt J, Ciancia M, Verli H, Pauly M, Bacic A, Olsen CE, Ulvskov P, Petersen BL, Somerville C, Iusem ND, Estevez JM (2011) O-Glycosylated Cell Wall Proteins Are Essential in Root Hair Growth. Science **332:** 1401-1403

Verhertbruggen Y, Marcus SE, Haeger A, Verhoef R, Schols HA, McCleary BV, McKee L, Gilbert HJ, Paul Knox J (2009) Developmental complexity of arabinan polysaccharides and their processing in plant cell walls. The Plant Journal **59:** 413-425

Verpoorte R, Lata B, Sadowska A (2007) Biology and biochemistry of Catharanthus roseus (L.) G. Don. Springer, [Dordrecht etc.]

Vicré M, Santaella C, Blanchet S, Gateau A, Driouich A (2005) Root Border-Like Cells of Arabidopsis. Microscopical Characterization and Role in the Interaction with Rhizobacteria. Plant Physiology **138:** 998-1008

Vissenberg K, Feijó JA, Weisenseel MH, Verbelen JP (2001) Ion fluxes, auxin and the induction of elongation growth in Nicotiana tabacum cells. Journal of Experimental Botany **52:** 2161-2167

Welinder KG (1992) Superfamily of plant, fungal and bacterial peroxidases. Curr. Op. Struct. Biol. **2:** 388-393

Welinder KG, Justesen AF, Kjærsgård IVH, Jensen RB, Rasmussen SK, Jespersen HM, Duroux L (2002) Structural diversity and transcription of class III peroxidases from Arabidopsis thaliana. European Journal of Biochemistry **269:** 6063-6081

Wen F, VanEtten HD, Tsaprailis G, Hawes MC (2007) Extracellular Proteins in Pea Root Tip and Border Cell Exudates. Plant Physiology **143:** 773-783

Wickström SA, Alitalo K, Keski-Oja J (2003) Endostatin Associates with Lipid Rafts and Induces Reorganization of the Actin Cytoskeleton via Down-regulation of RhoA Activity. Journal of Biological Chemistry **278:** 37895-37901

Willats WGT, Knox JP (1996) A role for arabinogalactan-proteins in plant cell expansion: evidence from studies on the interaction of β-glucosyl Yariv reagent with seedlings of Arabidopsis thaliana. The Plant Journal **9:** 919-925

Willats WGT, Marcus SE, Knox JP (1998) Generation of a monoclonal antibody specific to (1→5)-α-l-arabinan. Carbohydrate Research **308:** 149-152

Wojtaszek P, Smith CG, Bolwell GP (1999) Ultrastructural localisation and further biochemical characterisation of prolyl 4-hydroxylase from Phaseolus vulgaris: comparative analysis. Int J Biochem Cell Biol **31:** 463-477

Wu H-m, Wang H, Cheung AY (1995) A pollen tube growth stimulatory glycoprotein is deglycosylated by pollen tubes and displays a glycosylation gradient in the flower. Cell **82:** 395-403

Wu S, Baskin TI, Gallagher KL (2012) Mechanical fixation techniques for processing and orienting delicate samples, such as the root of Arabidopsis thaliana, for light or electron microscopy. Nat. Protocols **7:** 1113-1124

Wu Y, Williams M, Bernard S, Driouich A, Showalter AM, Faik A (2010) Functional Identification of Two Nonredundant Arabidopsis α(1,2)Fucosyltransferases Specific to Arabinogalactan Proteins. Journal of Biological Chemistry **285:** 13638-13645

Xie D, Ma L, Šamaj J, Xu C (2011) Immunohistochemical analysis of cell wall hydroxyproline-rich glycoproteins in the roots of resistant and susceptible wax gourd cultivars in response to Fusarium oxysporum f. sp. Benincasae infection and fusaric acid treatment. Plant Cell Reports **30:** 1555-1569

Xie F, Williams A, Edwards A, Downie JA (2012) A Plant Arabinogalactan-Like Glycoprotein Promotes a Novel Type of Polar Surface Attachment by Rhizobium leguminosarum. Molecular Plant-Microbe Interactions **25:** 250-258

Xin Z, Zhao Y, Zheng Z-L (2005) Transcriptome Analysis Reveals Specific Modulation of Abscisic Acid Signaling by ROP10 Small GTPase in Arabidopsis. Plant Physiology **139:** 1350-1365

Xu J, Tan L, Lamport DTA, Showalter AM, Kieliszewski MJ (2008) The O-Hyp glycosylation code in tobacco and Arabidopsis and a proposed role of Hyp-glycans in secretion. Phytochemistry **69:** 1631-1640

Yamada H, Kiyohara H (1999) Complement-activating polysaccharides from medicinal herbs. *In* H Wagner, ed, Immunomodulatory Agents from Plants. Birkhäuser Basel, pp 161-202

Yamasaki H, Sakihama Y, Ikehara N (1997) Flavonoid-Peroxidase Reaction as a Detoxification Mechanism of Plant Cells against H2O2. Plant Physiology **115:** 1405-1412

Yang J, Sardar HS, McGovern KR, Zhang YZ, Showalter AM (2007) A lysine-rich arabinogalactan protein in Arabidopsis is essential for plant growth and development, including cell division and expansion. Plant Journal **49:** 629-640

Yannarelli G, Noriega G, Batlle A, Tomaro M (2006) Heme oxygenase up-regulation in ultraviolet-B irradiated soybean plants involves reactive oxygen species. Planta **224:** 1154-1162

Yariv J, Graf L, Rapport MM (1962) Interaction of Glycosides and Saccharides with Antibody to Corresponding Phenylazo Glycosides. Biochemical Journal **85:** 383-&

Yariv J, Lis H, Katchals.E (1967) Precipitation of Arabic Acid and Some Seed Polysaccharides by Glycosylphenylazo Dyes. Biochemical Journal **105:** C1

Yates EA, Valdor J-F, Haslam SM, Morris HR, Dell A, Mackie W, Knox JP (1996) Characterization of carbohydrate structural features recognized by anti-arabinogalactan-protein monoclonal antibodies. Glycobiology **6:** 131-139

Yoder LR, Mahlberg PG (1976) Reactions of alkaloid and histochemical indicators in laticifers and specialized parenchyma cells of *Catharanthus roseus* (Apocynaceae). American Journal of Botany **63:** 1167-1173

Yoo S-D, Cho Y-H, Sheen J (2007) Arabidopsis mesophyll protoplasts: a versatile cell system for transient gene expression analysis. Nat. Protocols **2:** 1565-1572

Yoshida K, Ohnishi M, Fukao Y, Okazaki Y, Fujiwara M, Song C, Nakanishi Y, Saito K, Shimmen T, Suzaki T, Hayashi F, Fukaki H, Maeshima M, Mimura T (2013) Studies on Vacuolar Membrane Microdomains Isolated from Arabidopsis Suspension-Cultured Cells: Local Distribution of Vacuolar Membrane Proteins. Plant and Cell Physiology **54:** 1571-1584

Youl JJ, Bacic A, Oxley D (1998) Arabinogalactan-proteins from Nicotiana alata and Pyrus communis contain glycosylphosphatidylinositol membrane anchors. Proceedings of the National Academy of Sciences **95:** 7921-7926

Yu M, Zhao J (2012) The cytological changes of tobacco zygote and proembryo cells induced by beta-glucosyl Yariv reagent suggest the involvement of arabinogalactan proteins in cell division and cell plate formation. BMC Plant Biology **12:** 1-16

Yuasa K, Toyooka K, Fukuda H, Matsuoka K (2005) Membrane-anchored prolyl hydroxylase with an export signal from the endoplasmic reticulum. The Plant Journal **41:** 81-94

Zatón AML, Ochoa de Aspuru E (1995) Horseradish peroxidase inhibition by thiouracils. FEBS Letters **374:** 192-194

Zhang X, Henriques R, Lin S-S, Niu Q-W, Chua N-H (2006) Agrobacterium-mediated transformation of Arabidopsis thaliana using the floral dip method. Nat. Protocols **1:** 641-646

Zhang Y, Yang J, Showalter A (2011) AtAGP18 is localized at the plasma membrane and functions in plant growth and development. Planta **233:** 675-683

Zhang Y, Yang J, Showalter AM (2011) AtAGP18, a lysine-rich arabinogalactan protein in Arabidopsis thaliana, functions in plant growth and development as a putative co-receptor for signal transduction. Plant signaling & behavior **6:** 855-857

Zheng H, Wang G, Zhang L (1997) Alfalfa Mosaic Virus Movement Protein Induces Tubules in Plant Protoplasts. Molecular Plant-Microbe Interactions **10:** 1010-1014

Zhong J, Ren YJ, Yu M, Ma TF, Zhang XL, Zhao J (2011) Roles of arabinogalactan proteins in cotyledon formation and cell wall deposition during embryo development of Arabidopsis. Protoplasma **248:** 551-563

Zipor G, Oren-Shamir M (2013) Do vacuolar peroxidases act as plant caretakers? Plant Science **199–200:** 41-47

ANNEX

What chemical groups in the AGP molecules may be functioning as Prx substrate?

A.1 INTRODUCTION

An important question concerning the Prx-AGP interaction and the observed fact that AGPs are substrates of Prx, is the identity of the chemical group(s) in AGPs that may be oxidised by Prx. Although the precise identity of the chemical groups involved in the Prx-mediated cross-linking of cell wall glycoproteins and polysaccharides remains a matter of debate, several lines of data point to the participation of phenolic side-chains, including feruloyl residues of wall polysaccharides such as pectins, or Tyr residues of cell wall glycoproteins such as extensin (Fry, 2004; Held et al., 2004; Abdel-Massih et al., 2007). In AGPs, it is not likely that Tyr residues will be exposed for cross-linking, the most reasonable hypothesis being the cross-linking of feruloyl residues putatively esterified in the glycan chains. Ferulic acid is an hydroxycinnamic acid derivative and is able to form ester-linkages with sugar residues, normally arabinose or galactose, of cell wall polymers (Fry, 2004). By the action of Prx in the presence of H_2O_2, feruloyl residues yield radicals that form covalent bonds with each other (oxidative coupling), and the resulting diferuloyl residue has been speculated to form a cross-link between the polysaccharides to which the feruloyl residues were esterified. Polysaccharide-esterified phenolic oligomers formed by the oxidative coupling of more than two feruloyl groups have been shown to predominate over dimers in certain cell-types, and several specific trimers and tetramers were characterised (Fry et al., 2000; Bunzel et al., 2003; Bunzel et al., 2006).

In this supplemental section the work developed in Edinburgh in Fry's lab is described. The hypothesis was that the Prx-mediated AGP cross-linking involves phenolic groups ester-bounded to their glycosidic chains. Thus, in order to investigate the presence of phenolic groups ester-bounded to AGPs glycosidic chains, AGPs from gum arabic and *Brassica oleracea* were submitted to alkaline hydrolysis and the products obtained were analysed by TLC and HPLC. Furthermore, a kinetic radiolabelling experiment was performed to investigate the timing of incorporation of radioactive phenolic groups into the AGPs.

A.2 METHODOLOGY

A.2.1 Arabidopsis cell culture

Arabidopsis thaliana (L.) Heynh. 'Erecta' cells were grown at 21ºC under constant moderate illumination (25 µmol m^{-2} s^{-1}) on an orbital shaker at 135 rpm. The medium

was prepared as (May and Leaver, 1993) and cells were sub-cultured weekly by 10-fold dilution into fresh medium.

A.2.2 Isolation of AGPs from *Brassica oleracea* leaves

See section II.2.9.

A.2.3 Extraction of polymer-esterified phenolic compounds

Gum arabic or *B. oleracea* AGPs were incubated in the dark with 1 M NaOH for ON to saponify ester bonds. The reaction mixture was then acidified by the addition of 4 M trifluoroacetic acid (TFA) until pH 0.6-1. The solution was partitioned twice against ethyl acetate. After the addition of the ethyl acetate the samples were thoroughly mixed and then centrifuged at 3,500 *g* for 10 min to aid the separation of the aqueous and organic phases into two layers. The organic layer, which contained the saponified products, was removed, combined and dried in a speedvac. The samples were redissolved in propanol and stored at -20ºC.

A.2.4 TLC analysis

Thin-layer chromatography (TLC) was carried out on 20 x 20 cm plastic-backed silica gel plates with a fluorescent indicator (254 nm, Merck). Samples were loaded onto the TLC as spots or streaks 2 cm from the TLC edge. All samples were left to air dry thoroughly before being placed in the chromatography tank. The solvent used was benzene/acetic acid (9:1). During development, TLC plate was exposed to long wave (366 nm) UV light to keep hydroxycinnamates as a rapidly interconverting single spot of *cis*/*trans* isomers. The TLC was run for 2.5 h. Phenolic compounds were detected as dark spots under short wave (254 nm) UV light.

A.2.5 HPLC analysis

High-pressure liquid chromatography (HPLC) was used to separate phenolic compounds after their saponification from the glycosidic moieties of AGPs from *B. oleracea* and from gum arabic. Dionex HPLC with a Phenomenex Luna C_{18} column (250 x 4.6 mm, 5 µm particle size) was used to separate the phenolics which were then detected with a photo diode array detector. Separation was carried out with a column temperature of 35ºC. The injection volume of each sample was 30 µL. The method used was A = H_2O, B = 50% methanol, C = 100% methanol and D = 5% acetic acid, with a linear gradient: t = 0 min, A = 15%, B = 40%, C = 5% and D = 30%; t = 15.4 min, A = 3.6%, B = 68%, C = 4% and D = 24.4%; t = 37 min, A = 2%, B = 2%, C = 94% and

D = 2%; t = 39 min, A = 15%, B = 40%, C = 5% and D = 30%. The flow rate was 1 mL/min.

A.2.6 Preparation of cell-suspension culture of Arabidopsis for radiolabel feeding

Arabidopsis cell culture was filtrated through a single layer of muslin to remove large cell clumps. The filtrate, containing a suspension of fine-cell clumps, was used to prepare a 20% settled cell-volume cell-suspension culture of the required volume. After transfer to the experimental vessel, culture was left to adjust to their new environment for 1 h. [^{14}C]cinnamic acid (21 kBq/mL) was then fed to the culture. At each time point 1 mL of culture (cells + culture medium) was collected for further extraction of AGPs.

A.2.7 Extraction of AGPs from cells fed with [^{14}C]cinnamic acid

Cells were separated from the culture medium by centrifugation and then washed with distilled water. All subsequent manipulations were conducted at 4ºC.

To isolate the AGPs from the culture medium, AGPs were precipitated with the β-Yariv reagent by mixing the culture medium in an equal volume of β-Yariv and leaving ON at 4ºC. The insoluble Yariv–AGP complex was collected by centrifugation at 13,000 rpm for 1 h and washed 3 times with 1% NaCl and then twice in methanol. The pellet was dissolved in a minimum volume of DMSO and the β-Yariv was removed by adding a 10% (w/v) sodium dithionite solution and incubating at 50ºC until the mixture became a clear yellow colour. The resulting yellow solution was immediately dialyzed against water and finally the sample was freeze-dried.

To isolate the AGPs from cells, cells were ressuspended in 50 mM Tris-HCl pH 8.0, 10 mM EDTA, 0.1% β-mercaptoethanol and 1% (w/v) Triton X-100 and sonicated for 2 min. After a centrifugation at maximum speed for 10 min, the supernatant was precipitated with 5 volumes of cold ethanol for ON at 4ºC. The mixture was centrifuged at maximum speed for 20 min and the precipitate was left to evaporate the ethanol. The precipitate was then dissolved in 1% (w/v) NaCl. The insoluble material was removed by centrifugation, and the supernatant was retained. The pellet was again ressuspended in 1% (w/v) NaCl, and the soluble material (after centrifugation) was pooled with the first supernatant. AGPs were precipitated with the β-Yariv reagent by mixing with an equal volume of β-Yariv and leaving ON at 4ºC. The insoluble Yariv–AGP complex was collected by centrifugation at maximum speed for 1 h and washed 3 times with 1% NaCl and then twice in methanol. The pellet was dissolved in a minimum volume of DMSO and the β-Yariv was removed by adding a 10% (w/v) sodium dithionite solution and incubating at 50ºC until the mixture became a clear yellow

colour. The resulting yellow solution was immediately dialyzed against water and finally the sample was freeze-dried.

A.2.8 Detection of the radioactivity

Phenolic compounds were extracted from AGPs as in section A.2.6. 5% of each sample were assayed for total radioactive content by liquid scintillation counting. The rest of the samples were streaked onto TLC plates and were run as in section A.2.3. The presence of any phenolic compound [^{14}C]cinnamic acid derivative was detected by autoradiography.

A.3 RESULTS AND DISCUSSION

In order to investigate the presence of phenolic residues in AGPs, gum arabic and AGPs purified from *Brassica oleracea* were submitted to an alkaline hydrolysis to break the putative ester bonds of phenolic groups, followed by organic extraction and analyses by TLC (Figure A.1). In the TLC plate it was not visible any promising spot in both samples. This could happen because the amount of material extracted from the AGPs was very low to be detected with this technique.

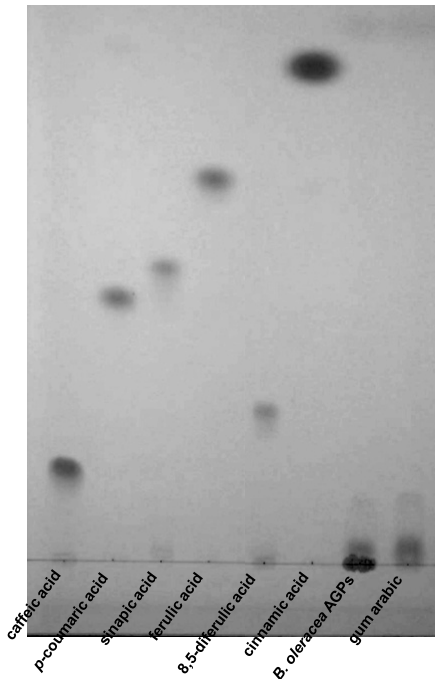

Figure A.1 – TLC plate of phenolic compounds extracted from AGPs of *B. oleracea* and gum arabic.

Therefore, the samples were analysed by HPLC, since it is a more sensitive technique (Figure A.2). Ferulic acid was clearly detected in the extract of hydrolysed *B. oleracea* AGPs (Figure A.2B), as well as for gum arabic, although in a lower amount (Figure

A.2C). This means that AGPs, in fact, contain feruloyl residues in their glycosidic chains that may thus function as Prx substrates. So, the next step was to perform cross-linking reactions of AGPs in the presence of Prx and H_2O_2 and to analyse the appearance of coupling products, for instance dimers or trimers of ferulic acid. This was tried once, but the result was inconclusive (data not shown). This work is being repeated using increased levels of isolated AGPs and improved analysis methods such as the ones cited by Bunzel (2010).

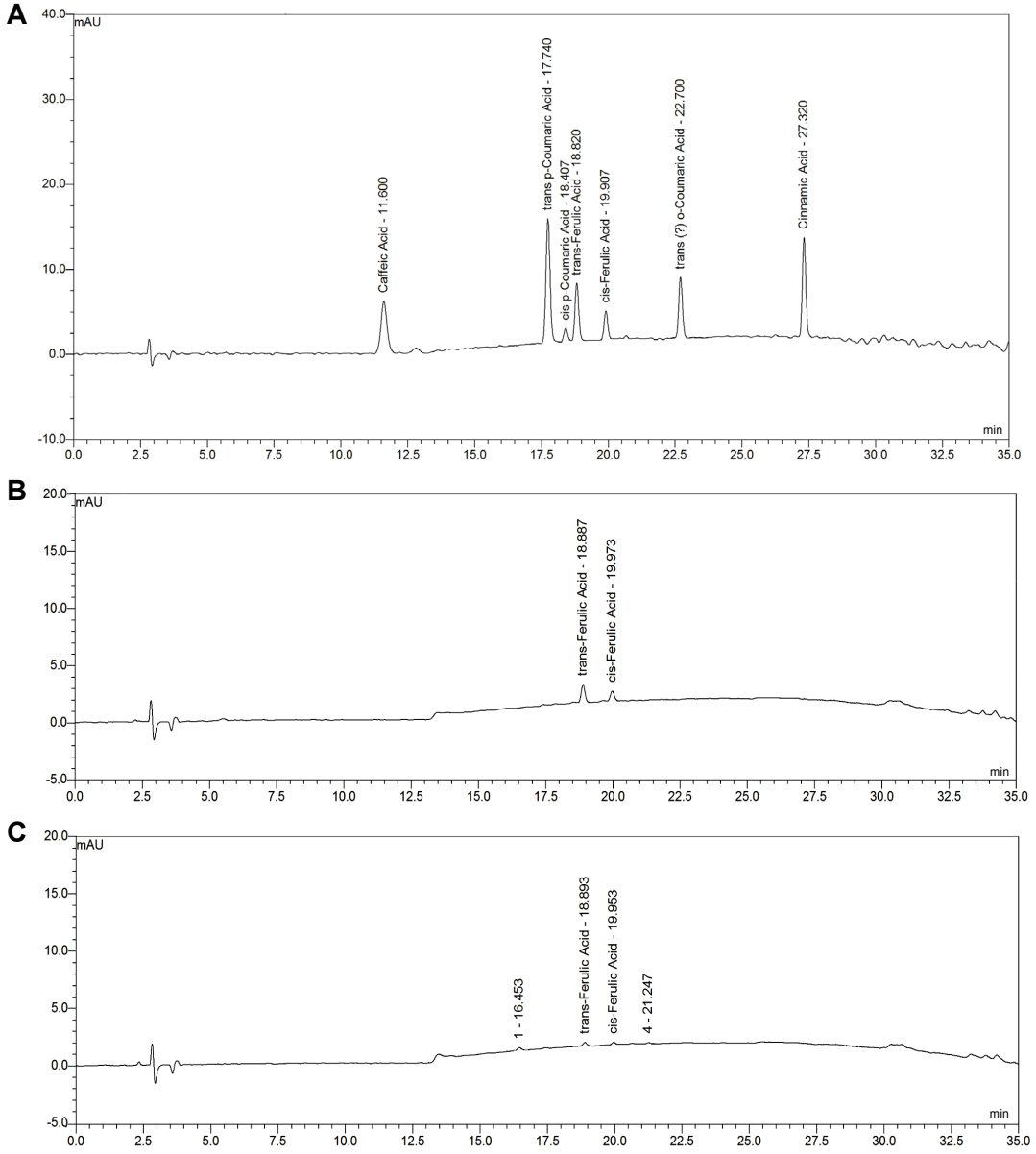

Figure A.2 – HPLC chromatograms of phenolic compounds extracted from AGPs. (A) Mixed markers. (B) *B. oleracea*. (C) Gum arabic.

Additionally, it was investigated the presence and the timing of incorporation of radioactive labelled phenolic precursors into AGPs. Arabidopsis cells were fed with

[^{14}C]cinnamic acid and during a time course AGPs were extracted from the cells and the culture medium. Cinnamic acid was chosen, because it is not a peroxidase substrate, so it is metabolically inert in the apoplast. This means that [^{14}C]cinnamic acid begins to be metabolised only when it is taken up by the cells. Furthermore, Lindsay and Fry (2008), demonstrated that Arabidopsis cells were capable to take up the [^{14}C]cinnamic acid from the culture medium. AGPs were hydrolyzed and the presence for radioactivity in the organic extracts was initially investigated by scintillation counting. It was noticeable that the early samples did not show any radioactivity and the latter samples presented almost none (data not shown). Nevertheless, the samples were run by TLC and the radioactivity was detected by autoradiography. However, the very low amount of radioactivity present in the samples was not possible to detect (data not shown). The cell debris from the extraction of AGPs was further analysed and it was evident that the cells incorporated [^{14}C]cinnamic acid (data not shown), however, during the 8 h of experiment, it was probably metabolized and incorporated in other cell compounds than in AGPs glycosidic chains.

A.4 LITERATURE CITED

Abdel-Massih RM, Baydoun EAH, Waldron KW, Brett CT (2007) Effects of partial enzymic degradation of sugar beet pectin on oxidative coupling of pectin-linked ferulates *in vitro*. Phytochemistry **68:** 1785-1790

Bunzel M, Ralph J, Brüning P, Steinhart H (2006) Structural Identification of Dehydrotriferulic and Dehydrotetraferulic Acids Isolated from Insoluble Maize Bran Fiber. Journal of Agricultural and Food Chemistry **54:** 6409-6418

Bunzel M, Ralph J, Funk C, Steinhart H (2003) Isolation and identification of a ferulic acid dehydrotrimer from saponified maize bran insoluble fiber. European Food Research and Technology **217:** 128-133

Fry SC (2004) Oxidative coupling of tyrosine and ferulic acid residues: Intra- and extra-protoplasmic occurrence, predominance of trimers and larger products, and possible role in inter-polymeric cross-linking. Phytochemistry Reviews **3:** 97-111

Fry SC, Willis SC, Paterson AEJ (2000) Intraprotoplasmic and wall-localised formation of arabinoxylan-bound diferulates and larger ferulate coupling-products in maize cell-suspension cultures. Planta **211:** 679-692

Held MA, Tan L, Kamyab A, Hare M, Shpak E, Kieliszewski MJ (2004) Di-isodityrosine is the intermolecular cross-link of isodityrosine-rich extensin analogs cross-linked *in vitro*. Journal of Biological Chemistry **279:** 55474-55482

Lindsay S, Fry S (2008) Control of diferulate formation in dicotyledonous and gramineous cell-suspension cultures. Planta **227:** 439-452

May MJ, Leaver CJ (1993) Oxidative Stimulation of Glutathione Synthesis in Arabidopsis thaliana Suspension Cultures. Plant Physiology **103:** 621-627